THE INFLUENCE OF STENT MATERIAL AND DIABETES ON MACROPHAGES TRANS-DIFFERENTIATION PATHWAYS IN THE PROGRESSION OF IN-STENT RESTENOSIS

Tiziano Poletti

A thesis submitted in partial fulfilment of the requirements of the University of Brighton for the degree of Doctor in Philosophy

June 2014

University of Brighton

DECLARATION

I declare that the research contained in this thesis, unless otherwise formally indicated within the text, is the original work of the author. The thesis has not been previously submitted to this or any other university for a degree, and does not incorporate any material already submitted for a degree.

Signed

Dated

ABSTRACT

The outcome of the deployment of cardiovascular stents in coronary arteries compromised by atherosclerosis may be affected by the deposition of a myofibroblast-driven neointimal tissue and consequent re-blockage of the vessel lumen known as in-stent restenosis (ISR). Its incidence is particularly high in people with diabetes unless drug-eluting stents (DES) are implanted as alternatives to the traditional bare metal stents (BMS) made of stainless steel (ST). However, the long-term outcome of the use of DES is under debate due to evidence of late thrombosis. Monocytes/macrophages (MM) play a key role in ISR participating in the different phases of the host response to the implant. This in-vitro study investigates differences in the distribution and response of MM that may be significant for a better understanding of the causes of the increased ISR occurrence among diabetic patients, particularly focusing on the trans-differentiation potential of MM into myofibroblast-like cells when in contact with ST. The overnight incubation of MM freshly isolated from blood from healthy donors (n=6) in high glucose (4500mg/L) and high free fatty acid (sodium palmitate 0.4mM) concentrations, alone or in combination, aimed at creating a diabetes-mimicking experimental model. MM response to ST seemed exacerbated by the synergistic effect of the palmitate and glucose as shown by the occurrence of features characteristic of activation as well as by their trend to fuse into the formation of giant cells as shown by scanning electron microscopy. Similarly results from RT-PCR (n=6) suggested an increase in the expression of the m-RNA for HAS3, the enzyme responsible for the synthesis of low molecular weight hyaluronic acid characteristic of the inflammatory process. Furthermore, the presence of MM positive for α-actin, as shown by immunocytochemistry, seemed to confirm the occurrence of early changes in their phenotype. This was accompanied by a significant ($p<0.05$ or $p<0.005$ after paired t-test) increase in the release of PDGF-BB, growth factor characterizing the post-inflammatory condition, as well as in the release of TNF-α confirming the short-term metal-induced inflammatory reaction from MM incubated on ST in comparison to control surfaces as shown by ELISA tests. Flow cytometry on buffy coats collected from three cohorts of donors (control, type 1 and type 2 diabetes) (n=7) suggested that variations among donors with diabetes in the number of circulating activated macrophages and haematopoietic progenitor cells may, once compared to clinical data, help to identify patients at high risk of developing ISR. The hypothesis of the contribution of MM in the deposition of restenotic neointimal tissue through the transformation into myofibroblasts was reinforced by results from flow cytometry that identified, both in freshly isolated buffy coats and after contact with surfaces, subpopulations co-expressing α-actin and markers for MM (CD14 or CD68). This was also supported by the immunostaining of the cells after overnight incubation on the surfaces where α-actin-positive cells were seen. Furthermore, ELISA test on the supernatants (n=10) suggested that ST triggered a significant increase in the release of PDGF-BB and TNF-α when compared to control surfaces. This study reinforced the hypothesis that MM can contribute to ISR through phenotypical changes and that the acute synergistic effect of glucose and lipids can affect their level of activation.

Acknowledgments

I would like to thank my supervisors for their help and support throughout this long journey: Dr. Moira Harrison for her precious advice on diabetes and English grammar; Prof. Matteo Santin for sharing his profound knowledge on biomaterials matter and for his consistent guidance; Dr. Anna Guildford for her help in laboratory and her support and motivation.

I would like to thank Dr. Anna Crown and Dr. Andrew Smith at the diabetes clinics at the Royal Sussex County Hospital in Brighton for giving me the possibility to access the clinic and for their help with the donor recruitment and data collection. A particular thanks goes to: Dr. Helen Stewart, Dr Paola Lanuti and the flow cytometry team at the Sussex Medical School in Brighton for helping me with the collection and interpretation of flow cytometry data; Dr. Bruschi and Dr. Colombo at the Niguarda Hospital in Milan for giving me the possibility to experience a real-life scenario and for providing me with images; Dr. Angela Sheerin and Dr. Clare Marriott for their help with the PCR; all the staff at the University of Brighton who shared their expertise and helped in many occasions.

Finally, I would like to give a special thanks to my mum and dad for their endless support and patience. Last but not least, a very special thanks goes to Sonia, Giancarlo, Claudia, nonna Barbara, Peter and all the people close to me for their love, support and encouragement that inspired me throughout my life and gave me the motivation and the energy to achieve this result.

CONTENTS

LIST OF FIGURES

LIST OF TABLES

LIST OF ABBREVIATIONS

ACBP	acyl-CoA binding protein
AGE	advanced glycation end product
BSA	bovine serum albumin
BMS	bare-metal stent
CHD	coronary heart disease
CVD	cardiovascular diseases
DES	drug-eluting stent
ECM	extra cellular matrix
FABP	fatty acid binding protein
FBS	foetal bovine serum
FFA	free fatty acid
FITC	fluorescein isothiocyanate
FSC	forward scatter
GAPDH	glyceraldehyde-3-phosphate dehydrogenase
HA	hyaluronic acid (hyaluronan)
HAS	hyaluronan synthase
HDL	high density lipoprotein
IGT	impaired glucose tolerance
ISR	*in-stent* restenosis
LDL	low density lipoprotein
PBS	phosphate buffered saline
PCR	polymerase chain reaction

PDGF	platelet-derived growth factor
PE	phycoerythrin
PTCA	percutaneous transluminal coronary angioplasty
PUFA	poly-unsaturated fatty acid
SEM	scanning electron microscopy
SMC	smooth muscle cells
SSC	side scatter
ST	stainless steel
TAE	tris acetate-EDTA
TCP	tissue culture plastic
TLR	toll-like receptor
TNF	tumour necrosis factor

CHAPTER 1

INTRODUCTION

1.1 BIOMATERIALS

1.1.1 Biomaterials: introduction and definition

The use of artificial materials to replace a part of the human body or its function can be traced back in history. The first examples of the aware use of synthetic materials in medicine date back to the nineteenth century with the use of a bone-substitute named "Plaster of Paris" and with the use of dental amalgam (Nicholson 2002). However, the introduction of the concept of biomaterials and their definition appeared in 1967 at the "International Biomaterials Symposium" at Clemson University (South Carolina) where they were defined as "a systemically, pharmacologically inert substance designed for implantation within or incorporation with a living system" used with the aim of replacing a part of human body or its function (Park & Lakes 1992, Park & Bronzino 2002, Nicholson 2002, Sharma 2005). The definition has been expanded since then to include different sources of biomaterials and better define their interaction with the human body. For example, Black defined biomaterials as "any pharmacologically inert material, viable or non-viable, natural product or man-made, that is a part of or is capable of interacting in a beneficial way with a living organism" (Sharma 2005). This was later expanded by Williams as "any non-living materials used in medical devices intended to interact with biological systems" (Sharma 2005). It appears clear that biomaterials include materials designed to interact with the human body with no induction of adverse reactions or toxicity (Sharma 2005). Therefore, biomaterials have to possess optimal physical, chemical, mechanical and structural properties in order to optimize the performance of the function they provide in the human body (Park & Lakes 1992). In addition, the materials used for their production must be biocompatible, thus characterized by a low degree of host response following implantation and interfacing with the living system. Ideal materials must be non-toxic, sterilizable

and stable during implantation as well as not corroding, degrading or being carcinogenic (Sharma 2005). The biocompatibility of biomaterials is now defined by a very broad concept that takes into account the general performance of the implants in the human body both in terms of the function provided and of the host response (Nicholson 2002). The host response includes all the interactions that biomaterials have with the body environment once implanted, such as cell adhesion, interaction with proteins and blood, effects of body fluids on the materials (i.e. corrosion, oxidation, dissolution) (Nicholson 2002). A more advanced definition of biocompatibility has been introduced to comprise the different uses of biomaterials. Initially the assessment of the biocompatibility of a material was focussed on the reduced toxicity, thrombogenicity, carcinogenicity, and immunogenicity. The more recent definition takes into consideration the context in which the material has to be used (Williams 2008). No truly inert material exists. In fact, any foreign body in contact with the human body will encounter some interaction with its components. Therefore, the new concept of biocompatibility takes into account how the biomaterial has to be used and its specific interaction with the human body. This is particularly important for materials that require a reaction with surrounding tissues in order to exert their function, or materials that must degrade after appropriate time (Williams 2008).
The use of biomaterials has become possible only after the introduction of aseptic surgical technique in 1860s (Park & Lakes 1992). The use and applications of biomaterials can be found in different sectors of the medical practice as illustrated in table 1.1 (Park & Lakes 1992).

Biomaterials can also be distinguished on the basis of their structure or source. The most common artificial materials used in medicine belong to the following categories (Park & Lakes 1992):

- Polymers (Nylon, Silicones, Teflon);
- Metals (Titanium, Stainless Steel, Co-Cr alloys, Gold);

- Ceramics (Aluminium oxide, Carbon, Hydroxyapatite);
- Composites (Carbon-Carbon).

Table 1.1 Examples of uses of biomaterials and their applications (Adapted from Park & Lakes, 1992)

Function of biomaterials	**Example of application**
Replacement of damaged organ/part	Orthopaedic artificial joints, kidney dialysis machine
Healing facilitation	Sutures, bone repairs and screws, wound dressings
Improvement of organ function	Cardiac pacemaker, contact lenses, stents
Correction of functional abnormalities	Harrington spinal rod
Correction of cosmetic problems	Mammoplasty, cosmetic implants
Diagnosis	Catheters, probes
Treatment	Catheters, drains

In addition, materials of biological origin (biological materials) such as tissues, proteins and polysaccharides can be used as biomaterials to replace an organ or facilitate the healing of a tissue. Biological materials are typically represented by composites containing a viable element (e.g. cells). Examples of those are represented by elastin, collagen, hyaluronic acid (Park & Lakes 1992, Park & Bronzino 2002).

1.1.2 Metallic biomaterials

Different metals and metallic alloys have been used as biomaterials for their electrical and thermal conductivity as well as their mechanical properties. As a

class of materials, metals are the most widely used for load-bearing implants (Park & Bronzino 2002).

The most common applications of metallic biomaterials is found in orthopaedic surgery for the production of artificial joints (e.g. hip, knee) and fracture healing aids (e.g. bone plates, screws). Metallic alloys are widely used in dentistry for implants or orthodontic devices and further applications include the production of vascular stents and catheter guides (Park & Lakes 1992, Park & Bronzino 2002, Nicholson 2002). Most metals present in nature (Iron, Chromium, Cobalt, Nickel, Titanium, Tantalum, Molybdenum, Tungsten) have been used to produce alloys that have found application as biomaterials (Park & Lakes 1992, Park & Bronzino 2002). The first and vastly used alloys for the production of medical devices are cobalt-chromium (Co-Cr) containing small amounts of molybdenum (Mo) and nickel (Ni) and 316L stainless steel. In addition, titanium (Ti) combined to a small percentage of aluminium and vanadium, has been increasingly used in the attempt to improve their biocompatibility (Nicholson 2002). Gold and platinum have been used pure or as main components of alloys for applications in dentistry. However, the choice of the alloys and metals is based on the cost-effectiveness, physicochemical properties and resistance to corrosion. In fact, this represents the main concern regarding the compatibility of these materials due to the high corrosive potential of the human body fluids (Park & Bronzino 2002, Nicholson 2002).

1.1.2.1 Stainless steel: definition and biocompatibility

Stainless steel is the name given to an alloy made of a composition of different metals other than iron and cobalt and giving origin to a material more resistant to corrosion than traditional steel. Stainless steels are regularly used by the medical, chemical, and pharmaceutical industries because of their corrosion resistance, biocompatibility, mechanical properties, ability to resist elevated temperatures and relative low cost (Park & Bronzino 2002, Nicholson 2002, Rokicki 2008). The

first stainless steel used to produce implants was the 18-8 stainless steel (type 302). This was then replaced by the 316 or 316L stainless steel in which the resistance to corrosion was improved by the addition of molybdenum and chromium in specific concentrations (Park & Lakes 1992, Park & Bronzino 2002, Nicholson 2002). In particular, grade 316 is the standard molybdenum-bearing grade. 316L stainless steel is the low carbon version of 316 (Park & Lakes 1992, Park & Bronzino 2002, Newson 2002, Nicholson 2002). The biomedical grade stainless steel, widely used nowadays for the production of orthopaedic and other medical devices, is the 316L whose composition is described in table 1.2 (Park & Bronzino 2002). Surgical stainless steel is a specific type of stainless steel including alloying elements of chromium, nickel and molybdenum conferring respectively scratch and corrosion resistance, smooth surface and hardness. The austenitic structure, a specific crystal structure obtained by increasing the temperature, also gives these grades excellent toughness and resistance to corrosion. Compared to chromium-nickel austenitic stainless steels, 316L stainless steel offers higher creep, stress to rupture and tensile strength at elevated temperatures (Newson 2002, Yang 2010).

The resistance to corrosion and wear once in contact with human fluids represents one of the main issues to be overcome when considering the biocompatibility of stainless steel. Therefore, stainless steels used for implants must be suitable for close and prolonged contact with human tissue (Kerber 2000, Yang 2010). Despite this concerns in the use of the metal for the production of biomaterials, the outcome has been overall satisfactory (Nicholson 2002). Stainless steel is rendered resistant to corrosion because of the development of a chromium-rich chromium oxide passive layer, typically on the order of 3 to 5 nm thick or about 15 layers of atoms, on the surface formed by an oxidation-reduction reaction in which the chromium is oxidized, and the passivating agent is reduced (Kerber 2000). If this layer is not allowed to form, or if the layer is broken, rapid general corrosion can follow. The surface chemistry of stainless steel ultimately depends

on the chemical as well as on the mechanical characteristics of the surface (Kerber 2000). Corrosion resistance in stainless steel may be enhanced by electropolishing and/or chemical treatments. The passivation treatment aims at increasing the amount of chromium in the area near the surface (Kerber 2000). The treatment is essential to improve the resistance to corrosion. In fact, the simple passivation due to exposure to the atmosphere is not sufficient to offer protection (Kerber 2000). Electropolishing is the surface treatment most extensively used to improve the resistance to corrosion of stainless steel (Rokicki 2008). The treatment has been further developed by combining it to a magnetic field, thus performing a magnetoelectropolishing (Rokicki 2008). For the chemical passivation different types of acid have been used (nitric, hydrofluoric, phosphoric, citric, EDTA) (Kerber 2000). The outcome of the passivation process is influenced by the combination of acid type, concentration, temperature and time (Kerber 2000).

Surgical grade stainless steel offers superior corrosion resistance compared with other steels. This is primarily due to the addition of chromium (at least 11% by weight) to the steel and the subsequent presence of chromium oxide on the outer surface. Compared with titanium and cobalt alloys, stainless steels are readily available and relatively inexpensive. The clinical requirements were the driver for the development of special 'implant' steels. These materials, now produced with enhanced chemical compositions, were originally developed from commercial-grade (316) stainless steel. Specific requirements for resistance to pitting corrosion apply to implant-grade stainless steels but do not apply to commercial stainless steels. Therefore, special production routes are required to obtain implant steels (Newson 2002).

Further surface treatments, such as the use of N^+ fluxes to form an ionic layer (ion-implantation) on the metal surface, have been attempted to protect stainless steel from the effect of corrosion (Nicholson 2002). Low temperature plasma surface alloying with nitrogen (nitriding), carbon (carburising) and both (carbonitriding) has been successfully employed in hardening medical grade

stainless steel by the formation of a modified layer better known as S-phase or expanded austenite. It has been shown that low-temperature treatments improved the localised corrosion and wear resistance of the medical grade stainless steel without affecting its biocompatibility (Buhagiar 2012).

The surface of stainless steel is a very good substrate for cell adhesion. This represents a key factor for its compatibility, particularly when considering the use of the metal for the production of orthopaedic prosthesis where the osteointegration is the critical factor for the positive outcome of the implantation (Nicholson 2002).

In addition, blood biocompatibility is a key factor for the reduction of adverse effects against the implanted material and it is essential in assessing the compatibility of cardiovascular implants (Nicholson 2002, Honess 2006). The roughness of the surface has been seen to influence the thrombogenicity of metal implants (Zhao 2003), particularly affecting the performance of devices used in cardiovascular procedures, such as coronary stents. A smoother surface was demonstrated to result in the reduction of platelet aggregation, thus reducing the formation of thrombi during the initial phases following implantation (Zhao 2003). The electrochemical polishing of the metal surface has been in fact used to reduce surface defects and successfully reduce the thrombogenicity of those devices (Zhao 2003).

1.1.3 Interaction of biomaterials with the human body

The implantation of biomaterials is generally associated with tissue injury as consequence of the surgical procedure. Although the tissue response varies depending on the site and on the procedure of implantation, the process of tissue repair is characterized by a common sequence of events leading to healing of the

tissue and summarized as follows (Parks & Lakes 1992, Nicholson 2002, Anderson 2008):

- Injury
- Acute inflammation
- Chronic inflammation
- Formation of granulation tissue
- Foreign body reaction
- Fibrosis

Table 1.2 Composition of 316L biomedical grade stainless steel. (Adapted from Park & Bronzino, 2002).

Element	**Composition (%)**
Carbon	0.03 maximum
Manganese	2.00 maximum
Phosphorus	0.03 maximum
Sulphur	0.03 maximum
Silicon	0.75 maximum
Chromium	17.00-20.00
Nickel	12.00-14.00
Molybdenum	2.00-4.00

1.1.3.1 Injury and blood clotting

Increased vascular permeability and blood flow at the site of the injury are the immediate consequences of the damage induced by the surgical procedure (Nicholson 2002) and leading to the process known as exudation. This is characterized by fluids rich in proteins and blood cells leaving the blood vessels

and accumulating at the site of the injury (Nicholson 2002). This is responsible for the activation of the inflammatory reaction that follows.

The injury is shortly followed by clotting of the blood surrounding the implanted material. Blood clotting is governed by platelets forming aggregates and catalysing the complex sequence of reactions characterizing the intrinsic and extrinsic pathways of the coagulation cascade thus leading to the thrombus formation and deposition of fibrin (Nicholson 2002). Although the thrombus formation is desirable and vital in order to stop the bleeding and initiate the tissue repair process, in the case of biomaterials this can represent a critical factor as large thrombi could be responsible for a life-threatening thrombosis (Nicholson 2002).

In addition, the contact of the materials with body fluids has as an immediate consequence represented by the formation of a layer of proteins, mainly fibrin derived from the coagulation process, depositing on the surface (Luttikhuizen 2006, Anderson 2008). This layer forms a provisional matrix around the struts providing a structural and biochemical basis driving the following inflammatory and foreign body reactions (Luttikhuizen 2006, Anderson 2008). It is in fact rich in mitogens and chemoattractant factors, cytokines, growth factors, and other bioactive agents able to modulate the activity of macrophages and to regulate the proliferation and activation of cell populations involved in the inflammatory response and wound healing process (Luttikhuizen 2006, Anderson 2008). Therefore, it appears clear that the surface characteristics, affecting the absorption of proteins, represent a key point for the modulation of the host response to the implanted device (Luttikhuizen 2006, Anderson 2008).

1.1.3.2 Inflammation

The term inflammation defines a series of reactions naturally occurring as the consequence of tissue damage which aim to isolate or eliminate the causative agent (Nicholson 2002). A complex sequence of events involving different cell

types and chemical mediators are involved in the process that results in the replacement of the damaged tissue or, if this is not possible, in the formation of scar tissue (fibrosis) (Nicholson 2002).

The initial phase of the inflammatory process, known as acute inflammation, is characterized by the presence of neutrophils (polymorphonucleated leukocytes) and mediated by the release of histamine from mast-cells and by the fibrinogen absorbed on material surfaces (Nicholson 2002, Anderson 2008). Acute inflammation is generally of short duration although it can last from hours to a few days depending on the severity of the injury (Nicholson 2002). The process is characterized by exudate (fluids and plasma) and by the presence of neutrophils that aim at removing the external agent responsible for the injury or damage (Nicholson 2002). Neutrophils generally disappear after 24-48 hours to be replaced by the infiltration of mononuclear cells (i.e. lymphocytes and monocytes) that, following extravasation and migration under the influence of chemokines and chemoattractant cytokines, start the process known as chronic inflammation (Nicholson 2002, Anderson 2008). This is characterized by the differentiation of monocytes into macrophages (Nicholson 2002, Anderson 2008). The inflammatory process is perpetrated for a period of time that can last up to a few weeks depending on the extent of the injury (Nicholson 2002, Anderson 2008). The recruitment, migration and differentiation of monocytes/macrophages at the site of the injury is sustained by the release from the same macrophages of chemoattractant and pro-inflammatory cytokines such as tumour necrosis factor alpha (TNF-α), interleukin-6 (IL-6), granulocyte-colony stimulating factor (GC-SF) and granulocyte macrophage colony stimulating factor (GMC-SF) (Luttikhuizen 2006, Anderson 2008). The platform of interaction between macrophages and biomaterials is represented by the plasma- and extracellular matrix-derived proteins absorbed on the strut surfaces, thus representing a key point for the modulation of the response to biomaterials as described above (Luttikhuizen 2006, Anderson 2008). In particular, cell (i.e. macrophages)

adhesion onto biomaterial surfaces is mediated by the interaction between receptors present on the surface of their cell membrane. These are composed of a combination of three different protein units known as integrins (Anderson 2008). Chronic inflammation is therefore characterized by the presence of mononuclear cells (monocytes/macrophages, lymphocytes) and plasma cells adhering onto the surface of the biomaterial and sustaining the immune and inflammatory reactions (Nicholson 2002, Anderson 2008). As part of the inflammatory process, adhering activated macrophages tend to fuse to form foreign body giant cells in the attempt to eliminate the foreign body through phagocytosis (Nicholson 2002, Luttikhuizen 2006, Anderson 2008). In addition to the formation of giant cells, macrophages aim to degrade the foreign body by releasing mediators such as enzymes, reactive oxygen species (ROIs) and acids in the area between cell membrane and biomaterial surface (Anderson 2008). However, with the exception of bio-degradable biomaterials, the phagocytic process is not able to eliminate the foreign body. The process of chronic inflammation, that generally lasts around two weeks, is followed by the deposition of granulation tissue, precursor of the formation of the fibrous capsule (fibrosis) around the strut (Anderson 2008).

1.1.3.3 Granulation tissue, foreign body reaction and fibrosis

Granulation tissue characterizes the process of wound healing following the implantation procedure (Nicholson 2002) as a consequence of the damage to endothelial and epithelial cells (Wynn 2008). The tissue is highly vascularized by the formation of new small blood vessels (pink granular aspect) deriving from the rearrangement of endothelial cells (Nicholson 2002). Furthermore, the cascade of events following the injury provokes the formation of extra-cellular matrix embedding the newly formed blood vessels under the influence of the growth factors and cytokines released throughout the reaction (Wynn 2008). In particular, collagen is deposited by the fibroblasts and myofibroblasts (fibroblasts expressing α-actin, a marker for smooth muscle cells) populating the granulation tissue in addition to inflammatory cells such as macrophages (Gabbiani 2004, Wynn 2008).

The extent of the formation of granulation tissue is related to the extent of the injury provoked by the implantation procedure (Nicholson 2002).

Fibrosis defines the final process of wound healing related to the implantation of biomaterials and it is characterized by the formation of a fibrous capsule around the device (Nicholson 2002). This is characterized by deposition of collagen forming the capsule as a consequence of an increase in the rate of collagen production by myofibroblasts populating the wound healing tissue compared to its degradation rate (Wynn 2008). In particular, the fibrotic process characterizes the implantation of biomaterials in soft tissues (Nicholson 2002).

The foreign body reaction is therefore the sequence of reactions induced by the implantation of biomaterials and characterized by the formation of foreign body giant cells and by the presence of the components of the granulation tissue such as macrophages, fibroblasts and small blood vessels (Nicholson 2002). The distribution in cell types varies depending on the characteristic of the implant, such as the structure of the surface (Nicholson 2002) and the components of the foreign body reaction can stay on the biomaterials throughout the entire life of the implant or be surrounded by the fibrous capsule (Nicholson 2002).

1.1.4 Cells in the reaction to biomaterials: macrophages and myofibroblasts

Different cellular components are involved in the complex cascade of events following implantation of biomaterials. Among those, macrophages play a key role in driving the inflammatory reaction and they are present alongside fibroblasts and myofibroblasts in the formation of granulation tissue and in the deposition of collagen forming the fibrous capsule (Nicholson 2002, Gabbiani 2004, Anderson 2008, Wynn 2008).

1.1.4.1 Haematopoiesis

Cellular components of circulating blood all derive from multipotent haematopoietic stem cells (HSCs), or haemocytoblasts, present in a small number in the bone marrow (Orkin 2008, Lilly 2011) through a process of differentiation known as haematopoiesis (Orkin 2008) as represented in figure 1. HSC can generate progenitor precursors that progressively differentiate into mature blood cells of the two main lineages, myeloid (erythrocytes, platelets and leukocytes) and lymphoid (lymphocytes) (Orkin 2008) (figure 1.1).

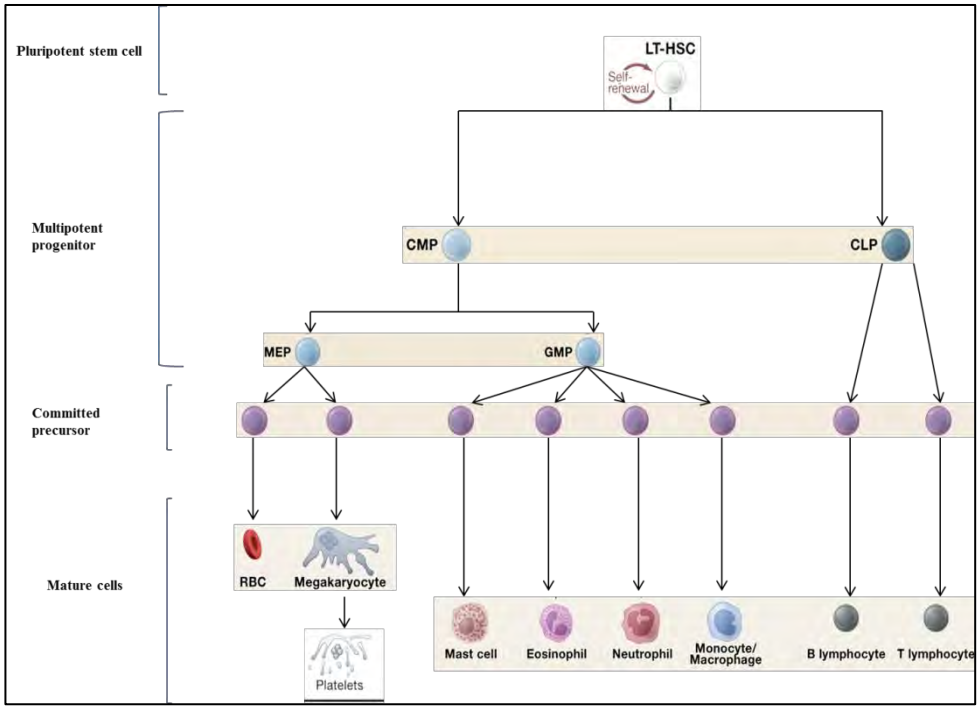

Figure 1.1 Schematic representation of the haematopoietic process. *Blood cells derive from a pluripotent self-renewing stem cell (LS-HSC) that differentiates into a common multipotent progenitor (haemocytoblast) in the bone marrow. This can in turn differentiate into progenitor of two different lineages, common myeloid progenitor (CMP) or common lymphoid progenitor (CLP). CMP differentiates into either the megakaryocyte-erythroid progenitor cell (MEP) or granulocyte-macrophage progenitor cell (GMP). These and the CLP generate all the cellular components of the circulating blood via formation of committed progenitor cells. Figure adapted from Orkin 2008.*

Haematopoietic stem cells are represented by a heterogeneous group of precursors capable of self-regeneration and residing in the bone marrow. They support the regular turnover of the whole range of cells constituting the blood throughout the entire life of an individual (Orkin 2008, Lilly 2011).

1.1.4.2 Monocytes and macrophages

Monocytes and macrophages are a heterogeneous group of leukocyte cells participating in the immune response (Takahashi 2001, Geissman 2010). Monocytes circulate in the bloodstream and reside in bone marrow and spleen (Geissmann 2010) following differentiation from the common myeloid progenitor in the bone marrow (figures 1.1, 1.2). They represent immune effector cells able to release cytokines that activate the inflammatory reaction in case of infections. They also present pathogen receptors able to mediate the migration of infected tissues under the stimuli of toxic molecules or pathogens (Geissmann 2010). Monocytes which have migrated to tissues can differentiate into macrophages and dendritic cells intervening in the immune reactions and perpetrating the inflammatory reaction (Geissmann 2010). In addition, they can differentiate into specialized cells (i.e.osteoclasts) (Gordon & Taylor 2005) confirming the heterogeneity of the population in size, granularity and nuclear morphology (Gordon & Taylor 2005). Monocytes differentiate from haematopoietic multipotent progenitor cells through progressive phases that include precursors such as monoblasts and promonocytes (figure 1.2) (Takahashi 2000). In particular, each monoblast generates two promonocytes and each promonocyte generates two monocytes (Takahashi 2000). Monocytes represent the 5-10% of leukocytes in humans (Geissmann 2010) and seem to lose their self-proliferation ability once mature and in the steady-state (Takahashi 2000, Geissmann 2010) when they remain in the circulating blood for several days before entering peripheral tissues to differentiate into macrophages (Geissmann 2010).

Macrophages are phagocytic cells resident in different tissues and organs (i.e. free or fixed macrophages in the spleen, in lymph nodes, in thymus; alveolar macrophages in the lungs) where they participate in tissue homeostasis through the elimination of senescent and apoptotic cells and the release of growth factors (Takahashi 2000, Teo 2003, Geissmann 2010). Macrophages in tissues have also been found to generate specialized cells participating in a similar way to the homeostasis of the tissue such as osteoclasts in the bone, Kupffer cells in the liver, and Langerhans cells in the epidermis (Takahashi 2000, Gordon & Taylor 2005). Therefore, macrophages represent a heterogeneous population showing different morphology and function according to the tissue they inhabit (Takahashi 2000).

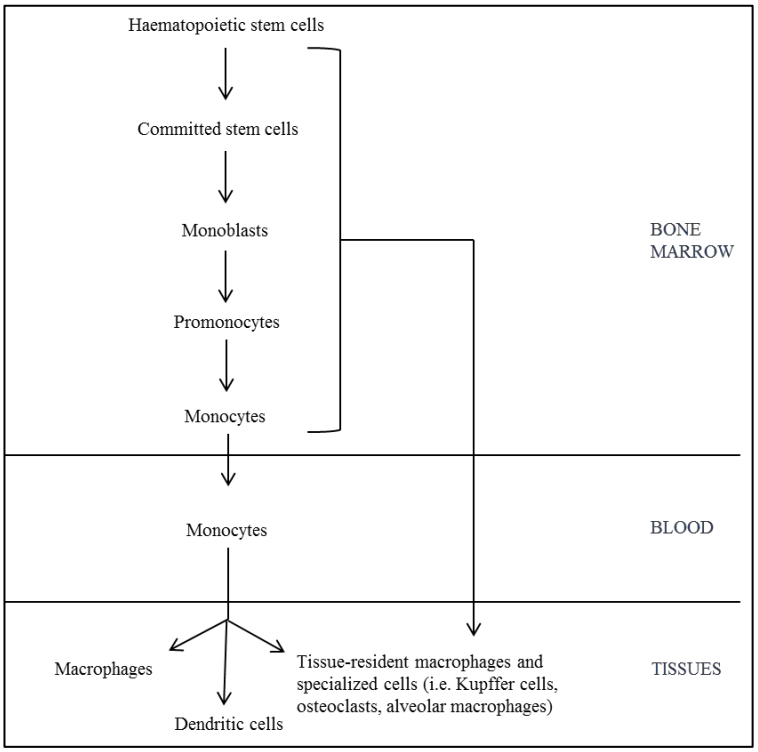

Figure 1.2. Differentiation pathways of monocytes and macrophages. *Monocytes derive from the differentiation of haematopoietic progenitor cells through subsequent steps involving the formation of monoblasts and promonocytes. Macrophages derive from the migration into infected tissues and further differentiation of circulating monocytes. Tissue-resident macrophages turn-over is also maintained by differentiation of precursors preceding the monocytic differentiation stage. Figure adapted from Takahashi 2000.*

During infections macrophages rich in pathogen recognition receptors intervene in the elimination of the infecting agents through phagocytosis. The phagocytic process is consequent of the inflammatory reaction triggered and sustained by the same cells through the release of pro-inflammatory cytokines (Takahashi 2000, Teo 2003, Geissmann 2010). In the case of acute infection or injury, macrophages populate the injured area through migration and differentiation of circulating monocytes in response to inflammatory stimuli (Takahashi 2000). Monocytes-derived macrophages are unable to self-renew thus deriving exclusively from the differentiation of circulating monocytes (Takahashi 2000) (figure 1.2). However, it was shown that, although in a steady-state, monocytes migrate to tissues to replenish the population of macrophages and tissue resident macrophages are capable of self-renewal (Takahashi 2000, Gordon & Taylor 2005). It was also shown that the origin of macrophages in tissues derives from the migration of precursors pre-ceding the monocytic stage and supporting the turn-over of macrophages in peripheral tissues and organs (figure 1.2) (Takahashi 2000, Gordon & Taylor 2005).

1.1.4.3 Myofibroblasts

As described in section 1.1.3.3 the tissue forming during the chronic inflammation or, more generally, during the wound healing process is characterized by the presence of fibroblasts and myofibroblasts within the reorganization of the extra-cellular matrix (Gabbiani 2004, Wight 2004, Wynn 2008). Myofibrobalsts represent the contractile status of fibroblastic cells occurring after injury (Hinz 2007). They have been identified in all fibrotic tissues as fibroblasts expressing contractile features typical of smooth muscle cells such as α-actin (Gabbiani 2004). The acquisition of the contractile status, i.e., the conversion of fibroblasts into myofibroblasts, is induced by the combination of different factors like the presence of TGF-β1, the action of specialised proteins in the extra-cellular matrix and the action of extra-cellular stress due to the remodelling of the matrix (Hinz 2007). It has been demonstrated that the remodelling of extra-cellular matrix, for

example in case of vascular disease, is characterized by the acquisition of a pro-inflammatory state. This is the result of the deposition of hyaluronan and versican under the influence of growth factors (TGF-β1 and PDGF), thus favouring the attachment of inflammatory cells and the migration and proliferation of smooth muscle cells from the vessel wall (Wight 2004). Different hypotheses have been proposed for the origin of myofibroblasts during fibrosis. Most commonly they are believed to originate from the differentiation of local fibroblasts (Gabbiani 2004, Wight 2005). However, additional sources such as the de-differentiation of surrounding vascular smooth muscle or the trans-differentiation of epithelial or mesenchymal cells have been suggested (Gabbiani 2004, Wight 2005). Different sources can also be tissue-specific. In fact, the differentiation of local haematopoietic stem cells as well as the presence of circulating precursors (fybrocytes) originating in the bone marrow have been proposed as sources of myofibroblasts (Gabbiani 2004, Wight 2005). In addition, different studies have recently demonstrated the trans-differentiation of macrophages into myofibroblasts in the fibrotic capsules (Mesure 2010) and after contact with stainless steel (Stewart 2009).

1.2 CARDIOVASCULAR DISEASE AND DIABETES

1.2.1 Cardiovascular disease and coronary heart disease: definition, epidemiology

The term cardiovascular disease (CVD) defines a broad range of morbidities characterized by alterations in the functionality of heart and blood vessels such as atherosclerosis, arrhythmia, heart failure, heart attack and myocardial infarction, heart valve disease, disorders of the aorta and its branches (British Heart Foundation 2010).

Cardiovascular disease represents the biggest cause of death in the UK. Despite a decrease in the number of deaths due to a better approach to reducing risk factors and improvements to therapies, in 2008 CVD still accounted for 191,000 deaths and 50,000 premature deaths in UK. CVD is the cause of the death of one in four men and one in five women under the age of 75 (British Heart Foundation, 2010). The financial impact of CVD on the NHS has been estimated to be around 30 billion pounds a year (British Heart Foundation, 2010).

The World Health Organization (WHO) estimated that in 2008 17.3 million people worldwide died from CVD, representing 30% of deaths globally (WHO, 2012). Among those, the 80% of deaths took place in low and medium-income countries and almost equally among men and women (WHO, 2012). WHO also estimated that by 2030 almost 25 million people will die worldwide from CVD, thus remaining the leading cause of death.

Coronary heart disease (CHD) includes diseases affecting the arteries supplying the heart (coronaries) due to narrowing or occlusion of the vessels caused by deposition of fat (atheroma), thus causing heart attack and angina (British Heart Foundation, 2010). In 2008 CHD was responsible for 88,000 of deaths related to CVD in the UK (British Heart Foundation, 2010).

1.2.1.1 Cardio vascular disease: risk factors

The identification of specific risk factors correlated to CVD and the appropriate targeting of these through government policy and health campaigns for prevention have resulted in a successful reduction in mortality related to these morbidities in the UK over the last decades (British Heart Foundation, 2010). Differences in CVD occurrence and mortality can be seen across genders, age groups, ethnicities and social conditions (British Heart Foundation, 2010). The most common risk factors identified as responsible for the occurrence of CVD are the following (Gregg 2005, British Heart Foundation 2010):

- **Overweight and obesity.** This is considered an independent risk factor associated with increase in blood pressure, blood cholesterol level and impaired glucose tolerance or diabetes. All those represent risk factors for the occurrence of CVD. A measure of the degree of overweight or obesity is the measurement of the body mass index (BMI) that is calculated by dividing the weight (expressed in kilograms) of an individual by their height (in metres) squared. A BMI value between 25 and 30 indicates overweight and a value bigger that 30 is indicative of obesity (Gregg 2005, British Heart Foundation 2010);
- **Blood cholesterol.** Research has shown that raised blood cholesterol levels are responsible worldwide for overall 8% of diseases and that 60% of CHD is due to total blood cholesterol levels above 3.8mmol/l (British Heart Foundation 2010). In particular, low levels of HDL (high density lipoprotein) cholesterol, participating in the removal of cholesterol from circulation, are associated with increased risk of CHD (British Heart Foundation 2010). The control of blood cholesterol levels can be achieved by changes in lifestyle such as dietary habits and physical activity, or by pharmacological treatment if the first are not sufficient.
- **Blood pressure**. An increase in the risk of CHD is directly correlated to increases in both systolic and diastolic blood pressure values. In particular, it has been estimated that an increase in 20mmHg in the usual systolic pressure and each increase of 10mmHg in the diastolic pressure doubles the possibility of death from CHD (British Heart Foundation 2010);
- **Diabetes.** An increase in the risk of CVD is directly associated with type 1 and type 2 diabetes (British Heart Foundation 2010). The topic will be discussed further in sections below.

1.2.2 Atherosclerosis

Atherosclerosis is generally considered to be related to the chronic inflammation of the artery walls leading to the deposition of a lipid plaque and consequent hardening of the vessels. The plaque deposition and stiffening of the vessel walls are responsible for the related morbidities and development of CHD (Chapman 1998, Kannel 1998, Fan & Watanabe 2003, British Heart Foundation 2010). Atherosclerosis has been identified as the main killer of the 21th century. The mechanisms of atherogenesis, a term identifying the process of plaque (atheroma) formation, are multiple and complex and different theories have been suggested (Chapman 1998, Fan & Watanabe 2003, Libby 2009). Different theories take into consideration the components responsible for the development of the disease such as alterations in blood lipid levels (dyslipidaemia), oxidative stress, endothelial dysfunction and inflammation. However, it is recognized that atherosclerosis, despite different pathways and risk factors associated with plaque formation, is always accompanied by a chronic inflammatory condition affecting the biology of the arterial wall (Chapman 1998, Fan & Watanabe 2003, Libby 2009).

1.2.2.1 Blood vessel structure

The structure of blood vessels is constituted by concentric layers (tunics) made of different types of tissues. Although the composition and distribution of the layers varies depending on the function and size of the vessel (veins, arteries, arterioles, capillaries), three main layers can be identified (Marieb 1991):

- **Tunica intima**: it constitutes the inner layer of the vessel and is composed of endothelial cells with a thin layer of supporting connective tissue. Damage in this layer can lead to atherosclerosis and clotting and its integrity is essential for the functionality of the vessel, being at the interface with the circulating blood.
- **Tunica media**: it is the middle layer of the vessel wall representing the muscular and elastic part of the vessels. It is in fact mainly composed of

smooth muscle cells and elastic tissue. This represents the thickest layer in the vessel wall.

- **Tunica adventitia**: it represents the outer layer of the vessel wall and it is mainly composed of fibrous connective tissue and elastin fibres.

In general, arteries conducting the blood from the heart to tissues and organs have proportionally more smooth muscle cells then veins of similar size (Marieb 1991).

1.2.2.2 Atherosclerotic plaque: characteristics and pathophysiology

The atherosclerotic plaque is generally composed by a necrotic core made of lipid and surrounded by a fibrotic cap made of smooth muscle cells and extracellular matrix (Fan & Watanabe 2003). The base of the cap (shoulder) contains macrophage derived foam cells and T lymphocytes and it determines the stability of the plaque. In particular, there are two main types of plaques that differ in terms of morphology and consequently in term of stability (Fan & Watanabe 2003):

- **Stable plaque**: composed of a small lipid core and surrounded by a thick fibrous cap
- **Unstable plaque**: composed of a large lipid core and a thin fibrous cap and containing a larger amount of inflammatory cells

Stable plaques represent a risk for vascular occlusions and stenosis because growing in size they can lead to the reduction of vascular lumen and to the consequent obstruction in blood flow (Fan & Watanabe 2003). Unstable plaques represent a major risk of fatalities as their rupture can occur regardless of their size and be the cause of thrombosis and acute coronary syndrome (Fan & Watanabe 2003).

It has been established that the formation of plaques is related to the infiltration of cells loaded with lipids, known as foam cells, in the sub-intimal layer of blood vessels. Foam cells originate from the differentiation of monocytes into

macrophages that consequently engulf oxidised lipoproteins (oxLDL) through surface scavenger receptors (Fan & Watanabe 2003). Circulating lipids originating from cholesterol are transported in the bloodstream in the form of lipoproteins, molecules composed of proteins and fat. The analysis of the composition of atherosclerotic lesions has shown that the atherogenic lipoproteins composing the plaques are mainly three types (Fan & Watanabe 2003):

- Low density lipoproteins (LDL);
- Very low density lipoproteins (β-VLDL);
- Lipoprotein (a).

Once deposited in the intima, LDL and VLDL are oxidized forming the atherogenic oxidized form that is phagocyted by macrophages for the formation of foam cells. In addition, oxidized lipoproteins exert a proinflammatory action favouring the expression of adhesion molecules on the endothelial cells of the vessel wall, thus triggering the adhesion of circulating monocytes to the intima (Fan & Watanabe 2003). It seems that Lipoprotein (a) is not normally oxidized and it never participates in the formation of foam cells. Although its role in atherogenesis is not entirely clear yet, its role as a pro-inflammatory mediator has been demonstrated (Fan & Watanabe 2003).

Although atherosclerotic lesions develop over a period of many years the process is initiated by the expression of adhesion molecules, such as vascular cell adhesion molecule-1 (VCAM-1) and intracellular adhesion molecule-1 (ICAM-1), on the endothelial cells of the intima favouring the adhesion of monocytes and T lymphocytes to the vessel wall. As mentioned above, the expression of adhesion molecules seems to be up-regulated by the increase of oxLDL, lipoprotein (a) and cytokines as demonstrated in vitro (Fan & Watanabe 2003).

Several studies have now concluded that there is a direct correlation of inflammation and immunity with the development of atherosclerotic lesions

identifying atherosclerosis as a chronic inflammatory disorder of blood vessels (Ross 1999, Fan & Watanabe 2003, Libby 2009).

1.2.3 Diabetes

As described by the World Health Organisation (WHO) consultation diabetes mellitus is a "metabolic disorder of multiple aetiology characterized by chronic hyperglycaemia with disturbances of carbohydrate, fat and protein metabolism resulting from defects in insulin secretion or action or both" (WHO Consultation 1999). In a more recent report published by the World Health Organization (WHO) in 2006 and concerning the diagnosis of diabetes mellitus and intermediate hyperglycaemia it was declared that an estimated 171 million people worldwide were affected by diabetes mellitus in 2000 and the figure was predicted to increase to 366 million by 2030 (WHO 2006). Similarly, data published by King *et al.* showed that between 1995 and 2025 the population with diabetes will increase 122% worldwide with a particular increase seen in the developing countries (King 1999).

The WHO report also defined the condition of metabolic syndrome as precursor of, or concomitant to, type 2 diabetes and characteristic of the more developed countries. Metabolic syndrome is characterised by impaired glucose tolerance (IGT) accompanied by alterations of the metabolic system and their consequences such as hypertension, dyslipidaemia, central obesity and microalbuminuria (WHO 1999). IGT is defined as an intermediate state between normal glucose homeostasis and diabetes, thus characterized by difficulties in controlling post-prandial blood glucose levels. Individuals falling into this category generally present a normal glucose level under fasting conditions but are unable to regulate blood glucose levels after meals. Therefore, they represent a category at risk of developing type 2 diabetes if not promptly controlled through changes in lifestyle (WHO 1999). Symptoms of hyperglycaemic condition are characterized by thirst,

polyuria, frequent infections, blurring of vision, drowsiness and weight loss. These symptoms are thought to be the result of a higher than 6.1mmol/l (threshold for normoglycaemia) fasting venous glucose concentrations which, if not treated, can lead to coma and death due to ketoacidosis, particularly in the case of type 1 diabetes (WHO 1999). Symptoms occur more severely and acutely in type 1 diabetes due to the depletion of insulin related to the lack insulin producing β-cells. This condition can quickly lead to ketoacidosis and death if not treated with insulin replacement therapy (Lambert & Bingley 2006). Type 2 diabetes is generally a consequence of the degeneration of an acute phase inflammatory state involving in particular adipose tissue and leading to a progressive insulin resistance. For this reason occurrence of symptoms can take long time and the diagnosis can be delayed (Sjoholm & Nystrom 2006). The differentiation between the two main forms of diabetes (type 1 and type 2) is now based on the aetiology of the disease represented by the causing agent and mechanisms of development (WHO 1999) as detailed in the sections below.

1.2.3.1 Type 1 Diabetes

Type 1 diabetes is characterized by the destruction of pancreatic insulin-producing islets of Langerhans (beta cells) mainly due to an autoimmune reaction identified by the presence of specific auto-antibodies (Lambert 2006). The development of autoantibodies can begin in the early childhood and it can occur over a period of time that can extend up to 5-8 years (Lambert 2006). However, it has been demonstrated that the destruction of pancreatic cells is not due to the direct action of the antibodies but it is an immune process mediated by T lymphocytes and inflammatory cells (Zacher 2002, Lamhamedi-Cherradi 2003, Homo-Delarche & Drexhage 2004, Lambert 2006). It is recognized that type 1 diabetes represent a multifactorial autoimmune disease where the destruction of β-cells in the pancreatic islets of Langerhans is the result of the intervention of T lymphocytes, macrophages and dendritic cells around the islets (Zacher 2002, Lamhamedi-Cherradi 2003, Homo-Delarche & Drexhage 2004). The process is orchestrated by

the expression of multiple inflammatory genes in the islets and both human and rodent models of the disease have shown that the islets are destroyed by the intervention of inflammatory cells (Lamhamedi-Cherradi 2003). Helper T-lymphocytes intervene in the initiation of the process in cooperation with macrophages for the triggering and maintenance of the inflammatory cascade leading to the destruction of β-cells. Cytotoxic T lymphocytes are effectors of the cell destruction (Zacher 2002). Similar clinical scenarios correlated to the destruction of β-cell may be initiated by the action of different viruses (WHO 1999). Because of the absence of insulin, type 1 diabetes is generally characterized by a rapid onset of acute symptoms that can easily lead to ketoacidosis and related coma and death if not diagnosed promptly. Type 1 diabetes manifests more typically during childhood or adolescence and individuals are lean. The only available treatment is daily insulin replacement through injection or insulin pump (Lambert 2006).

1.2.3.2 Type 2 diabetes

Type 2 diabetes is a condition of insulin resistance in which the production of insulin by beta cells is maintained but its action is not sufficient to reduce blood glucose concentration to the normoglycaemic threshold (Sjoholm & Nystrom 2006). It is characterized by insulin deficiency related to defects in insulin secretion or action or their concomitance (WHO 1999). The levels of insulin can be normal but its action is not effective in reducing blood glucose levels (insulin resistance). The glucose level in blood is maintained by the balance between the production processes of gluconeogenesis and glyconeogenesis in the liver and by disposal of glucose by insulin-insensitive tissue such as brain and by insulin-sensitive tissues such as muscles, fat and heart (O'Rahilly 1994). Insulin resistance is characterized by a loss in sensitivity to insulin action in tissues thus resulting in increased blood glucose levels. The extent of the process marks the difference between the conditions of impaired glucose tolerance and type 2 diabetes (O'Rahilly 1994, WHO 1999, Wellen & Hotamisligil 2005, Sjoholm &

Nystrom 2006). Type 2 diabetes is therefore a condition that occurs over time accompanied by the development of metabolic syndrome and obesity. Metabolic syndrome is characterized as a multifactorial condition presenting the concomitant presence of different cardiovascular risk factors such as abdominal obesity, dyslipidaemia, raised blood pressure, insulin resistance and glucose intolerance, proinflammatory and prothrombotic states (WHO 1999, Beilby 2004). A direct connection between insulin resistance, obesity and diabetes has been demonstrated in various studies that focussed on the direct connection between metabolism and immune system.

Obesity has been characterized as a chronic inflammatory condition associated with the overproduction of pro-inflammatory cytokines such as TNF-α and IL-6, and of messenger molecules known as adipokines (leptin, adiponectin) from muscles and adipose tissue of obese individuals (Wellen & Hotamisligil 2005, Sell 2006). Accumulation of macrophages in the adipose tissue participates in the activation and progression of an inflammatory condition in adipocytes of obese individuals paving the way for the development of insulin resistance (Weisberg 2003, Permana 2006). The abundance of visceral fat characterizing obesity generates insulin resistance in skeletal muscles and potentially diabetes (Sell 2006). In particular, hyperlipidaemia is connected to increase of fatty acid uptake by muscle cells that generates metabolites activating the inflammatory cascade. Elevated amounts of free fatty acids and the action of TNF-α seem to modify the receptor for insulin on insulin-sensitive tissues such as skeletal muscles (Moller 2000, Wellen 2005, Mlinar 2007) thus causing insulin resistance and diabetes on a longer term (Wellen 2005, Mlinar 2007). Similarly the release of adipokines is associated to occurrence of insulin resistance (Mlinar 2007).

Type 2 diabetes is a condition traditionally affecting adult populations (although obesity and sedentary lifestyle are resulting in an increase in type 2 in children and adolescents) and correlated to metabolic dysfunction. The aetiology of the disease is related to genetic predisposition and lifestyle risk factors such as low physical activity and diet (Tuomilehto 2001, Spranger 2003). The correction of

lifestyle habits can control the development of type 2 diabetes in individuals with insulin resistance (Tuomilehto 2001). The UK prospective diabetes studies (UKPDS) have shown the relevance of the thigh control of blood glucose levels, including strict dietary programs, on the reduction of the incidence of diabetes-related complications and on the progression of the disease (King 1999, Riddle 2000, American Diabetes Association 2002, Mazzone 2010). Therefore, the control of blood glucose is not only reducing the occurrence of early complications and mortality in the development of type 2 diabetes but could also play an important role in the incidence of complications in individuals with type 1 diabetes in which diabetes is diagnosed at young age in the absence of co-morbidities related to the general metabolic disorder characterizing the origin of type 2 diabetes (King 1999, American Diabetes Association 2002, Mazzone 2010).

1.2.3.3 Long term complications of diabetes: advanced glycation end products (AGEs)

Irrespective of the type of diabetes, people with poorly controlled diabetes are at risk of developing long-term complications as a consequence of prolonged hyperglycaemia. Diabetes is a co-morbid condition which puts those with the disorder at risk of an increase in atherosclerotic disease and cardiovascular, peripheral vascular and cerebrovascular disease, all consequences of long-term hyperglycaemia (WHO Consultation 1999, Nathan 1993). In addition common complications associated to long-term diabetes are retinopathy, nephropathy and neuropathy (Nathan 1993).

Hyperglycaemia leads to the formation of advanced glycation end products (AGEs) which are the result of the reaction between reducing sugars and amino groups leading to irreversible changes to lipids and proteins in the body (Price 2004, Goldin 2006). The reaction consists in non-enzymatic glycation and oxidation of long-lived proteins. This occurs through the formation of Amadori products and Schiff bases following the reaction between aldoses (sugars) and

proteins amino groups. Further rearrangement of the Amadori products involves irreversible reactions leading to the formation of AGEs through oxidative and non-oxidative pathways (Goldin 2006) (Figure 1.3). Amadori products present highly reactive carbonyl groups that interact with functional groups of proteins leading to the formation of AGEs as a result of reactions of denaturation, browning and cross-linking. The process is known as "carbonyl stress" (Goldin 2006). AGEs can in turn produce reactive oxygen species (ROS) generating oxidative stress, cross-link to molecules, modify the extracellular matrix and interact with cellular receptor (RAGE) modifying the action of hormones, cytokines and free radicals (Goldin 2006). AGEs form under hyperglycaemic conditions and are responsible for vascular damage and other complications of diabetes through extracellular and intracellular mechanisms.

Alterations in cellular structure due to cross-linking between molecules and alterations in cell functions through receptor binding and formation of intracellular proteins which leads to structural and functional alterations in tissues are particularly relevant for the occurrence of disorders in the cardiovascular system (Peppa 2003).

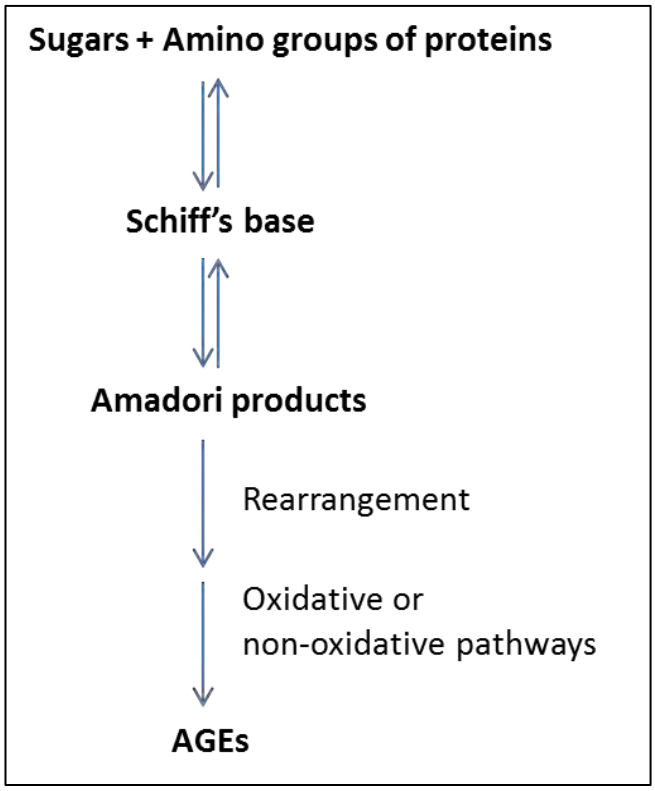

Figure 1.3. Schematic representation of the pathways involved in the formation of advanced glycation end products (AGEs). *The formation of AGEs derives from a process of glycation and oxidation of long-lived proteins due to the reaction (Maillard reaction) between sugars and amino groups and leading to the formation of Schiff's bases and Amadori products (reversible reactions). These intermediate represent highly reactive carbonyl compounds (carbonyl stress) that, after rearrangement, interact with functional groups of proteins thus leading to the formation of AGEs.*

AGEs accumulate in the vessel wall interacting with smooth muscle cells, macrophages and endothelial cells, and quenching the endothelial release of NO (nitric oxide) often resulting in the progressive stiffening of the arterial wall which is clinically associated with an accelerated atherosclerotic process through a complex network of receptor-dependent and independent mechanisms (Peppa 2003, Price 2004, Goldin 2006). Vessel wall alterations are associated with an increased inflammatory reaction and the recruitment of leukocytes which, in turn, are related to the release of TNF-α and IL-6. This leads to an increase in C-reactive protein production, well recognised risk marker of CVD (Price 2004).

1.3 CARDIOVASCULAR STENTS AND IN-STENT RESTENOSIS

Atherosclerosis is the main cause of CVD compromising life expectation. The deposition of the atherosclerotic plaque may lead to a blockage in the lumen of the blood vessel which, when the occlusion is located in the coronary arteries, may cause major cardiovascular events such as angina, stroke and heart attack (Kannel 1998). The most common surgical treatments used to re-establish the patency of the occluded lumen, known also as revascularization procedure, are coronary by-pass graft and percutaneous balloon angioplasty (Alderman 2000).

1.3.1 Percutaneous balloon angioplasty and stent placement

The use of percutaneous transluminal coronary angioplasty (PTCA) has widely increased since its introduction by Gruentzig in 1977 (Santin 2005) as it represents a less invasive and risky technique compared to by-pass graft (Bertrand 1998). The procedure consists of the insertion of a balloon-tipped catheter driven to the site of the lesion through a major artery. The balloon is then inflated, deflated and removed to re-open the occluded vessel (Santin 2005). Despite the procedure representing a valid and less invasive alternative to bypass grafting and leading to an immediate success rate of revascularization of around 90% (Herrmann 1992), complications still affect the outcome of the intervention. These are mainly related to the effect of vasospasm, thrombus formation and elastic recoil of the vessel wall resulting in incomplete restoration of the lumen patency affecting at least 10% of the procedures (Herrmann 1992). In addition, the formation of restenosis (secondary vascular occlusion) connected to vascular elastic recoil and negative remodelling of the vessel affects up 30-40 % of cases (Liu 1999, Santin 2005). Concerns about death and myocardial infarction following the procedure have been raised in different studies evaluating the outcome of PTCA (Herrmann 1992, Alderman 2000).

The PTCA technique has been developed further by the deployment of a stent, an expandable tubular metallic mesh that is loaded onto the balloon and delivered during PTCA (figure 1.4) (Santin 2005). The stent is placed at the site of the lesion to support the blood vessel and maintain the lumen patency ensuring the success of revascularization procedure (figure 1.5). The presence of the metallic structure reduces the chances of elastic recoil and consequently improves the outcome of the procedure (Gross 2000, Santin 2005). Despite the deployment of stents representing a relevant improvement in the angioplastic procedure, complications still affect the general outcome in up to 35% of patients when considering the implantation of traditional bare metal stents in more complex scenarios (Gross 2000, Santin 2005, Singh 2010).

1.3.1.1 Typologies of cardiovascular stents

The tubular metallic mesh forming the strut of cardiovascular stents traditionally used for angioplasty in coronary arteries was made of iron-chromium nickel alloys (stainless steel), cobalt-chromium alloys, alloys with titanium such as Nitinol (nickel-titanium) and tantalum (Gotman 1997). The continuous attempts to develop the material constituting the struts and its coatings aimed to optimize the strength and mechanical properties reducing the thickness of the strut and maintaining the radio-opacity needed during the surgical procedure (Santin 2004, O'Brien & Carroll 2009). The reduction of the thickness of the strut has resulted in a reduction in the restenosis rate. In order to optimize structural properties of the struts, different coatings were used to ensure radio-opacity and optimize the bio-compatibility of the devices (Santin 2004, O'Brien & Carroll 2009).

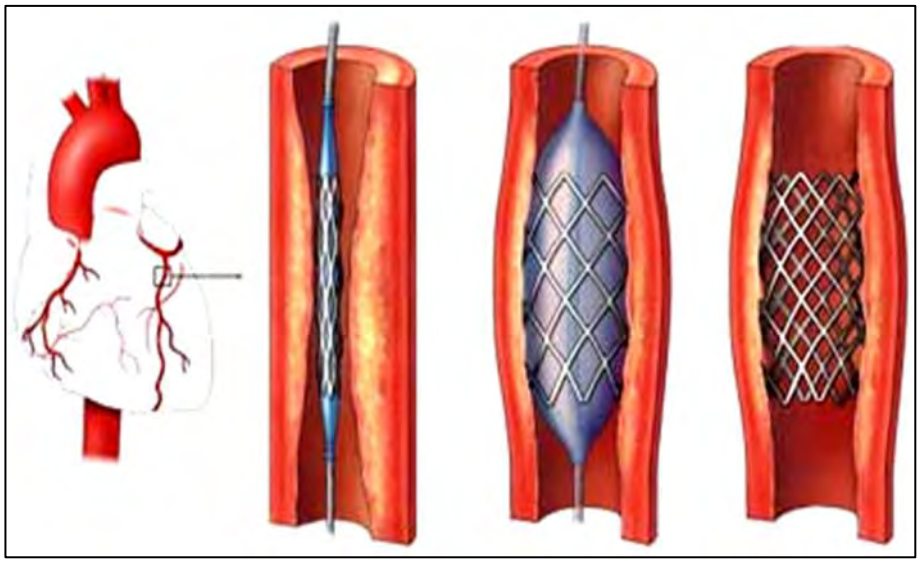

Figure 1.4 Schematic representation of the procedure of stent deployment in a coronary artery. *A balloon-tipped catheter bearing the stent is driven to the site of the lesion where after inflation, deflation and retrieval of the baloon the stent remains to maintain the lumen patency. Copyright © 2005 Nucleus Communications, Inc. All rights reserved. www.nucleusinc.com 2005 Nucleus*

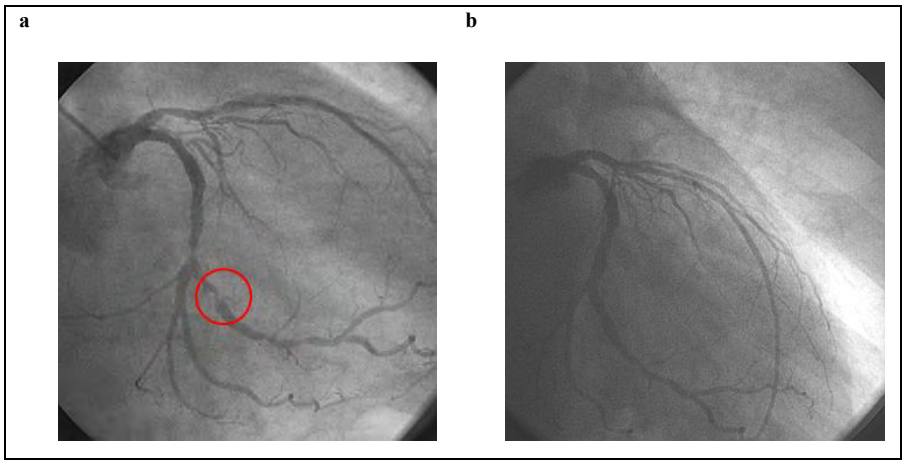

Figure 1.5 Images of revascularization following stent implantation. *The figure shows the angiogram of coronary arteries in a patient with a more than 20 mm long lesion occluding the 90% of the diameter of the left circumflex artery (a) and the angiogram of the same region following revascularization obtained through the deployment of a cardiovascular stent (b). Images obtained from Niguarda Hospital, Milan (Italy).*

Gold, carbon, different inorganic coatings such as titanium oxides and polymers were tested to obtain the optimal compromise between strut-thickness, opacity and biocompatibility. However, none of the coatings showed an improvement in the biocompatibility of the devices in terms of restenosis rate compared to stainless steel alone which remains the material of choice for the production of cardiovascular stents and other medical devices thanks to its strength, hardness, corrosion resistance, biocompatibility, fatigue resistance, and ease of sterilization (O'Brien & Carroll 2009, Umoru 2009).

Further attempts to reduce the rate of restenosis have been represented by the production of drug-eluting stents (DES). In those cases the metallic strut is coated with a multilayer polymeric coating controlling the release of the embedded drug aiming at reducing the cellular proliferation responsible for the formation of the restenotic plaque (O'Brien & Carroll 2009). The successful first generation of DES has been widely used in clinical applications in the last decade. Among those the Cypher (Cordis/Johnson & Johnson, NY, USA) is formed by a strut coated with three polymeric layers releasing Sirolimus (Barlis 2007, O'Brien & Carroll 2009). This is an immune-suppressant drug that inhibits the reaction of T-lymphocytes and inflammatory cells also reducing the proliferations of smooth muscle cells (Santin 2005, O'Brien & Carroll 2009). The second commercially successful DES is the Taxus (Boston Scientific, MN, USA) where the strut is coated by a single polymeric layer containing Paclitaxel, a cytostatic drug acting as mitotic inhibitor (Santin 2005, Barlis 2007, O'Brien & Carroll 2009). The use of first generation DES has resulted in improved restenosis rate in the short-term follow up analysis after PTCA. However, controversy arose related to the long-term benefit of the use of DES due to correlation with late thrombosis published in many studies (Santin 2005, Joner 2006, Barlis 2007, Jensen 2007, Somberg & Weinberger 2007, O'Brien & Carroll 2009, Singh 2010) as discussed further in the following sections.

Further developments have been attempted to improve the outcome and the technology of drug release from polymeric coatings of DES. The second generation of DES included the Everolimus-eluting Xience V (Abbott laboratories, Abbot Park, IL, USA) stent that showed promising results for short and long term use (O'Brien & Carroll 2009). More drug-delivery systems have been explored for the use in stent struts in order to optimize the delivery and obtain a better biocompatibility. Those included the use of biodegradable polymers for the coating or modification in the structure such as the use of microtextured stainless steel. Furthermore, the coating with nano-porous aluminium oxide and the delivery from macro reservoirs have been investigated (O'Brien & Carroll 2009). However, none of the most advanced devices have so far found a relevant clinical application as a valid alternative to the traditional bare-metal stents or to the first generation DES. Those, in fact, still represent the first choice in large scale surgical procedures due to the better cost-effectiveness of the treatment (O'Brien & Carroll 2009). The "Technology Appraisal 71" published by the National Institute for Health and Clinical Excellence (NICE) in October 2003 (NICE Technology appraisal 71, 2003) admitted the use of two types of drug-eluting stents represented by the Cypher (Sirolimus-eluting stent) and the Taxus (Paclitaxel-eluting stent).

The implantation of drug-eluting stents (DES) instead of the traditional bare metal stents (BMS) has commonly been adopted to reduce the occurrence of in-stent restenosis in patients at high risk of cardiovascular complications. Due to their relatively high cost, the technology appraisal 71 published within the NICE guidelines states that within the NHS the use of DES should be limited to the following cases:

- target artery less than 3 mm in calibre;
- lesion more than 15 mm long;
- more than one artery need stenting;

- treatment of myocardial infarction

1.3.2 In-stent restenosis

Although BMS implantation has widely improved the clinical outcome when compared to PTCA alone, the procedure still suffers complications in up to 35% of cases (Santin 2005, Singh 2010). The main impediment to the technique is as a result of a secondary occlusion inside the stent, a phenomenon termed in-stent restenosis (ISR). The histological analysis of restenotic stented arteries has demonstrated that neo-intimal growth represents the main mechanism responsible for the occurrence of *in-stent* restenosis rather than tissue remodelling or stent recoil as previously hypothesized (Moustapha 2001, Chung 2002, Farb 2002).

Different elements were shown to participate in favouring the development of neo-intimal tissue. Histological evaluation of neo-intimal growth showed that the increase in the extent of the arterial injury is directly correlated to an increase in neo-intimal proliferation. Consequently, an increase in the size of the strut can generate a bigger injury, in turn correlating to an increase in the restenosis rate (Farb 2002). Similarly, the same study demonstrated the direct correlation between penetration of the strut within the lipid core and the incidence of restenosis (Farb 2002). The depth of strut penetration has been therefore correlated to the degree of inflammation of the neointima, determinant factor of neo-intimal growth (Farb 2002). As a result, surgical techniques have been improved in an attempt to reduce ISR related to implantation injury (Santin 2005).

1.3.3 Features of the restenotic plaque

The individual features of the plaque associated with ISR have been described by numerous groups (Turley 2001, Bayes-Genis 2002, Chung 2002). It is generally

accepted that stent implantation is followed by clot formation which is normally reabsorbed within 12 days. During this phase neutrophils are recruited to the site of the lesion as a consequence of an increased release of chemokines and chemoattractant cytokines. It is the binding of platelets by these neutrophils which is thought to be responsible for the activation of the inflammatory response (Welt & Rogers 2002). The clot formation is followed by a thickening of the neointima. The histological evaluation of the new tissue has shown it to be characterized by the deposition of a proteoglycan (versican and hyaluronan)-rich extracellular matrix colonised with smooth muscle cells (SMC) and macrophages, a situation often associated with non-healing wound tissue (Bayes-Genis 2002).

The ECM of the restenotic plaque is comprised of collagen and glycosaminoglycans, such as hyaluronan (HA). In wound healing tissue it is the hyaluronan which mediates the interactions between the cells and the matrix to close the wound. Hyaluronan also traps water causing swelling, a possible contributing factor towards increased neointimal growth at the site of the lesion (Travis 2001). Together with its role in the proliferative and remodelling phases of restenosis (Toole & Tammi 2002), hyaluronan is also an important contributor to the first phase of inflammation where it favours cellular migration and the production of TNF-α, an important cytokine in macrophage maturation and activation (Boyce 1997). Histological evaluation of the neointimal tissue also supports a decrease in cellularity of the tissue over time. Indeed, samples retrieved after 18 months following implantation showed the prevalence of myoxid tissue with stellated-shaped smooth muscle cells scattered in a loose proteoglycan-rich ECM (Chung 2002, Santin 2005,).

1.3.4 Role of inflammatory cells and growth factors in in-stent restenosis

Inflammatory cells, in particular monocyte-derived macrophages, play a key role in the development of *in-stent* restenosis (Santin, 2005). They are present at the

site of the lesion during the early stage development and are thought to drive the inflammatory reaction via the secretion of different chemokines, cytokines and growth factors (Tashiro, 2001). Platelet derived growth factor (PDGF-BB) is one of the growth factors associated with ISR. It is secreted by different cell types including platelets, SMC, endothelial cells and macrophages, and is known to exert mitogenic and chemotactic stimuli on mesenchymal derived cells including SMC (Krettek, 2001), possibly contributing to the formation of the neointimal tissue. Transforming growth factor–beta (TGF-β1) is another important growth factor implicated in the formation and accumulation of ECM associated with ISR. More specifically it is involved in the synthesis of different ECM components, such as hyaluronan, through the stimulation of SMC (Chung, 2002).

The contribution of monocyte-derived macrophages to ISR is not only related to the activation of the inflammatory reaction through the release of cytokines and growth factors, as mentioned above. Indeed, recent studies have demonstrated that the cells also possess phenotypical plasticity under specific stimuli. In particular, it has been demonstrated that monocytes can express SMC-α-actin in vitro, indicative of a myofibroblast-like phenotype (Bayes-Geni, 2002). As described in section 1.1.4.3 myofibroblasts are collagen-forming cells which possess features of both SMC and fibroblasts, they form the main cellular components of the late neointimal tissue. As a result, the ability of macrophages to alter their phenotype to myofibroblast-like cells may be of great importance to the development of ISR. (Bayes-Geni 2002). Indeed, a recent study has confirmed the expression of SMC-α-actin in monocytes/macrophages with corresponding changes in morphology after one week of incubation on surfaces made of stainless steel (Stewart 2009). This has been further investigated by Dinnes et al (2007), who demonstrated macrophage plasticity and inflammatory state to be dependent on the surface chemistry of the substrate material. Indeed, the adaptation of the inflammatory cell response appeared to be achieved through cellular remodelling involving changes in intracellular and cytoskeletal structure (Dinnes 2007).

1.3.5 Bare-metal stents versus drug-eluting stents

The use of DES during PTCA has replaced BMS in complex scenarios such as bigger and longer lesions (≥20 mm), small vessels (diameter ≤ 2.5 mm) and in patients at major risk of developing restenosis such as people with diabetes or with a history of cardiac events (Yan 2008). Different studies have compared the outcome following implantation of the two types of stents. The benefit of DES in the treatment of patients with complications and in more complex lesions appear clear when considering the short-term follow up. Different studies have shown a reduction in the restenosis rate and in the need of a secondary re-vascularization when DES were implanted (Joner 2006, Barlis 2007, Jensen 2007, Somberg & Weinberger 2007, Patti 2008, Yan 2008, Singh 2010). The reduction of the rate of restenosis in native coronary arteries obtained with the use of DES compared to the use of BMS was calculated as up to the 70% (Singh 2010). However, the same studies showed controversial results concerning the long-term outcome of DES implantation. It seems, in fact, that the use of DESs can be accompanied by an increase in late stent thrombosis. The traditional BMS were affected by thrombosis at different stages following implantation but generally within one year after the procedure (Somberg & Weinberger 2007). Thrombosis after use of BMS can occur around the implant within 7 days following the procedure, at an early stage within 30 days or at a later stage within 1 year. The occurrence of thrombosis is in this case affected by the implantation technique and by the use of anti-platelet therapies. Only rarely thrombosis has occurred after one year following implantation in the case of bare metal stents (Somberg & Weinberger 2007). In the case of DES an increased rate of very late thrombosis (more than one year following implantation) was seen. The dispute concerning this data is still open as issues in terms of criteria of population selection and power calculations can affect those results (Barlis 2007, Jensen 2007, Somberg & Weinberger 2007, Patti 2008, Yan 2008, Singh 2010). However, a study demonstrated a delay in the arterial healing after implantation of DESs correlated

to a prolonged persistence of fibrin in the site of the lesion and prolonged incomplete endothelization of the same lesion (Jonsen 2006). This could represent a platform for the explanation of the long-term issues affecting the use of those devices. This is also confirmed by studies demonstrating the critical input of the anti-platelet therapy on the DESs implantation outcome. The outcome was in fact greatly improved by the addition of an anti-platelet drug (Clopidogrel) for at least 6 months following intervention. In more complex conditions the therapy needs extending for the year following implantation (Jensen 2007, Somberg & Weinberger 2007, Yan 2008).

Overall, the critical factors affecting the outcome of the stenting procedure are represented by the surgical procedure technique, the choice of appropriate size of the strut to be implanted and the appropriate anti-platelet therapy following intervention. The appropriate combination of those critical points has been shown to improve the clinical outcome independently from patient conditions (Ruygrok 2001, Ruygrok 2003).

1.3.6 In-stent restenosis and diabetes

As discussed in section 1.3.5, patients with diabetes are considered to be at a higher risk of developing ISR. When analysing the data following implantation of traditional bare metal stents the rate of restenosis affecting diabetic patients was between 41% and 70% (Kornowski 1997). This was shown to be correlated to the excessive intimal hyperplasia characterizing those patients (Kornowski 1997). The increased risk of developing ISR characterizing diabetes mellitus is in fact related to the promotion of proliferation of smooth muscle cells in the injured vascular area and to dysfunctions in the endothelium as a consequence of the hyperglycaemic condition (Patti 2008) as described in section 1.2.3.3. This is supported by recent data from a clinical study which highlights a correlation between the occurrence of ISR, metabolic syndrome and type 2 diabetes,

identifying this as a condition at particular risk of ISR (Kitoga 2008). Indeed, recent long-term data evaluating the cardiac outcome in patients with diabetes treated with DES emphasized the relevance of other risk factors such as age, treatment with insulin or hypoglycaemic agents, size and location of the lesions rather than the typology of implanted stent (Moses 2003, Kitoga 2008). However, many studies have demonstrated the improvement in the restenosis rate and consequent reduction in the necessity of intervening with a secondary revascularization within 6-12 months following the stent implantation in diabetes patients when DES were implanted in comparison to BMS (Abizaid 2003, Gilbert 2004, Kumbhani 2008, Patti 2008, Frobert 2009). In particular the RAVEL trial emphasized the ability of Sirolimus-eluting stents in reducing the neointimal hyperplasia in diabetic patients (Abizaid 2003). This has made of DES the stents of choice for the treatment of coronary occlusions in people with diabetes.

Restenosis in diabetic patients still represents an open challenge as they remain the population more affected by ISR (Frobert 2009). In addition, the evaluation of the overall cost-effectiveness of DES is still under debate (Greenberg 2004) thus reinforcing the interest in the understanding of the mechanisms of in-stent restenosis in diabetes particularly related to the use of traditional bare metal stents.

1.4 AIM OF THE STUDY

Restenosis remains an open challenge affecting the use of traditional bare metal stents particularly within the diabetic population. The controversies associated with the long term outcome of drug-eluting stents implantation and the attempts to improve the cost-effectiveness of the procedure ensure the interest in the use of bare metal stents.

Therefore, this study aims to investigate the molecular mechanisms leading to the adverse reaction to bare metal stent implantation and to the higher incidence of *in-stent* restenosis in patients with diabetes. This will be achieved by evaluating the inflammatory response of mononuclear cells in contact with stainless steel, material of choice for the production of traditional bare metal stents. The response of cells from different groups of donors will be assessed to determine whether the inflammatory reaction to foreign surfaces in people with diabetes is the cause of the increased *in-stent* restenosis.

This will be achieved by:

- Characterization of blood-derived inflammatory cell subpopulations from healthy donors and donors with diabetes to identify the predisposition of diabetic patients for increased inflammatory cell activation.

- Development of an *in vitro* model of diabetes to determine the effect of glucose and lipid concentrations on inflammatory cell response to stainless steel.

- Comparison of the experimental results to clinical data of recruited patients and to a clinical database.

CHAPTER 2

CHARACTERIZATION OF CELL SUB-POPULATIONS IN BUFFY COATS AND COMPARISON TO CLINICAL DATA IN THE DIABETIC POPULATION

2.1 INTRODUCTION

The deployment of cardiovascular stents has been widely adopted to improve the outcome of percutaneous balloon angioplasty, a common non-invasive surgical procedure performed to restore the lumen patency in occluded coronary arteries (Farb 2002, Moses 2003) as described in section 1.3.1. Vessel recoil and the formation of a secondary occlusion, known as restenosis, represent common complications of the procedure (Santin 2005). In particular, bigger and more complex lesions, small calibre vessels, calcified lesions and diabetes represent risk factors for the occurrence of restenosis (Ruygrok 2001, Farb 2002, Klein 2002, Ruygrok 2003, Barlis 2007). *In-stent* restenosis still affects the general outcome of angioplasty representing a complication leading to potentially fatal cardiovascular events such as myocardial infarction and to the necessity of secondary revascularisation (Moses 2003). Partial reduction in the incidence of *in-stent* restenosis has been achieved by improvements of the surgical procedure in order to reduce the stress on the blood vessel wall and to limit the penetration of the metal strut during implantation (Farb 2002, Santin 2005). The administration of antiplatelet agents such as Clopidogrel following implantation reduces the risks of thrombus formation, while cholesterol lowering drugs such as Statins protect from cardiovascular complications (Bunch 2002). However, *in-stent* restenosis still remains a challenge in the treatment of coronary artery occlusions by stent deployment.

2.1.1 Drug-eluting stents (DES) versus bare metal stents (BMS)

Different technological attempts to improve and develop new stents have been carried out over the last decades at the aim of reducing the impact of the stent implantation (for details see section 1.3.1.1). However, the most widely used and

studied stent devices are still represented by traditional bare metal stents (BMS), mainly produced with 316L stainless steel, and drug-eluting stents (DES) as described in sections 1.3.1.1 and 1.3.5. People with diabetes represent the major population at risk of cardiovascular diseases and prone to develop *in-stent* restenosis. The incidence of *in-stent* restenosis following implantation of BMS in diabetic patients is significantly higher than in people without diagnosed diabetes (Abizaid 2003, Gilbert 2004, Kumbhani 2008, Patti 2008, Frobert 2009). Indeed, the incidence of *in-stent* restenosis has been reduced since DES were chosen for the treatment of vessel occlusions in diabetic patients (Abizaid 2003, Gilbert 2004, Kumbhani 2008, Patti 2008, Frobert 2009).

Different meta-analyses have compared the clinical outcome of DES versus BMS based on follow-up data. Those studies showed a clear benefit in the deployment of DES compared to BMS particularly in the short and intermediate follow-up periods. The use of DES has led to a reduction in the incidence of myocardial infarction, cardiac events and the need for a secondary revascularization intervention (Barlis 2007, Jensen 2007, Mauri 2007, Yan 2008). However, data related to long-term benefits and in particular to the occurrence of late thrombosis, still remain controversial (Garg 2008). In fact, some studies showed an increased risk of late thrombosis after deployment of DES. However, it was hypothesised that the differences observed in the outcome may be related to differences in the pharmacological treatments following implantation in high-risk patients or to the methods adopted for the collection of data and the criteria applied (Jensen 2007).

2.1.2 Cell types involved in *in-stent* restenosis

In-stent restenosis is characterized by the deposition of a neointimal tissue around the stent strut characterized by a high content of a proteoglycan (versican and hyaluronan)-rich extracellular matrix colonised by smooth muscle cells (SMC)

and macrophages, a histological pattern often associated with non-healing wound tissue (Bayes-Genis 2002).

Inflammatory cells (neutrophils and macrophages) have been found infiltrating the thrombi deposited around the stent strut during the initial phases of healing following stent expansion. In addition, macrophages were found throughout all the stages of the neointimal formation whereby smooth muscle cells and myofibroblasts have been shown to populate the hyaluronan-rich neointimal tissue characterising the later stages of tissue formation (Santin, 2005). Understanding the origin of myofibroblasts in the restenotic tissues would therefore identify the cellular components directly involved in the development of the restenotic process.

The analysis of the neointimal tissue has shown that monocyte-derived macrophages are one of the cellular components playing a fundamental role throughout the whole restenotic process. They were in fact observed in association with smooth muscle cells that are responsible for the tissue deposition and of the vasculature contraction (Tashiro 2001, Santin 2005).

2.1.3 Cell types and markers

The distribution of cellular components in blood varies among individuals and in response to pathological conditions.

2.1.3.1 Monocytes and macrophages

Monocytes are part of the circulating mononuclear cells produced in the bone marrow from the progenitor common to neutrophils. They are released in the blood stream where they constitute 5-10% of the human leukocytes. Monocytes are represented by a heterogeneous population of cells that can vary in size, nuclear morphology and granularity (Gordon & Taylor 2005). They circulate in

the blood stream and under specific stimuli they migrate to peripheral tissues to differentiate into macrophages or dendritic cells (both taking part in the immune reaction) or into osteoclasts. Circulating monocytes are identified by the presence of different markers. In particular, CD14 is commonly recognised as the marker for circulating monocytes. It is in fact present on monocytes able differentiate into phagocytes after leaving the blood stream and on monocytes able to differentiate into different cellular components of the mesenchymal lineage as demonstrated in recent studies (Kuwana 2003, Varol 2009). Although CD14 remains expressed during different phases of the differentiation into macrophages, the expression of the marker is down-regulated in conjunction with their differentiation. The marker for activated macrophages is classically identified as CD68. CD68 is an 110KDa trans-membrane glycoprotein that is expressed at very low levels in most cell types, but it is highly-expressed in monocytes and tissue macrophages (Holness & Simmons 1993).

Monocytes and macrophages also express the common leukocyte antigen represented by CD45. This is a trans-membrane phosphatase expressed by all mature nucleated cells of the haematopoietic lineage, excluding erythrocytes and platelets (Dahlke 2004).

2.1.3.2 Endothelial progenitor cells.

Recent studies have focussed their attention on the characterisation of cells of the haematopoietic lineage expressing the marker CD34. This is a surface antigen expressed by all the haematopoietic and stem cells. CD34 is also expressed outside the lymphohaematopoietic system by vascular endothelial cells (Delia 1993). Recent studies have also demonstrated the presence of circulating endothelial progenitor cells positive for the marker CD34. Circulating immature cells of the haematopoietic lineage, derived from bone marrow, participate in the regeneration and repair of different tissues, not limited to the haematopoietic lineage (Fadini 2006). It has been hypothesized that those cells can be precursors

of endothelial cells participating in the tissue repair following endothelial injury and cardiac events. The amount of circulating CD34+ cells has in fact been seen to vary rapidly in consequence of cardiac events. Their amount seemed to be inversely proportional to the presence of cardiovascular risk factors (Fadini 2006). For these reasons the amount of circulating cells expressing CD34 has been identified as a potential useful indicator for cardiovascular events with applications for diagnostic or therapeutic purposes (Fadini 2006).

2.1.4 Diabetes, cardiovascular risk and *in-stent* restenosis

The report published by the World Health Organization (WHO) in 2006 and concerning the diagnosis of diabetes mellitus and intermediate hyperglycaemia declared that an estimated 171 million people worldwide were affected by diabetes mellitus in 2000 and the figure was predicted to increase to 366 million by 2030 (WHO 2006).

Despite the differences in the aetiology of the type 1 and type 2 diabetes as described in section 1.2.3, cardiovascular disease represent one of the major causes of mortality among the diabetic population. Studies have shown that the mortality among people with diabetes following myocardial infarction is significantly higher than in people without diabetes (Miettinen 1998). In fact they have a myocardial infarction risk levels similar to people without diabetes that have had a prior myocardial infarction.

The increased cardiovascular risk in people with diabetes has been traditionally connected to alterations in the vascular endothelium due to prolonged exposure to hyperglycaemic conditions (Peppa 2003, Price 2004, Goldin 2006). Hyperglycaemia has been traditionally identified as the major factor responsible for long-term complications of diabetes due to the formation of advanced glycated end (AGE) products (Peppa 2003). The increase in cardiovascular risk associated

with diabetes is the result of a more complex scenario. AGE products can accumulate in vascular tissues causing alteration in the function of endothelial cells, macrophages and smooth muscle cells together with interacting with AGE-binding molecules on cell surfaces and triggering pro-oxidising and pro-inflammatory events. AGE products also facilitate the oxidisation of LDL cholesterol favouring its deposition within the vessel wall and causing atheroma. This, in addition with the AGE-crosslinking within the arterial wall, causes vessels stiffening (Peppa 2003). The cardiovascular alterations associated with diabetes have also been shown to be accompanied by inflammation, leukocyte and immune cell activation and consequent increase in the release of pro-inflammatory cytokines (Hu 2001). In addition, AGE products can react with dendritic cells changing their phenotype and function and causing the immunological alterations characterising diabetes (Price 2004).

The close connection between diabetes and cardiovascular disease has in fact led to the development of the "common soil" hypothesis suggesting that diabetes and cardiovascular disease share common genetic and environmental circumstances, resulting from an underlying pathophysiological condition (Hu 2001). According to this theory common conditions and lifestyle habits would be the responsible for the development of alterations in metabolism resulting in increased cardiovascular risk and increase in the development of type 2 diabetes rather than one condition being the consequence of the other (Hu 2001).

In an interesting publication Wellen & Hotamisligil (2005) described the connection between inflammation, obesity and diabetes particularly demonstrating the close connection between the metabolic and immune system. Obesity is a low-grade inflammatory condition that leads to insulin-resistance and consequently to type 2 diabetes. The study showed in fact that a basic inflammatory condition favours a catabolic state suppressing anabolic functions, such as insulin signalling pathway, with the consequent reduction of action of insulin and occurrence of insulin-resistance (Wellen & Hotamisligil 2005). Overproduction of TNF-α, the

prevailing pro-inflammatory cytokine, was found in adipose tissue and muscle of obese patients. It was also demonstrated that macrophages accumulate in white adipose tissue of obese individuals where their function overlaps with adipocytes mediating the inflammatory response through the release of cytokines. Macrophages also mediate the formation of atheromas, storing lipids and turning into atherogenic foam cells. Co-localisation of macrophages and adipocytes is not the only mechanism justifying the inflammatory condition connected to obesity. Obesity is in fact correlated to endoplasmatic reticulum stress with the consequent overproduction of reactive oxygen species from mitochondria and activation of the inflammatory cascade (Wellen & Hotamisligil 2005).

2.2 AIMS

Clinical success has been achieved by replacing bare metal stents with drug-eluting stents in complex arterial lesions and in subjects suffering with diabetes. However, the controversial opinions on the long-term outcomes and the attempt to improve the balance of cost-benefits have raised interest in exploring the biomolecular mechanisms responsible for *in-stent* restenosis correlated to the use of traditional stents made of stainless steel. In particular, the work described here focused on the investigation of the role of monocyte-derived macrophages, which play a central role throughout all the phases of the restenotic process.

The work described in this chapter aimed to verify the predisposition of diabetic patients to inflammatory cell activation, paving the way to a better understanding of the increased *in-stent* restenosis occurrence in diabetes. This was achieved through:

- Characterization of the sub-populations forming the fraction of circulating mononuclear cells in healthy donors and donors with type 1 or type 2 diabetes.
- Assessment of the potential links between cell sub-population patterns and biochemical blood parameters obtained from blood tests.

2.3 MATERIAL AND METHODS

2.3.1 Recruitment of volunteers and blood collection

2.3.1.1 Recruitment criteria and procedure

Non diabetic control subjects were recruited from staff and students at the University of Brighton or from non-diabetic people accompanying diabetic donors at the time of attending the weekly diabetes clinic at the Royal Sussex County Hospital (Brighton, East Sussex). Ethical approval was obtained respectively from the Pharmacy and Biomolecular Sciences Ethics Committee at the University of Brighton and from the Brighton West Research Ethics Committee of the NHS (reference number 07/Q1911/40). The ethical approval from the Brighton West Research Ethics Committee of the NHS (reference number 07/Q1911/40) was also obtained for the recruitment of donors with diabetes attending the weekly clinic for diabetes at the Royal Sussex County Hospital (Brighton, East Sussex). In order to obtain approval standard operating procedure and donor information leaflets were produced (Appendix 1).

Control subjects were selected among healthy adults (18-60) (total of n=12) to represent a source of mononuclear cells not chronically exposed to elevated blood glucose level or conditions affecting their response to foreign materials. For this reason the exclusion criteria applied in the recruiting process were a diagnosis of diabetes or metabolic syndrome, the presence of chronic inflammatory diseases or

diseases affecting the immune system, the use of immunosuppressor or cytostatic drugs and the presence of current or previous morbidities involving the cardiovascular system.

Donors with diabetes were recruited among the patients attending the weekly diabetes clinic at the Royal Sussex County Hospital and divided into two groups:

- Subjects with type 1 diabetes (T1) (total of n=13)
- Subjects with type 2 diabetes (T2) (total of n=12)

In order to standardize the response of mononuclear cells, people with chronic inflammatory or autoimmune diseases, individual using immunosuppressant or cytostatic drugs, subjects with diseases affecting immune response and cancer were excluded from the study. Clinical data of the patients were obtained from the hospital database, stored and used anonymously. The following clinical data were collected from the Royal Sussex County Hospital database: serum creatinine to assess kidney functions, total cholesterol, glycated haemoglobin (Hb1Ac) and blood pressure. General information such as height and weight, personal and family clinical history, and medications were collected through a questionnaire that donors were asked to complete immediately before blood collection.

The data were then anonymized and stored in password-locked computers at the University of Brighton in compliance with the Ethics regulation and the Human Tissue Act.

2.3.1.2 Collection and treatment of the blood

After obtaining informed consent, 30ml of blood was collected by venipuncture in heparinised tubes (Greiner Bio-One Ltd; cat number 455051) and treated within three hours according to Boyum's method (Boyum 1968). This technique consists of a centrifugation (400xg for 30 min) on polysucrose gradient (Histopaque 1077– Sigma-Aldrich; cat 10771) in 15ml polypropylene tubes (Fisher Scientific, UK) to separate blood components into different layers as described in previous studies

(Boyum 1968). To optimize the outcome of the separation process 6 ml of blood was gently overlaid on 3 ml of Histopaque-1077 and the tubes were spun (400xg for 30 minutes) shortly afterwards to avoid spontaneous precipitation of the blood within the gradient. The spinning resulted in the formation of four different layers. Red blood cells and granulocytes precipitated at the bottom of the tube forming a dense layer overlaid by the Histopaque. The top layer was formed by platelet-rich-plasma (PRP). At the interface between plasma and Histopaque layers an opaque layer representing the buffy coat composed chiefly of mononuclear cells (lymphocytes and monocytes) formed. PRP and the buffy coats were gently collected using Pasteur pipettes, transferred to clean tubes and used for the experiments. Buffy coats were washed three times by adding 8ml of sterile Phosphate Buffered Saline solution (PBS) followed by a spinning at 250xg for 15 minutes. Final mononuclear cells pellets were suspended in 1 ml of Dulbecco's Modified Eagle's Medium (DMEM; PAA Laboratories or Sigma Aldrich) at physiological concentration of glucose (1000 mg/L) added with 10% Foetal Bovine Serum (FBS; PAA Laboratories) and Penicillin/Streptomycin (PAA Laboratories), and cells were counted.

2.3.2 Flow cytometry

2.3.2.1 Principles of the technique

Flow cytometry is a powerful technique for counting and examining microscopic particles resulting from the combination of immunostaining with light scattering and spectrometry (Brown 2000). Modern polychromatic equipment allow for conducting a multiparametric analysis of the physical and chemical characteristics of up to thousands of particles per second (Perfetto 2004). Following staining after incubation with fluorophore-tagged antibodies binding to specific cell markers, cell mixtures are suspended in a stream of isotonic fluid forming a laminar flow. This ensures that cells pass individually through the interrogation

point represented by an electronic detection apparatus (Perfetto 2004). Commonly a beam of light (usually laser light) of a single wavelength is directed onto the stream of fluid and the light is scattered by the particles whilst fluorescence is simultaneously emitted by the fluorophores attached to the same particles. Modern apparatus contain up to four different lasers emitting at different wavelengths allowing measurement of up to nineteen different parameters within the same sample (Perfetto 2004). The physical properties of the particles in each sample can be determined through the combined evaluation of the size and of the internal complexity provided by the detection of signals respectively from forward side scatter (FSC) and side scatter (SSC). The simple morphological characterization can be sufficient to distinguish among two different cell populations (Brown 2000). The addition of specific fluorophore-tagged antibodies allows the identification of specific cellular markers and consequently of cell sub-populations as widely used in haematology (Brown 2000). Scattered light and fluorescence are collected by a complex detection system, and the signal is transferred to and analysed by the electronic interface. In particular, a number of detectors are aimed at the point where the stream passes through the light beam. A detector is in line with the light beam (FSC) and several detectors are positioned perpendicular to it (SSC). Those are combined with fluorescent detectors specific for each emission wavelength in order to selectively measure the emission of every fluorochrome. The photomultiplier unit of the detection system is composed of dichroic mirrors that reflect and transmit photons and are coupled to filters to further selected the emission wavelength (Perfetto 2004). Each suspended particle passing through the beam scatters the ray and fluorescent chemicals found in the particle or attached to the particle may be excited into emitting light at a longer wavelength than the light source. FSC correlates with the cell size and SSC depends on the inner complexity of the particle and its morphology (Brown 2000). Different control steps are needed when obtaining flow cytometric measurements with the polychromatic machines. One of the most relevant issues is represented by the background fluorescence mainly generated by the natural autofluorescence

of cells. This can be overcome by conducting a preliminary titration experiments to determine the best concentration of antibody providing the best positive fluorescent signal versus background (Perfetto 2004). Another issue can be related to the overlapping in the spectral emission of fluorochromes. This is generally corrected by a step known as "compensation" and represented by the application of a mathematical deconvolution deducting the unspecific emission due to spectrum overlapping from the specific fluorochrome-related emission in order to ensure proportionality between fluorescent signal and dye (Perfetto 2004). In modern polychromatic machines the compensation is calculated by the software associated to the flow cytometer after collecting the fluorescence for each fluorochrome from sample prepared by adding the labelled antibodies to standard microbeads supplied by the companies (Perfetto 2004, Perfetto 2006).

2.3.2.2 Limitations of the technique

Flow cytometry represents an advanced and precise technique widely used for the characterization and quantification of cell populations. The appropriate selection of markers and the use of modern multiparametric equipment have allowed the simultaneous detection of different parameters and subpopulations. The advanced technology characterizing the modern machines has improved the outcome of the analysis by reducing unspecific signals and the variability of the results and their interpretations. However, limitations can still derive from the weakness of the signal of the fluorochrome binding the antibody or affecting the signal once the antibody is binding the marker. This could potentially affect the analysis of populations scarcely represented in the original samples. Cell loss occurring during the isolation process could also affect the quantification obtained with flow cytometry. Consequently the quantification of cell populations does not represent the total amount in the whole blood but exclusively the percentage in the test tubes.

2.3.2.3 Characteristics of the instrument

Flow cytometry was performed using the LSR II flow cytometer (Becton, Dickinson and Company Biosciences, USA) within the laboratories of the Brighton and Sussex Medical School (Brighton, UK) and data collected and analysed. Data were analysed using the software FlowJo-Flow cytometry data analysis (Tree Star Inc., USA). LSR II is a bench polychromatic flow cytometer able to analyse up to nineteen parameters using four fixed-aligned air-cooled lasers. In particular there are three solid-phase lasers emitting in the blue (20mW at 488 nm; Coherent Sapphire), in the violet (25mW at 405 nm; Coherent VioFlame PLUS) and in the UV (20mW at 355 nm; Lightwave Xcyte) regions of spectrum. In addition to solid phase lasers a Helium/Neon laser (18 mW at 633 nm; HeNe) allows the detection of a broader range of dyes. The collection optics consist of octagon and trigon optical arrays each able to collect emission at different colours.

2.3.2.4 Selection of antibodies

Markers were chosen in order to obtain a complete characterization of the cell subpopulations extracted with the centrifugation on Histopaque-1077 gradient focusing in particular on the cell types participating in the restenotic process and involved in the inflammatory response to foreign body. In particular, the selected antibodies were the following: CD3 (T lymphocytes), CD19 (B lymphocytes), CD14 (Monocytes), CD68 (Activated macrophages), CD45 (General marker for leukocytes), CD34 (Haematopoietic and endothelial progenitor cells).

The working dilution for each antibody as listed in table 2.1 was determined through an initial titration experiment by labelling cells with increasing concentration of antibody and evaluating the optimal response. In addition, suggestions from manufacturers were taken into account to determine the optimal working dilutions.

Antibody mixtures were prepared by combining three different antibodies in each tube. This was made possible by the selection of antibodies that were conjugated to three fluorochrome molecules emitting at different wavelengths. This permitted the optimization of the outcome of the analysis by increasing the number of samples tested with the limited amount of cells available after collection of buffy coats. The triple-staining technique also enabled the identification of the co-expression of markers and related cell sub-populations as described in chapter 3.

Table 2.1 List of antibodies and their dilutions used for cell identification in flow cytometry experiments.

Cells identification	**Marker**	**Dilution**	**Antibody**
Leukocytes	CD45	0.1 μg/1x10^6 cells	PE/Cy5-conjugated anti-hCD45 Immunotools GmbH
Haematopoietic and endothelial progenitor cells	CD34	0.1 μg/1x10^6 cells	PE-conjugated anti-hCD34 Immunotools GmbH
T Lymphocytes	CD3	0.1 μg/1x10^6 cells	PE/Cy5-conjugated anti-hCD3 Immunotools GmbH
B Lymphocytes	CD19	0.1 μg/1x10^6 cells	PE-conjugated anti-hCD19 Immunotools GmbH
Monocytes	CD14	0.1 μg/1x10^6 cells	FITC-conjugated Anti-hCD14 Immunotools GmbH
Activated macrophages	CD68	1 μg/1x10^6 cells	FITC-conjugated anti-hCD68 Santa Cruz Biotechnology, Inc.
Smooth muscle cells	α-actin	0.25 μg/1x10^6 cells	PE-conjugated anti-h-α-smooth muscle cells actin R&D Systems

The antibodies were combined as follows:

- CD3-PECy5,CD19-PE,CD14-FITC;
- CD3-PECy5, CD19-PE, CD68-FITC;
- CD45-PECy5, CD34-PE, CD14-FITC;
- CD45-PECy5, CD34-PE, CD68-FITC

2.3.2.5 Preparation of cells

Buffy coats collected as described in section 2.3.1.2 from a total of 21 donors (7 per each group) were analysed for the expression of the markers listed in table 2.1.

Pellets of cells isolated according to the Boyum's were re-suspended in physiological glucose concentration (1000mg/L) DMEM (PAA Laboratories) containing 10% FBS (PAA Laboratories) and penicillin/streptomycin (PAA Laboratories) at a final concentration of $5x10^6$ cells/ml. $2x10^6$ cells from the suspension (400µl) were transferred to each BD FACS 5ml round bottom tubes and prepared for flow cytometry by initially incubating cells in a 20mM solution of EDTA in washing buffer (0.1% sodium azide and 0.5% BSA in PBS) for 10 minutes at 37^{o}C. EDTA was added as a chelating agent in order to obtain a single cell staining suspension. After a washing step with washing buffer followed by a centrifugation step at 400xg for 8 minutes at 4^{o}C, cells were incubated for 30 minutes at 4^{o}C in the dark with the antibody mixtures (as detailed in paragraph 2.4.2.3). A total of 100µl of antibody mixture solution was added to the pellets of cells. Cells were then briefly incubated in BD FACS lysing solution (BD Biosciences, USA; cat 349202) followed by further washing steps. The lysing solution is used to eliminate residues of red blood cells from the samples. However, it has been demonstrated that lysing solution has permeabilizing properties on leukocytes membranes (Tiirikainen 1995). In the case of intracellular markers cells were further permeabilized with a short incubation step

in BD FACS permeabilizing solution 2 (BD Biosciences, USA; Cat 340973). After the last washing steps supernatants were decanted from the tubes and cells stored overnight at 4^{o}C in the dark before acquiring the data.

2.3.2.6 Negative control and criteria for the selection of the desired population

Prior to each reading session a negative control represented by cells without the addition of antibodies was tested in order to exclude the non-specific natural autofluorescence and optimise the deduction of the background fluorescence. Regular readings of microbeads (Compbeads-Beckton, Dickinson, USA) labelled with the antibodies selected for the experiments were obtained in order to perform the correct compensation of the fluorescence. The results were expressed as percentage of the population positive for the specific fluorochrome over the total amount of particles counted in the tube.

Before proceeding with the acquisition of the final results, preliminary steps for the selection of the appropriate gate were applied. The gating strategy was at first based upon morphological characterization of the population. The morphology was analysed comparing size of the particles as recorded by the FSC with the internal complexity of the particles recorded from the SCC as shown in figure 2.1a. This step is followed by a more restricted selection to eliminate the wider peak detected with the FSC in order to exclude cell aggregates that would affect the number of positive events counted in the experiment (Figure 2.1b).

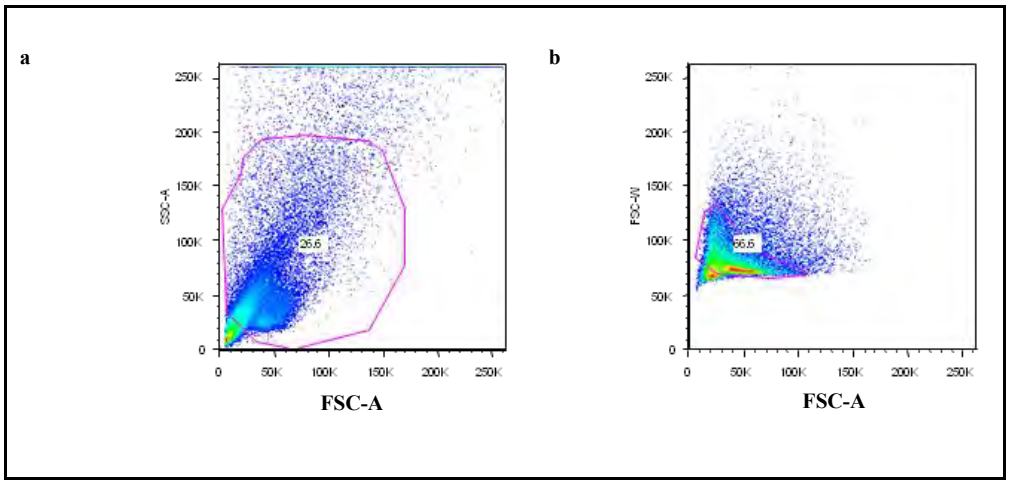

Figure 2.1 Example of the applied strategy for the selection of the population during flow cytometry analysis*. The first step of the selection of the gate (gating strategy) was based upon morphological criteria such as cells size and complexity (Fig. 2.1a). The second step was based on the exclusion of wide-peak signals in order to exclude cells aggregates (Fig. 2.1b).*

Negative controls were prepared before each reading in order to test the background fluorescence. Cells for negative controls were treated with all the steps of the staining protocol omitting the addition of the specific antibodies. Diagrams showed the influence of background noise due to unspecific fluorescence as represented in figure 2.2.

2.3.2.7 Statistical analysis

The distribution of data obtained from flow cytometry on the buffy coats was analysed with Minitab and was found to be not normal for most of the populations, thus requiring the application of non-parametric statistical analysis. The significance among groups was therefore verified by using Mann-Whitney test in Minitab 16 and results expressed as median value followed by the range of values.

Differences between clinical data from donors were analysed using t-test in Minitab 16 and results expressed as average ± standard error.

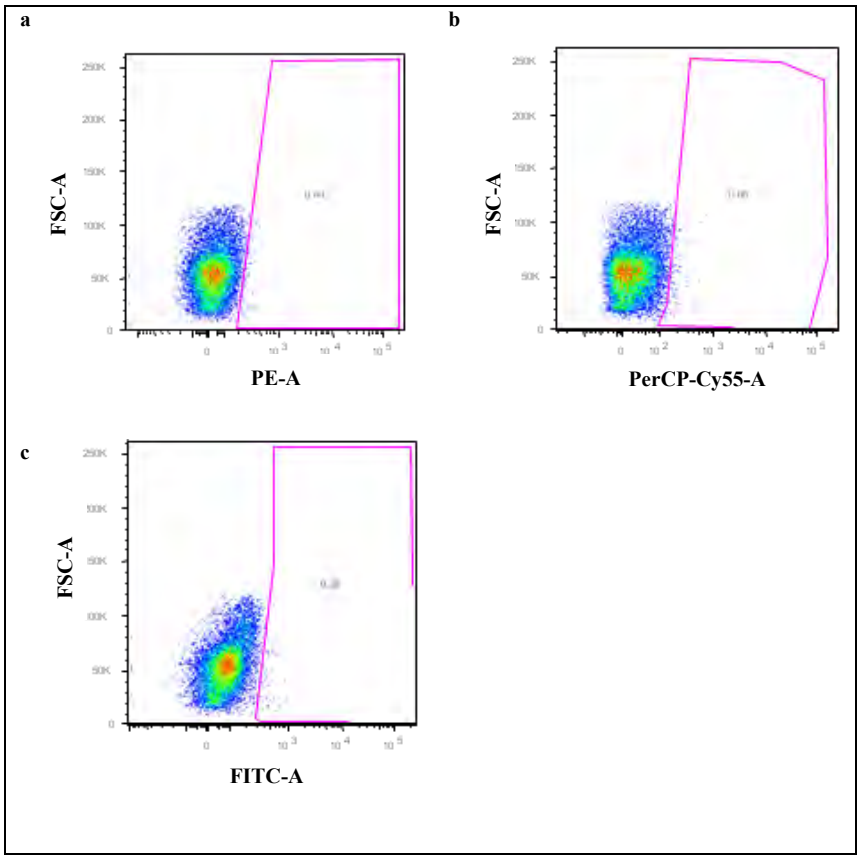

Figure 2.2 Example of readings obtained from negative controls on three different channels. *The diagrams show the signal due to background noise and related to unspecific fluorescence generated by unlabelled cells from the buffy coats on the channel for PE (fig. 2a), for PerCPCy55 (fig. 2b) and for FITC (fig. 2c).*

2.4 RESULTS

The analysis of the data provided information about the individual distribution among donors and a general comparison of the sub-population distribution among the three cohorts of donors. Table 2.2 shows the results obtained from flow cytometry on seven donors from each group. Significance was verified with Mann-Whitney test for non-parametric distribution using Minitab 16 and the

results for each group were expressed as median value followed by the range of the values (minimum and maximum values recorded) (table 2.2).

2.4.1 Lymphocytes

The flow cytometric analysis in this study revealed the presence of both T lymphocytes and B lymphocytes in buffy coats from the donors (table 2.2). Charts in figure 2.3 show the morphological homogeneity across the cohorts of the population identifying T lymphocytes. The median values of the total amount of T lymphocytes in the buffy coats was similar across the three cohorts ranging from 1.5% in buffy coats from control subjects to 2.5% in donors with type 1 diabetes and to 1.4% in donors with type 2 diabetes (table 2.2). No significant differences were found between the groups. Furthermore, variability among donors was observed as shown by the wide ranges recorded particularly from donors with diabetes (table 2.2) and represented in figure 2.4.

The amount of B lymphocytes detected with flow cytometry was consistent among donors and sub-groups (table 2.2; figure 2.5). The median values of the total amount of cells expressing the marker for B lymphocytes (CD19) was 0.4% in control subjects (table 2.2), 0.8% in donors with type 1 diabetes (table 2.2) and 0.4% in donors with type 2 diabetes (table 2.2). Even analysing the distribution across donors from the three cohorts the amount was consistent (figure 2.5) and in every case below 5% (figure 2.5).

Table 2.2 Distribution of cell populations in buffy coats across donors (n=7 per cohort). The quantification of cell sub-populations obtained from flow cytometry of buffy coats extracted from the three cohorts of donors (control, type 1 and type 2 diabetes) is expressed as percentage of the cells positive for the selected marker on the total amount of cells counted in each tube. The values in the table are expressed as median value among the group and range (minimum-maximum) values from the same group. The statistical analysis was done applying Mann-Whitney test in Minitab 16 which showed that the amount of activated macrophages (CD68+), highlighted in the table, was significantly higher (p=0.0215) in buffy coats from donors with type 1 diabetes than in buffy coats from control subjects.

		Median values of the distribution of cell sub-populations and ranges of values within the groups (Percentages)		
Marker	**Cells Identification**	**Control (n=7)**	**Type 1 Diabetes (n=7)**	**Type 2 Diabetes (n=7)**
CD3	**T Lymphocytes**	**1.5%** 0.2-3.5	**2.5%** 0.7-11.2	**1.4%** 0.3-30.8
CD19	**B Lymphocytes**	**0.4%** 0.2-2.6	**0.8%** 0.12-2.3	**0.4%** 0.1-3.6
CD14	**Monocytes**	**12.4%** 9.6-23.38	**13.3%** 2.8-36.6	**13.2%** 7.4-20.0
CD68	**Activated macrophages**	**1.5%** 0.53-1.8	**5.4%** 0.7-32.6	**0.4%** 0.27-9.19
CD34	**Endothelial progenitor cells**	**0.3%** 0.0-0.6	**0.4%** 0.1-0.74	**0.6%** 0.1-12.0
CD45	**Leukocytes**	**5.6%** 0.3-24.8	**12.5%** 6.5-34.0	**23.5%** 2.5-94.5

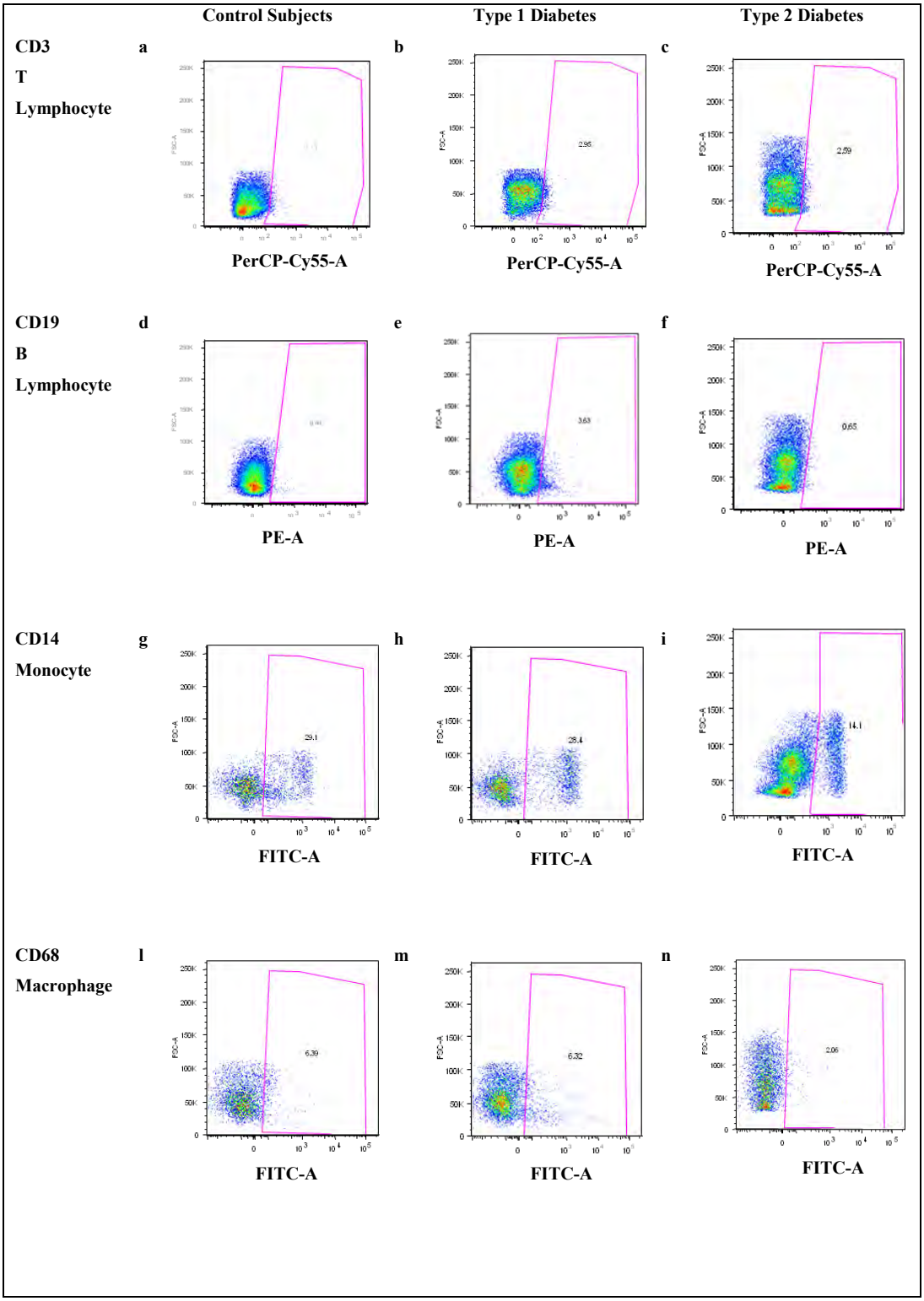
Control Subjects
Type 1 Diabetes
Type 2 Diabetes
CD3
T
Lymphocyte
a
b
c
PerCP-Cy55-A
PerCP-Cy55-A
PerCP-Cy55-A
CD19
B
Lymphocyte
d
e
f
PE-A
PE-A
PE-A
CD14
Monocyte
g
h
i
FITC-A
FITC-A
FITC-A
CD68
Macrophage
l
m
n
FITC-A
FITC-A
FITC-A

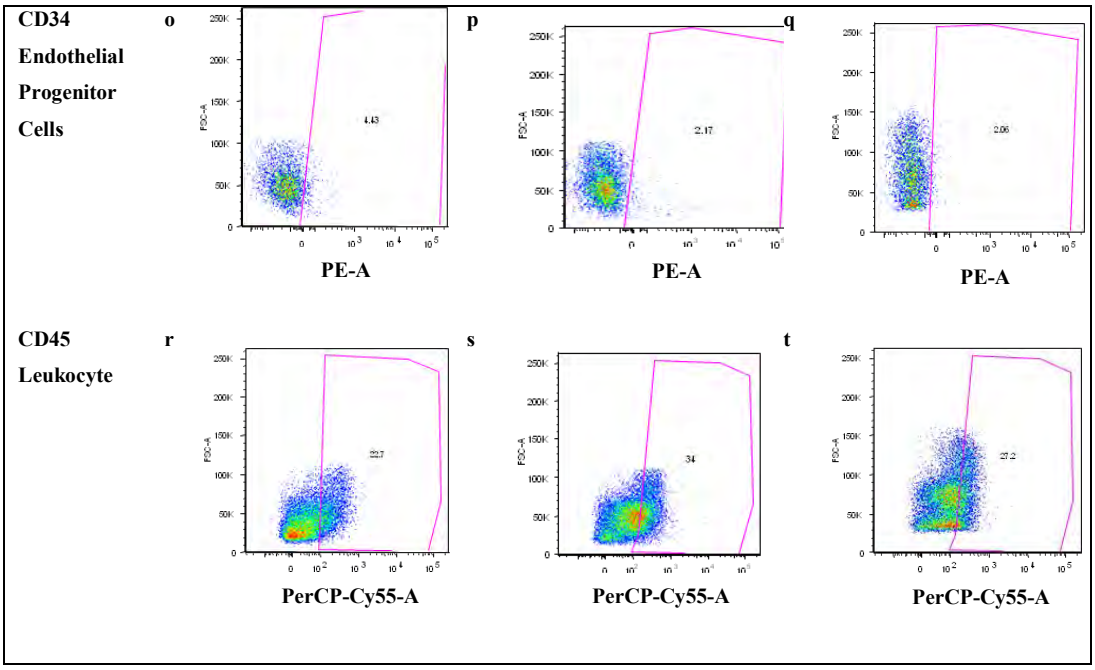

Figure 2.3 Flow cytometry identified the presence of different cell sub-populations in buffy coats from all the donors. *The figure shows the representation of flow cytometric analysis of buffy coats extracted from one donor per each cohort. The selection of the population positive to the marker of interest is contained within the pink line and it is represented by signals shifted from the "core" population along the selected channel correspondent to the different fluorophores (PE-, PerCP-Cy55 and- FITC-).*

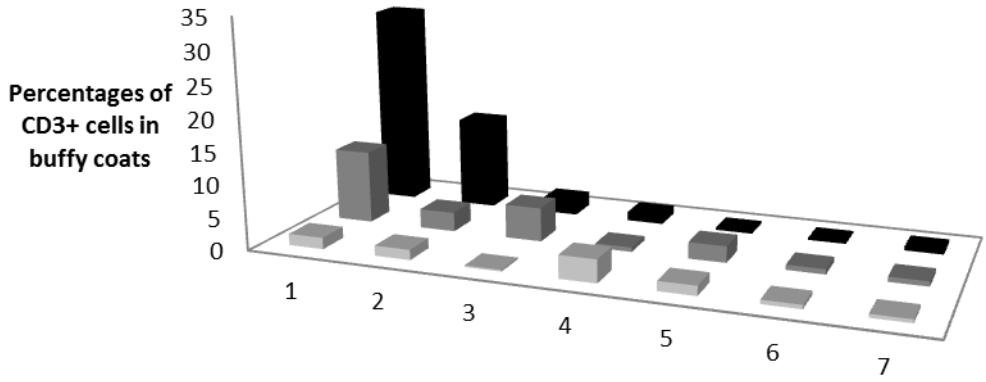

Donors	1	2	3	4	5	6	7
Control	1.8	1.6	0.2	3.5	1.5	0.6	0.5
Type 1 Diabetes	11.2	3.0	5.2	0.7	2.5	0.8	0.8
Type 2 Diabetes	30.8	13.9	2.2	1.4	0.3	0.3	0.6

Figure 2.4 The amount of T Lymphocytes (cells positive to CD3) in buffy coats was variable among donors with diabetes (n=7). *The diagram illustrates the variations in the amount of circulating cells positive to CD3 (marker for T Lymphocytes) expressed as percentage of cells positive to CD3 on the total amount of cells counted in each tube as obtained by flow cytometry. The figure shows that there was a greater individual variability in the number of T lymphocytes among donors with type 1 diabetes (dark grey columns) and in donors with type 2 diabetes (black columns) compared to donors in the control group (light grey columns).*

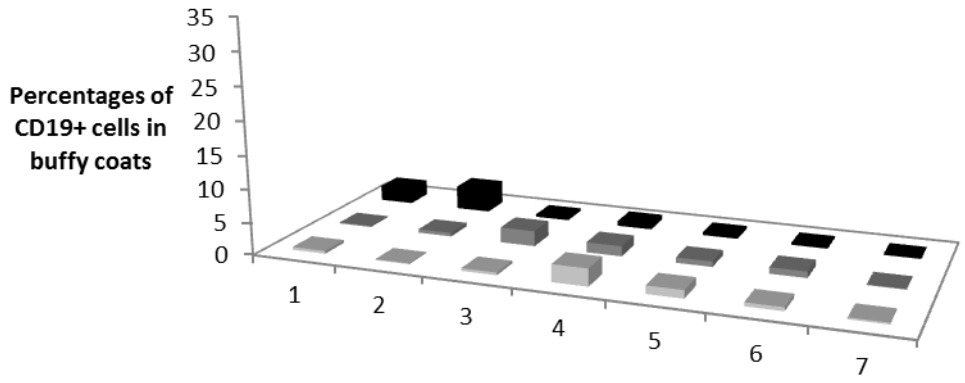

Donors	1	2	3	4	5	6	7
Control	0.4	0.1	0.4	2.6	1.2	0.6	0.3
Type 1 Diabetes	0.2	0.5	2.3	1.5	0.8	1.0	0.1
Type 2 Diabetes	2.4	3.6	0.4	0.8	0.4	0.3	0.1

Figure 2.5 The amount of B Lymphocytes (cells positive to CD19) in buffy coats was consistent across donors (n=7). *The flow cytometric analysis provided the amount of cells positive to CD19 (marker for B Lymphocytes) expressed as percentage of cells positive to CD19 on the total amount of cells counted in each tube. The figure shows that the amount of B lymphocytes in the analysed Buffy coats was consistent across the donors in each group and across the three cohorts. The total amount was consistently <3.6%.*

2.4.2 Leukocytes and monocytes/macrophages

The general marker for leukocytes (CD45) was used to identify the overall population of white blood cells obtained through the isolation method. The results obtained were extremely variable across samples. The median values of the total amount of cells positive for CD45 ranged from 5.6% in control subjects, to 12.5% in donors with type 1 diabetes and to 23.5% in donors with type 2 diabetes (table 2.2). Donors with diabetes, particularly with type 2, showed the widest variability ranging from 2.5% to 94.5% (table 2.2). The amount of total leukocytes isolated in the buffy coats through a single centrifugation on poly-sucrose gradient can

vary due to the isolation technique (Almeida 2000) in correlation with the variability in the amount of lymphocytes. Further purification steps or advanced technique of cell sorting coupled to flow cytometry are commonly used to purify the population obtained from the Boyum's method. This can partially explain the variability of the amount of CD45+ found in different samples. Analysis of the results also showed that in the more recent experiments the amount of CD45+ seemed to decrease progressively suggesting the degradation and loss of the signal from the antibody used (data not shown). For these reasons the amount of CD45 cannot be used for quantitative determinations but it provided sufficient information for the characterisation of sub-populations where the marker was co-expressed with other markers as described in chapter 3.

CD14 was used as marker for the identification of monocytes (Kuwana 2003). The median values of the total amount of monocytes (CD14+) in the test tubes was variable across individuals (figure 2.6) but the average consistent across groups, this being represented by 12.4% in the control subjects, 13.3% in donors with type 1 diabetes and 13.2% in donors with type 2 diabetes (table 2.2). Diagrams obtained from the three cohorts of donors (control in figure 2.3g; type 1 diabetes in figure 2.3h; type 2 diabetes in figure 2.3i) showed the homogeneity of the morphology of populations.

Median values of the total amount of activated macrophages (CD68 positive) within buffy coats from donors with type 1 diabetes was higher (5.4%) than the value in controls (1.5%) and in donors with type 2 diabetes (0.4%) as shown in table 2.2. The statistical analysis using Mann-Whitney test for non-parametric distribution revealed a significant difference ($p=0.0215$) between the total amount of CD68+ cells in buffy coats from control subjects compared to buffy coats from donors with type 1 diabetes.

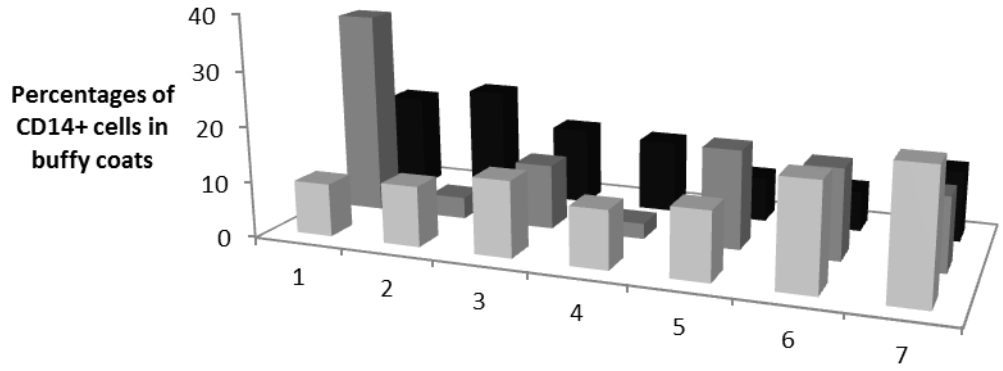

Donors	1	2	3	4	5	6	7
Control	9.6	10.9	13.8	10.6	12.4	19.2	23.4
Type 1 Diabetes	36.6	3.9	11.7	2.8	17.8	16.4	13.3
Type 2 Diabetes	17.5	20.0	14.1	13.2	8.1	7.4	12.8

Figure 2.6 The amount of monocytes (cells positive to CD14) in buffy coats was variable across donors (n=7). *The flow cytometric analysis provided the amount of cells positive to CD14 (marker for monocytes) expressed as percentage of cells positive to CD14 on the total amount of cells counted in each tube. The figure shows the variability of CD14+ cells across donors.*

The significant difference between the values obtained from the groups was maintained, although reduced, even when the unusually high result obtained from donor A with type 1 diabetes (32.6%) was removed (p=0.045). The recruited healthy control subjects showed a consistent percentage of activated macrophages that was always below 1.8% (figure 2.7). The percentage of CD68 positive cells among donors with type 1 diabetes ranged between 0.7% and 32.6% (table 2.2), particularly being over the 2% in all of the donors except for one (figure 2.8). In donors with type 2 diabetes the amount of CD68+ cells ranged between 0.16% and 9.19% (table 2.2; figure 2.7). In particular, all the donors with type 1 diabetes except for one showed an amount of activated macrophages (CD68+) in buffy coats higher than the median value of the amount of CD68+ in buffy coats from

control subjects (1.5%). Within the group of donors with type 2 diabetes only three showed an amount of CD68+ higher than 1.5% (figure 2.7).

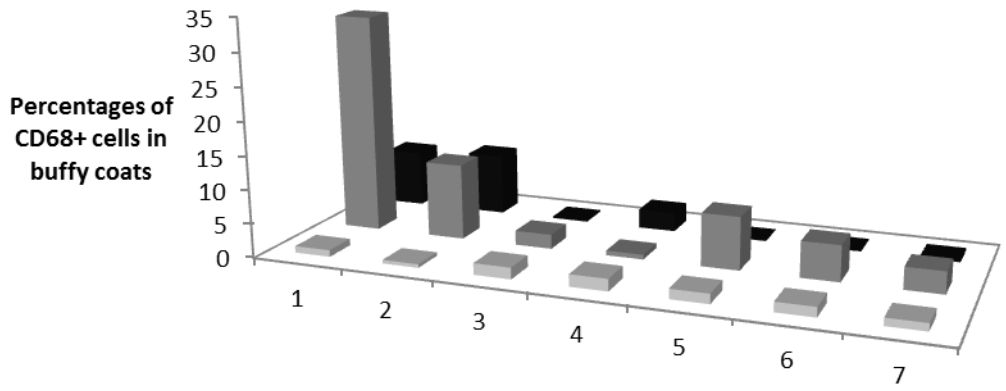

Donors	1	2	3	4	5	6	7
Control	1.0	0.5	1.7	1.8	1.5	1.5	1.1
Type 1 Diabetes	32.6	11.3	2.2	0.7	7.9	5.4	3.3
Type 2 Diabetes	8.5	9.2	0.3	2.9	0.2	0.2	0.4

Figure 2.7 The amount of activated macrophages was consistent in buffy coats from control subjects and variable in buffy coats form donors with diabetes (n=7)*. Results show that control subjects the amount of activated macrophages (expressing CD68) was generally low and consistent among the group except from one donor. Donors with diabetes showed a wide variability in the amount of circulating activated macrophages.*

2.4.3 Endothelial progenitor cells

The median value of total amount of cells responding positively to CD34 was similar in buffy coats collected from donors with type 2 diabetes (0.6%), from control subjects (0.3%) and from donors with type 1 diabetes (0.4%) (table 2.2). However, a great variability among donors with type 2 diabetes was found (figure 2.8). Results showed that among control subjects and donors with type 1 diabetes the amount of cells positive to CD34 was consistent, representing less than the

0.8% of events in the test tubes. In two of the donors with type 2 diabetes the amount of cells positive to CD34 was particularly high representing the 8.09% and the 12% of the total amount of events counted in the test tubes (figure 2.8).

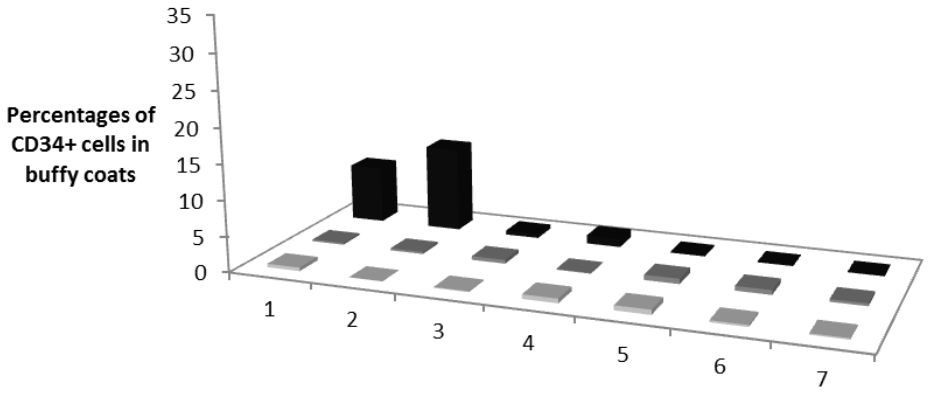

Donors	1	2	3	4	5	6	7
Control	0.5	0.0	0.1	0.6	0.7	0.3	0.2
Type 1 Diabetes	0.2	0.3	0.5	0.1	0.7	0.7	0.4
Type 2 Diabetes	8.1	12.0	0.6	1.2	0.2	0.1	0.1

Figure 2.8 The amount of endothelial progenitor cells was low in buffy coats from most donors. Different trend in donors with type 2 diabetes (n=7). *Results showed that in buffy coats from control subjects and donors with type 1 diabetes the amount of cells positive to CD34 (endothelial progenitor cells) was consistent and always below the 0.7% of events. Different trend was observed among donors with type 2 diabetes showed a bigger variability.*

2.4.5 Biochemical blood results

Donors with diabetes were recruited among patients attending the weekly diabetes clinic at the Royal Sussex County Hospital in Brighton and Hove (East Sussex). After obtaining informed consent, patients were asked to fill in a brief questionnaire (see appendix 1) about their general health condition, particularly providing their height and weight in order to calculate their Body Mass Index (BMI). Biochemical blood test results were also collected from the hospital

database as described in paragraph 2.3.1.1. Table 2.3 shows the summary of the donors clinical data obtained compared to the amount of activated macrophages (positive to CD68) and endothelial progenitor cells (positive to CD34) in their buffy coats .

The group of the recruited patients with type 2 diabetes was on average significantly older than patients with type 1 diabetes ($p<0.01$) and on average their BMI (29.86±1.81 Kg/m^2) was significantly higher ($p<0.05$) than the BMI of donors with type 1 diabetes (24.81±0.92 Kg/m^2) (table 2.3). In particular, the average of the BMI from patients with type 2 diabetes fell at the threshold between values identifying overweight and obese conditions (30 Kg/m^2). The average of the BMI from donors with type 1 diabetes fell within the threshold value separating normal and overweight condition (25 Kg/m^2).

The amount of glycated haemoglobin (HbA1c) represents a quantification of the long-term effect of high blood glucose levels on proteins and an indication of the prolonged management of diabetes. According to the World Health Organisation (WHO) diabetes can be diagnosed when the HbA1c value is higher than 6.5% (WHO 2006). The therapeutic target for the HbA1c values in people with diabetes recommended by NICE guidelines is contained between 6.5% and 7.5% in order to ensure an appropriate management of blood glucose levels. The values obtained from the different donors varied from 6.7% to 9.5% among donors with type 1 diabetes (table 2.3) and from 6% to 15.1% among patients with type 2 diabetes (table 2.3), thus indicating a different degree of success in blood glucose management among donors.

The total cholesterol was chosen to represent the general control of lipid levels in the blood. The values obtained from all donors were under the level considered as normal in UK (5.5 mmol/L in men and 5.6 mmol/L in women). However the optimal target for total cholesterol in order to control its impact of cardiovascular risk is considered below 5mmol/l. In this scenario only one donor among donors

with type 1 diabetes (row C) had a value above the target, likely related to the fact that the vast majority of donors were prescribed cholesterol lowering agents such as Statins.

The amount of creatinine in blood is used as an indicator of kidney function. Creatinine is a product of aminoacid metabolism and it is derived from muscles. Its turn-over is exclusively regulated by kidneys, thus representing an ideal indicator of the renal function and used as indicator of diabetes-related kidney disease and correlated to increased cardiovascular risk (Wannamethee 1997).

Data in table 2.3 compares the biochemical and clinical data from the recruited donors with diabetes to the percentages of activated macrophages (CD68+) and of endothelial progenitor cells (CD34+) obtained from flow cytometry on buffy coats from the same donors.

The clinical data underlined represent values above the values considered as normal, thus contributing to increase in cardiovascular risk. The average of CD68+ cells obtained from buffy coats from control subjects (1.3%) was used as an average value of circulating activated macrophages.

The values of CD68+ cells above 1.3% are underlined in table 2.3. Data shows all the donors with type 1 diabetes except from one (row D) had an amount of activated macrophages higher than the average in control subjects. All of the donors with diabetes except from one (row A) showed at least one of the values identifying cardiovascular risk factors higher than the normal optimal value. All the control subjects recruited for the study had a BMI within the "normal weight" range (20-25 Kg/m^2) (data not shown).

Table 2.3 Comparison of the clinical data from donors with type 1 and type 2 diabetes with the flow cytometric readings of cells in buffy coats (n=7). The table lists the biochemical parameters obtained from blood from two groups of donors from the Royal Sussex County Hospital database and from questionnaire filled at the time of recruitment. Clinical data are compared to the flow cytometry readings obtained from buffy coats from the same donors for the identification of circulating activated macrophages (CD68+) and endothelial progenitor cells (CD34+). The clinical results underlined represent values above the normal range. Values of the percentage of CD68+ cells in buffy coats underlined were higher than the maximum value obtained from control subjects (1.8%).

Donors and type of diabetes		**Age**	**BMI (Kg/m^2)** Normal weight between 20 and 25	**HbA1c (%)** Target values: Between 6.5 and 7.5%	**Total Cholesterol (mmol/l)** Optimal value: below 5	**Blood Pressure** Optimal values between 90/60 To 130/80	**Creatinine (µmol/l)** Optimal values: 45-90 (women) 60-110 (men)	**CD68+ % in Buffy Coat**	**CD34+ % in Buffy Coat**
A	**Type 1**	50	22.29	6.7	4.2	115/65	NA	**32.6**	0.4
B	**Type 1**	44	**28.4**	7.2	3.4	100/70	90	**11.3**	0.8
C	**Type 1**	60	23.63	6.1	**5.1**	**140/72**	86	**2.1**	0.5
D	**Type 1**	35	**27.43**	**7.7**	4.2	**142/90**	83	0.7	0.1
E	**Type 1**	51	23.46	**9.5**	4	124/70	82	**7.9**	0.7
F	**Type 1**	59	22.58	**9.4**	3.3	**145/75**	69	**5.4**	0.7
G	**Type 1**	49	**25.88**	6.9	3.3	120/80	69	**3.3**	0.4
H	**Type 2**	61	**28**	7.3	3.5	NA	**111**	**8.5**	8.1
I	**Type 2**	51	**35.83**	6.4	3.1	**140/82**	82	**9.2**	**12**
J	**Type 2**	63	**26.51**	6	2.9	NA	Na	0.27	0.6
K	**Type 2**	69	**25.34**	**9.6**	3.2	**140/78**	84	**2.9**	1.2
L	**Type 2**	66	**33.38**	**8.1**	3	125/78	Na	0.0	0.2
M	**Type 2**	70	**35.19**	7	2.8	122/52	Na	0.2	0.1
N	**Type 2**	58	24.75	**15.4**	3.5	NA	71	0.9	0.3

2.5 DISCUSSION

In-stent restenosis still represents a complication affecting the outcome of coronary balloon angioplasty accompanied by deployment of stents. The occurrence of the complication is particularly exacerbated in patients with diabetes and in complex scenarios such as longer or thicker lesions (Yan 2008, Singh 2010). In the case of people with diabetes the incidence of in-stent restenosis after the use of bare metal stents was between the 41% to the 70% (Kornowski 1997). The clinical approach of replacing traditional bare metal stents with drug-eluting stents has been shown to be successful in the reduction in the need for short-time revascularization in these patients. However, clinical data related to long-term follow-up after implantation still generate controversy due to potential increase in long-term thrombotic events (Barlis 2007, Jensen 2007, Somberg & Weinberger 2007, Patti 2008, Yan 2008, Singh 2010). This, in addition to the cost reduction associated with the use of bare metal stent made of stainless steel, implies that it is still of great importance to achieve a better understanding of the pathways leading to in-stent restenosis after bare metal stents implantation. In particular, this study is focussed on the occurrence of in-stent restenosis in people with diabetes and on the role of inflammatory cells derived from circulating monocytic population throughout the restenotic process. Indeed, the first part of this study aimed at providing an overall characterization of the fraction of circulating monocytic cells obtained from people with diabetes and from control subjects also comparing the results with biochemical values in the case of diabetic people.

The collection of mononuclear cells after centrifugation on poly-sucrose gradient has been previously shown to provide buffy coats variably rich in lymphocytes (Almeida 2000), those representing the second more abundant population obtained through Boyum's method (Boyum 1968). This study identified relevant

amounts of both T lymphocytes and B lymphocytes in buffy coats from the three groups of donors (table 2.2). Interestingly, T lymphocytes appeared to show a higher variability among donors, particularly among donors with diabetes (figure 2.4). The amount of B lymphocytes was consistent in donors from all groups (figure 2.5). The variability in T lymphocytes was likely to be due to the different conditions of the donors. In fact, T lymphocytes represent the main components responsible for the cell-mediated immunity. The amount in circulating blood varies among individuals both under normal conditions and in reaction to pathological conditions.

Inflammatory cells, in particular monocyte-derived macrophages, play a key role in the development of *in-stent* restenosis participating in all of the steps following stent implantation and particularly in the activation of the inflammatory response to the material through the release of cytokines and chemotactic factors (Santin 2005). Different studies have identified an increase in the amount of macrophages populating the adipose tissue in obese people (Di Gregorio 2005) demonstrating the correlation between obesity and macrophage infiltration of the adipose tissue (Weisberg 2003), thus confirming the inflammatory vascular condition characterizing obesity and metabolic syndrome as responsible for the development of insulin resistance and type 2 diabetes (Kahn & Flier 2000, Hu 2001, Wellen & Hotamisligil 2005) .

Differences in the amount of circulating cells positive to CD68 (representing activated macrophages) can be correlated to a general inflammatory condition of the donor and, consequently, this might be connected to an increase in the probability of developing in-stent restenosis after implantation of the device. However, it is important to take into account the possibilities of co-morbidities or temporary pathological conditions potentially correlated to an inflammatory condition, thus affecting the amount of circulating cells expressing CD68. Results showed that control subjects had an amount of circulating activated macrophages consistently below the 1.8% (figure 2.7). Different scenarios were seen analysing

the distribution of activated macrophages in donors with diabetes (figure 2.7). In particular, all the donors with type 1 diabetes showed higher levels of circulating activated macrophages relative to control subjects. Donors with type 2 diabetes showed a mixed scenario despite being on average significantly older and with a significantly higher BMI value than donors with type 1 diabetes (table 2.3). The comparison of clinical and biochemical blood results with the amount of circulating activated macrophages did not provide a direct connection between their trend lines. However, the increase in cardiovascular risk is emphasised by the co-existence of different risk factors. In particular, elevated BMI, blood pressure, age, total cholesterol, serum creatinine and HbA1c contribute synergistically to the occurrence of cardiovascular complications. Nearly all the donors with diabetes recruited in this study showed alterations in at least one of the risk factors. The limited amount of donors recruited for the study did not allow sufficient data for a statistically significant analysis of the trend correlating clinical data with population distribution. In addition, the clinical scenario of people with diabetes is generally complex and particularly affected by the duration of the disease and by the use of medications that can interfere with the vascular condition of patients. No studies were found quantifying the expression the expression of CD68 within the mononuclear cell fraction of circulating blood in pathological conditions. Therefore, a defined threshold for the identification of a clinical relevant up-regulation of the marker cannot be used for the comparison of the results from this study. However, old studies reported a flow cytometric quantification of the content of cells expressing CD68 within buffy coat to be around the 2% (Strobl 1998). This is in line with the results obtained from buffy coats isolated from control subjects in this study. This study mainly aimed to compare the expression of the marker between control and diabetic subjects to verify whether the potential up-regulation of CD68+ can identify the predisposition of developing in-stent restenosis in relation to the activation of inflammatory cells. Results from this study seemed to confirm that diabetes, well-known for being associated with an increased cardiovascular risk, can also be

associated with an increase in circulating activated macrophages. However, considering the limited sample size, it is important to take into account that the variability within the population expressing CD68 may be associated with transient or chronic inflammatory conditions not necessarily related to diabetes. Nevertheless, the results identified alterations in the circulating inflammatory cells characterizing the diabetic population reinforcing the inflammatory nature of the disease and potentially identifying the basis for the predisposition for developing in-stent restenosis.

Cells positive for the marker for haematopoietic and endothelial progenitor cells (CD34) have been identified as precursors of endothelial cells intervening in the repair of vascular injury (Fadini 2006). The amount of circulating cells positive to CD34 seem to increase temporarily immediately after cardiac events thus representing a diagnostic or therapeutic target respectively for the prevention or repair of cardiovascular injury (Yin 1997, Boilson 2008). Data obtained from the analysis of buffy coats demonstrated a variability of results particularly among donors with type 2 diabetes. This seemed to confirm that the amount of cells positive for CD34 can be extremely variable among different donors. The amount of cells positive to CD34 detected during the experiment was generally consistent across groups and among donors. Previous studies have also shown that the amount of circulating CD34+ cells can vary rapidly following vascular injury and cardiac events. This explains the individual variability of the results and suggests that the level of CD34+ cells could represent an important diagnostic tool for identifying patients at risk of developing cardiovascular complications.

2.6 CONCLUSIONS

The histological analysis of restenotic stented coronary arteries has determined that neointimal growth is proportionally correlated to the amount of inflammatory cells surrounding the strut as well as to the depth of the strut penetration within the lipid core and to the damage to the vessel wall provoked by the surgical procedure (Farb 2002). These findings emphasized the relevance of the degree of activation of the inflammatory process characterizing the initial phases following stent implantation, thus suggesting that anomalies in the inflammatory condition of patients at the moment of intervention could represent a parameter for the identification of the predisposition of developing in-stent restenosis. Results from this small pilot study suggested that people with diabetes may present an increased amount of circulating activated macrophages even in subjects in which the analysis of the clinical data suggests a well-controlled basic health condition. In particular, the increased amount of macrophages was observed in most of the donors with type 1 diabetes and in only two of the recruited donors with type 2 diabetes. The extension of the study to an appropriate sample size could determine specific trends correlating diabetes with circulating macrophages and health conditions, thus potentially recognizing the quantification of circulating activated macrophages as an independent factor for the identification of individual prone to developing in-stent restenosis. Therefore, the quantification of circulating activated macrophages could become a useful diagnostic tool for the prediction of the outcome of the procedure prior to intervention. Results also suggested that a more complete evaluation of the scenario may derive by the quantification of circulating haematopoietic progenitor cells, demonstrated to be related to endothelial damage and cardiovascular risk (Fadini 2006).

Previous studies have demonstrated the phenotypical plasticity of monocyte-derived macrophages being able to differentiate into myofibroblasts thus

contributing to the formation of neointima during the later stages of ISR and, more generally, to different phases of the foreign body reaction (Stewart 2009, Mesure 2010). More studies have identified sub-populations in the circulating blood derived from monocytes and able to differentiate in cells of the mesenchymal lineage, endothelial cells and smooth muscle-like cells (Kuwana 2003, Rehman 2003, Boilson 2008, Pilling 2009, Forte 2010). Therefore, the next step of this work analysed mononuclear cells isolated from buffy coats in order to confirm the presence of circulating sub-populations with the ability to the trans-differentiate in order to confirm the findings published in literature and identify potential links between their distribution and the predisposition of developing *in-stent* restenosis. In addition, the comparison of sub-population distribution between people with diabetes and control subjects may elucidate on the links between trans-differentiation potential of inflammatory cells and increased occurrence of in-stent restenosis in diabetes.

CHAPTER 3

CHARACTERIZATION OF CELL SUB-POPULATIONS IN BUFFY COATS: ANALYSIS OF TRANS-DIFFERENTIATION POTENTIAL OF MONOCYTES

3.1 INTRODUCTION

It has been widely demonstrated that circulating monocytes do not represent exclusively the precursors of activated macrophages responsible for the phagocytic activity in peripheral tissues (Kuwana 2003). They are in fact characterized by morphological heterogeneity (Gordon & Taylor 2005) with the ability to generate different cell populations under specific stimuli (Kuwana 2003, Gordon & Taylor 2005, Waldo 2008).

Previous studies have demonstrated a possible contribution of monocyte-derived macrophages to the formation of the restenotic plaque associated to their phenotypical plasticity. In particular, monocytes were shown to express α-actin *in vitro* (Bayes-Geni 2002, Stewart 2009). This is a recognised marker for smooth muscle cells (SMC) and its presence on macrophages was indicative of a myofibroblast-like phenotype *(*Bayes-Geni 2002, Stewart 2009). Myofibroblasts are collagen-forming cells which possess secretive/proliferative phenotype features of both SMC and fibroblasts. They represent the main cellular components of the late neointimal tissue and they characterize the capsule surrounding non-degradable implant in the foreign body reaction as well as the granulation tissue in the wound healing process (Mesure 2010). Myofibroblasts are specialized cells also known as "mesenchyme-like interstitial cells" that participate to tissue repair following vascular injury under specific pathophysiological conditions (Forte 2010). They are responsible for the contraction of granulation tissue, the production and remodelling of extra-cellular matrix and the production of angiogenic and pro-inflammatory factors as well as the generation of tensile forces (Forte 2010). Their presence in restenosis has been associated to contribution to neointimal formation as well as to the thickening of the tunica media and to the remodelling of extra-cellular matrix. Overall, their contribution to the restenotic process is associated to contractile, proliferative and

remodelling activities as well as to the synthesis of growth factors favouring the proliferative phases of neointimal formation and of glycosaminoglycan forming the matrix of the restenotic plaque (Forte 2010).

The ability of macrophages to modify their phenotype and turn into myofibroblast-like cells may therefore be of great importance to the development of *in-stent* restenosis (Bayes-Geni 2002). Indeed, a recent study has confirmed the expression of SMC-α-actin in monocytes/macrophages with corresponding changes in morphology after one week of incubation on surfaces made of stainless steel (Stewart 2009). This has been previously investigated by Dinnes et al (2007), who demonstrated macrophage plasticity and inflammatory state to be dependent on the surface chemistry of the substrate material. Indeed, the adaptation of the inflammatory cell response appeared to be achieved through cellular remodelling involving changes in intracellular and cytoskeletal structure (Dinnes 2007). Further contribution to the understanding of the origin of smooth muscle cell-like cells in tissues has derived by a study that demonstrated the presence of a population of α-actin positive cells in the low density fraction of mononuclear cells freshly isolated from human blood by centrifugation (Sugiyama 2006).

3.1.1 Origin of myofibroblasts

The origin of myofibroblasts can be attributed to different contributions as illustrated in figure 3.1. Indeed, they can derive from the differentiation of surrounding fibroblasts but they can also originate from the trans-differentiation of smooth-muscle and endothelial cells through a process called endothelial-mesenchymal transition (EMT) (Forte 2010). The differentiation into myofibroblasts (expressing α-smooth muscle cells actin) is commonly preceded by the differentiation into precursors named proto-myofibroblasts, not yet expressing smooth-muscle cells α-actin (figure 3.1) (Forte 2010). In the case of vascular myofibroblasts, their origin can be attributed to the differentiation of

circulating precursors named fibrocytes (Forte 2010). Fibrocytes differentiate from cells of the monocytic lineage expressing CD14, marker for monocytes. Fibrocytes have been identified by the concomitant expression of CD34 (marker for haematopoietic progenitor cells), CD45 (general marker for leukocytes) and collagen I (Pilling 2009, Forte 2010). However, the characterization of the population can be affected by difficulties related to the progressive loss of CD34 and CD45 by fibrocytes and by the expression of the same markers by a broad range of different cell types (Pilling 2009).

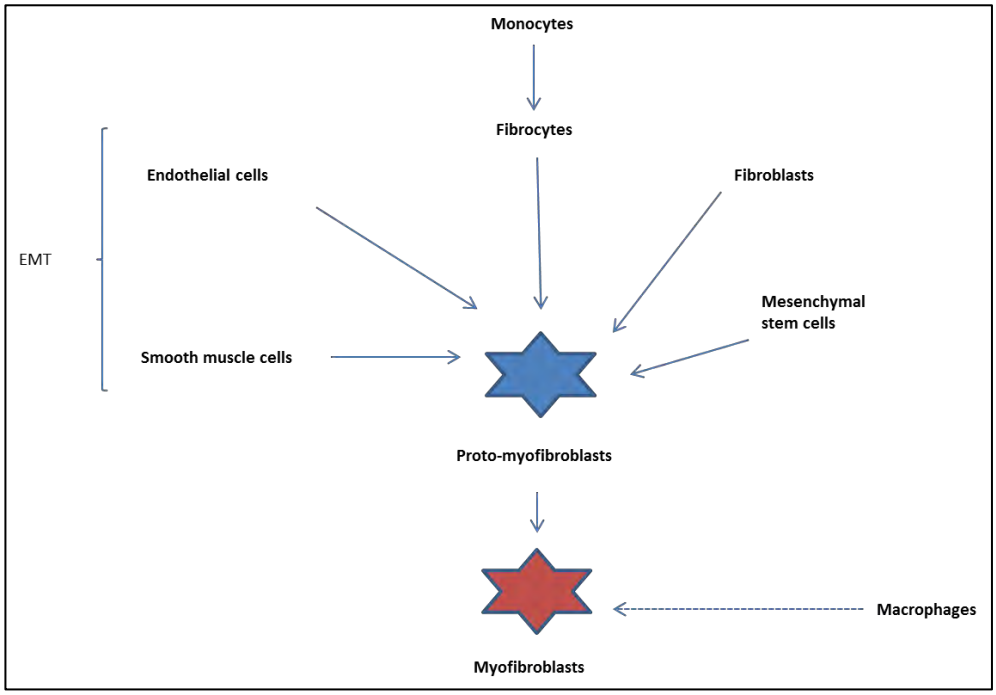

Figure 3.1 Schematic representation of the multiple origins of myofibroblasts. *Myofibroblasts can derive from the differentiation of different cell types. The trans-differentiation of smooth muscle and endothelial cells is known as endothelial-mesenchymal transition (EMT). The final cell is preceded by precursors (proto-myofibroblasts) that, opposite to myofibroblasts, do not yet express α-actin (marker for smooth muscle cells). Precursors of fibrocytes were found among monocytes as confirmed by the expression of specific markers. Myofibroblasts populating the neointima that forms following vascular injury in models of restenosis were found to derive from precursors derived by circulating blood. Among those precursors, cells co-expressing the marker for macrophages were found, thus reinforcing the contribution of trans-differentiation of macrophages in the restenotic process. Figure adapted from Forte et al. 2010.*

The repair process following vascular injury has traditionally been considered as driven by myofibroblasts derived by fibroblasts resident in the adventitia that migrate under the effect of cytokines (Forte 2010).

However, different studies investigating the formation of neointimal tissue during the restenotic process have suggested the multiplicity of myofibroblasts origin, in particular showing that they can derive from precursors isolated from peripheral blood (Wilcox 2001, Forte 2010). In addition, a study reproducing vascular injury in a porcine model showed that, following vascular injury, the 5% of cells populating the neointima co-expressed the marker for smooth muscle cells and macrophages (Bayes-Geni 2002). This finding was then reinforced by evidence about the contribution of the differentiation of inflammatory cells in circulating blood to the formation of myofibroblasts participating in the restenotic process published by Stewart et al. (2009) (Bayes-Geni 2002, Forte 2010).

3.1.2 Trans-differentiation potential of circulating mononuclear cells

The ability of monocytes, identified by the marker CD14, to differentiate into different lineages under specific stimuli has been demonstrated in previous studies (Kuwana 2003, Gordon & Taylor 2005, Varol 2009). In particular, Kuwana *et al.* (2003) identified a population of monocytes, thus positive to the CD14 marker, acting as progenitor of mesenchymal lineages and able to intervene in osteogenesis, chondrogenesis, myogenesis and adipogenesis under specific in-vitro culture conditions (Kuwana 2003). More specifically, the same study identified a subpopulation co-expressing markers for monocytes (CD14), leukocytes (CD45), haematopoietic and endothelial progenitor cells (CD34) and type I collagen. These cells were identified as a monocyte subpopulation presenting a fibroblast-like morphology and able to generate different cell types of the mesenchymal lineage when cultured on fibronectin under different cultural conditions. This sub-population was named monocyte-derived mesenchymal

progenitor (MOMP) (Kuwana 2003). The flow cytometric analysis of adhering cells identified different lineages according to the phenotypical expression of markers. In particular, the study demonstrated that the CD14-expressing precursor, derived from a sub-population of monocytes, was able to differentiate into different mesenchymal lineages. The study demonstrated that monocyte differentiation is triggered by the binding with fibronectin and by the interaction with soluble factors, thus hypothesizing that monocytes could infiltrate into peripheral tissues as a response to injury. Once reached the tissues, they would interact with tissue fibronectin and soluble factors released during the inflammatory process to differentiate as a repair response to injury. These findings demonstrate that mononuclear cells participate in tissues homeostasis, replacing cells damaged by injuries or physiological turnover, thus representing a potential therapeutic target for the regeneration of damaged vasculature as well as a key factor for the development of the restenotic process (Kuwana 2003).

3.1.3 Endothelial progenitor cells and monocytes

Previous studies have demonstrated the correlation between circulating haematopoietic progenitor cells (identified as a cell population expressing the marker CD34), cardiovascular risk and metabolic syndrome (Fadini 2006). More recent studies have defined the CD34+ cell population as formed by different sub-populations based on the co-expression of markers which are correlated to the origin and differentiation potential of the haematopoietic cells. In particular, studies seem to agree in the identification of two sub-sets of cell populations of the haematopoietic lineage and positive to CD34 based on the co-expression of the common leukocyte marker (CD45). They identified cells expressing CD34 but not expressing CD45 as endothelial progenitor cells (EPC) of haematopoietic origin and forming exclusively endothelial cells in culture. Cells co-expressing CD34 and CD45 were identified as circulating angiogenic cells (CAC) or

alternatively as culture-modified mononuclear cells (CMMC) (Rehman 2003, Boilson 2008). CAC were shown to form spindle-like shaped cells after 7 days in culture not forming pure endothelial cells but spindle-shaped cells expressing haematopoietic and endothelial markers and possessing differentiation potential. They represent the majority of the CD34+ subpopulations and the only sub-population reduced in number in patients with endothelial dysfunctions (Boilson 2008).

3.1.4 Smooth muscle cells in circulating blood

Smooth muscle cells represent the population characterising the neointima in the restenotic plaque (Santin 2005). Previous studies have demonstrated that the mononuclear fraction of human blood can differentiate in culture under the presence of specific cytokines such as TGF-β and PDGF-BB into cells showing morphology and phenotype of SMC. Alpha–actin, primordial marker for smooth muscle cells, was used to identify the presence of cells expressing SMC-like phenotype. Therefore, the studies hypothesised the presence of precursor of SMC of monocytic origin in the circulating blood as the cells expressed the marker for monocytes (CD14) (Simper 2002, Sugiyama 2006). Furthermore, the study by Sugiyama (2006) divided the mononuclear population into two fractions, depending on their density and showed that exclusively the low density fraction contained monocytic cells able to differentiate into SMC (Sugiyama 2006). This confirmed the heterogeneity of the circulating mononuclear population.Table 3.1 summarises the sup-populations identified so far by recent studies able to differentiate *in vitro* into endothelial cells or myofibroblasts or smooth muscle-like cells under specific culture conditions and potentially intervening in the vascular repair process representing the focus for a better understanding of the restenotic process.

Table 3.1. Summary of sub-populations derived by mononuclear cells potentially participating in vascular repair after trans-differentiation. Different subpopulations within the mononuclear cells fraction of the blood were identified as progenitor possessing trans-differentiation potential.

Sub-population identification	Phenotypical identification	Role and differentiation potential	Function *in-vivo*	Reference
MOMPs (Monocyte-derived mesenchymal progenitor)	CD14+CD45+ CD34+type I collagen+	In-vitro differentiation in cells of mesenchymal lineage	Tissue homeostasis. Replacement of cells in tissue damaged by injuries or during physiological turn-over	Kuwana et al. (2003)
CACs (circulating angiogenic cells) or **CMMCs** (culture-modified mononuclear cells)	CD34+CD45+(CD14)+	Formation of spindle-shaped cells in culture. Expression of endothelial and haematopoietic cell markers. Differentiation potential	Differentiation into endothelial cells participating in vascular repair	Rehman *et al*. (2003), Boilson *et al.* (2008)
EPCs (endothelial progenitor cells)	CD34+CD45-CD14-	Exclusive formation of endothelial cells	Formation of endothelial cells	Rehman *et al*. (2003), Boilson *et al.* (2008)
SMPCs (smooth muscle progenitor cells)	CD14+-CD105+-α-actin+	Circulating source of smooth muscle cells	Differentiation in to smooth muscle cells participating in vascular repair and wound healing	Sugiyama *et al.* (2006)

3.2 AIMS

The work described in this chapter aimed to characterize the mononuclear cell sub-populations in buffy coats isolated from donors with type 1 and type 2 diabetes, and from healthy control subjects. The characterization was performed on the basis of the ability to co-express a combination of specific markers in order to provide evidence of the presence of sub-populations derived from monocytes possessing trans-differentiation potential. In particular, the study focused on the understanding of the contribution of mononuclear cells to the formation of myofibroblasts, thus consequently representing key factors for the deposition of the neointima during the later stages of the restenotic process. The comparative analysis between healthy donors and individuals with diabetes aimed at unveiling potential differences in cell sub-population distribution to determine how diabetes can affect their distribution and their trans-differentiation potential, hence having a potential impact on *in-stent* restenosis.

3.3 MATERIAL AND METHODS

3.3.1 Recruitment of volunteers and collection of buffy coats

Data discussed in this chapter were obtained from the same group of donors as described in section 2.3.1.1. However, only the results from three donors per each group (total of nine donors) were available to be analysed in terms of cell sub-population distribution. In the case of the samples stained with the antibody for α-actin only a total of eight donors were available. The procedure for the collection of blood and its treatment are described in Section 2.3.1.2.

3.3.2 Flow cytometry

The characteristics of the instruments and the procedure for cell preparation and labelling are described in sections 2.3.2.1, 2.3.2.3 and 2.3.2.5. The selection of antibodies used for the procedure of triple staining is described in section 2.3.2.4. In addition, some of the tubes (n=8) with cells from donors from different groups were tested for the identification of α-actin, marker typically expressed by smooth muscle cells. The antibody for the detection of human smooth muscle cells α-actin (conjugated to PE; R&D Systems) was added to the tubes at the concentration of 0.25μg per one million cells. The tubes were stained with triple staining combining CD45-PECy5, α-actin-PE and CD14-FITC. This allowed the identification of cell sub-populations co-expressing markers for monocytes and α-actin in the circulating blood.

Controls were used and limitations of the technique apply as described in Section 2.3.2.5 and 2.3.2.2.

Results were analysed using the software FlowJo and expressed as percentage of the populations of interest in the total amount of cells counted in each test tubes. In order to characterize the composition of each population on the basis of the sub-population distribution the results were than expressed as percentage of each sub-population on the total amount of marker expressed in the tube as described below in section 3.4.

3.4 RESULTS

Tubes were triple stained mixing different antibodies as described in sections 2.3.2.4, 2.3.2.5 and 3.3.2. Considering the limited amount of cells available in each experiment, this procedure allowed the expansion of the analysis of each

marker necessary to the characterisation of cellular components. The combined use of different antibodies also allowed the identification of the co-expressed markers in the same sample. Results obtained from a total of nine donors (three donors per each group), with the exception of samples stained with the antibody for α-actin (only a total of eight donors were available) were collected. A quantitative and statistically valid analysis was not applicable due to the limited amount of data (n=3 per cohort). However, results were analysed qualitatively to depict the variability in the distribution of sub-populations among donors and to confirm the presence of different sub-populations in buffy coats. The results presented in this chapter derive from donors belonging to the same batch recruited for experiments described in the previous section. However, for the experiments in this chapter, due to the limited amount of donors per group, the mean of the three readings per cohort was chosen to represent the distribution rather than the median, which was previously chosen as best representative of the non-parametric results obtained. In addition, the percentages expressed in this chapter represent the sub-population distribution rather than the total marker expression in the buffy coats. Each tube was marked for three different markers and the software was able to provide a figure for the total expression of each marker as well as the figures indicating the sub-populations forming the total amount of each marker on the basis of the co-expression of the other markers used in the tubes. For instance, if in one tube cells were labelled with the combination of marker A, marker B and marker C, the software provided the total amount of cells expressing the marker A (A_{tot}), thus representing the 100% for the specific marker, as well as the amount of each sub-population forming the 100% and co-expressing one of the other markers, both and none (A only). In this example the population expressing the marker A would be split as follows:

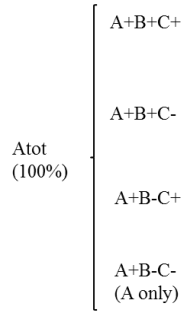

Therefore, if every sub-population is expressed by the instruments as its percentage over the total amount of "event" (particles) counted in the correspondent tube; the results in the following paragraphs are expressed as the mean of the percentage expressing each sub-population over the total expression of the marker in each tube. For instance, in the case of the sub-population co-expressing all the markers (A+B+C+), data would be expressed as follows:

$$\frac{\%\ A+B+C+}{\%\ Atot} \quad X \quad 100$$

3.4.1 Distribution of sub-populations within monocyte and macrophages in buffy coats

The previous chapter illustrated differences among the total amount of cells positive to the marker for monocytes (CD14) and activated macrophages (CD68). The analysis of the results in terms of marker co-expression demonstrated that there was a partial co-expression of the signal identifying CD14 or CD68 with signal identifying the marker for emdothelial progenitor cells (CD34) (figures 3.2a-d). The co-expression can be in fact observed in the plots in figures 3.2(a-d), this being represented by the partial overlapping of the area identifying the population emitting on the channel for the fluorochrome FITC (figures 3.2a-d) to the area representing the population emitting on the channel for PE (figures 3.2a-d). In particular, figures 3.2a and 3.2b show the co-expression of CD34 (black area) and CD14 (blues dots) in buffy coats from respectively donors with type 1

and type 2 diabetes. Similar finding were observed in buffy coats from control subjects (data not shown). Similarly, the population representing circulating activated macrophages (positive to CD68) and represented by blue dots in figures 3.2c and 3.2d was partially overlapping with the areas representing the population positive to the marker for haematopoietic and endothelial progenitor cells (positive to CD34) in buffy coats from the same donors with type 1 diabetes and type 2 diabetes.

The population positive for the marker for monocytes (CD14) was analysed to determine the amount of cell sub-populations on the basis of the co-expression of the different markers used for the triple staining of the test tubes. Data were obtained from the software Flow-Jo and expressed as percentage of the sub-population in the total amount of events counted by the instrument as described in the previous section. Results showed that the population of monocytes (CD14+) was composed mainly of cells expressing exclusively the specific marker (CD14) in all the groups of donors ranging from 66.2% in donors with type 1 diabetes, to 69.5% in control subjects and to 79.9% in donors with type 2 diabetes (figure 3.3). Data are expressed as mean of the percentage of each sub-population over the total amount of cells positive to CD14 [i.e. (%CD14+CD45+/%totalCD14+) x 100]. The second more abundant population (CD14+CD45+) was represented by cells co-expressing the general marker for leukocytes (CD45) in association to the marker for monocyte (CD14). The remaining cells co-expressed the marker for haematopoietic and endothelial progenitor cells (CD34) in concomitance with the marker for monocytes (CD14+CD34+). The amount of the last population ranged from 0.6% in donors with type 2 diabetes, to 1.4% in control subjects and to 1.6% in donors with type 1 diabetes. A similar amount of CD14+ cells were co-expressing both the general marker for leukocytes and the marker for monocytes (CD14+CD34+CD45+). The value obtained from the donors with type 2 diabetes (0.6%) was low and equal to the value obtained from the same group and identifying the CD14+CD34+ population, thus suggesting that the recorded

signal, although slightly variable among the three donors (data not shown), was close to background noise. The amount of sup-populations within the monocytes positive to the three markers was 1.1% in control subjects and 1.2% in donors with type 1 diabetes (figure 3.3). Summing the percentages of the cell expressing exclusively CD14+ and of the CD14+CD45+ sub-population the results demonstrated that the vast majority (97.5% of the recruited control subjects, 97.2% of donors with type 1 diabetes and 98.7% of donors with type 2 diabetes) of the population was identified by monocytes not expressing the marker for haematopoietic progenitor cells (CD34). The sub-population of monocytes co-expressing the marker for haematopoietic stem cells in the donors recruited in the study was never above 2.5% (figure 3.3).

Similarly, the population positive to the marker for activated macrophages (CD68) was differentiated based on the co-expression of the different markers as described for the CD14+ population. Data were expressed as percentage of the sub-populations on the total amount of activated macrophages (CD68+) cells thus splitting the population of activated macrophages into different sub-populations. The results showed that activated macrophages in buffy coats of donors from all groups were mainly formed by cells expressing exclusively CD68, those representing 58.8% of activated macrophages in buffy coats from control subjects, 64.0% of activated macrophages in buffy coats from type 1 diabetes and 61.1% in buffy coats from donors with type 2 diabetes (figure. 3.4).

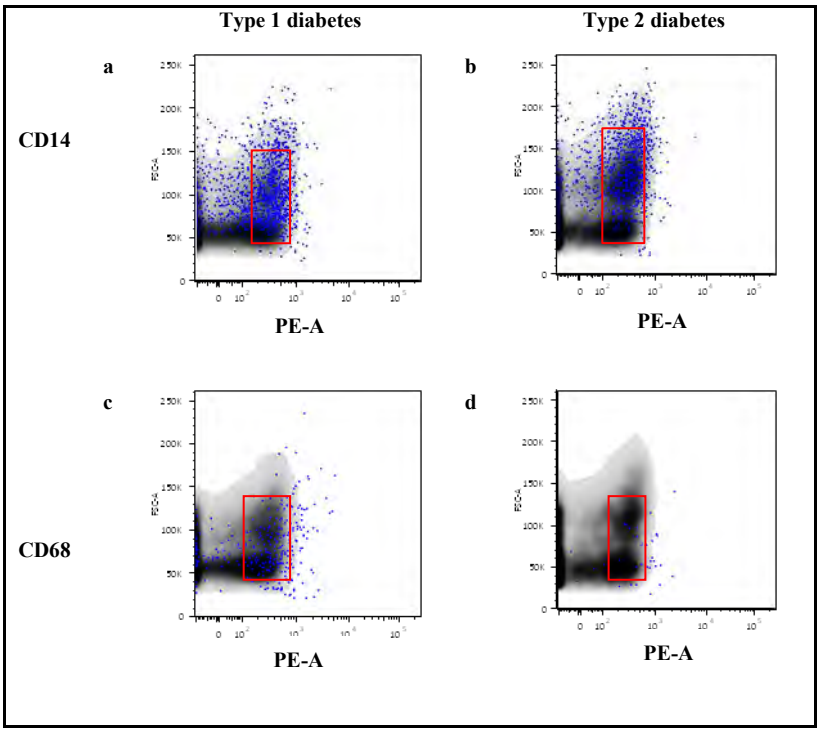

Figure 3.2 Cells in buffy coats co-expressed the markers for monocyte (CD14) or activated macrophages (CD68) with the marker for haematopoietic and endothelial progenitor cells (CD34). *The plot representing monocytes (CD14+) population (blue dots in figure 3.2a and 3.2b) partially overlapped the population positive to CD34 representing the endothelial progenitor cells (the black area) in buffy coats of the donor with type 1 diabetes (fig. 3.2a) and with type 2 diabetes (fig. 3.2b) as represented by the area included in the red rectangular. Buffy coats from a donor with type 1 diabetes (fig.3.2c) and with type 2 diabetes (fig.3.2d) contained cells positive to the marker for activated macrophages (CD68) (blue dots) co-expressing the marker for haematopoietic and endothelial progenitor cells (CD34) (black area)*

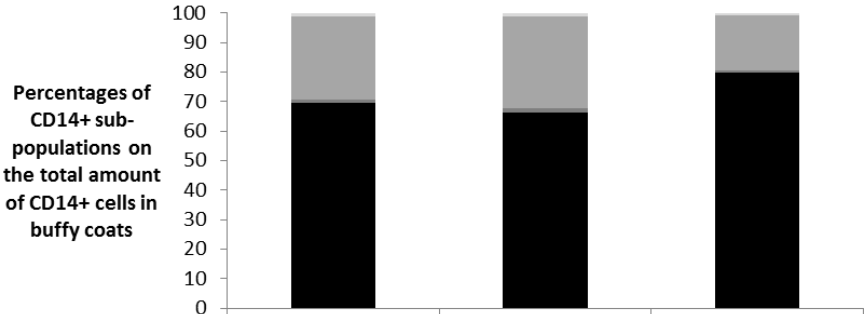

	Control	Type 1 Diabetes	Type 2 Diabetes
CD14+CD34+CD45+	1.2	1.2	0.7
CD14+CD45+	28.0	31.0	18.8
CD14+CD34+	1.4	1.6	0.7
CD14 Only	69.5	66.2	79.9

Figure 3.3 Percentage of cells among monocytes co-expressing CD34 (n=3 per cohort). *Mononuclear cells population in buffy coats was mainly composed of cells expressing exclusively the marker for monocytes (CD14 only). Values are expressed as the average of the values from each donor in the group. The second more represented sub-population was co-expressing the marker for monocytes (CD14) and leukocytes (CD45). Between the 1.2% to the 1.6% of monocytes co-expressed the marker for haematopoietic and endothelial progenitor cells (CD34) with or without the general marker for leukocytes (CD45) among control subjects and donors with type 1 diabetes. No co-expression was seen in donors with type 2 diabetes.*

The second more abundant sub-population among the activated macrophages across the groups was represented by cells co-expressing the general marker for leukocytes (CD45) that is commonly expressed in different phases of monocytes life (figure 3.4). A cell sub-population co-expressing the marker for haematopoietic progenitor cells in combination with both the marker for activated macrophages (CD68) and haematopoietic and endothelial progenitor cells (CD34) (CD68+CD34+CD45+) was also found as represented in figure 3.4. This particular sub-population was particularly high in buffy coats of the donors with type 2 diabetes selected in this study (15.7%) compared to the amount found in buffy coats from control subjects (7.3%) and from donors with type 1 diabetes

(4.1%) (figure 3.4). In addition the CD68+CD34+ sub-population was found in buffy coats from all the donors (figure 3.4).

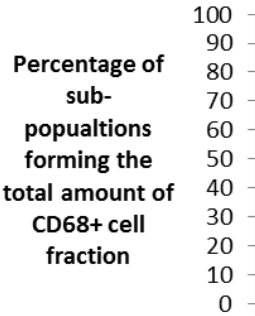

	Control	Type 1 Diabetes	Type 2 Diabetes
CD68+CD34+CD45+	7.3	4.1	15.7
CD68+CD45+	28.8	29.3	19.3
CD68+CD34+	5.1	2.6	3.9
CD68 Only	58.8	64.0	61.1

Figure 3.4 Percentage of cells among macrophages co-expressing CD34 in buffy coats (n=3 per cohort)*. The population of activated macrophages in buffy coats was composed mainly by cells expressing exclusively the marker for activated macrophages (CD68 only). Values are expressed as mean of the values from each donor in the group. The sub-population co-expressing the marker for haematopoietic progenitor cells with markers for activated macrophages and leukocytes (CD68+CD34+CD45+) was particularly abundant (15.7%) in donors with type 2 diabetes and well represented in control subjects (7.3%) and donors with type 1 diabetes (4.1%).*

3.4.2 Distribution of sub-populations among cells positive to the marker for haematopoietic and endothelial progenitor cells

The antibody against CD34 was used in two different mixtures according to the triple staining technique as described in sections 2.3.2.4, 2.3.2.5 and 3.3.2. This allowed the parallel characterization of the haematopoietic progenitor cell population on the basis of the co-expression of the marker for monocytes (CD14) and for activated macrophages (CD68), both in conjunction with the general marker for leukocytes (CD45)

Results are expressed as mean of the percentages of each sub-population in the total amount of cells positive for the marker for haematopoietic and endothelial progenitor cells (CD34). As shown in Section 2.4.2.2 the antibody for the detection of CD34 was combined to the antibody for CD14 (monocytes) and to the antibody for the general marker for leukocytes (CD45) to stain some of the tubes.

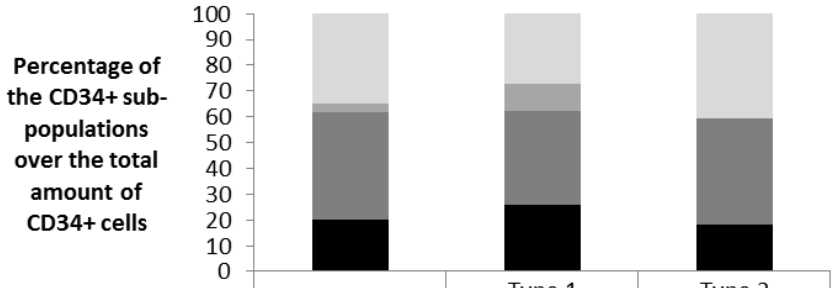

	Control	Type 1 Diabetes	Type 2 Diabetes
CD34+CD14+CD45+	35.1	27.2	40.9
CD34+CD45+	3.3	10.4	0.0
CD34+CD14+	41.3	36.5	40.9
CD34 Only	20.3	25.9	18.3

Figure 3.5 Percentage of CD34 positive cells co-expressing markers for monocytes and leukocytes in buffy coats (n=3 per cohort). *Results showed that only 18.3% in donors with type 2 diabetes, 20.3% in control subjects and 25.9% in donors with type 1 diabetes of the haematopoietic stem cells expressed exclusively the specific marker (CD34). Despite with differences across the groups, the majority of cells positive to CD34 showed to co-express the marker for monocytes and/or the marker for leukocytes (CD45).*

antibodies and containing buffy coats from the same groups of donors showed that only a limited amount of cells across the groups were exclusively positive to CD34, the percentage ranging from 18.3% in donors with type 2 diabetes, to 20.3% in control subjects and to 25.9% in donors with type 1 diabetes (figure 3.5). In all of the donor groups the most represented sub-populations were identified by the cells co-expressing the marker for monocytes (CD14) or both the marker for monocytes (CD14) and the general marker for leukocytes (CD45). No CD34+CD45+ were found in buffy coats of donors with type 2 diabetes but 3.3%

of them was found in buffy coats of control subjects and 10.4% was found in buffy coats from donors with type 1 diabetes.

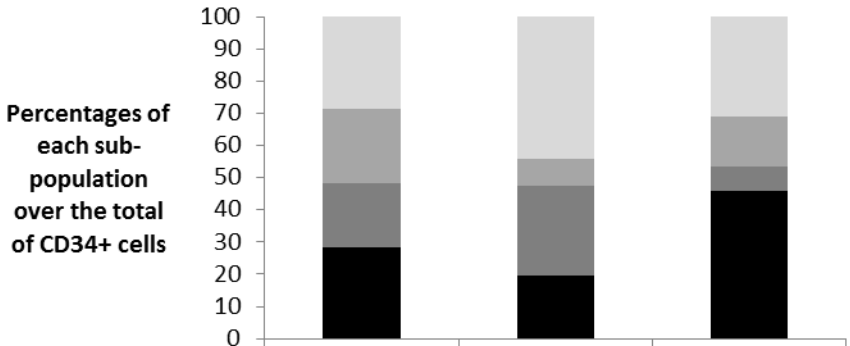

	Control	Type 1 Diabetes	Type 2 Diabetes
CD34+CD68+CD45+	28.6	44.2	30.9
CD34+CD45+	23.3	8.4	15.8
CD34+CD68+	19.8	28.0	7.6
CD34 Only	28.3	19.5	45.8

Figure 3.6 Percentage of circulating endothelial progenitor cells co-expressing the marker for activated macrophages and/or leukocytes (n=3 per cohort). *The majority of cells expressing the marker for haematopoietic progenitor cells (CD34) was formed by sub-populations co-expressing marker for activated macrophages (CD68) and/or the general marker for leukocytes (CD45). The amount of cells expressing exclusively CD34 was much higher in donors with type 2 diabetes (45.8%) than in control subjects (28.3%) and donors with type 1 diabetes (19.5%). Data are expressed as mean of the percentage of each sub-population over the total amount of CD34+ cells in test tubes.*

The analysis of results obtained from tubes labelled with a mixture containing antibodies for the marker for haematopoietic and endothelial progenitor cells (CD34), activated macrophages (CD68) and leukocytes (CD45) showed that recruited donors with type 2 diabetes contained 45.8% of the circulating haematopoietic stem cells in buffy coats formed of cells expressing exclusively CD34 (figure 3.6) and the 30.9% of CD34+CD68+CD45+ cells (figure 3.6). In

buffy coats from donors with type 1 diabetes cells exclusively positive to CD34 were representing 19.5% of the total amount of circulating haematopoietic stem cells and 44.2% was represented by CD34+CD68+CD45+ cells (figure 3.6). In buffy coats from control subjects the ratio of the two populations was represented by 28.3% of cells expressing exclusively the CD34 and by 28.6% of CD34+CD68+CD45+ cells (figure 3.6).

3.4.3 Characterization of α-actin positive population in buffy coats

Buffy coats from a total of eight donors (four control subjects, three donors with type 1 diabetes and one donor with type 2 diabetes) were analysed for the characterization of cell sub-populations positive to α-actin on the basis of the co-expression of the marker for monocytes (CD14) and of the general marker for leukocytes (CD45). Figure 3.7 illustrates that in buffy coat from a control subject (figure 3.7a), from a donor with type 1 (figure 3.7b) and type 2 (figure 3.7c) diabetes a population positive to α-actin was found. No differences could be identified among the group of donors and the quantitative analysis was not possible because of the limited amount of data for the specific characterisation. However, the results from flow cytometry confirmed the concomitant expression of the marker for monocytes (CD14) and for α-actin. The population positive to CD14 and represented by blue dots as shown in Figures 3.7d, 3.7e and 3.7f (respectively for control subject, donor with type 1 diabetes and donor with type 2 diabetes) was in fact partially overlapping with the area representing the core population positive to α-actin (black area in figures 3.7d-f). In particular, buffy coats were triple stained combining antibodies for CD45 (leukocytes), α-actin (smooth muscle cells) and CD14 (monocytes) as described in Section 3.3.2. Results showed how the population positive to α-actin could be differentiated into sub-population analysing to concomitant expression of the different markers.

Despite the semi-quantitative character of the study, figure 3.8 compares the mean values of the percentages representing the different sub-populations forming the actin-positive cells within the buffy coats from the three groups of donors. Differences were seen among donors when data from control subjects were compared to data from the donors with type 1 diabetes. The sub-population expressing exclusively α-actin ("actin only" in figure 3.8) represented vast majority of the sub-populations ranging from 47.9% in the donor with type 2 diabetes, to 53.5% in donors with type 1 diabetes, to 69.8% in control subjects when calculated as percentage of the average of the sub-population on the total amount of actin positive population.

In all of the donors the second major sub-population was the one co-expressing CD14 (monocytes) and α-actin. In the case of the donor with type 2 diabetes this population was present at a similar rate (47.2%) as the population expressing exclusively actin (47.9%) (figure 3.8). Only a small percentage represented the co-expression of CD45 (general leukocytes) with α-actin or all the markers.

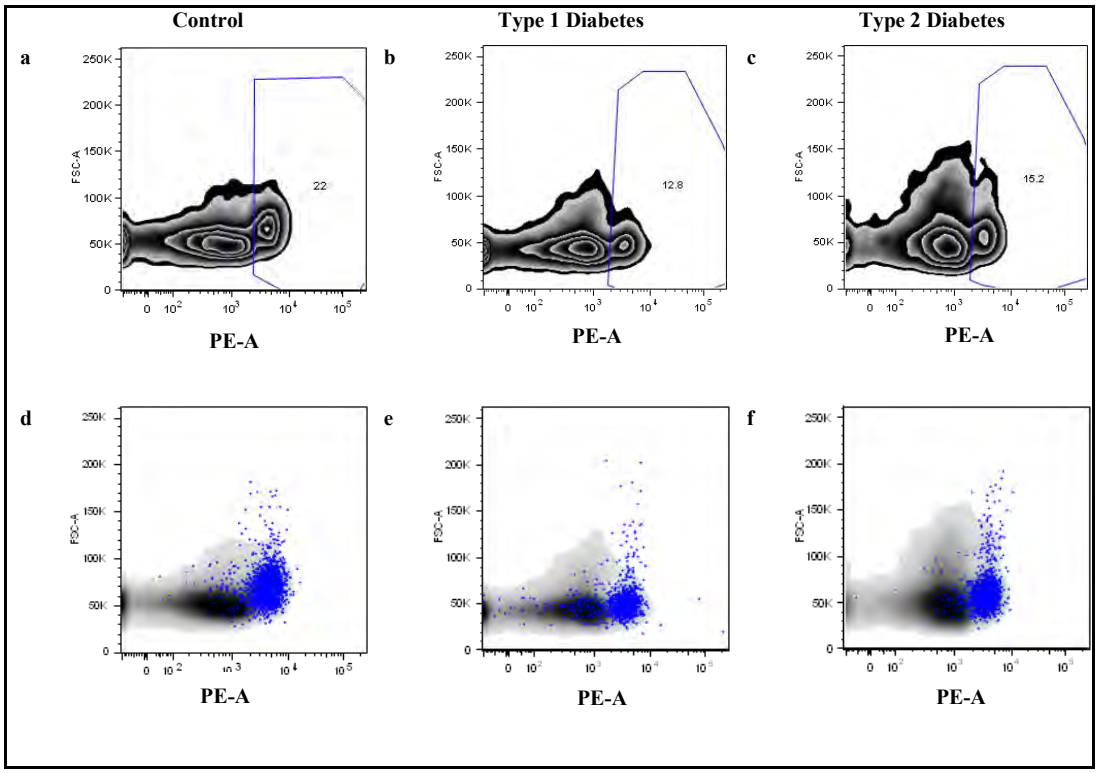

Figure 3.7 Cell sub-populations co-expressing α-actin with the marker for monocytes. *Results obtained from flow cytometry on buffy coats from a control subject (3.7a), from a donor with type 1 diabetes (3.7b) and from a donor with type 2 diabetes (3.7c). Mononuclear cells contained a sub-population expressing the marker for smooth muscle cells (α-actin) represented by the area included in the blue line (fig. 3.7a-c). The overlapping of the area identifying α-actin+ cells (blue dots in fig. 3.7d-f) with the area representing cells positive to the marker for monocytes (CD14) (black area in fig 3.7d-f) confirmed the presence of a sub-population co-expressing the two markers*

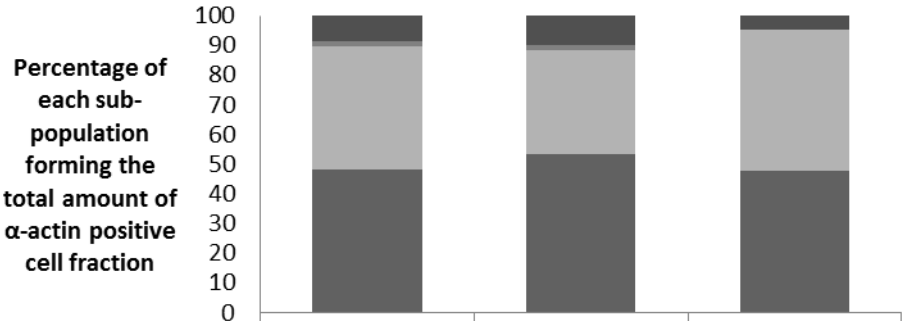

	Control	Type 1 Diabetes	Type 2 Diabetes
Actin+CD14+CD45+	8.6	9.8	4.6
Actin+CD45+	1.8	1.8	0.2
Actin+CD14+	41.5	34.9	47.2
Actin Only	48.1	53.5	47.9

Figure 3.8 Percentage of cells positive to α-actin co-expressing the marker for monocytes (CD14) in buffy coats as a fingerprint of trans-differentiation potential of mononuclear cells into myofibroblasts (n=8 in total). *Further characterisation of the sub-population positive to α-actin in buffy coats showed that cells expressing exclusively the marker for α-actin (actin only) were the most abundant across the groups of donors ranging from 47.9% in the donor with type 2 diabetes to 53.5% in donors with type 1 diabetes. A similar amount of cells co-expressed α-actin and CD14 (actin+CD14+). Data are expressed as the mean of the percentage of the sub-population on the total amount of cells positive to α-actin.*

3.5 DISCUSSION

Results discussed in the previous chapter suggested alterations within the distribution of the mononuclear cell sub-populations in circulating blood among people with diabetes. In particular, results advocated an increase in the amount of circulating activated macrophages (CD68+) and possible variations in the amount of circulating cells positive to the endothelial progenitor cell marker (CD34+). Those findings suggested that the nature of diabetes as an inflammatory condition might have an impact on the outcome of *in-stent* restenosis due to the presence of a higher amount of circulating activated macrophages, thus enhancing the

inflammatory response in the early phases following implantation (Farb 2002). In particular, the quantification of the cell sub-populations may represent an independent risk factor for the identification of the predisposition in developing *in-stent* restenosis at the moment of intervention in addition to the traditional risk factors represented by clinical and biochemical data.

Different studies have demonstrated the ability of monocyte-derived macrophages to differentiate into myofibroblasts *in-vitro* under different stimuli (Kuwana 2003, Rehman 2003, Boilson 2008) or in contact with foreign material such as stainless steel (Stewart 2009). *In-vitro* studies have shown that after 5-7 days the adhering monocytes tend to assume a spindle-like shape typical of myofibroblasts, cellular component expressing morphological and functional characteristic of both SMC and fibroblasts (Stewart 2009). This suggests that monocytes/macrophages intervene in the deposition of the neointimal tissue during the later phases of restenosis due to their phenotypical plasticity in addition to the leading role played during the initial inflammatory reaction following vascular injury and strut deposition (Santin 2005, Stewart 2009, Mesure 2010).

The trans-differentiation potential of circulating mononuclear cells has been investigated in recent studies where the role of monocytes was expanded from exclusive precursor of phagocytic cells such as macrophages and dendritic cells acting as scavengers and pro-inflammatory cells in the immune reaction to a potential source of precursor of different cell types, thus contributing to tissue homeostasis and to repair processes following tissue injuries (Kuwana 2003, Gordon 2005, Waldo 2008). In particular, in a study published by Kuwana et al. (2003) a cell sub-population expressing the marker for monocytes (CD14) in conjunction with the marker for haematopoietic and endothelial progenitor cells (CD34), the general leukocyte marker (CD45) and the type I collagen was identified. The sub-population was shown to act as a progenitor able to differentiate into cell types of the mesenchymal lineage in *in-vitro* cultures under specific growth factors. It has therefore been hypothesized that those cells can

infiltrate peripheral tissues to contribute to the tissue homeostasis replacing damaged or senescent cells (Kuwana 2003). More studies have identified cell sub-populations co-expressing markers for haematopoietic progenitor cell (CD34) with the general marker for leukocytes (CD45) and with the marker for monocytes (CD14). Those were shown to be able to generate spindle-like cells in culture and to differentiate into endothelial-like cells to participate in the regeneration of the vasculature (Rehman 2003, Boilson 2008). In addition, fibrocytes have been identified as progenitor of vascular myofibroblasts intervening in processes of tissue repair, wound healing and *in-stent* restenosis. The identification of fibrocytes has been attributed to the co-expression of the marker for haematopoietic progenitor cells (CD34), the general marker for leukocytes (CD45) and collagen I (Pilling 2009, Forte 2010).

Furthermore, a circulating cellular sup-population expressing the marker for monocyte (CD14) in conjunction with α-actin has been identified as precursor of smooth muscle-like cells, thus confirming the potential contribution of cells of the monocytic lineage to generate myofibroblasts under specific stimuli (Sugiyama 2006).

Therefore, blood mononuclear cells seem to play an important role in the physiological turn-over and tissue repair mechanisms due to their trans-differentiation potential. A better understanding of the distribution of cell sub-populations in the mononuclear cell fraction of the blood could therefore fully elucidate the role of monocytes in the deposition of neointima responsible for the formation of the restenotic plaque and more in general on their role in processes of tissue repair.

Results from this experiment showed that the population of monocytes identified by the expression of CD14 presents a small amount of cells co-expressing the marker for haematopoietic and endothelial progenitor cells (CD34) alone or in combination with the general leukocyte marker (CD45) with the exception of the

recruited donors with type 2 diabetes (figure 3.3). This reinforced the results published by Kuwana *et al.* (2003) confirming the presence in the circulating blood of a sub-population co-expressing the three markers (CD14-CD34-CD45) and identified as progenitor cells of monocytic origin able to differentiate in cells of the mesenchymal lineage and to participate in tissue repair and homeostasis. This cell type can play a key role in the contribution of monocytes to the formation of neointimal tissue during the restenotic process. This finding also corroborates the presence in circulating blood of a sub-population of monocytic origin that previous studies have identified as fibrocytes, progenitor of myofibroblasts intervening in processes of vascular repair and in-stent restenosis (Pilling 2009, Forte 2010). Due to the limited amount of donors available to this study, a statistically significant comparison between the groups was not possible. In addition, the individual variability related to blood composition requires a greater amount of data in order to identify a significant trend in the patient groups. The amount of circulating CD34+, identifying endothelial progenitor cells, was in fact shown to vary rapidly as a consequence of cardiac events and in the presence of cardiovascular risk factors (Fadini 2006). The parallel characterisation of the CD34+ population in buffy coats from the same donors showed that the vast majority of it was represented by cells co-expressing CD14, alone or in combination with CD45 (figures 3.5). This represented a further development of the findings from Kuwana et al. (2003) and of Boilson et al. (2008) who differentiated the CD34+ on the basis of the co-expression of CD45. In particular, Boilson et al. (2008) identified the population co-expressing CD34 and CD45 as cells generating spindle-like cells in culture in opposition to the cells expressing exclusively CD34 and identified as pure precursor of endothelial cells. It was also shown that the CD34+CD45+ sub-population was the only one changing at the variation of cardiovascular conditions being reduced in patients with endothelial dysfunctions (Boilson 2008), thus representing the key-subpopulation in the repair process following cardiovascular injury. The presence of a similar sub-population within the circulating blood, as demonstrated in this study, reinforces the

importance of the trans-differentiation potential of monocytes for their contribution to tissue repair and restenotic processes. In addition to the individual variability, the characterization of those sub-populations can be affected by the difficulties related to the identification of the population in readings obtained with flow cytometry. The signal from CD34+CD45- cells is in fact detected at low frequency and due to their low percentage of this type of cells in the circulating blood the discrimination between signal and background noise could have affected the results (Boilson 2008).

Results showed that, among the circulating population positive to the marker for activated macrophages (CD68), a variable amount ranging from 6% to 20% of cells were co-expressing the CD68 marker alone or in combination with CD45 (figure 3.4). The parallel characterization of the expression of CD34+ showed that the sub-populations co-expressing CD68 alone or in combination with CD45 represented the majority of the CD34 population in recruited control subjects and donors with type 1 diabetes and the 38% of the CD34+ population in the recruited donors with type 2 diabetes (figure 3.6). Data associated with the expression of CD68 showed a higher variability across groups and donors, possibly related to the different degrees of activation and basic inflammatory condition as shown in the previous chapter. The identification of the CD34+CD68+ sub-population in circulating blood is particularly important for the understanding of the restenotic process as a recent study demonstrated that CD34+CD68+ can differentiate in myofibroblasts intervening in the foreign body reaction (Mesure 2010).

In addition, mononuclear cells from buffy coats were treated to identify sub-population of monocytic origin positive to α-actin. Sugiyama et al. (2006) demonstrated the presence in the low density fraction of the mononuclear cells of sub-populations positive to CD14 and α-actin representing a precursor able to form smooth muscle-like cells. The presence of the sub-population represents a further confirmation of the contribution of monocytes-macrophages to the development of restenosis in its later stages. Despite on a small amount of donors,

results from this experiment confirmed the presence of α-actin positive cells in the buffy coats of the donors (figure 3.7). In particular, the main components of the population, although with extremely variable distribution among donors, were represented by cells expressing exclusively the α-actin and by cells expressing α-actin in combination with CD14 (figure 3.8). The results confirmed findings previously published by Sugiyama et al. (2006) and by Simper et al. (2002) demonstrating the presence of precursors of SMCs in human blood (Simper 2002, Sugiyama 2006). The variability across donors in addition to individual differences in blood cell distribution can also be related to the extraction procedure. It has been in fact shown that only the lower density fraction of the mononuclear cells extracted by poly-sucrose gradient contained cells positive to α-actin (Sugiyama 2006).

Although the distribution of the different sub-populations seemed to be generally consistent across the groups, the study analysed a limited amount of donors insufficient to obtain a statistically significant analysis of the data. In addition, the individual variability characterising blood cell distribution highlights the necessity of recruiting a greater amount of donors allowing the identification of possible trends correlating groups of donors or cardiovascular risk factors to a specific sub-population distribution. However, the presence of the sub-populations identified cellular components derived from monocytes potentially contributing to the later phases of the restenotic process, thus representing a focal point for the understanding of the development of the restenotic process. Interestingly, the data seemed to show that the sub-populations presenting a broader variability among donors were the ones positive for CD68 and α-actin. Results presented in this chapter derive from the same group of donors presented in chapter 2. However, the characterization of cell sub-population distribution was possible only for three donors per each group, thus limiting the possibility of any quantitative and statistical analysis of the results. Therefore, results were expressed as mean of the three readings per each cohort, rather than median and range as in the previous

chapter when a statistical analysis on the non-normally distributed data was conducted. Differences in the presence of CD68+ cells (activated macrophages) shown in the previous chapter seemed to be correlated to different degrees of basic inflammatory condition characterizing different donors. This reinforces the hypothesis of the relevance of the characterisation of blood sub-populations to identify individual with increased predisposition to ISR. In addition, an eventual difference in circulating α-actin+CD14+ sub-population could represent a further indication of the predisposition to ISR.

3.6 CONCLUSIONS

The data presented in this chapter confirmed that the mononuclear fraction of circulating blood is composed of sub-populations characterised by a trans-differentiation potential as identified in previous studies (Kuwana 2003, Rehamn 2003, Boilson 2008, Pilling 2009, Forte 2010). In particular, results confirmed the presence of sub-populations identified as precursor of myofibroblasts intervening in the formation of the neointimal plaque in the restenotic process. This suggested that the sub-populations may be identified as potential therapeutic or diagnostic targets for the identification of the predisposition or for the prevention of the development of *in-stent* restenosis at the moment preceding the intervention. In addition, results discussed in this chapter provided a characterization of circulating mononuclear cell populations on buffy coats freshly isolated from healthy donors and donors with diabetes. Despite no differences among groups were possible to be identified due the limited amount of donors, this study provided a novel contribution to the data previously published that identified the sub-populations in *in vitro* studies following cellular stimulation with medium spiked with specific growth factors. Furthermore, the study suggested that a thorough analysis on the sub-population distribution in a greater amount of donors

could provide with a better understanding of the sub-population majorly involved in the trans-differentiation process. In addition, a more extended comparison of sub-population distribution among cells from selected donors with diabetes and healthy subjects could provide with a better insight in the contribution of the trans-differentiation of sub-populations to the restenotic process.

Variations in the phenotypical expression of macrophages were seen after long-term contact with stainless steel, material of choice for the production of bare metal stents (Stewart 2009).

The next steps of this study will be represented by the investigation of the acute effect (overnight incubation) of monocytes-derived macrophages to the metal. In particular, the analysis will investigate potential changes in the cell sub-population distribution, in the phenotypical expression and in the release of growth factors from mononuclear cells isolated from the three cohorts of donors.

CHAPTER 4

BIOMATERIAL SUBSTRATE INFLUENCE ON MONONUCLEAR CELL TRANS-DIFFERENTIATION

4.1 INTRODUCTION

Histological analysis of stented coronaries has shown the presence of macrophages throughout all the phases of the restenotic plaque formation (Farb 2002, Santin 2005). The role attributed to inflammatory cells has therefore been extended from key players in the activation of the implant-induced inflammatory response during the early phases to direct participants in the neointimal tissue formation. It has been hypothesized that macrophages contribute to the in-growth of neointimal tissue both through the release of growth factors promoting the proliferation of smooth-muscle cells (SMC) and through their trans-differentiation into smooth muscle cells capable of synthesising new hyaluronan-rich extra-cellular matrix and to their differentiation into myofibroblasts (Bayes-Genis 2002, Santin 2005, Stewart 2009). Previous work and data collected and presented in chapters 2 and 3 demonstrated the presence of mononuclear sub-populations in the circulating peripheral blood that are able to differentiate into myofibroblast- and smooth muscle cell-like cells. Sub-populations of these cells appear to undergo trans-differentiation *in vitro* under specific stimuli. Therefore, results suggested that the quantification of their percentage in an isolated buffy coat sample could allow the identification of patients prone to develop *in-stent* restenosis. Previous *in vitro* studies have also demonstrated that mononuclear cells incubated for seven days on stainless steel develop a phenotype characteristic of myofibroblasts, assuming a spindle-like shape and expressing α-actin, a typical marker identifying SMC (Stewart 2009). Studies have also shown an increase in the release of post-inflammatory cytokines at different incubation times of macrophages on stainless steel *in vitro* (Santin 2004, Harrison 2007).

4.1.1 Foreign body reaction

4.1.1.1 Definition and characteristics

The complex cascade of non-specific reactions driven by the immune system following contact with foreign materials is defined as foreign body reaction (FBR) as previously described in section 1.1.3.3. The initial process is a result of tissue injury and can be compared to a wound healing process altered by the presence of the foreign body that is the medical device (Luttikhuizen 2006). The process is characterized by increased permeability of the vascular wall to facilitate the extravasation of cells under the influence of chemokines and other inflammatory mediators released by platelets following the activation of the coagulation cascade (Luttikhuizen 2006). Leukocytes attracted to the site of the lesions trigger the inflammatory response through the release of pro-inflammatory cytokines such as TNF-α, IL-1 and IL-6 and the promotion of local vascularisation. Macrophages are attracted to the site of the lesion to protract the inflammatory reaction and to facilitate the wound healing both through their phagocytic properties (clearing the site of bacteria and tissue fragments) and through their later secretion of growth factors able to recruit tissue cells (Luttikhuizen 2006). The adsorption of fibrinogen and other proteins on the surface of biomaterials are a key factor in cell adhesion and activation of macrophages. In the development of biomaterials the chemistry of the surface is of great importance as it influences the composition of the adsorbed protein layer as well as the conformation of the adsorbed proteins that can acquire antigenic properties thus inducing the inflammatory response (Santin 2004, Luttikhuizen 2006). In the case of degradable biomaterials the reaction is protracted until the material is completely removed from the site by phagocytes (neutrophils and macrophages). In the case of non-biodegradable biomaterials of a size too big to be phagocytized, a capsule is formed to “wall-off” the foreign material from the surrounding tissue (Luttikhuizen 2006, Mesure 2010).

4.1.1.2 Macrophages and FBR

As described in section 1.1.3.3, macrophages are attracted to the site of the lesion by fibrin, antibodies and proteins adhering on the material surface. Once in the site of the injury, macrophages release pro-inflammatory cytokines such as interleukin-1 (IL-1), IL-6 and TNF-α to sustain the inflammatory reaction (Luttikhuizen 2006). The release of pro-inflammatory cytokines by macrophages was shown to be influenced by the chemistry of the material surface and consequent protein adsorption (Luttikhuizen 2006). Following activation, macrophages tend to fuse to form poly-nucleated giant cells in the attempt to eliminated particles that are too large to be phagocytized by single cells. However, in the case of non-degradable materials phagocytosis is not possible and macrophages play a key role in the formation of the capsule surrounding the foreign body. This is in fact mainly formed of an internal layer of macrophages surrounded by different layers of myofibroblasts (Mesure 2010). A recent study has hypothesized that in this case macrophages abandon their classical role of phagocytic cell, switching from pro-inflammatory status towards the promotion of wound healing through the release of growth factors that enhance the deposition of extra-cellular matrix (Mesure 2010) and consequently the activation of SMC. The same study has shown that, during FBR, primitive cells are attracted to the site to generate myofibroblasts, main components of the tissue forming the capsule. The study demonstrated the presence of a CD68+CD34+ population in the fibrotic tissue generated during the FBR. The sub-population was shown to be responsible for the formation of myofibroblasts, thus confirming the direct intervention of macrophages in the formation of myofibroblasts. The same study demonstrated that the CD68+CD34- sub-population was not able to differentiate into myofibroblasts (Mesure 2010).

4.1.2 Cytokines

Cytokines represent a heterogeneous group of small proteins synthesized by the majority of cells and acting as signalling molecules. They coordinate intercellular communication and cell migration, thus regulating immunity, inflammation and haematopoiesis in response to noxious events requiring cell intervention (Dinarello 2000, Dinarello 2007). Cytokines are involved in cell proliferation, differentiation and migration intervening in reaction to infectious disease and regulating inflammatory response following injuries. Deregulations in cytokine functions can have pathological consequences (Dinarello 2007). Based on their role played in the inflammatory reaction cytokines can be divided into:

- Pro-inflammatory cytokines
- Anti-inflammatory cytokines

Pro-inflammatory cytokines regulates the expression of genes secreting factors that sustain the inflammatory reaction. Anti-inflammatory cytokines suppress or reduce the production or the activity of pro-inflammatory cytokines reducing the intensity of the inflammatory cascade. The balance between the secretion of pro- and anti-inflammatory cytokines modulates the impact of the disease (Dinarello 2000).

In addition, chemokines are cytokines released by activated inflammatory and endothelial cells. They stimulate the transfer of leukocytes to tissues favouring their activation and the degranulation of neutrophils in order to coordinate the immune response and intervening in the development of angiogenesis (Luttikhuizen 2006).

4.1.2.1 Tumour Necrosis Factor Alpha (TNF-α)

Tumour necrosis factor-alpha (TNF-α) is a pro-inflammatory cytokine primarily produced by macrophages and monocytes. It activates the inflammatory cascade in cooperation with other pro-inflammatory cytokines (Dinarello 2000). TNF-α is

released by macrophages after contact with ceramic and metal particles (Catelas 1999, Suska 2003) in combinations with pro-inflammatory interleukins to trigger inflammatory response. TNF-α is low in cells in the absence of external stimuli and it is synthesized *de novo* by live cells under specific inflammatory stimuli (Catelas 1999, Suska 2003). In addition, TNF-α has been shown to act synergistically with IL-2 to induce endothelial adhesion molecules favouring the migration of leukocytes at the site of inflammation (Dinarello 2000, Suska 2003).

Interestingly, the role played by TNF-α in cell growth, differentiation and apoptosis has been shown to be relevant to cardiac homeostasis. The amount of circulating TNF-α is increased in individuals with heart failure, demonstrating a correlation between the cytokine and heart disease and identifying the cytokine as potential therapeutic target for individuals prone to cardiovascular disease (Sack 2002).

4.1.2.2 Platelet-Derived Growth Factor-BB (PDGF-BB)

Platelet-derived growth factors are mitogenic and chemotactic molecules that stimulate the migration and proliferation of mesenchymal cells including smooth muscle cells (Krettek 2001). PDGF is secreted by a variety of cell types such as platelets, smooth muscle cells, endothelial cells and macrophages. It can be present as a hetero- or homo-dimer of aminoacidic chain A and B linked by disulphide bonds (Hammacher 1988, Krettek 2001). The homodimer PDGF-BB was shown to have an essential role during the development of atherosclerosis through modification of macrophages and smooth muscle cells in the vascular wall. This growth factor was shown to stimulate the proliferation of smooth muscle cells, to inhibit the secretion of macrophage stimulating factor (MCSF) and to induce the expression of scavenger receptors in macrophages thus favouring the initial formation of the atherosclerotic plaque (Shimada 1992, Inaba 1993). PDGF exerts a strong effect on SMC migration and proliferation, representing a key component in tissue remodelling. In addition, PDGF-BB is the

only isoform of the growth factor interacting with all the PDGF receptors (Pintucci 2005). PDGF-BB isoform also exerts an angiogenic role through the interaction with the receptor PDGF-β (Battegay 1994). Furthermore, PDGF and TGF-β1 synergistically increase the synthesis of versican and hyaluronan in the extra-cellular matrix in arterial SMC confirming the importance of PDGF in the homeostasis of the vascular endothelium and in its remodelling during the early phases of atherosclerosis (Wight 2004).

4.1.3 Macrophages, cytokines and *in-stent* restenosis

Macrophages are able to synthesize different cytokines to sustain the inflammatory reaction in the early phases of FBR (Luttikhuizen 2006). Macrophages were shown to synthesize pro-inflammatory cytokines, particularly TNF-α, in response to contact with material surfaces or particles (Catelas 1999, Suska 2003, Luttikhuizen 2006) and in contact with stainless steel (Santin 2004). However, the release of TNF-α did not seem to be predominant following contact with stainless steel compared to growth factors such as TGF-β1 and PDGF-BB, a biochemical activity typical of a post-inflammatory status of macrophages that favours proliferation of SMCs and ECM deposition (Santin 2005). Furthermore, a study investigating the release of TNF-α from macrophages in contact with biomaterials provided evidence of individual variability in the release of the pro-inflammatory cytokine (Schachtrupp 2003). Further studies investigated the release of cytokines and growth factors by macrophages in contact with stainless steel at different incubation times or conditions. A recent study showed that macrophages from healthy donors and donors with diabetes incubated on stainless steel in high glucose concentration (hyperglycaemia-mimicking conditions) showed a significant increase in the release of TGF-β1 and PDGF-BB after three hours of incubation on stainless steel, thus suggesting that the contact with the metal stimulates respectively ECM production and SMC proliferation (Harrison

2007). Similar findings were confirmed by a study demonstrating significant increase in the release of TGF- β1 and PDGF-BB from macrophages incubated on stainless steel for seven days (Stewart 2009).

4.2 AIMS

The experimental work described in this chapter aimed to assess whether the inflammatory condition associated with diabetes can be related to differences in their response to stainless steel and to the predisposition to *in-stent* restenosis. The comparison of the mononuclear cell activation when in contact with the metal surface and with extra-cellular matrix (ECM) was chosen in the attempt to elucidate the differences in the contribution of the two substrates to the development of *in-stent* restenosis (Stewart 2009). The acute response triggered by the contact of mononuclear cells from healthy and diabetic donors with stainless steel was assessed through:

- Phenotypical characterization of mononuclear cells and their sub-populations adhering on the surfaces.
- Measurement of the release of pro- and post-inflammatory cytokines after overnight incubation on the surfaces of stainless steel simulating the stent surface and of extra-cellular matrix mimicking the blood vessel wall surface after de-endothelialisation caused by the device expansion.

4.3 MATERIALS AND METHODS

4.3.1 Recruitment of volunteers and blood collection

Data discussed in this chapter were obtained from the same group of donors as described in chapter 2. The recruitment process and the criteria applied in the selection of donors are explained in Section 2.4.1.1. The procedure for the collection of blood and its treatment are described in Section 2.4.1.2.

4.3.2 Experimental surfaces and conditioning

Experiments aimed to assess the differences in inflammatory reactions and cell behaviour when in contact with different artificial surfaces relevant to the understanding of the restenotic process. Three different surfaces were tested:

- Stainless steel (St; AISI 316L) discs of 15 mm diameter provided by Goodfellow, UK (024-275-44). The discs were disinfected with 70% (v/v) Ethanol/deionised water mixture and washed three times with sterile PBS prior to use. Stainless steel was chosen because it represents the material of choice for the production of traditional bare metal stents.
- ECM-coated wells were obtained by layering a commercially-available ECM gel extracted from Engelbreth-Holm-Swarm murine sarcoma (Sigma Aldrich, UK, catalogue number E1270). The gel was suspended in physiological glucose concentration DMEM-5.5mM glucose (PAA Laboratories or Sigma Aldrich, UK) and stored at 4^{o}C in order to maintain it in its liquid form. The bottom of the wells were coated with 150µl of soluble ECM gel that was transferred into each well of a 24-well tissue culture plate under sterile, cold conditions and then incubated for 30 minutes at 37^{o}C to induce gel formation and to obtain complete coating of

the wells. ECM was chosen to mimic the environment surrounding the stent strut after implantation and expansion of the device particularly representing the de-endothelialized vessel wall (Stewart 2009)

- Tissue culture plate plastic was tested as a control surface.

All the surfaces were pre-conditioned with an incubation of 30 minutes at 37^{o}C with 200µl per well of freshly isolated human platelet-rich-plasma collected after centrifugation of the blood on Histopaque gradient. The incubation with plasma induced the adsorption of proteins onto the surfaces in order to mimic the conditioning of the surface after their exposure to the circulating blood (Santin 2004, Stewart 2009). Indeed, when biomaterials are implanted, proteins from the surrounding environment tend to adhere onto their surfaces with different pattern according to the differences in the physico-chemical composition of the material. The layer of adsorbed proteins represents a key point in the future interaction between biomaterial and human body mediating the inflammatory response (Luttikhuizen 2006).

After rinsing the surfaces three times with sterile PBS to remove the excess of plasma proteins, $5x10^5$ cells were seeded and incubated in 1ml of low glucose (1000mg/l) DMEM (Sigma Aldrich or PAA Laboratories) for 3 hours at 37^{o}C. The culture medium was then replaced with fresh medium in order to remove the non-adherent cells mainly represented by lymphocytes that do not grow on surfaces (Haston & Wilkinson 1982). Culture medium was replaced with fresh medium and cells incubated overnight at 37^{o}C at 5% CO_2.

Overnight incubation was chosen in the attempt to highlight differences in the acute response of inflammatory cells to the contact with the metal across groups of donors. This could elucidate on the differences in the reactivity of macrophages at the moment or immediately after the implant procedure. A previous study has shown changes in the phenotype of macrophages as the effect of a prolonged (7 days) contact with stainless steel (Stewart 2009), thus showing that the contact

with the metal may trigger phenotypical changes regardless of the conditions of the donors. The choice of overnight incubation could highlight differences between groups of donors in relation to morbidities and basic health conditions correlated to the diabetic condition. An increased activation and an early trend in switching the phenotype could in fact be related to a different degree of activation of the inflammatory cells potentially correlated to the development of in stent restenosis.

4.3.3 Collection of supernatants

Cells were seeded into tissue culture plates as described above and incubated overnight at 37^{o}C in 5% CO_2. After incubation, supernatants were collected in 1.5 ml Eppendorf polypropylene tubes, centrifuged at 10,000xg for 5 minutes in order to sediment floating cells and debris and the resulting supernatants were finally transferred in a fresh 1.5 ml Eppendorf tube to be frozen at -70^{o}C until use.

4.3.4 Immunocytochemistry

4.3.4.1 Immunochemistry: description of the technique

Immunocytochemistry is a technique used to assess the presence of a protein or antigen in cells by using a specific antibody, which binds to it thus allowing visualization and examination under a microscope (Bocksteins 2012). It is a valuable tool for understanding the expression, localization and interactions of proteins at the cellular level. The preparation of samples to be used for immunocytochemical analysis differs depending on the experiment. The technique is therefore extremely versatile and widely used for cells or cell component identification in research as well as representing a valid diagnostic tool for clinical application (Bocksteins 2012).

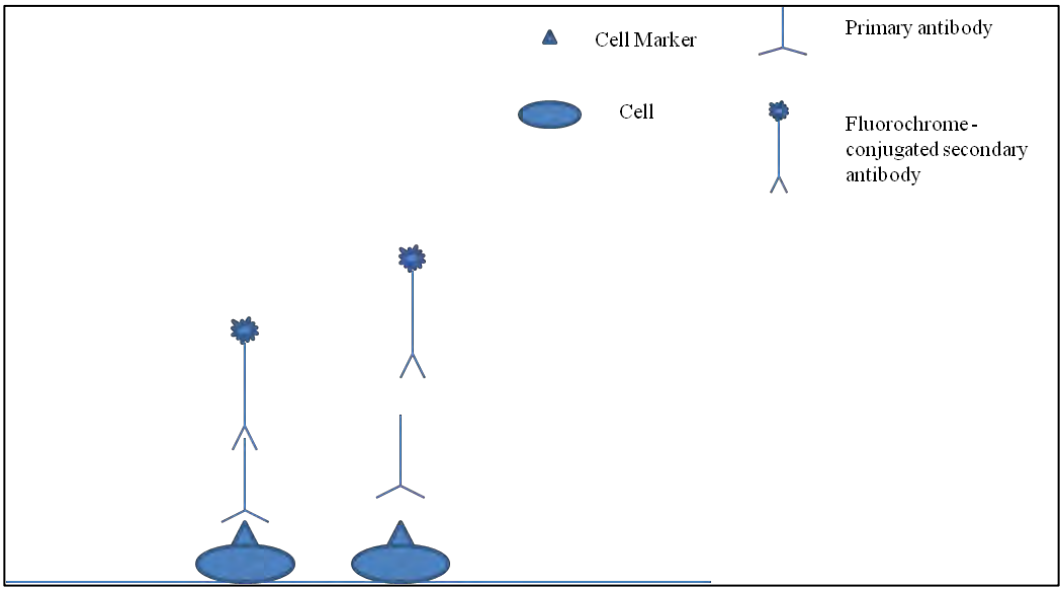

Figure 4.1 Schematic representation of immunocytochemistry on adhering cells. *Immunochemistry is based on the specificity of the bond of a primary antibody specific for a specific domain of a protein (e.g. a typical cell marker). The secondary antibody conjugated to the fluorochrome allows the visualization of the complex under fluorescence microscope.*

Cells to be stained can be attached to a solid support to allow easy handling. The shared feature of the various types of available protocols is that the whole cell is present on the slide surface. Reactions taking place in the nucleus or the identification of intracellular components require the use of permeabilizing cells using detergent (Triton X-100 or Tween-20) and the use of organic fixatives (acetone, methanol, or ethanol) becomes necessary (Bocksteins 2012).

The experimental procedure applied in this study is illustrated in figure 4.1. Cells adhering in monolayers on different surfaces were stained to evaluate their phenotypical expression after incubation on the experimental surfaces. Following fixation, cells were incubated with primary antibodies specific for the markers of interest followed by incubation with a species-specific secondary antibody. The specificity of the bond of primary antibody-cell marker is crucial for the

identification of the protein of interest. The secondary antibody was conjugated to a molecule exhibiting fluorescence allowing visualization of the marker of interest under fluorescence microscope.

Results from immunocytochemistry can be affected by unspecific binding of antibodies. A "blocking" step with a protein solution (i.e. albumin) is therefore used prior incubation with primary antibody to block all the potential unspecific sites the antibody could bind, thus originating a false positive. Control samples are generally prepared to verify the absence of unspecific binding or cross-reactivity between the selected antibodies (Bocksteins 2012).

4.3.4.2 Immunochemistry of mononuclear cells adhering on tested surfaces

After overnight incubation and removal of supernatants, cells adhering on surfaces were washed three times in sterile PBS and fixed with an incubation of 30 minutes in 3.7% (v/v) paraformaldehyde (Sigma Aldrich, UK) in PBS at room temperature. After three washes with PBS, cells to be stained for intracellular markers were permeabilized with an incubation of 10 minutes in a 0.2% (v/v) solution of Triton X-100 (Sigma Aldrich, UK) in PBS. The cells that did not need to be stained for intracellular markers were left in PBS during the incubation with Triton. After further three washes with PBS, cells were incubated with 100µl or 200µl of solutions of primary antibodies as described in Table 4.1 diluted in 1% (w/v) Bovine Serum Albumin (BSA-Sigma Aldrich,UK; catalogue number A7030) in PBS for 2 hours at room temperature. The working dilutions for each antibody were chosen either following manufacturers' instruction or through titration experiments in which serial dilutions of the antibodies were tested in order to determine the optimal concentration. The list of primary antibodies used in the experiment and their working dilutions are reported in Table 4.1. Negative controls to verify the specificity of the recorded fluorescence were prepared by adding secondary antibody to wells where cells were not seeded.

After completing the incubation with primary antibody solutions, cells were washed three times with PBS followed by incubation for 1 hour at room temperature in the dark with 100 µl of a 1:5000 solution of the secondary antibody (table 4.2) in 0.1% (w/v) BSA in PBS. Cells were then washed three times with PBS and counterstained with DAPI to identify the cell nuclei. Images were taken using an inverted-light fluorescence microscope at different magnifications (x20 and x40).

Table 4.1 Primary antibodies used for immunocytochemistry. List of primary antibodies and their working dilutions used for cell phenotypical characterization through immunocytochemistry.

Cells identification	Marker	Dilution	Antibody/Company
Activated macrophages	CD68	1:100	Mouse monoclonal anti-human CD68(KP1) Santa Cruz Biotechnology, Inc. Cat No sc-20060
Haematopoietic and endothelial progenitor cells	CD34	1:100	Mouse monoclonal anti-human CD34 Caltag Laboratories.
Smooth muscle cells (SMC)	α-actin	1:100	Mouse monoclonal anti-human smooth Muscle Actin Dako-Cytomation UK L.t.d

4.3.5 Preparation of cells retrieved after overnight incubation on surfaces for flow cytometry

Cells isolated through the Boyum's method as described in section 2.4.1.2 were incubated overnight onto surfaces as described in section 4.3.2. After collection of supernatants as described in section 4.3.3 cells were washed with PBS and detached from the surfaces

through incubation for 5-10 minutes in 200µl of TrypLe Express (Gibco-Life Technologies) at 37°C.

Table 4.2 Secondary antibody used for immunocytochemistry. Secondary antibody and working dilutions used for the immunolabelling in the immunocytochemistry experiments.

Antibody	Fluorescent molecule-Colour	Working dilution	Company
FITC-Goat Anti-Mouse IgG+IgA+IgM	Fluorescein Isothiocyanate (FITC)- (Green)	1:5000	Zymed Laboratories

TrypLe Express is a trypsin-free solution able to detach the cells through the action of EDTA and more gentle than trypsin-based medium on the cell surface. It was chosen to reduce damages to proteins on the cell surface in order to optimize results for flow cytometry. The reaction was stopped by the addition of 400µl of DMEM and the cell suspension spun at 2000xg for 5 minutes to obtain the pellet. Cell pellets were then re-suspended in 400 µl of DMEM and prepared for flow cytometry according to the protocol described in 2.3.2.5. Following staining, cells were immediately sent to the laboratory to be analysed via flow cytometry. The tubes were triple-stained combining CD45-PECy5, α-actin-PE and CD68-FITC using antibodies and working dilutions as described in sections 2.3.2.5 and 3.3.2.

4.3.6 Enzyme-linked Immunosorbent Assay

4.3.6.1 Principle of the method

Enzyme-linked immunosorbent assay (ELISA) is an immunoassay used to determine and quantify the amount of proteins or antibodies in samples. It is widely used as a diagnostic tool to verify the presence of disease-related

antibodies in blood or for its quantification potential in research experiments (Crowther 2001). ELISA combines the specificity of the bond antibody-antigen with the sensitivity of simple enzyme assays. The assay is generally used to measure the amount of a specific protein in the samples through the addition of a protein-specific antibody followed by secondary interaction with a secondary antibody coupled to reagents that generate measurable reactions following interaction with a specific substrate added. Most commonly ELISA kits use secondary antibodies coupled to enzymes that develop colorimetric reactions following interaction with the substrate. The colour developed can be measured with a spectrometer and the obtained optical density values will be proportional to the protein of interest binding the antibodies. The quantification requires comparison to a standard curve obtained with increasing known amounts of the protein to be detected. Different variations in the sequence of reagents used in the assay can be found. In this experiment the kits used the "sandwich ELISA" technique. This involved the use of a "capture" antibody attached to the bottom of the wells in 96-well plates. The protein to be measured bound the capture antibody. A "detection" antibody recognizing the same protein was added, supporting the development reaction and allowing identification and quantification. This can be directly coupled to the enzyme generating the colorimetric reaction with the substrate or the addition of a conjugated-secondary antibody can be necessary (figure 4.2) (Crowther 2001).

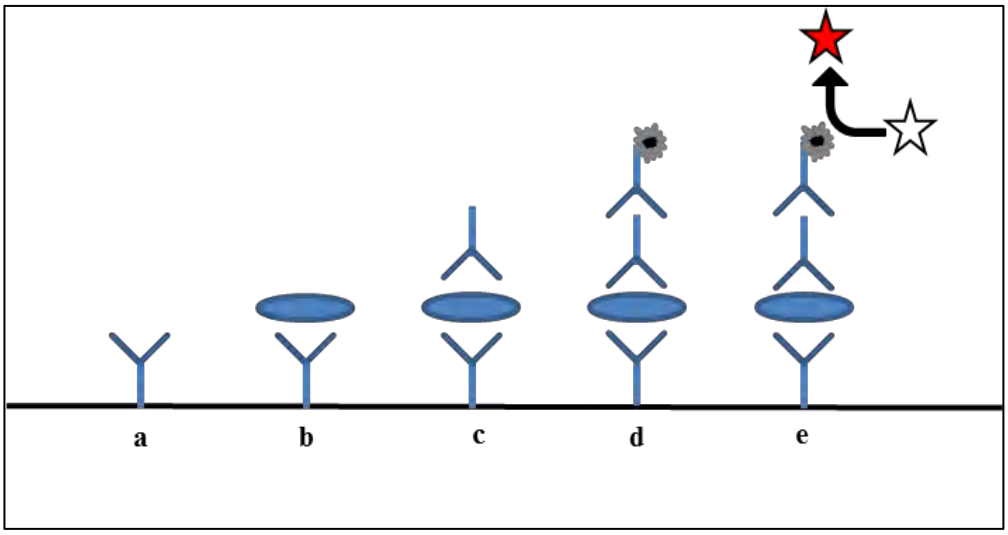

Figure 4.2 Schematic representation of a sandwich ELISA. *Different steps involved in a sandwich ELISA procedure involve the coating of plate with a capture antibody (4.2a) able to bind to the protein of interest in the samples (4.2b). An antibody specific for the same protein (detecting antibody) binds specifically to the protein of interest (4.2c) followed by incubation with an enzyme-linked secondary antibody that in turn binds to the detecting antibody (4.2d). The addition of a substrate reacting with the enzyme develops the colorimetric reaction (4.2e).*

The performance of the assay can be influenced by the choice of the pair of antibodies based on the specificity of their binding to the antigen epitopes. Key factors in the experimental procedure are represented by the "washing steps" intercalating the incubation with antibodies in order to eliminate excess of reagents and avoid non-specific binding or undesired background. Background noise must be verified using control wells containing the medium samples are dissolved in. In addition, the concentration of the protein of interest in the samples must be included in the optimal range measurable through the assay to ensure linearity between concentration and measured optical density (Crowther 2001).

4.3.6.2 ELISA of cytokines and growth factors released by mononuclear cells adhering on test substrates

Supernatants (1ml per sample) collected as described in section 4.3.3 were used to assess the amount of cytokines playing an essential role in the development of in-stent restenosis released during the overnight incubation of monocytes-derived macrophages on experimental surfaces. The release of cytokines was tested using solid phase sandwich ELISA as described below. All results obtained from the tests were normalized dividing the amount of cytokine in the original sample by the overall amount of proteins measured through the method described by Bradford (Bradford 1976) and explained in section 4.3.6.5. The amount of proteins found in samples was considered proportional to the amount of cells adhering onto the surfaces. The normalization of the data aimed to reduce artefacts due to measurement of increase in the amount of cytokines due to higher number of cells rather than to effect due to contact with biomaterials or environmental conditions.

Each sample (n=10 per cohort of donor and experimental surface) was loaded in duplicate. Results are expressed as mean ± standard error and analysed using paired student t-test.

4.3.6.3 TNF-α ELISA

The release of Tumour Necrosis Factor-alpha (TNF-α) was measured using the Human TNF-α ultrasensitive kit purchased from Invitrogen Corporation (Cat. Number KHC3014C). The use of ultrasensitive kit allowed measuring low levels (ranging from 0 to 32pg/ml) of TNF-α in the samples. The amount of TNF-α in the samples was first assessed through preliminary experiments to ensure that the amount of TNF-α in samples corresponded to the detectable range of the kit. All samples were therefore diluted 1:4 with standard diluents buffer supplied by the company prior loading into the wells in order to obtained concentrations of TNF-α measurable within the optimal range of the ultrasensitive kit. All samples were

loaded in duplicate and two wells with culture medium (DMEM+10%FBS+penicillin/streptomycin) were prepared as background. The test was conducted according to the instructions provided by the company. The kit was based on a solid phase sandwich ELISA providing 96-well plates pre-coated with an antibody specific for human TNF-α and following incubation with biotynilated anti-TNF-α antibody. The colorimetric reaction developed through the reaction of the complex biotin-HRP-conjugated streptavidin with TMB-based reagent and stopped with the provided stop solution. Results were measured at 450nm.

The standard curve was prepared using the human TNF-α standard provided according to the instructions of the company producing a dilution series (0-32 pg/ml) and obtaining the following:

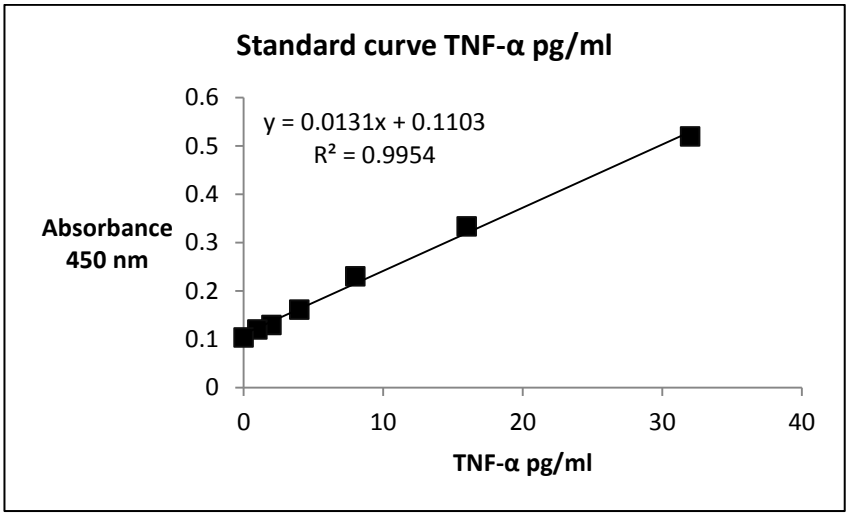

Figure 4.3 Standard curve for TNF-α ELISA. *The standard curve was obtained plotting the absorbance read at 450nm generated by a serial dilution (0-32 pg/ml) of the TNF-α standard supplied by the manufacturer. The data series generated a line with* R^2*=0.9954.*

4.3.6.4 PDGF-BB ELISA

The measurement of the release of Platelet Derived Growth Factor-BB (PDGF-BB) in samples was obtained using the human PDGF-BB ELISA kit from Abcam (Cat. Number ab100625). Samples (100 µl) were loaded in each well in duplicate. The kit was based on a solid phase sandwich ELISA technique. The 96-well plates were pre-coated with an antibody specific for human PDGF-BB. Samples were incubated in the plate for 2.5 hours at room temperature followed by incubations with biotynilated antibody, Horse Radish Peroxidases-conjugated streptavidin, tetramethylbenzidine (TMB)-based substrate and stop solution as described in the manufacturer's instruction. Results from the colorimetric reaction were measured at 450nm.

The standard curve was obtained using the human PDGF-BB standard supplied by the company and producing a serial dilution ranging from 0 to 400pg/ml. However, the values obtained from the highest concentrations of the standard solution were excluded from the standard curve because the results obtained were out of scale and the linearity of the curve was affected. The range of values obtained from the experimental samples fell within the range (0-44.44 pg/ml) as represented in the standard curve (figure 4.4).

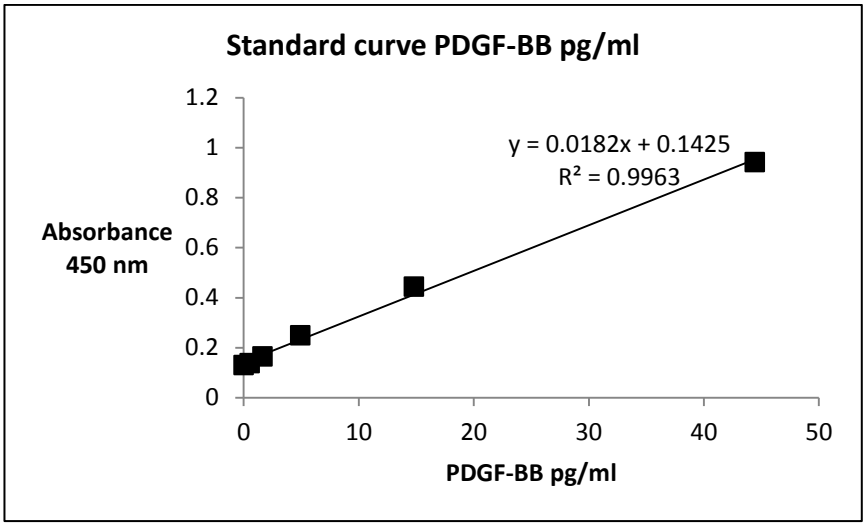

Figure 4.4 Standard curve for PDGF-BB. *The standard curve was obtained plotting the absorbance read at 450nm generated by a serial dilution (0-44.44 pg/ml) of the PDGF-BB standard supplied by the manufacturer. The data series generated a line with* $R^2 = 0.9963$.

4.3.6.5 Protein assay (Bradford method)

In order to normalize the results obtained from the ELISA test, the overall amount of protein in the tested supernatants was evaluated using the Bio-Rad reagent for protein assay. The procedure is a dye-binding assay based on the reaction of Coomassie Brilliant Blues G-250 with the basic and aromatic amino acid residues contained in a protein. Once bound to protein residues the colour of the dye turns from red to blue and the absorbance from 465 nm to 595 nm. For experiments described in this chapter the Bio-Rad Protein Assay reagent was used (Cat Number 500-0006) was used. The reagent was diluted 1 in 5 with deionised water and 200µl were added in each well with 10µl of samples or standards. BSA (Sigma Aldrich, UK) was used as a standard protein as suggested by manufacturer. After producing a serial dilution (0-1000 µg/ml) of a stock solution of 10 mg/ml of BSA in PBS a linear standard curve was obtained (Figure 4.5).

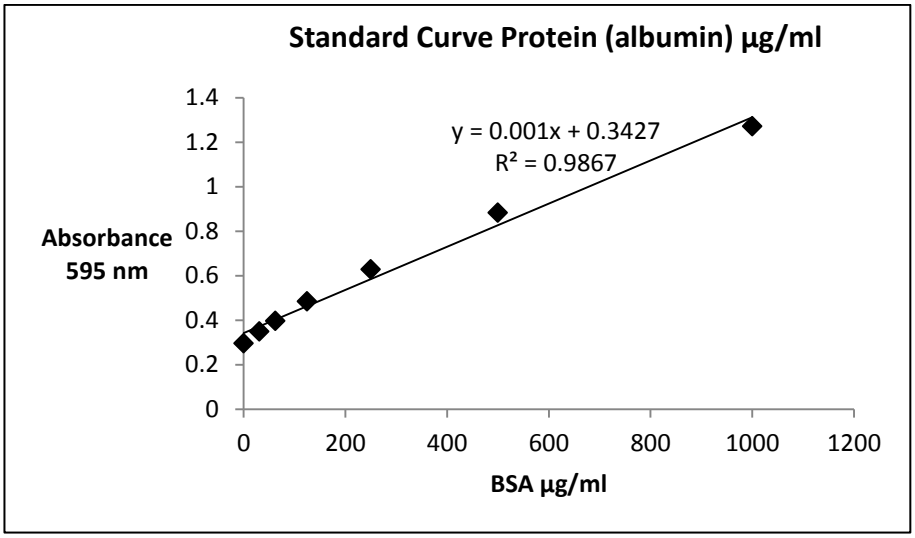

Figure 4.5 Standard curve for protein assay (Bradford method). *The standard curve was obtained plotting the absorbance read at 595 nm corresponding to a serial dilution (0-1000 µg/ml) of bovine serum albumin (BSA). The data series generated a line with* R^2*=0.9867*

After five minutes of incubation at room temperature the absorbance was read at 595nm and the results analysed against the standard curve.

4.4 RESULTS

Mononuclear cells extracted from freshly isolated human blood from healthy donors and from donors with type 1 and type 2 diabetes were incubated overnight on stainless steel to evaluate the response of monocytes-derived macrophages to the material. The response to stainless steel was compared to the response to tissue culture plate plastic and to extra-cellular matrix. The overnight incubation was chosen to evaluate the acute response immediately after implantation. The inflammatory cell response was evaluated through analysis of changes in

phenotypical expression and through the measurement of the release of pro- and post-inflammatory cytokines.

4.4.1 Immunocytochemistry

The images obtained from DAPI counterstain showed that stainless steel represents a good substrate for cell adhesion (figures 4.6c,d) suggesting that, following implantation, macrophages will adhere onto the stent strut initiating the inflammatory reaction. Furthermore, immunostaining confirmed that the adhering cells from donors from all groups expressed the marker for activated macrophages (CD68) after overnight incubation on stainless steel (figures 4.7a,b,c) as well as on tissue culture plastic (figures 4.7d,e,f) and on extra-cellular matrix (figures 4.7g,h,i).

Among the adhering population, cells positive for α-actin were found thus confirming the presence of cells expressing a smooth muscle cell-like phenotype. In particular, the comparison of nuclei counterstain to images of cells stained for CD68 and α-actin across the surfaces showed that while the majority of adhering cells was expressing CD68 (figures 4.8a,b; 4.9a,b; 4.10a,b), only some of the adhering cells were expressing α-actin (figures 4.8c,d; 4.9c,d; 4.10c,d) when incubated overnight on stainless steel. A limited amount of adhering cells were positive to CD34, marker for haematopoietic and endothelial progenitor cells (figures 4.8e,f; 4.9e,f; 4.10e,f). Although the amount of CD34+ cells was variable across donors and areas, the overall amount of CD34+ cells was generally lower than the amount of cells expressing α-actin. Similar scenario was observed across donors and surfaces (figure 4.11).

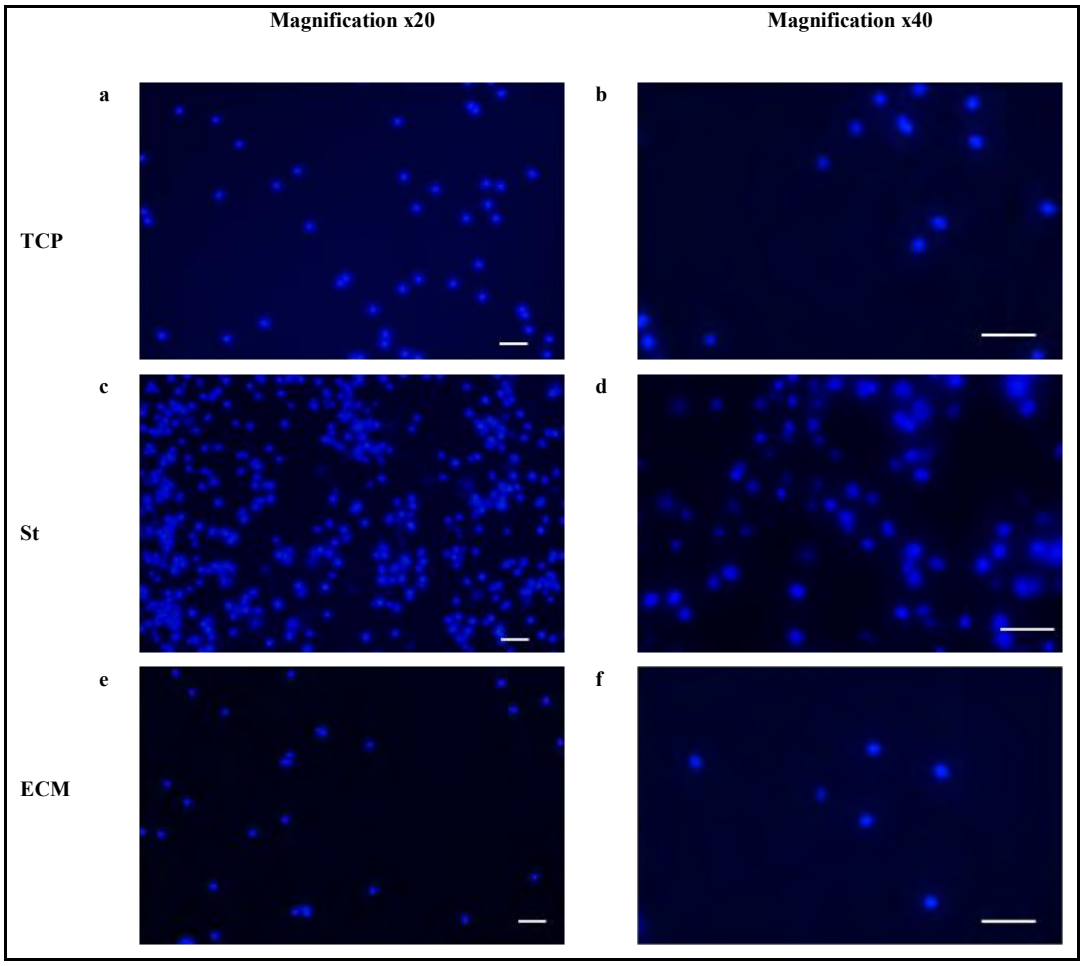

Figure 4.6 Adhesion of mononuclear cells on the experimental surfaces. *DAPI nuclei counterstain of cells from buffy coats from a control subject incubated overnight on TCP, St and ECM. The figure shows that stainless steel is a good surface for cell adhesion (figures 4.6c magnification x20 and 4.6d magnification x40) when compared to TCP (figures 4.1a magnification x20 and 4.6b magnification x40) and ECM (figures 4.6e magnification x20 and 4.6f magnification x40). Size bars indicate 50µm.*

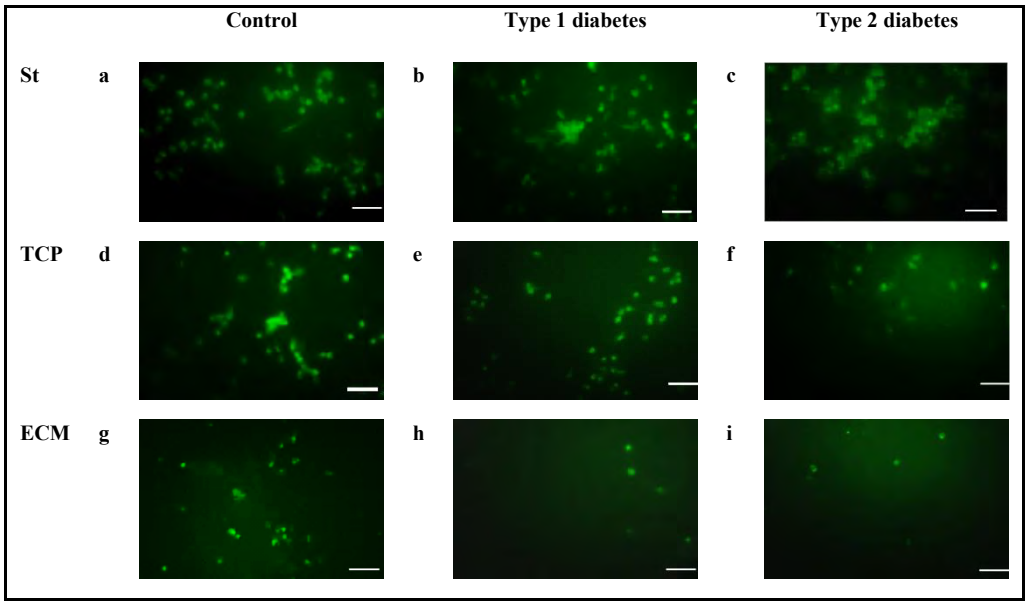

Figure 4.7 Expression of CD68 among mononuclear cells after overnight incubation on the tested surfaces. *The figure illustrates the expression of the marker for activated macrophages (CD68) isolated from one donor per each group after overnight incubation on stainless steel (figures 4.7a,b,c), tissue culture plastic (figures 4.7d,e,f) and extra-cellular matrix (4.7g,h,i) . The trend of the expression of CD68 was similar across groups of donors. Magnification: X40. Size bars indicate 50µm.*

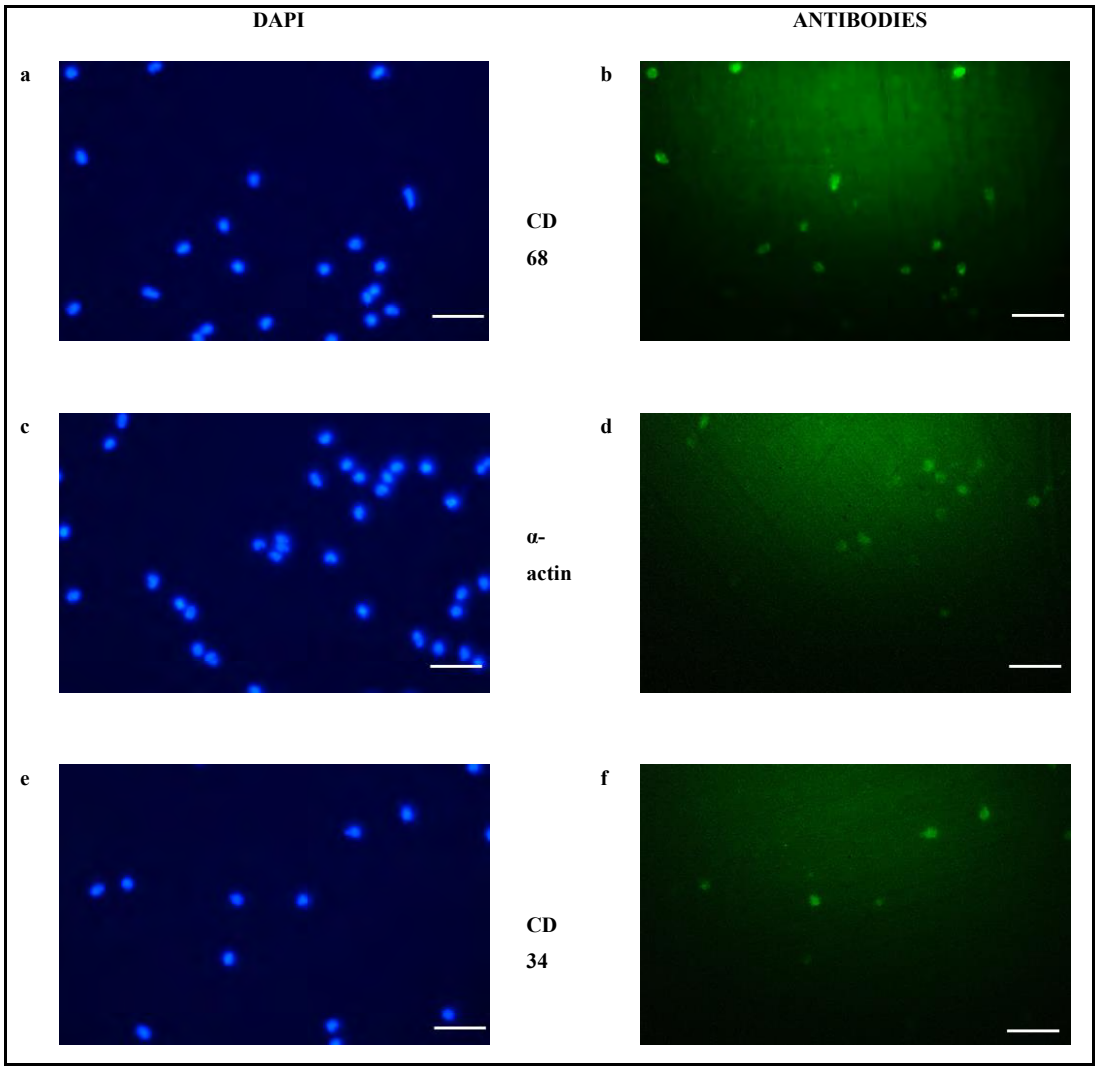

Figure 4.8 Phenotypical expression of mononuclear cells after overnight incubation on stainless steel. *Immunostaining on cells from a control subjects incubated overnight on St with nuclei counterstained by DAPI showed that the adhering cells expressed CD68 (figure 4.8a,b), α-actin (figure 4.8c,d) and CD34, marker for haematopoietic progenitor cells (figures 4.8e, f). Magnification: X40. Size bars indicate 50µm.*

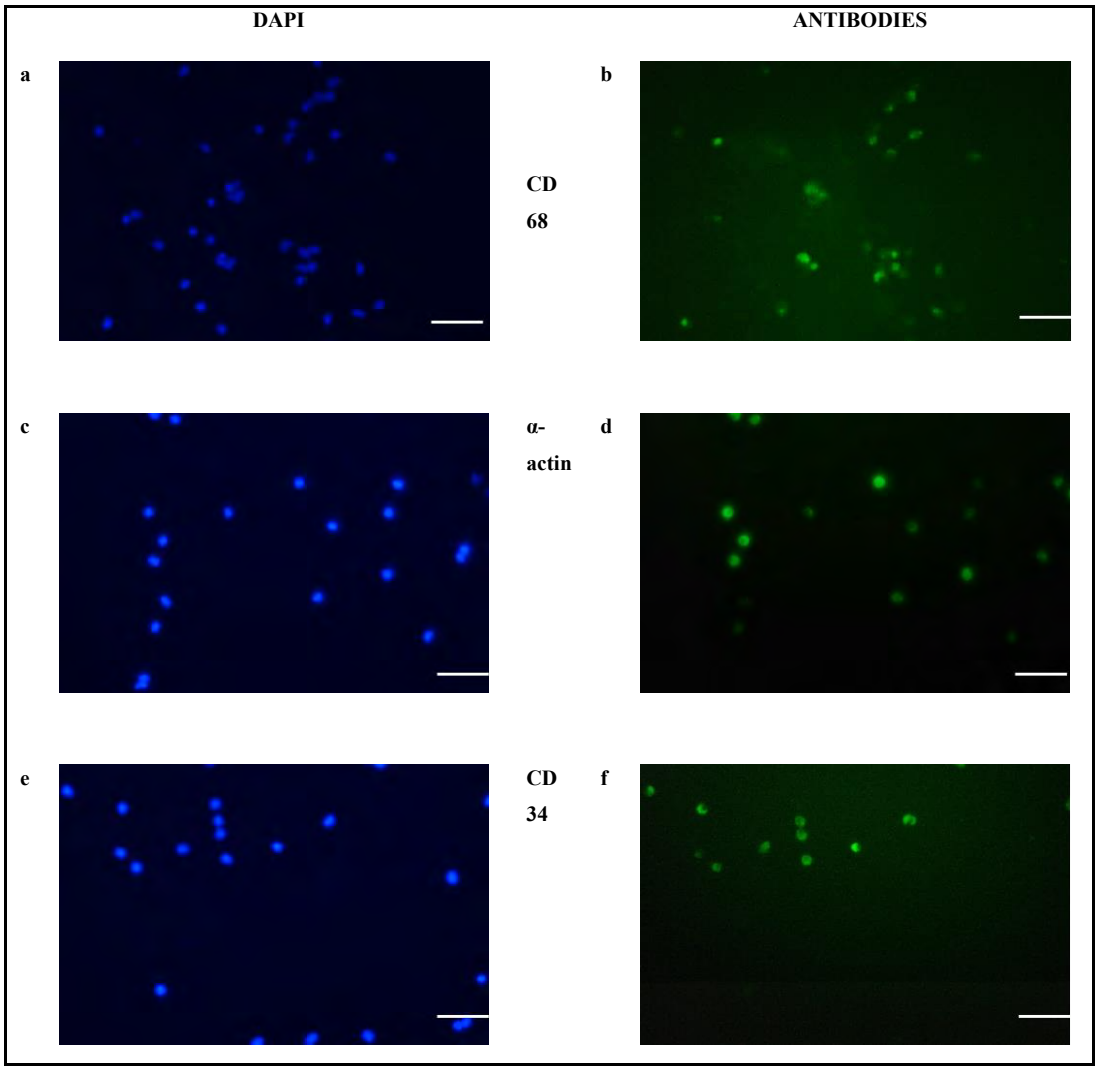

Figure 4.9 Phenotypical expression of mononuclear cells after overnight incubation on extra-cellular matrix. *Immunostaining on cells from a control subjects incubated overnight on ECM with nuclei counterstain by DAPI showed that the adhering cells expressed CD68 (figure 4.9a,b), α-actin (figure 4.9c,d) and CD34, marker for haematopoietic progenitor cells (figures 4.9e,f) . Magnification: X40. Size bars indicate 50µm.*

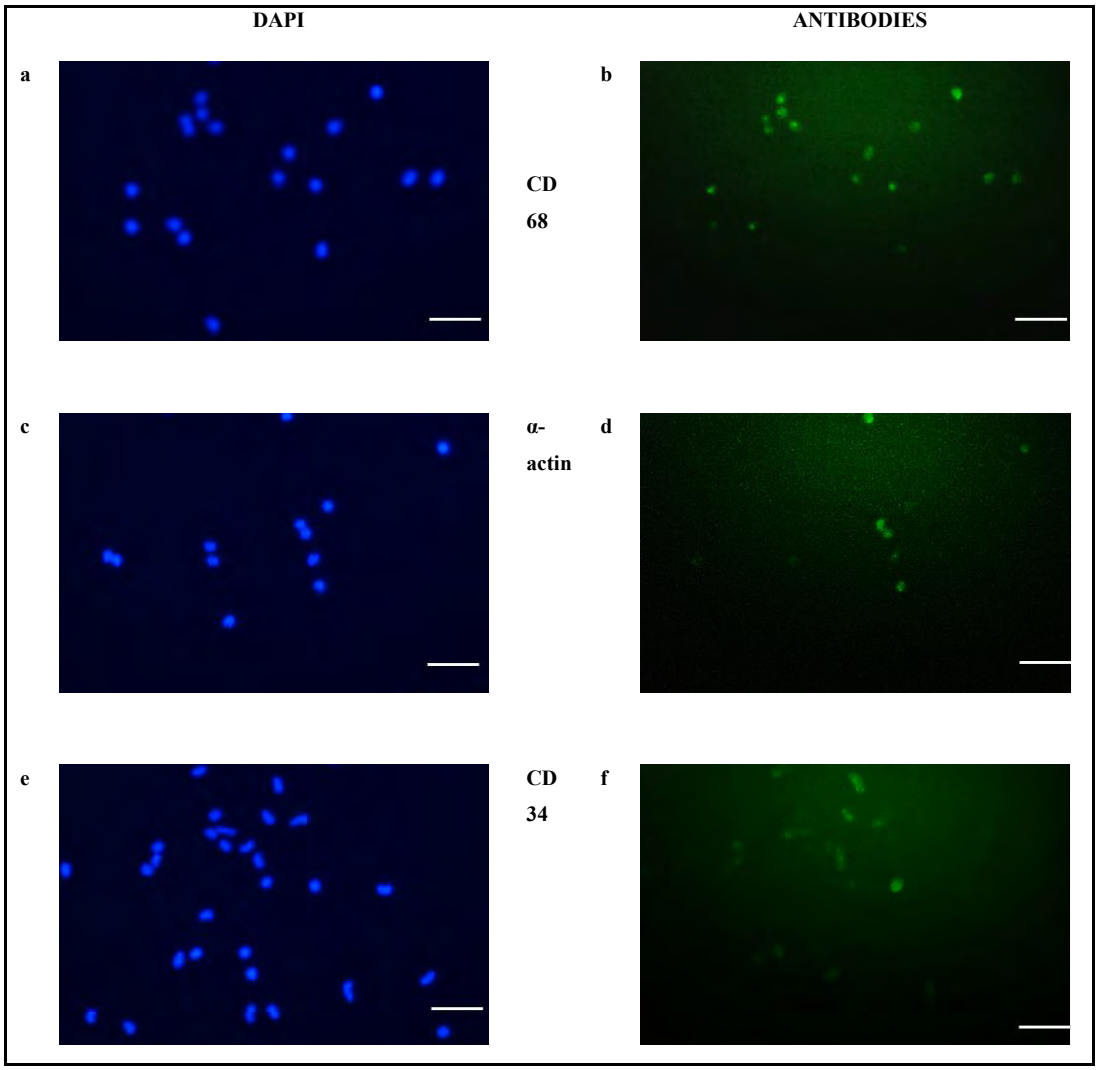

Figure 4.10 Phenotypical expression of mononuclear cells after overnight incubation on tissue culture plastic. *The immunostaining on cells from a control subjects incubated overnight on TCP with nuclei counterstain by DAPI showed that the adhering cells expressed CD68 (figure 4.10a,b), α-actin (figure 4.10c,d) and CD34, marker for haematopoietic progenitor cells (figures 4.10e,f) . Magnification: X40. Size bars indicate 50μm.*

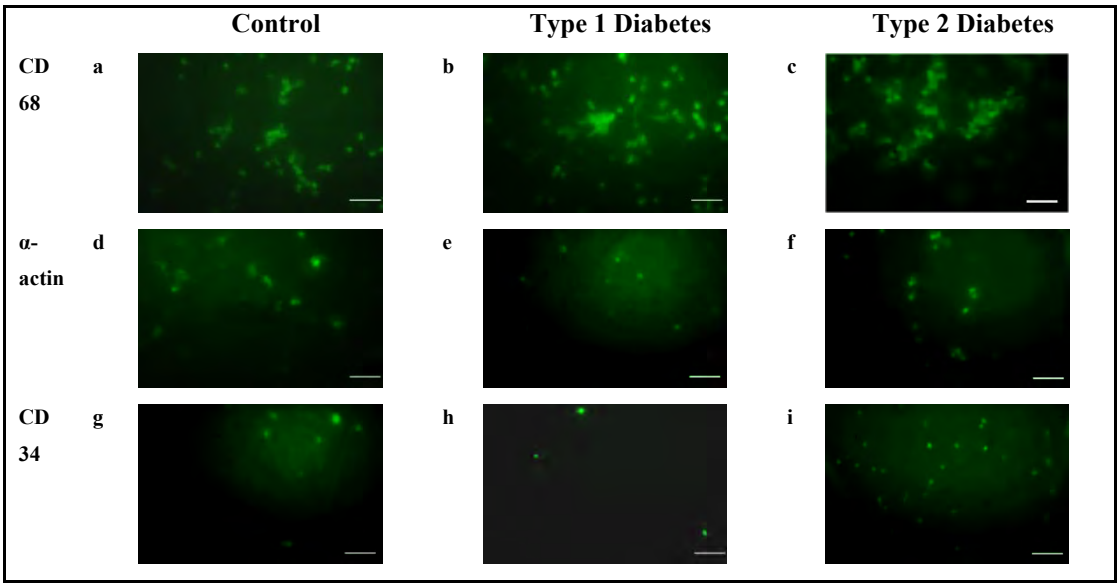

Figure 4.11 Expression of CD34 and α-actin among macrophages form different cohorts of donors and incubated overnight on stainless steel. *Immunostaining for the markers for activated macrophages (CD68), smooth muscle cells (α-actin) and haematopoietic endothelial progenitor cells (CD34) on mononuclear cells from a healthy donor and from donors with type 1 and type 2 diabetes incubated overnight on St showed that the majority of cells incubated overnight on St expressed CD68 in all of the donors (figure 4.9a: control subject; 4.9b: donor with type 1 diabetes; 4.9c: donor with type 2 diabetes). A variable amount of cells from control subjects (figure 4.9d), from donors with type 1 diabetes (figure 4.9e) and from donors with type 2 diabetes (figure 4.9f) expressed α-actin under the same conditions. Magnification: X40. Size bars = 50μm.*

4.4.2 Flow cytometry

Mononuclear cells retrieved after overnight incubation on St, TCP and ECM were characterized by flow cytometry for the expression of α-actin, CD68, CD45 and CD34. A population expressing α-actin was found among cells after incubation on surfaces.

Figure 4.12 illustrates the flow cytometric characterisation of cells isolated from one donor from each group. In particular, it compares the images identifying the population positive to α-actin prior incubation on surfaces (in buffy coats) (figures

4.12a,d,g) to the images obtained after overnight incubation on stainless steel (figures 4.12b,e,h). The population positive to α-actin increased variably across donors after incubation on stainless steel. Figures 4.12c,f,i show that in all donors the image identifying activated macrophages (CD68) partially overlapped to the core of the image representing cells expressing α-actin, thus confirming the presence of a sub-population co-expressing the markers. Similar scenario was observed across donors and surfaces.

Figure 4.13 compares the co-expression of actin and CD68 in cells isolated from one donor per each group and incubated on stainless steel, extra-cellular matrix and tissue culture plastic. A similar scenario was found across donors and surfaces. Interestingly the morphology of the actin+CD68+ population in the images obtained from stainless steel in the three donors (figures 4.13c,f,i) seemed to spread when compared to the images obtained from cells incubated on extra-cellular matrix (figures 4.13a,d,g) and tissue culture plastic (figures 4.13b,e,h).

A statistical analysis of the data obtained from flow cytometry was not possible due to the limited amount of data available (three donors per each group). However, figure 4.14 shows the trend in the amount of cells expressing the marker for monocytes (CD14) (figure 4.14a) and for activated macrophages (CD68) (figure 4.14b) in buffy coats and among cells retrieved after incubation on the experimental surfaces. Across all donors a slight increase in the percentage of cells positive to CD14 was seen among cells retrieved from surfaces and comparable in all surfaces and across groups with the exception of cells from the donors with type 1 diabetes after detachment from extra-cellular matrix (figure 4.14a).

A more evident increase in the percentage of cells positive to CD68 was observed among cells detached from the tested surfaces in comparison to the percentage obtained from buffy coats from the same donors (figure 4.14b) although with individual variability.

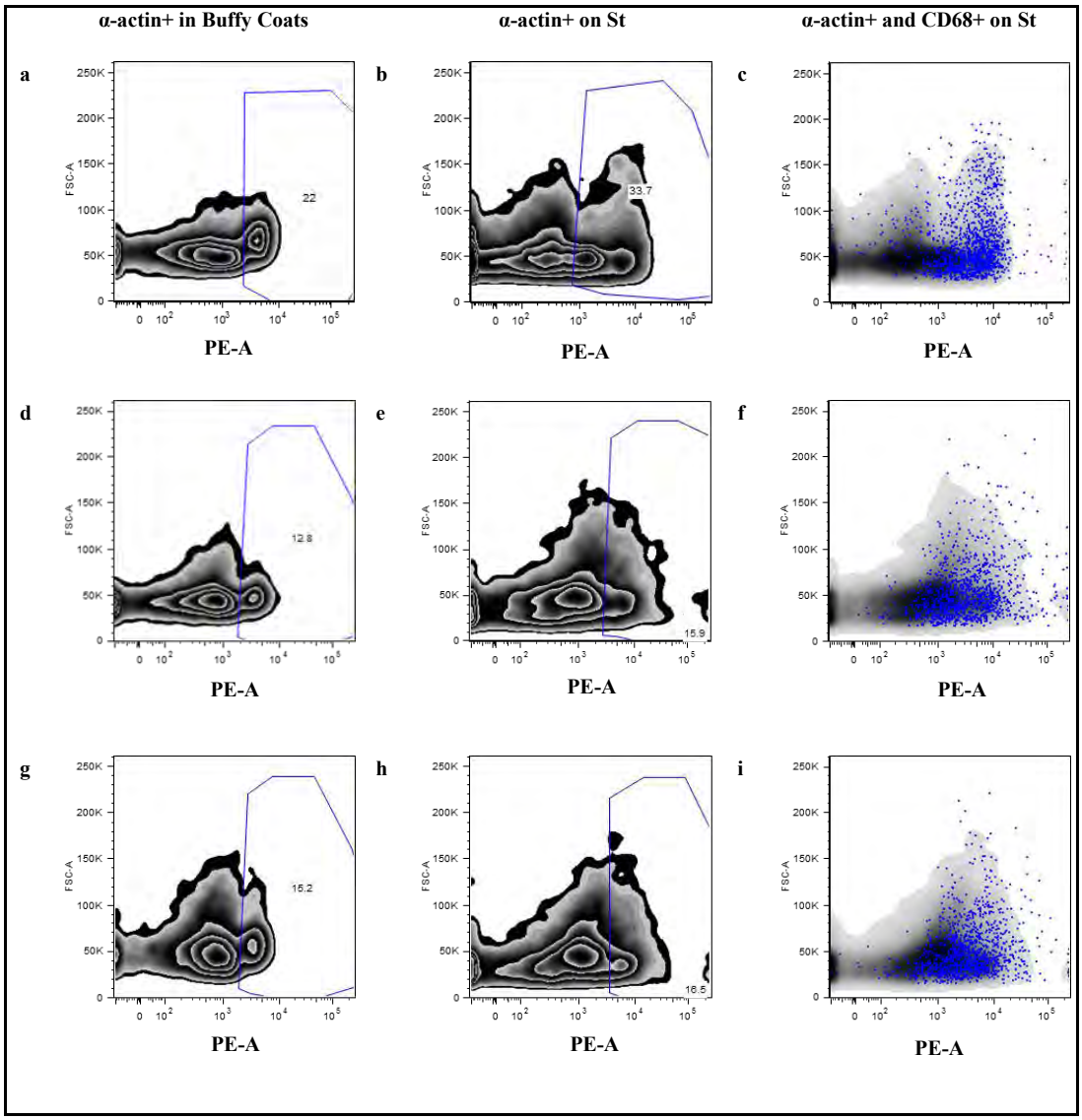

Figure 4.12 Co-expression of markers for smooth muscle cells (α-actin) and for activated macrophages (CD68) in cells incubated overnight on stainless steel. *Flow cytometry showed a cell sub-population positive to a-actin in buffy coats from a control subject (Figure 4.12a) and from a donor with type 1 (figure 4.12d) and type 2 (figure 4.12g) diabetes. Among cells from the same donors a sub-population of cells positive to α-actin was found after overnight incubation on stainless steel (figures 4.12b, 4.12e and 4.12h respectively). The actin positive population in cells retrieved from the surfaces was co-expressing the marker for activated macrophages (CD68) as represented by the overlapping of the area represented by blue dots (CD68+) with the area representing the actin positive cells (grey area) with similar trend in the control subject (figure 4.12c) and in the donor with type 1 (figure 4.12f) and type 2 (figure 4.12h) diabetes.*

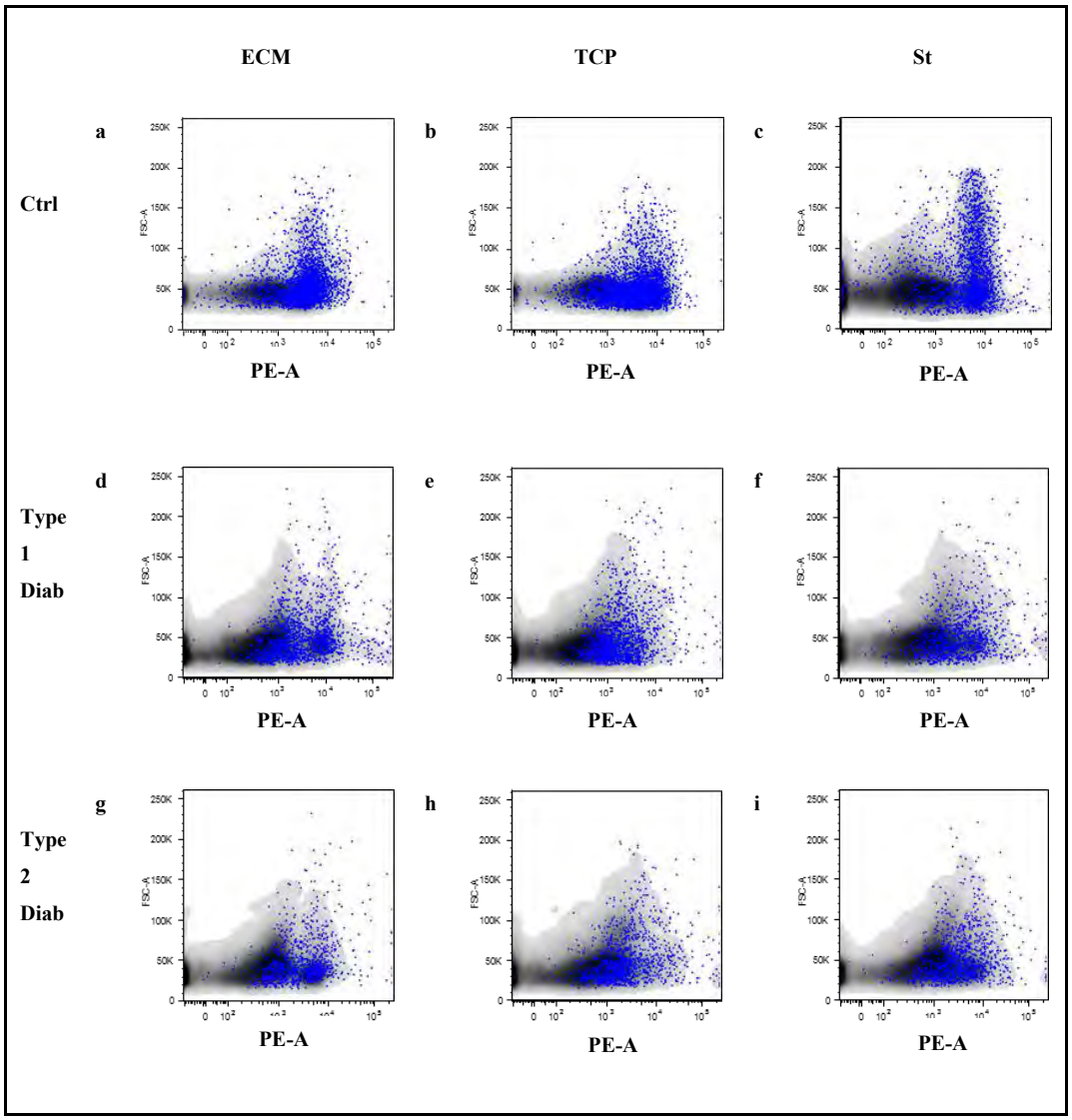

Figure 4.13 Flow cytometry of cell sub-populations co-expressing actin and CD68. *The figure shows a partial overlapping of the core of the signals recorded on the channel for PE (grey-black area in the plot), representing the α–actin positive sub-population (marker for SMC), with the signals recorded on the channel for FITC, identifying the sub-population positive to CD68 (marker for activated macrophages). This indicated the presence of a cell sub-population co-expressing both the markers after overnight incubation on ECM (figures 4.13a, 4.13d, 4.13g), on St (figures 4.13b, 4.13e, 4.13h) and on TCP (figures 4.13c, 4.13f, 4.13i) across all groups of donors.*

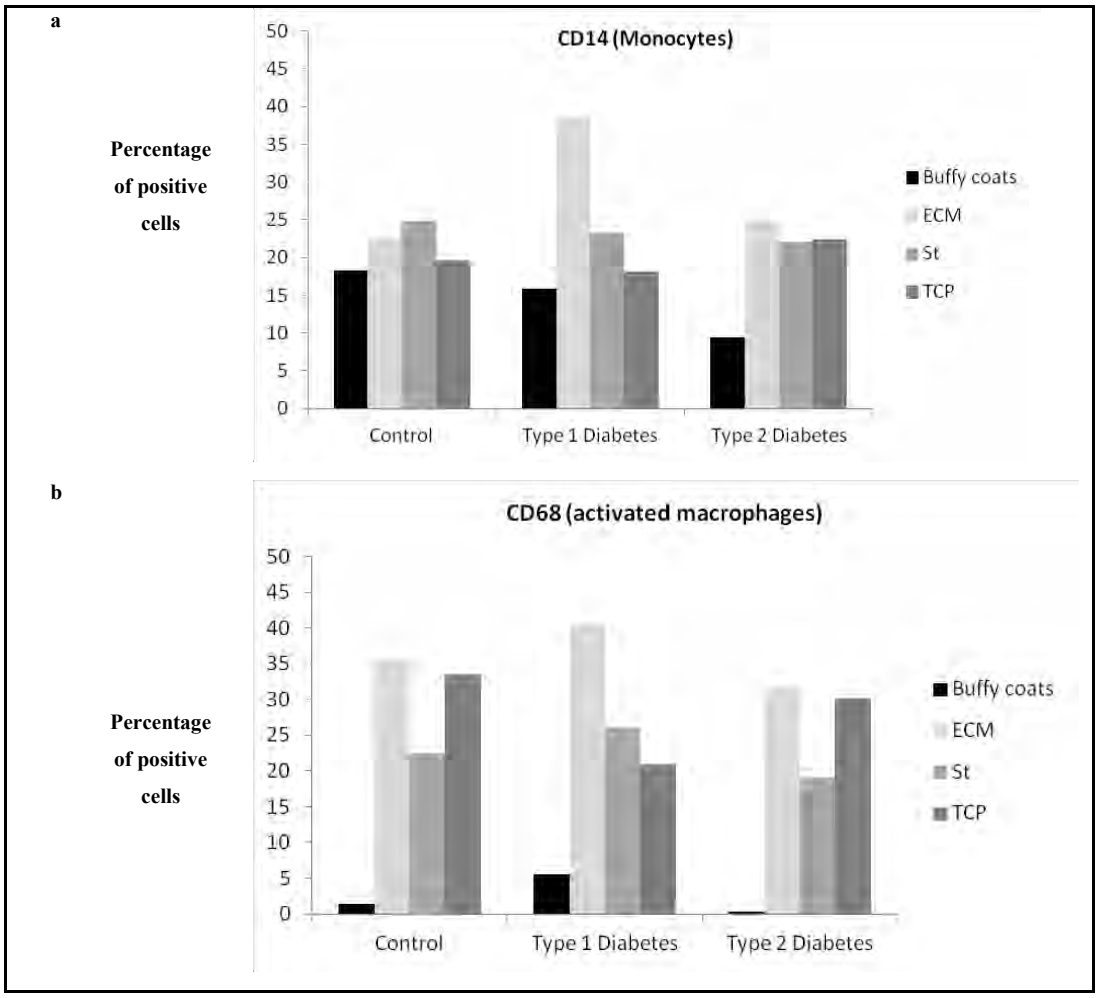

Figure 4.14 Expression of CD14 and CD68 among mononuclear cells after overnight incubation on the tested surfaces (n=3). *The figure illustrates the mean of percentages of cells positive to the marker for monocytes (CD14) and to the marker for activated macrophages (CD68) in buffy coats and after overnight incubation on surfaces detected with flow cytometry. The amount of monocytes and activated macrophages detected with flow cytometry after overnight incubation of cells from three donors per each group showed an increase of CD14+ cells in the population retrieved after incubation on TCP, St and ECM-coated wells (figure 4.14a). Similarly, the amount of activated macrophages among cells retrieved after incubation on the experimental surfaces was much higher than the amount detected in buffy coats from the same donors (figure 4.14b).*

Results from flow cytometry seem in contrast with the images obtained from immunocytochemistry (figures 4.6 and 4.7). In those cases stainless steel seemed to be a better surface for the adhesion of mononuclear cells when compared to

ECM or TCP. Results represented in figure 4.14 seem to override the previous findings. This is likely to be related to the different sensitiveness of the procedures. In the preparation of cells for flow cytometry the adhering population was gently detached from the surfaces and transferred in the tubes where the labelling protocol and the final reading was executed, thus resulting in the reduction of cell loss during the procedure. In particular, the numerous washing, fixation and labelling steps involved in the immunocytochemistry technique might have implied the loss or damage of some of the cells incubated on ECM, substrate that peeled easily during the phases of cell preparation. This surface seemed in fact to present a reduced overall amount of adhering cells (figure 4.6) and of cells expressing CD68 (figure 4.7).

Data from flow cytometry after overnight incubation of cells on the tested surfaces were used to characterise the sub-populations forming the actin+ and the CD34+ adhering cell populations. As shown in figure 4.15 the total amount of cells expressing actin was constituted only minimally by cells expressing exclusively the marker for SMC (actin only in the figure) in healthy donors (3.14%-4.73%) and in donors with type 2 diabetes (3.3.1%-8.95%). Despite the variability across groups, the most abundant sub-population was represented by cells co-expressing CD45 alone or in combination with CD68 in conjunction with α-actin (respectively actin+CD45+ and actin+CD68+CD45+ sub-populations), thus suggesting that most of the actin+ cells were derived from a progenitor of leukocytic origin. The sum of the percentages representing the two sub-populations in cells from all groups and after contact with all the experimental surfaces was in fact always above the 80% of the total amount of actin+ cells with the exception of cells from donors with type 1 diabetes retrieved from ECM where the two sub-populations represented the 67.57% of the total actin+ cells and a much higher percentage (24.06%) of cells expressing exclusively actin was found. The remainder was represented by a sub-population of cells co-expressing CD68 and actin.

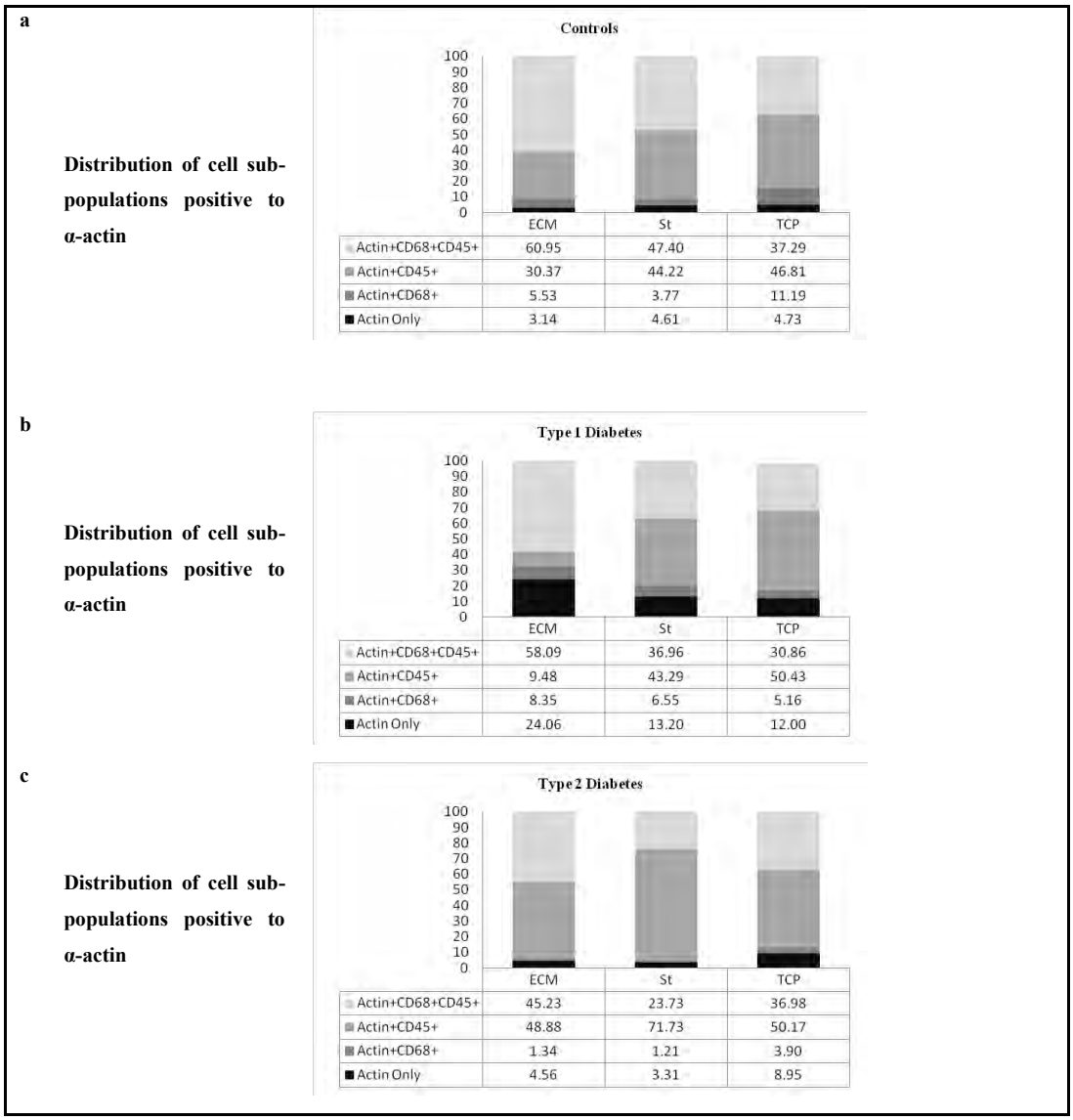

Figure 4.15 Flow cytometry of adhering cells positive to α–actin within the sub-populations co-expressing CD68 and CD45 (n=3). *Flow cytometric characterization of the sub-populations forming the total amount of cells from three donors per each group positive to actin (smooth muscle cells) after overnight incubation on tissue culture plastic (TCP), stainless steel (St) and extra-cellular matrix-coated wells (ECM). Results showed that across donors and after incubation on all the surfaces the majority of cells expressing α-actin were composed of sub-populations co-expressing the general marker for leukocytes (CD45) alone or in combination with the marker for activated macrophages (CD68). Data were expressed as mean of percentage of sub-populations on the total amount of cells positive to α-actin in each test tube and results collected from three donors from each group.*

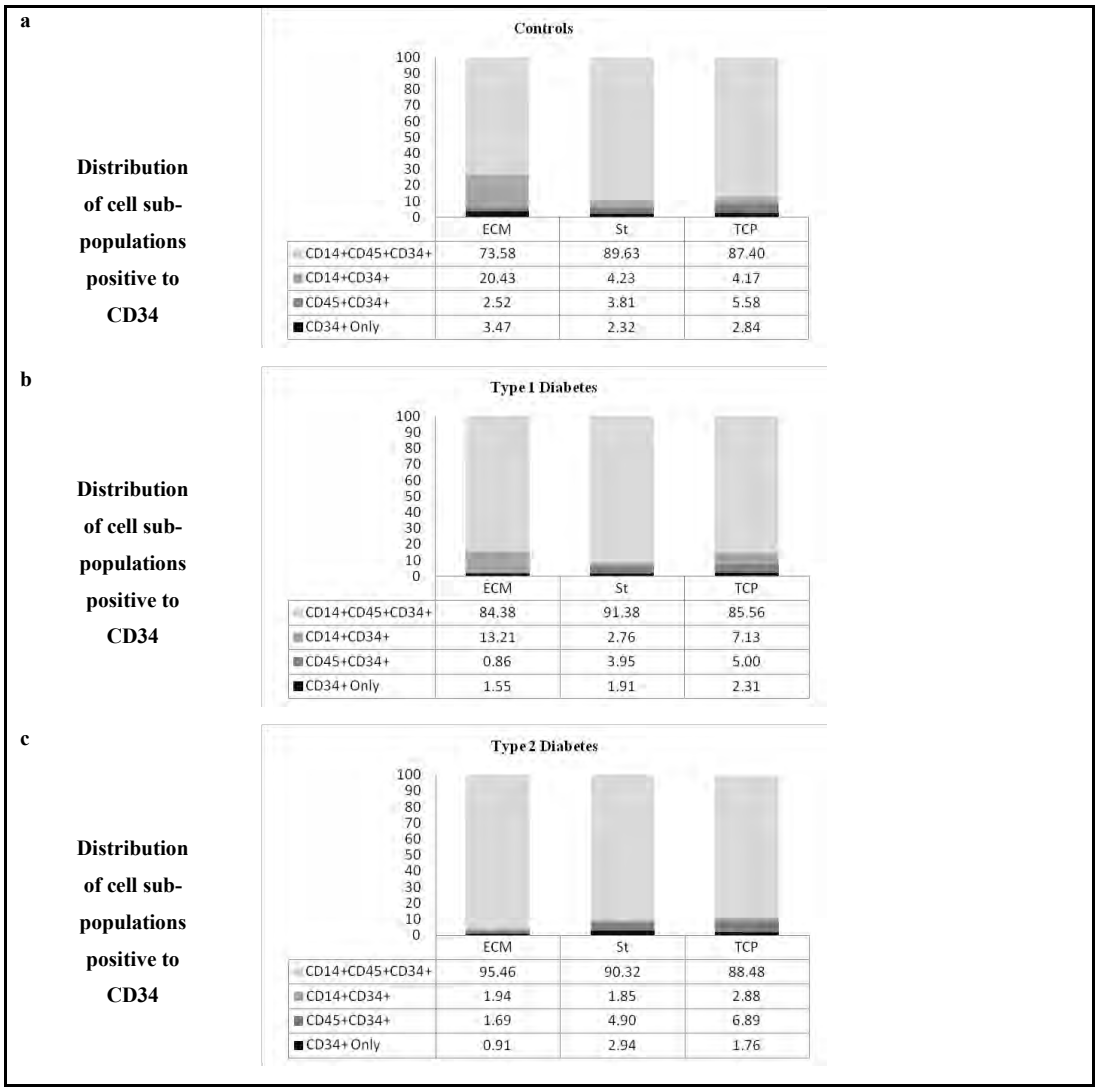

Figure 4.16 Percentage of sub-populations expressing CD34 (marker for endothelial progenitor cells) (n=3). *The flow cytometric characterization was performed on mononuclear cells isolated from three donors per each cohort and incubated overnight on ECM, TCP and St. The majority (73.58%-95.46%) (figures 4.16a-c) of cells positive to CD34 was composed of a sub-population co-expressing CD34 with the marker for monocytes (CD14) and the general marker for leukocytes (CD45) across donors from all groups. Only little amount of CD34+ cells expressed exclusively CD34 (0.91%-3.47%) (figures 4.16a-c). Data were expressed as mean of the percentage of the sub-populations on the total amount of CD34+ cells in each experimental tube and results collected from three donors from each group.*

Results from flow cytometry were also analysed for the characterization of cell sub-populations forming the total amount of cells expressing the marker for haematopoietic and endothelial progenitor cells (CD34). Only a very small fraction of CD34+ was represented by cells expressing exclusively CD34 ranging from 0.91% to 3.47% across the three groups of donors (figures 4.16a,b,c). The majority of the adhering CD34+ cells was represented by a sub-population co-expressing CD14 and CD45 (CD34+CD14+CD45+), whose percentage ranged from the 73.58% to the 95.46% of the total CD34+ population (figures 4.16a,b,c). The remaining CD34+ population was formed by cells co-expressing either CD14 or CD45.

4.4.3 ELISA

ELISA tests were used to quantify the release of PDGF-BB and TNF-α by macrophages incubated overnight on the experimental surfaces. The raw data obtained from ELISA and Bradford tests are listed in Appendix 2. The amount of PDGF-BB and TNF-α measured in the samples was normalized on the total amount of proteins measured in the correspondent sample through Bradford test in order to avoid artefact due to differences in the amount of adhering cells. The statistical differences were assessed using paired t-test.

4.4.3.1 PDGF-BB

Results from ELISA test are represented in table 4.3. The table shows that the trend in PDGF-BB release was similar when comparing the values before and after normalization on the total amount of proteins obtained from the Bradford test.

Table 4.3 Overview of the results obtained from the ELISA test for the measurement of PDGF-BB (n=10 per group of donors). The table represents the means of the amount of PDGF-BB measured in the samples (pg/ml) through ELISA test and their normalization on the total amount of proteins in the same samples. This is expressed as ratio PDGF-BB/total proteins (pg/µg ± standard error).

	PDGF-BB measured in samples (pg/ml)			PDGF-BB normalized on total amount of proteins in samples (pg/µg) ± standard error		
Group of donors	**TCP**	**St**	**ECM**	**TCP**	**St**	**ECM**
Control	28.85	43.28	31.37	0.024±0.0034	0.036±0.0049	0.026±0.0028
Type 1 Diabetes	28.91	38.80	26.40	0.025±0.0050	0.032±0.0069	0.021±0.0053
Type 2 Diabetes	29.04	40.44	29.66	0.024±0.0037	0.033±0.0055	0.024±0.0045

In supernatants collected from healthy donors and incubated overnight on St, TCP and ECM the release of PDGF-BB from cells incubated on St (0.036±0.0049 pg of PDGF-BB in µg of protein in the sample) was significantly higher than the release of PDGF-BB from cells from the same donors incubated on TCP (0.024±0.0034 pg/µg; p=0.0036) and from cells incubated on ECM (0.026±0.0028 pg/µg; p=0.028) (figure 4.17a).

The release of PDGF-BB from cells from donors with type 1 diabetes and incubated on St (0.032±0.0069 pg/µg) was significantly higher (p=0.032) than the release measured from cells incubated on ECM (0.021±0.0053 pg/µg) (figure 4.17b). The release of PDGF-BB from cells from the same donors incubated on TCP (0.025±0.0050 pg/µg) was lower than the one measured from cells on St but not significantly different (p=0.22) (figure 4.17b).

The release of PDGF-BB from cells of donors with type 2 diabetes incubated on St (0.033±0.0055 pg/µg) was significantly higher (p=0.041) than the release from cells incubated on TCP (0.024±0.0037 pg/µg) (figure 4.17c). The amount of PDGF-BB measured in samples from cells from the same donors incubated on ECM (0.024±0.0045 pg/µg) was equal to the amount measured from cells on TCP

and lower than the one measured from cells on St but not significantly different (figure 4.17c).

Comparing the release of PDGF-BB from cells incubated on the same surfaces but across groups of donors no significant differences were found.

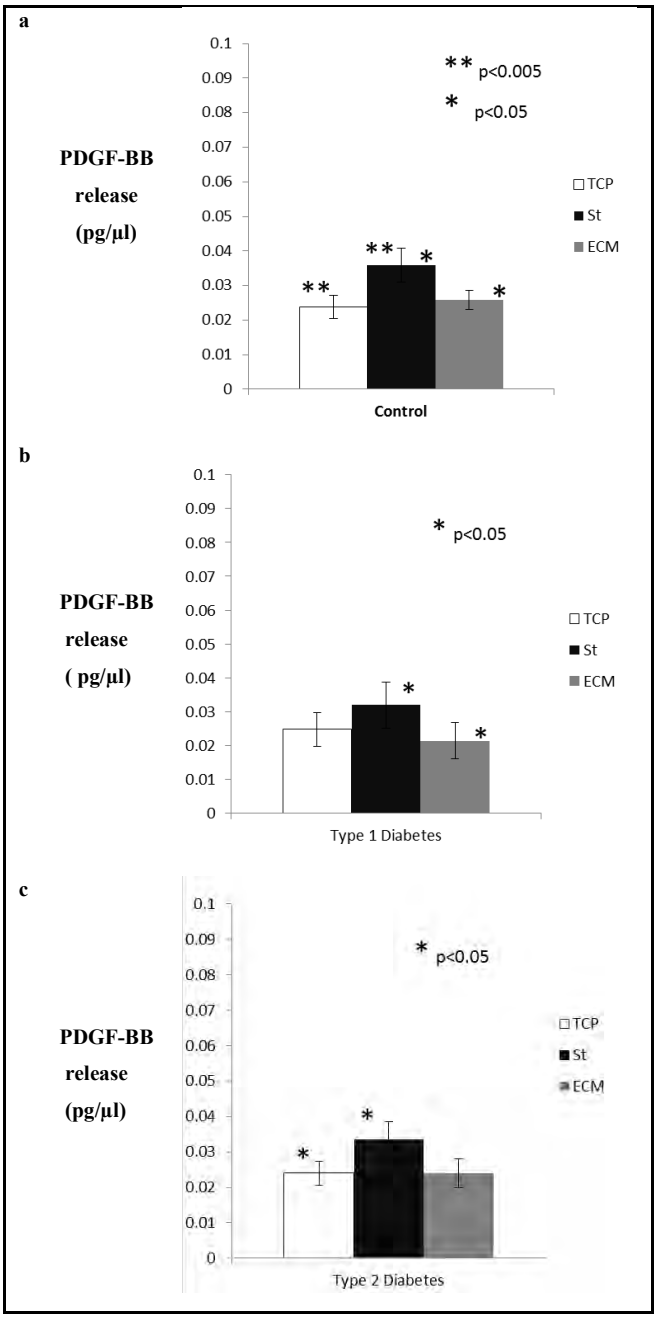

Figure 4.17 PDGF-BB release from cell after overnight incubations on the tested surfaces. *Values are expressed as mean of PDGF-BB (pg) measured in each sample through ELISA test over the total amount of proteins in the same sample (µg) measured via Bradford test. Data were analysed using paired t-test. The release of PDGF-BB was significantly higher after incubation on stainless steel compared to tissue culture plastic in control subjects (p=0.0036) (figure 4.17a) and in donors with type 2 diabetes (p=0.041) (figure 4.17c). In donors with type 1 diabetes there was a significantly higher (p=0.032) release of PDGF-BB in cells incubated on stainless steel compared to cells incubated on extra-cellular matrix (figure 4.17b). Cells from control subjects showed a significant increase in the release of PDGF-BB when incubated on stainless steel when compared to ECM (p=0.028) (figure 4.17a).*

4.4.3.2 TNF-α

Table 4.4 represents the means of results obtained from the ELISA test for the measurement of TNF-α and deriving from the raw data shown in Appendix 2. Table 4.4 shows that the trend in TNF-α release was similar when comparing the values before and after normalization on the total amount of proteins obtained from the Bradford test.

Table 4.4 Overview of the results obtained from the ELISA test for the measurement of TNF-α (n=10 per group of donors). The table represents the means of the amount of TNF-α measured in the samples (pg/ml) through ELISA test and their normalization on the total amount of proteins in the same samples. This is expressed as ratio TNF-α /total proteins (pg/µg) ± standard error.

	TNF-α measured in samples (pg/ml)			TNF-α normalized on total amount of proteins in samples (pg/µg)		
Group of donors	**TCP**	**St**	**ECM**	**TCP**	**St**	**ECM**
Control	294.60	365.91	270.07	0.24±0.047	0.31±0.038	0.22±0.026
Type 1 Diabetes	334.92	440.21	330.03	0.28±0.036	0.36±0.033	0.26±0.021
Type 2 Diabetes	239.24	434.02	161.54	0.19±0.050	0.36±0.025	0.13±0.037

The release of the pro-inflammatory cytokine TNF-α from cells after overnight incubation on the experimental surfaces was measured and expressed as ratio of TNF-α (pg) released over the total amount of proteins (µg) measured in the same supernatant through Bradford assay.

Cells from healthy donors incubated overnight on stainless steel released a significantly higher (p=0.0047) amount of TNF-α (0.31±0.038 pg/µg) than cells from the same donors incubated on extra-cellular matrix (0.22±0.026 pg/µg). The amount of TNF-α in supernatants collected from cells on stainless steel was also significantly higher (p=0.048) than the TNF-α measured in supernatants from cells incubated on TCP (0.24±0.047 pg/µg) (figure 4.18a).

Similarly, TNF-α measured in supernatants collected from cells from donors with type 2 diabetes incubated on St (0.36±0.025 pg/µg) was significantly higher (p=0.0030) than the amount measured in supernatants from cells on extra-cellular matrix (0.13±0.037 pg/µg). The amount in supernatants from cells on stainless steel was also significantly higher (p=0.026) than the amount measured from cells on tissue culture plastic (0.19±0.050 pg/µg) (figure 4.18c).

A similar scenario was found in supernatants from cells from donors with type 1 diabetes where the amount of TNF-α measured in supernatants from cells on St (0.36±0.033 pg/µg) was significantly higher (p=0.0023) than the amount measured in supernatants from cells on extra-cellular matrix (0.26±0.021 pg/µg) (figure 4.18b). Despite the amount of TNF-α measured in supernatants from cells on tissue culture plastic (0.28±0.036 pg/µg) being lower than the amount measured from cells on stainless steel and closer to the result obtained from cells incubated on extra-cellular matrix there was no statistically significant difference between the series of data.

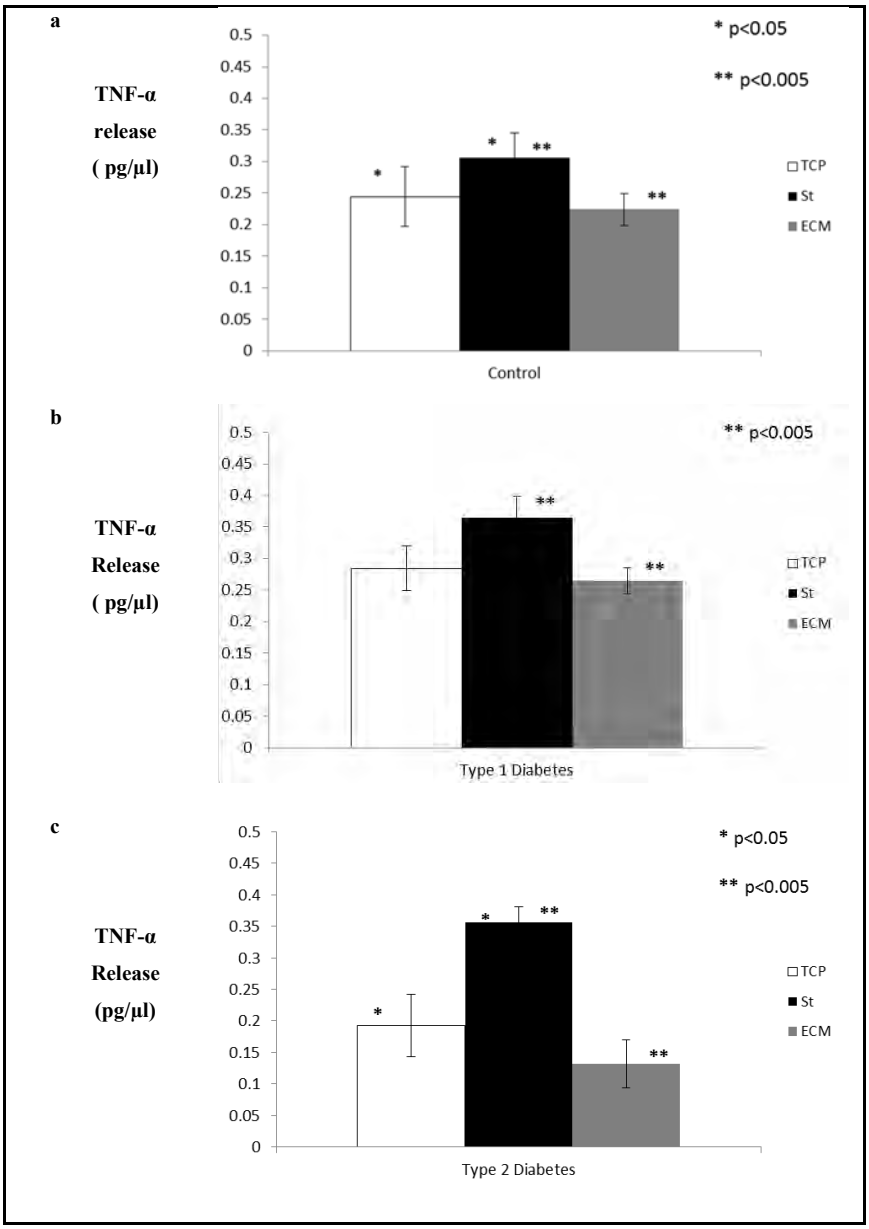

Figure 4.18 TNF-α release from cells after overnight incubation on the tested surfaces (n=10). *Data were expressed as mean of the ratio of TNF-α measured by ELISA (pg/ml) over the total amount of proteins measured with the Bradford method (µg/ml) ± standard error. Data were analysed using paired t-test. The incubation of cells on stainless steel triggered a significant increase in the release of TNF-α when compared to TCP in both cells from control subjects (p=0.048) (figure 4.18a) and cells from donors with type 2 diabetes (p=0.026) (Figure 4.18c). Similar trend, but not significant, was found in samples from donors with type 1 diabetes. In all the group of donors incubation on stainless steel triggered a significant increase in the release of TNF-α when compared to ECM with a p=0.0047 in control subjects, p=0.0023 and p=0.0030 respectively in donors with type 1 and type 2 diabetes (figures 4.18 a,b,c).*

higher ($p<0.005$) than the amount measured in supernatants from cells incubated on extra-cellular matrix.

The comparison of the release of TNF-α across the groups of donors revealed that cells from the recruited donors with type 1 diabetes released a significantly higher ($p=0.042$) amount of TNF-α than cells from the recruited donors with type 2 diabetes (figure 4.19). No statistically significant difference was seen between cells from donors with type 1 diabetes and control subjects (figure 4.19).

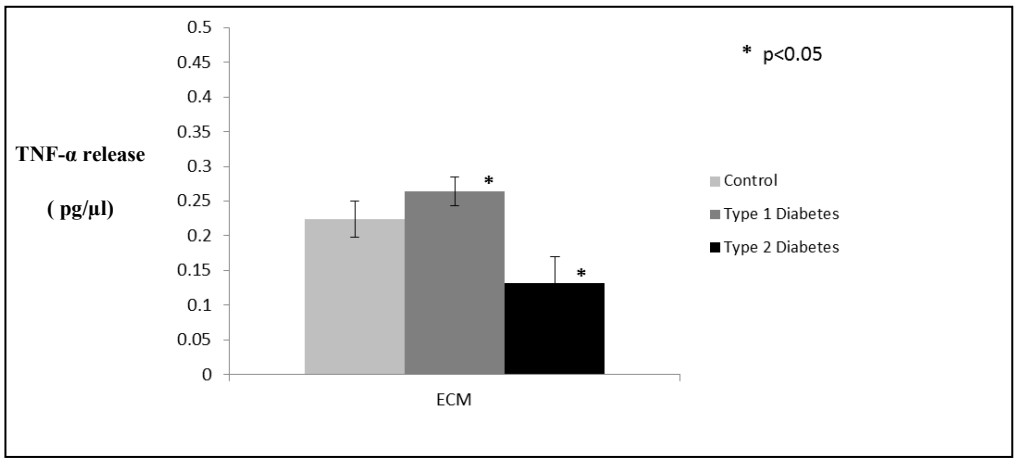

Figure 4.19 TNF-α release by cells adhering on ECM. *The release of TNF-α from macrophages incubated on extra cellular matrix among the three groups of donors was significantly lower ($p=0.042$) in cells from recruited donors with type 2 diabetes compared to the cells from recruited donors with type 1 diabetes. Data were analysed using paired t-test.*

4.5 DISCUSSION

Previous studies have shown that the cellularity of the restenotic plaque decreases with time (Chung 2002, Santin 2005). The initial phases following implantation see the intervention of platelets, neutrophils and inflammatory cells to sustain the response to the injury and the physiological reaction to the foreign body (Farb

2002). Restenotic tissue older than three months is characterized by a proteoglycan-rich matrix with smooth muscle cells and myofibroblasts characteristic of a healing wound. Specimens analysed after 18 months following implantation are in fact characterized by myoxid tissue constituted by stellated-shaped smooth muscle cells distributed in extra-cellular matrix rich in proteoglycan (mainly versican and hyaluronan) (Chung 2002, Santin 2005).

Macrophages can be found throughout all the phases of the restenotic process (Farb 2002, Santin 2005). In the development of the foreign body reaction macrophages intervene in the early phases of the inflammatory response reaching the injured area under stimuli of chemokines in order to sustain the inflammatory process and to remove the foreign body through phagocytosis (Luttinkhein 2006). In the case of non-degradable materials macrophages modify their role differentiating into a wound healing phenotype. In particular, a study from Mesure et al. (2010) demonstrated that a sub-population expressing the marker for activated macrophages (CD68) in conjunction with the marker for haematopoietic progenitor cells (CD34) actively participate in the formation of myofibroblasts characterizing the fibrotic tissue surrounding the implant. This confirmed the hypothesis of macrophages contributing in the development of the restenotic tissue through their ability to trans-differentiate. Previous studies have shown that after seven days of incubation on stainless steel macrophages expressed α–actin acquiring a spindle-like morphology, both typical of smooth muscle cells and myofibroblasts. As discussed in chapter 3 the trans-differentiation potential of macrophages has been investigated in different studies that demonstrated the presence in circulating blood of sub-populations able to differentiate in different cell type of the mesenchymal lineage under specific stimuli *in vitro* (Kuwana 2003, Gordon & Taylor 2005, Varol 2009).

This study evaluated the phenotypical expression of monocytes-derived macrophages isolated from healthy donors and donors with diabetes in contact with stainless steel. The experimental conditions chosen for the study aimed to

investigate the early response of inflammatory cells to the material reproducing the environment surrounding the stent strut shortly after implantation and potentially highlighting differences in the immediate response among donors rather than exclusively induced by the contact with the metal. Cells were in fact incubated overnight rather than for seven days as utilised in a previous study that demonstrated phenotypical changes after incubation on stainless steel (Stewart 2009). In addition, the choice of a low glucose medium, reproducing physiological blood glucose concentrations, emphasized the effect of the material on the cells thus highlighting possible differences across groups of donors. Immunocytochemistry confirmed that stainless steel is a favourable substrate for cell adhesion (figure 4.6), thus suggesting that, following implantation, monocytes which migrate from the circulating blood and from the surrounding atherosclerotic tissue may adhere with greater affinity to the stent struts. The cells adhering on the experimental surfaces expressed CD68, thus identifying them as activated macrophages (figure 4.7). Among those, cells expressing α-actin were found, thus confirming the presence of sub-populations able to generate myofibroblasts (figures 4.8, 4.9, 4.10). Some of the adhering cells expressed the marker for haematopoietic progenitor cells (CD34) (figures 4.8, 4.9, 4.10, 4.11). Therefore, results suggested that part of the myofibroblast-like cells observed may derive from a change in phenotype of the macrophages triggered by the contact with artificial surfaces such as stainless steel. No relevant differences were observed among the three different groups of donors (control, type 1 and type 2 diabetes) and a similar trend was observed in cells adhering an all the experimental surfaces.

Results from flow cytometry provided the phenotypical characterization of the adhering cells sub-populations. The comparison of the distribution of populations in buffy coats and among cells detached after contact with the tested surfaces showed a relative increase in the amount of cells expressing the marker for monocytes (CD14) (figure 4.12). This can be explained by the removal of non-

adhering cells through the replacement of the medium after three hours of incubation. The step aimed in fact to remove the non-adhering lymphocyte population leaving on the surfaces a population mainly represented by monocytes, i.e. CD14+ cells. More interestingly, a greater increase in the amount of activated macrophages (CD68+) was found among cells retrieved from surfaces (figure 4.14) indicating that the overnight incubation on stainless steel triggered the activation of monocyte into macrophages, thus confirming the findings obtained by immunocytochemistry. In addition, flow cytometry results showed that the population of adhering cells expressing the marker for smooth muscle cells (α-actin) was mainly composed of sub-populations co-expressing CD68 alone or in combination with CD45, the general marker for leukocytes (figure 4.15). Only a very small amount of cells expressed exclusively α-actin (figure 4.15). Therefore, the findings confirmed that the sub-populations possessing the potential to differentiate into myofibroblasts were derived from macrophages. Furthermore, flow cytometry showed that the main sub-population forming the cells positive to the marker for haematopoietic progenitor cells (CD34) co-expressed the marker for monocytes (CD14) and the general marker for leukocytes (CD45) (figure 4.16) thus confirming the presence of progenitors deriving from monocytes and able to differentiate into cells of the mesenchymal lineage as discussed in the previous chapter.

The complex cascade of events characterizing the inflammatory reaction in the early phases of the foreign body reaction is driven by the release of pro- or anti-inflammatory cytokines that regulate cell responses (Luttikhuizen 2006). Macrophages in contact with metallic or ceramic particles were shown to release TNF-α, one of the main pro-inflammatory cytokine (Dinarello 2000). Macrophages in contact with stainless steel showed an increase in the release of TNF-α likely connected to their activation (Santin 2004). However, different studies have shown that TNF-α does not represent the predominant cytokine in the restenotic process (Santin 2005). Studies have in fact shown that restenosis is

mainly characterised by the presence of TGF-β and PDGF-BB, cytokines promoting proliferation of smooth muscle cells and the formation of extra-cellular matrix (Santin 2005). Studies have also shown that the contact with stainless steel promote a significant release of TGF-β and PDGF-BB by macrophages after seven days incubation (Stewart 2009) or after three hours at high glucose concentration in the medium (Harrison 2007).

This study confirmed that overnight incubation on stainless steel triggered the release of PDGF-BB by macrophages (figure 4.17). The effect of stainless steel was particularly evident in cells from control subjects where the release of the growth factor was significantly higher compared to both tissue culture plastic and extra-cellular matrix. The contact with stainless steel also triggered an increase in the release of PDGF-BB in donors with type 1 and type 2 diabetes. In those cases a significant increase was observed respectively in comparison to extra-cellular matrix and tissue culture plastic (figure 4.17). Results showed that even after overnight incubation in glucose concentration similar to physiological blood level stainless steel promotes the post-inflammatory status in macrophages. A similar trend was observed in all the groups, it appeared to be emphasised in healthy donors, thus suggesting that donors with diabetes might be characterized by higher basic level of activation partially masking the effect of the metal.

After overnight incubation, the contact with stainless steel activated the adhering macrophages as confirmed by the significant increase in the release of TNF-α in all the groups of donors. In particular, the release of TNF-α was significantly higher when compared to the release from cells in contact with extra-cellular matrix ($p<0.005$) (figure 4.18). Higher release of TNF-α was observed also in comparison to cells incubated on tissue culture plastic with the trend being significantly different only in control subjects and in donors with type 2 diabetes (figure 4.18). The reason for that can be in part due to the reaction to the tissue culture plastic that, representing an artificial surface, can trigger partial activation of macrophages. In addition, donors with type 1 diabetes showed a higher basic

level of activation demonstrated by the significant difference in the release of TNF-α from cells from donors with type 1 diabetes when compared to the release from cells from donors with type 2 diabetes incubated on extra-cellular matrix (figure 4.19), the surface adopted in this study to mimic the de-endothelialized blood vessel wall that is supposed to support only a limited activation of macrophages.

4.6 CONCLUSIONS

This experiment confirmed the likelihood that, following implantation, macrophages migrate towards the stent struts where they become activated and transform the early acute inflammatory response to the foreign body into a chronic event. However, during this process activated macrophages also switch their phenotype soon acquiring a wound healing, post-inflammatory phenotype capable of secreting PDGF-BB. The growth factor promotes the proliferation of smooth muscle cells and myofibroblasts, thus potentially intervening in sustaining the formation of the restenotic plaque. The phenotypical switch emphasized by the contact with the metal found further confirmation by the characterization obtained from flow cytometry demonstrating the presence of sub-populations derived from monocytes and macrophages contributing to the formation of myofibroblasts. This corroborated findings discussed in the previous chapter and published in previous studies (Pilling 2009, Stewart 2009, Forte 2010). Results discussed in previous chapters suggested the occurrence of variations within the distribution of activated macrophages and their sub-populations among donors with diabetes. Results from ELISA showed a difference in the release of TNF-α from donors with type 1 diabetes in comparison to donors with type 2 diabetes. Results from this and previous chapters showed that the subjects with type 1 diabetes recruited during this study were characterized by an increase in the level of circulating

activated macrophages. This may represent an indication of the association of diabetes with anomalies in inflammatory cell distribution and in their response to the metal. Therefore, the metal-induced activation of macrophages in association with differences in sub-population distribution may represent a key factor for the increased risk of developing *in-stent* restenosis that deserves further investigation to better define the extent of the correlation.

Results obtained from the analysis of macrophages from people with diabetes were characterized by variability due to differences in the clinical and pathological conditions among the donors. The following part of the study aimed to utilize experimental conditions in order to investigate the effect of high glucose and lipid concentration, alone or in combination, on the response of monocytes-derived macrophages to the contact with stainless steel surface. This will in fact eliminate differences related to co-morbidities, extent of the diabetes-induced damage and therapies in order to evaluate solely the acute effect of hyperglycaemia, hyperlipidaemia and their synergistic effect on the inflammatory cells.

CHAPTER 5

EFFECT OF PALMITATE AND HIGH GLUCOSE ON THE RESPONSE OF MACROPHAGES TO STAINLESS STEEL

5.1 INTRODUCTION

The analysis of the distribution of cell sub-populations in buffy coats described in chapter 2 revealed that diabetic subjects may present variations in the amount of circulating activated macrophages, indicating chronic inflammatory conditions and a relatively high percentage of circulating endothelial progenitor cells that is widely recognised as an indicator of endothelial dysfunction and increased cardiovascular pathology risk (Fadini 2006). This suggested that the characterization of circulating cell populations, alongside the traditional evaluation of general clinical conditions and biochemical markers, could represent a further step in the identification of individuals prone to develop both cardiovascular disease and *in-stent* restenosis upon coronary stent implantation. However, it is widely accepted that a complex clinical scenario characterises donors with diabetes where many variables influencing the increase in cardiovascular risk and alterations in vascular endothelium are involved (Hu 2001, Peppa 2003, Price 2004, Goldin 2006). The connection between diabetes, obesity and inflammation (Wellen & Hotamisligil 2005) suggests that alterations in blood lipid levels and consequent metabolic dysfunction represent a key factor in the understanding of the increased inflammatory response in diabetic people, thus representing an important element in the response of inflammatory cells to biomaterials.

5.2 FREE FATTY ACIDS

The rapid increase in obesity in recent years has been correlated to the increase of metabolic diseases including heart disease and diabetes (Lakka 2002, Hu 2011). Studies have demonstrated the correlation between alterations in lipid metabolism and insulin resistance, pancreatic cell death, hypertension and metabolic

syndrome (Hansen 1999, Hu 2011). Lipids introduced by diet are hydrolysed to free acids before being absorbed and utilized for lipid synthesis (Rustan 2005). Recent studies have demonstrated a correlation between an increase in plasma levels of saturated fatty acids, derived from an increase in fat intake from the diet, and the occurrence of insulin resistance (Lee 2006, Kennedy 2008, Hu 2011).

5.2.1 Definition and metabolism

Fatty acids are formed by a long carbon chain with a methyl and a carboxyl group respectively at the –ω and –α terminal. They are differentiated between saturated and unsaturated fatty acids depending on the presence of double bonds between carbon atoms as follows (Rustan & Drevon 2005, Aas 2006):

- Saturated fatty acids are long chains (commonly 12-22) of single-bonds carbon-carbon.
- The unsaturated fatty acids contain one (monounsaturated) or more (polyunsaturated) double bonds between carbon atoms along the chain.

The roles of fatty acids, either free or as part of more complex molecules, comprise (Rustan & Drevon 2005):

- metabolic fuel (energy storage and metabolism) providing 37kJ/g;
- transferable form of energy as part of lipids in blood;
- components of cells membranes as part of phospholipids;
- thermal, electrical and mechanical insulation;
- gene regulators as part of molecules (eicosanoids) influencing transcription signals.

Free or unesterified fatty acids are present, although in small amounts, in all living tissues. Lipids in tissues can be hydrolysed to free fatty acids by a variety of lipolytic enzymes before being metabolized in various ways including oxidation, desaturation, elongation or re-esterification (Rustan & Drevon 2005). As free

acids they can interact with a wide range of enzyme systems in both specific and non-specific ways. They must be rapidly sequestered in tissues by various means to ensure that their activities are closely regulated. Free monomeric fatty acids have very low solubility in aqueous media (Rustan & Drevon 2005). In serum, they are transported between tissues bound to the protein albumin, which has up to six strong binding sites in addition to a large number of weak binding sites. In this way, the concentration of a long-chain fatty acid in serum can be increased by as much as 500 times above its normal maximum (Spector 1969, Spector 1975). However, the bound fatty acids can diffuse into the aqueous phase, where they are rapidly taken up into the outer leaflet of the plasma membrane by non-enzymatic mechanisms.

Figure 5.1 illustrates the main pathways of fatty acid metabolism. Following digestion of ingested fat in the small intestine, free fatty acids (FFA) are re-absorbed by the intestinal mucosa and transferred to the circulation. Once FFA reaches the circulation they are transported across the bloodstream as serum albumin-bound forms. Circulating FFA are captured by cells through a "transporter" situated on the membrane and transported within the cells by fatty acid-binding proteins (FABP). Recent studies have confirmed the presence of different proteins functioning as transporters for FFA on cell membranes that was previously thought to occur by simple diffusion (Schwenk 2010). The transporters identified include the protein CD36, plasma membrane-associated fatty acid-binding protein (FABP(pm)), and a family of fatty acid transport proteins (FATP1-6) (Schwenk 2010). The transporters facilitate the absorption of free fatty acids within the cells but they also participate in fatty acid uptake regulation. Under specific stimuli such as muscle contractions or insulin the intracellular proteins migrate to the membrane to facilitate the fatty acid uptake. This suggests the critical role played by the transporters in the occurrence of metabolic disease such as diabetes and insulin resistance, identifying the proteins as potential targets for lipid regulation in future treatments (Glatz 2010, Schwenk 2010). Inside the

cells FFA are activated by interaction with a group of enzymes (Acyl-CoA) and transported by the Acyl-CoA binding protein (ACBP) to mitochondria or peroxisomes responsible for their oxidation with consequent formation of energy in the form of ATP or heat (Rustan & Drevon 2005). Alternatively ACBP can transfer FFA to the endoplasmic reticulum where they will form, following esterification, different forms of lipids (phospholipids, triglycerides and cholesteryl esters) important for a structural role and lipid homeostasis (Rustan & Drevon 2005). In addition, certain FFA can regulate gene expression through binding of transcription factors (Rustan & Drevon 2005).

The intracellular amount of FFA can also be increased by excess of glucose in the bloodstream. The excess of glucose is transformed intra-cellularly into FFA via lipogenesis (figure 5.1) (Rustan & Drevon 2005).

5.2.2 FFA: functions, biological effects and impact on cardiovascular disease

FFA intervene in the biological system through different mechanisms. Polyunsaturated fatty acids (PUFA) are precursors of eicosanoids, a group of signalling molecules such as leukotrienes, prostaglandins and thromboxanes that are important cellular mediators intervening in platelet aggregation, chemotaxis for blood cells and cell growth, particularly essential in the early phases of the inflammatory process (Rustan & Drevon 2005). FFA are components of phospholipids forming cell membranes. The nature of FFA included in the membrane can affect its fluidity and flexibility. In particular, the membrane flexibility increases with increase of PUFA within the membrane. This is important for the impact on the cardiovascular system as a high amount of PUFA intake can “soften” the structure of low-density lipoproteins (LDL), thus reducing their atherogenic potential (Rustan & Drevon 2005). In addition, lipid peroxidation is responsible for the formation of oxidized LDL that triggers the formation of atherosclerotic plaques. The composition of FFA forming LDL was

shown to be important in determining their atherogenic potential, thus demonstrating that high intake of PUFA versus saturated fatty acid can reduce the risk of coronary heart disease (Rustan & Drevon 2005, Aas 2006).

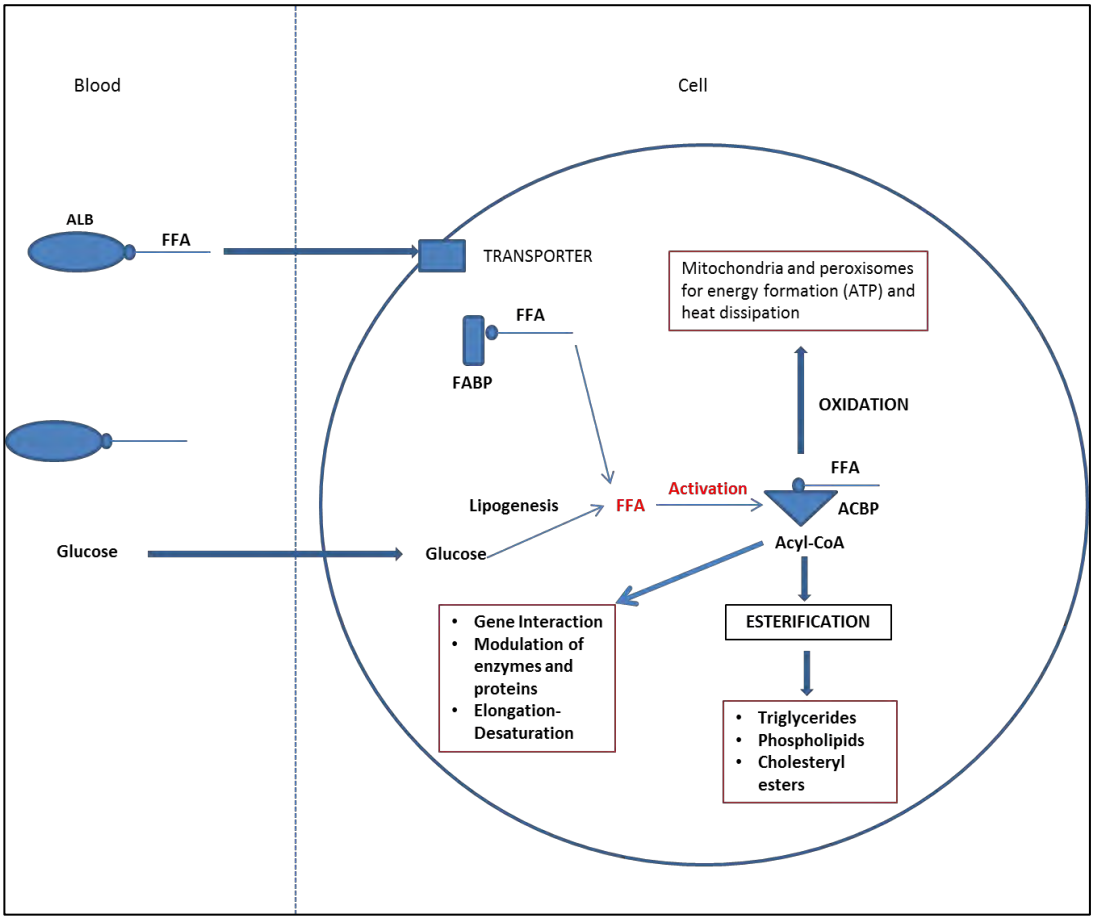

Figure 5.1 Metabolism of free fatty acid. *Free fatty acids reaching circulation after digestion are transported bound to serum albumin (ALB) and absorbed by cells through a "transporter" present on their membrane. FFA are transported intracellularly through fatty acid-binding proteins (FABP) and activated through interaction with enzymes (Acyl-CoA). Once activated the complex is transported by Acyl-CoA binding protein (ACBP) to mitochondria or peroxisomes for oxidation leading to energy formation in form of ATP or heat. Alternatively, the complex is transported to endoplasmic reticulum where following esterification FFA form different classes of lipids (i.e. phospholipids). Certain FFA or Acyl-CoA can participate to gene regulation through binding to transcription factors. Excess of glucose can also be transformed into FFA intracellularly. Diagram adapted from Rustan & Drevon (2005).*

Furthermore, FFA can bind covalently to proteins (acylation of proteins) affecting the functions of membrane proteins. It has been shown that saturated fatty acid can bind to protein through a stronger bond than PUFA (Rustan & Drevon 2005).

The attention of researchers has been recently focussed on the negative effects of a diet rich in saturated fatty acids, recognised as responsible for an increase in the occurrence of cardiovascular disease and metabolic dysfunctions (Kennedy 2008, Hu 2011). Saturated fatty acids have been shown to directly increase inflammation and insulin resistance and to increase the release of pro-inflammatory cytokines (IL-6 and TNF-α) in skeletal muscle cells through induction of inflammatory gene expression (Lee 2006, Kennedy 2008, Hu 2011). Saturated fatty acids were shown to expand the white adipose tissue, increasing size and number of adipocytes. Stimulated adipocytes release pro-inflammatory cytokines, thus resulting in the promotion of systemic inflammation. This is followed by death of the adipocytes with consequent release of their contents and recruitment of neutrophils and macrophages on site (Kennedy 2008). The chronic basic inflammatory condition associated with obesity is the consequence of excess fat intake, particularly if rich in saturated fatty acid (Kennedy 2008). Furthermore, the increase in inflammation due to the effect of saturated fatty acids on white adipose tissue was also shown to be due to the intracellular mechanisms such as promotion of oxidative stress on endoplasmic reticulum, production of reactive oxygen species and protein kinase C signalling (Kennedy 2008).

As mentioned above, an increase in saturated fatty acid can be associated with the occurrence of a chronic basic inflammatory condition accompanied by alterations in protein stiffness and increase of insulin resistance through lipid accumulation within skeletal muscle cells (Rustan & Drevon 2005, Lee 2006, Kennedy 2008, Hu 2011). Different studies have investigated the protective effect of PUFA on cardiovascular system and metabolic dysfunction. Indeed, an increase in the amount of circulating PUFA results in a direct effect on lowering circulating lipids and reducing the atherogenicity of oxidized LDL (Rustan & Drevon 2005).

In addition, recent studies have demonstrated the protective effect of PUFAs on the occurrence of insulin resistance reducing the lipid accumulation within skeletal muscle cells (Lee 2006, Hu 2011).

5.2.2.1 Palmitic acid: characteristics and interaction with macrophages

The most abundant saturated free fatty acid in mammals is palmitic acid, formed of a chain with 16 carbon atoms, and stearic acid, formed of a chain of 18 carbon atoms (Rustan & Drevon 2005). Palmitate and stearate represent 90% of saturated fatty acids circulating in human plasma (Haversen 2009). Figure 5.2 illustrates the chemical structure of palmitic acid, containing sixteen carbon atoms with the molecular formula $C_{16}H_{32}O_2$.

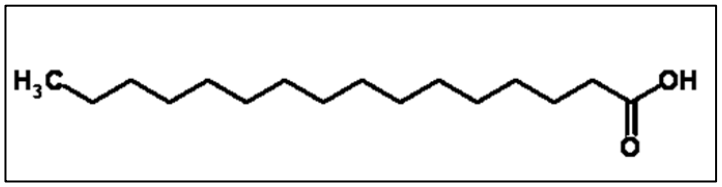

Figure 5.2 Chemical structure of palmitic acid. *Palmitic acid is the most common saturated fatty acid in animal food, thus predominant component of diets rich in saturated fatty acids. It is formed of a chain of 16 carbon atoms linked by single C-C bonds and ending with the carboxylic group. The molecular formula is $C_{16}H_{32}O_2$, molar mass is 256.42 g/mol and its melting point is at 62.9^{O}C. Image adapted from www.spiderchem.com (RSC).*

Palmitate has been used in different studies to evaluate the effects of saturated FFA on the chronic inflammatory condition characterizing obesity (Suganami 2005, Li 2008). Studies have demonstrated the increase of macrophage infiltration in white adipose tissue of obese individuals, thus identifying macrophages as responsible for sustaining the inflammatory condition through interaction between adipocytes and macrophages (Rustan & Drevon 2005, Suganami 2005, Li 2008). It was shown that saturated fatty acids triggered the release of pro-inflammatory cytokines by macrophages, an effect not seen with unsaturated fatty acid. The co-

culture of macrophages and adipocytes showed an increase in the production of TNF-α triggered by saturated fatty acid. It was shown that the white adipose tissue releases fatty acid that activated resident macrophages or recruited new ones (Rustan & Drevon 2005). TNF-α was identified as key mediator of inflammation in adipose tissue (Suganami 2005)

In addition it was shown that high concentrations of palmitate and stearate induced the release of pro-inflammatory cytokines, in particular TNF-α, by macrophages in culture (Haversen 2009).

Saturated fatty acids were shown to trigger the release of TNF-α and IL-10 by macrophages and adipocytes through the activation of Toll-like receptors (TLR), pro-inflammatory receptors implicated in the activation of the immune system in inflammatory diseases (Curtiss & Tobias 2009, Dasu 2011). The activation of TLR leads to the activation of transcription factors within the cells, in particular Nuclear Factor-Kappa B (NFkB) and c-Jun N-terminal Kinase (JNK), thus leading to the release of cytokines (Rustan & Drevon 2005, Dasu 2011). In particular, it was shown that palmitate and stearate increased the release of TNF-α, IL-1 and IL-8 by macrophages mediated by the action on TLR of ceramide, a product of the metabolism of long chain saturated fatty acids. A similar action was not demonstrated for unsaturated fatty acids (Haversen 2009). Details of intracellular mechanisms leading to saturated fatty acid-induced inflammation have not yet been unveiled. Different studies demonstrated that the saturated fatty acid induced the expression of TLR-2 and TLR-4 on macrophages leading to the activation of pro-inflammatory gene expression (Chait 2010, Dasu 2011, Huang 2012). Similarly, low glucose concentration, as well as insulin, have been has been shown to be associated with an overall anti-inflammatory effect in diabetics (Collier 2008). A study showed that, similarly to saturated fatty acids, high glucose induces the expression of TLR-2 and TLR-4 in monocytes as a consequence, respectively, of the activation of protein kinase C (PKC)-alpha and -delta, and through the stimulation of NADPH oxidase (Dasu 2008). The inhibition

of the pathways in monocytes has in fact shown the inhibition of inflammatory cytokine secretion (Dasu 2008). In addition, a recent study demonstrated the synergistic activity of saturated fatty acid and high glucose concentration on the activation of pro-inflammatory cytokines and transcription factors in monocytes providing further insight in the mechanisms characterizing the inflammatory condition of diabetes and metabolic syndrome (Dasu 2011).

5.3 AIMS

The work described in this chapter aimed to evaluate the effect of glucose and lipids (represented by palmitate) on the acute response of macrophages to contact with stainless steel.

The overall aim was to assess whether hyperlipidaemia and hyperglycaemia could exacerbate the activation of cellular pathways leading to *in-stent* restenosis following the implantation of a stainless steel non-medicated stent.

This was obtained by creating a basic experimental model of diabetes and metabolic syndrome characterized by the use of culture medium with modified concentrations of glucose and lipids alone or in combination. The effect of the changes in cultural conditions was assessed through:

- The analysis of changes in the phenotypical expression of mononuclear cells adhering on stainless steel.
- The analysis of morphological changes on mononuclear cells adhering on stainless steel evaluating the potential synergistic effect of high glucose and lipid concentrations and the contact with the metal.

- The measurement of the release of pro- and post-inflammatory cytokines after overnight incubation on the experimental surfaces under different cultural conditions.

5.4 MATERIAL AND METHODS

5.4.1 Recruitment of volunteers, blood collection and treatment

Cells of the mononuclear lineage were isolated from informed healthy volunteers (18-60). Donors were chosen to provide a source of mononuclear cells not chronically exposed to elevated blood glucose level or conditions affecting their response to foreign materials. For this reason exclusion criteria applied in the recruiting process were: subjects with a diagnosis of diabetes or metabolic syndrome, the presence of chronic inflammatory diseases or diseases affecting the immune system, the use of immunosuppressant or cytostatic drugs and the presence of current or previous morbidities involving their cardiovascular system.

Ethical approval for the study was obtained from the Pharmacy and Biomolecular Sciences Ethics Committee from the University of Brighton. In order to obtain approval, standard operating procedures and donor information leaflets (Appendix 1) were produced and informed consent was obtained by donors. Blood (30ml) was collected in heparinised tubes (Greiner Bio-One Ltd; Cat number 455051) by venepuncture and treated according to the procedure described in section 2.3.1.2 within three hours after collection.

5.4.2 Preparation of material substrate and their surfaces conditioning

The experimental surfaces were chosen and treated as described in Section 4.3.2. Cells were seeded on the surfaces as follows:

$5x10^5$ cells per well for plates to be used for immunocytochemistry and scanning electron microscopy;

- $1x10^6$ cells per well in plate to be used for RNA extraction and PCR (described in chapter 6).

5.4.3 Experimental conditions

In order to evaluate the reaction of monocytes/macrophages to stainless steel after exposure to high glucose and/or lipid concentration, four experimental conditions were used as it follows:

- Physiological blood glucose concentration (5.5mM):

  Cells were incubated overnight at 37^oC and 5%CO2 in DMEM (Sigma Aldrich, UK or PAA laboratories) with glucose concentration comparable to physiological level (1000mg/L) added with 10% (v/v) FBS (PAA laboratories) and penicillin/streptomycin (PAA laboratories).

- High glucose concentration (25mM):

  Cells were incubated overnight in DMEM (Sigma Aldrich, UK or PAA Laboratories) containing high glucose concentration (4500 mg/L) and added with 10% (v/v) FBS (PAA Laboratories) and penicillin/streptomycin (PAA Laboratories).

- Effect of high free fatty acid concentration alone or in combination with high glucose concentration:

Physiological or high glucose concentration DMEM was added with sodium palmitate (Sigma Aldrich, UK Cat.P9767) at a concentration of 0.4mM. Sodium palmitate was chosen because it represents the predominant fraction of circulating saturated free fatty acids and its effect on different cell types alone or in combination with glucose had previously been investigated in different studies (Briaud 2001, Dasu 2011). In previous studies the effect of palmitate in the culture medium was investigated at a range between 0 and 0.6mM. The experimental concentration of sodium palmitate used in this study was determined observing the effect of increasing concentrations (0.2, 0.4 and 0.5mM) of palmitate on cells grown under different conditions as described in section 5.3.6.

5.4.4 Preparation of sodium palmitate solution

A 100mM stock solution of sodium palmitate was obtained by dissolving the lipid powder (Sigma Aldrich, UK Cat.P9767) in a 1:1 (vol:vol) solution of deionized water and ethanol at 50^{o}C. The stock solution was then stored at -20^{o}C for up to four weeks and used to obtain a 5mM solution of sodium palmitate in 10% (w/v) BSA (BSA-Fatty acid free, Sigma Aldrich, UK; Cat A7030). The solution was prepared by diluting the 100mM stock solution with a 10% (w/v) solution of BSA in deionized water with gentle stirring for one hour at 37^{o}C to allow the formation of the palmitate-BSA complexes. After cooling, the final solution was sterilized by filtering with 0.45µM filters (Sartorius Stedium- Minisart Cat 16555). The palmitate/BSA molar ratio in the final solution was approximately 3:1. As previously reported, the final solution was stored at -20^{o}C for a maximum of four weeks and pre-heated at 50^{o}C prior addition to the culture medium.

5.4.5 Optimisation of the experimental conditions

The concentration of sodium palmitate to be added to the culture medium was determined based on data from literature and through preliminary experiments assessing the toxicity of increasing concentrations of palmitate on adhering mononuclear cells. Previous studies used concentration of BSA-complexed palmitate of 0.5mM to reproduce hyperlipidaemic conditions (Briaud & Poitout 2001, Haversen 2009). In particular, a study showed the occurrence of toxic effects on human macrophages using 0.6mM palmitate in the culture medium (Haversen 2009). To optimise the experimental conditions for this work, freshly isolated macrophages were incubated for 24 and 48 hours on tissue culture plastic with increasing concentrations of sodium palmitate (0.2mM, 0.4mM, 0.5mM) prepared according to the protocol described in section 5.3.4. The samples were tested for cell viability, proliferation and morphology using respectively Hoechst-Propidium Iodide (HPI) staining, staining for Ki67 and scanning electron microscopy (SEM).

5.4.5.1 Hoechst-Propidium Iodide (H/PI)

Cell viability was determined by staining the adhering cell nuclei with the combination of Hoescht 33258 (BisBenzimide; Sigma Aldrich, UK) and propidium iodide (Sigma Aldrich, UK). Cells were isolated and seeded on the plates as described in sections 5.4.1, 5.4.2 and 5.4.3. Cells were incubated overnight or for 48 hours and washed three times with PBS. A mixture of Hoescht and propidium iodide, each at a final concentration of 0.05 mg/ml in the culture medium was added to the wells and cells observed using an inverted-light fluorescence microscope. The two dye molecules intercalate with DNA bases thus generating fluorescence. Hoescht absorbs in the UV range of the spectrum emitting blue fluorescence. Propidium iodide emits red fluorescence. Propidium iodide cannot permeate intact cell membranes, thus being visible only in dead cells with altered membranes. Hoescht, due to its smaller size, can penetrate live

or apoptotic cells with intact membranes. The staining allows therefore the identification of live cells (blue), necrotic (red) and apoptotic (bright blue).

5.4.5.2 Immunocytochemistry for Ki-67

Ki-67 is a protein expressed by the cell nuclei throughout all the phases of cell proliferation. In particular, during the interphase of the cell cycle the protein is situated in the nucleus and it is relocated on the chromosome surface during mitosis (Scholzen & Gelden 2000). The protein is consequently expressed during all the active phases of the cell cycle (G1, S, G2 and mitosis) with the exception of the quiescent phase (G0). This makes of Ki-67 the ideal marker for the identification of proliferating cells (Scholzen & Gelden 2000). More specifically, antibodies for Ki-67 have been used in techniques such as immunocytochemistry to detect cells in proliferative stage. All the cells in a sample would in fact express Ki-67 with the exception of cells in the phase G0 (Scholzen & Gelden 2000).

In this work, macrophages prepared according to the protocol described in sections 5.4.1, 5.4.2 and 5.4.3 and adhering on tissue culture plastic were incubated overnight and for 48 hours at 37^{o}C. Following incubation, cells were rinsed three times with PBS and fixed with incubation at -20^{o}C for 15 minutes in a 1:1 mixture of methanol and acetone. Non-specific binding sites were blocked through a further incubation of the cells in a 1% (w/v) solution of BSA in PBS (30 minutes at room temperature) and incubated for 1 hour in a 1:50 solution of rabbit anti-human anti-Ki67 antibody (Abcam, UK; Ab16667) in 1% (w/v) BSA in PBS (room temperature). The step was followed by incubation with a 1:50 solution of the fluorochrome-tagged secondary antibody (Anti-rabbit Alexafluor-Red fluorescence) in PBS (room temperature in the dark) and nuclei counterstained by further addition of DAPI. Between all the steps of the staining process cells were rinsed three times with PBS. Cell culture samples (n=3) were observed by an epi-fluorescence microscope (Inverted NIKON Elipse TE2000U) equipped with a Canon LM Scope camera and images acquired with Image Pro-Insight software.

Micrographs were taken at X40 magnification. Six fields were analysed from each sample.

5.4.5.3 Scanning Electron Microscopy (SEM)

Scanning electron microscopy was used to verify the morphology of the adhering macrophages. After incubation of cells prepared as described in sections 5.4.1, 5.4.2, 5.4.3, adhering cells were rinsed with PBS and fixed by incubation in a 1:1 solution of methanol and acetone (15 minutes at -20^{o}C). Following further rinses with PBS cells were dehydrated by incubation with increasing concentration of ethanol/water (25%, 50%, 75% and 96% by volume; 15 minutes at room temperature for each step). Cells were then air dried and stored at -20^{o}C. Cells were coated with platinum (4nm) before images were acquired using Zeiss-Sigma scanning electron microscope (Zeiss EVO LS15 taken at 5kV).

5.4.6 Collection and storage of supernatants

Cells were seeded into tissue culture plates as described above and left in incubation overnight at 37^{o}C in 5% CO_2 and humidity. After incubation supernatants were collected in Eppendorf 1.5 ml polypropylene tubes, centrifuged at 10,000xg for 5 minutes to precipitate floating cells and debris and finally transferred to clean 1.5 ml Eppendorf tube and frozen at -70^{o}C.

5.4.7 Preparation of cells for double-stain immunocytochemistry

After overnight incubation and removal of supernatants, cells adhering on surfaces were washed three times in sterile PBS and fixed with an incubation of 30 minutes in 3.7% (v/v) paraformaldehyde (Sigma Aldrich, UK) in PBS at room temperature. After three washes with PBS cells to be stained for intracellular markers were permeabilized with an incubation of 10 minutes in a 0.2% (v/v)

solution of Triton X-100 (Sigma Aldrich, UK) in PBS. The cells that did not need to be stained for intracellular markers were left in PBS. After further three washes with PBS cells were incubated with 100µl or 200µl of solutions of primary antibodies, as described in table 5.1, diluted in 1% (w/v) BSA (BSA-Sigma Aldrich,UK; Cat A7030) in PBS for 1.5-2 hours at room temperature. The working dilutions for each antibody were chosen following manufacturers' guidelines or by titration experiments in which different dilutions of the antibody were tested in order to select the condition that provided the better balance between staining outcome and background noise. The list of antibodies used in different experiments and their working dilutions is represented in table 5.1. A double immunostaining technique was used to bypass the restriction due to the limited amount of cells extracted from each donor. Each well was incubated with a mixture of two primary antibodies, each at the final concentration listed in table 5.1. The antibodies were selected of different species (mouse and rabbit) in order to avoid cross-reactivity. Secondary antibodies were specific for the species and conjugated to different flurophores to show different colour fluorescence during the final examination.

After completing the incubation with primary antibodies solutions, cells were washed three times with PBS, followed by a 1-hour incubation at room temperature and in the dark with 100µl or 200µl of 1:100 solution of secondary antibodies (anti-mouse Alexafluor Invitrogen, green fluorescence; anti-rabbit Alexafluor, red fluorescence) in 0.1% (w/v) BSA in PBS. The cells were then washed three times in PBS and counterstained with DAPI to identify the cell nuclei.

Negative controls were prepared to verify non-specific binding and background noise. To this purpose, cells were stained with the same protocol omitting the incubation with primary antibodies (prim.). This step was replaced by incubation with 1% (w/v) BSA in PBS. Results showed that despite the presence of a background staining, no relevant

unspecific binding of secondary antibodies (sec.) to cell surfaces occurred (figures 5.3a,b,c).

Table 5.1. List of primary antibodies and their working dilutions used for cells phenotypic characterisation by immunocytochemistry

Cell identification	Marker	Dilution	Antibody
Endothelial Progenitor Cells	CD34	1:100	Mouse monoclonal anti-human CD34 antibody, Abcam plc, UK. Cat No Ab54208
Blood Mononuclear Cells	CD14	1:100	Mouse monoclonal anti-human CD14 antibody, Abcam plc, UK. Cat No Ab63319
Activated macrophages	CD68	1:50	Rabbit polyclonal anti-human CD68 antibody, Abcam plc, UK. Cat No Ab74208
Smooth muscle cells	α-actin	1:100	Rabbit polyclonal anti-human alpha smooth muscle actin, Abcam plc, UK. Cat No Ab97375

Negative controls were prepared to verify absence of cross reactivity between primary and secondary antibodies. Those were prepared by adding the antibody mixtures to wells without seeded cells. No positive reaction was seen in those wells (figures 5.3d,e,and f).

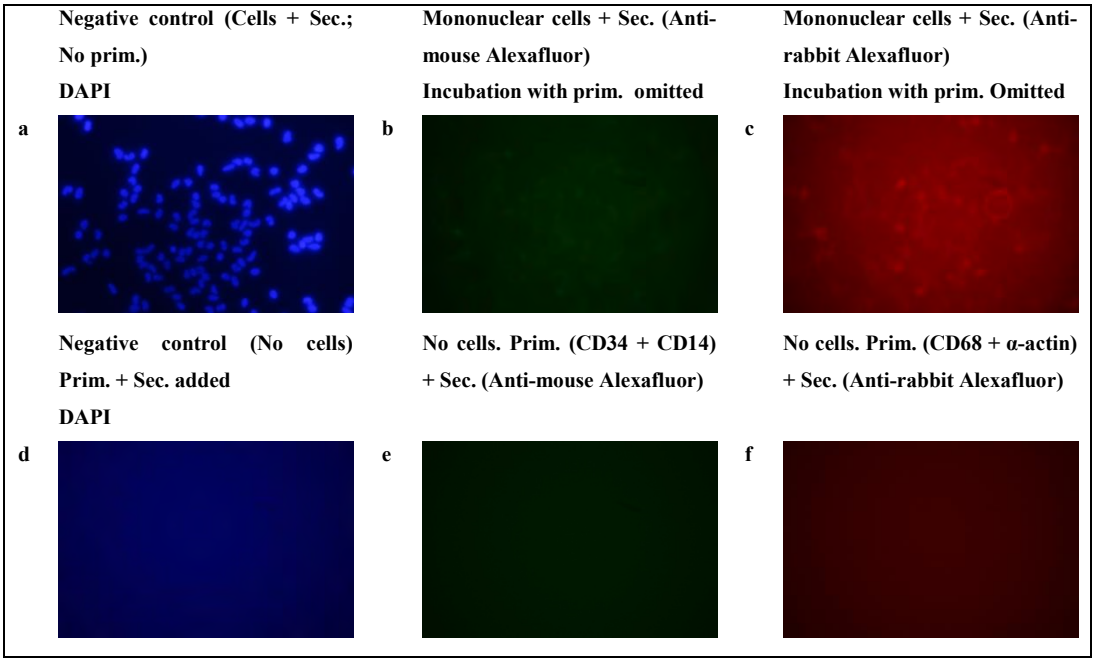

Figure 5.3 Negative controls for immunostaining. *Negative controls were prepared by replacing the incubation with primary antibody mixtures with incubation in 1% (w/v) BSA in PBS. This showed the presence of a low background noise due to the interaction between cells and secondary antibodies (figures 5.3a,b,and c). The absence of cross-reactivity between antibodies or between antibodies and protein layer coating the surfaces after pre-conditioning was verified by staining wells where no cells were seeded (figures 5.3d,e,f). Images taken at epi-fluorescence microscope. Magnification X40.*

5.4.8 ELISA test

Supernatants (1ml per sample) collected as described in section 5.4.6 were used to assess the amount of cytokines relevant to the restenotic process released during the overnight incubation of the monocytes-derived macrophages on experimental surfaces. The release of cytokines was tested using solid phase sandwich Enzyme Linked-Immuno-Sorbent Assay (ELISA) as described in section 4.3.6. All the results obtained from the tests were normalised by dividing the amount of cytokine measured in each sample by the amount of total proteins present in the same sample which was using the method described by Bradford (Bradford 1976). The amount of proteins found in samples was considered proportional to the

amount of cells adhering onto the surfaces. The normalization of the data aimed at reducing the possibility of artefacts related to differences in the amount of adhering cells. Normalizing the amount of cytokine by the total amount of proteins that is considered proportional to the amount of adhering cells, the differences in cytokines would be exclusively correlated to the effect of the contact with biomaterials or to changes in the environmental conditions.

Each sample (n=6 per cohort of donor and per experimental surface) were loaded in triplicate. Results are expressed as mean ± standard error and analysed using paired student t-test.

5.4.8.1 PDGF-BB ELISA

The measurement of the release of Platelet Derived Growth Factor-BB (PDGF-BB) in samples was obtained by using the human PDGF-BB ELISA kit from Abcam (Cat. Number ab100625) as described in section 4.3.6.4 and performed on n=6 samples. The standard curve was obtained using the human PDGF-BB standard supplied by the company and producing a serial dilution ranging from 0 to 400pg/ml. However, the values obtained from the highest concentrations of the standard solution were excluded from the standard curve because the results obtained were out of scale and the linearity of the curve was affected. The range of values obtained from the experimental samples fell within the range represented in the standard curve (0-44.44 pg/ml) (figure 5.4).100µl of DMEM (Sigma Aldrich, UK) added with the 10% (v/v) FBS (PAA Laboratories) and penicillin/streptomycin (PAA Laboratories) were loaded in duplicate to verify the background absorbance due to the culture medium.

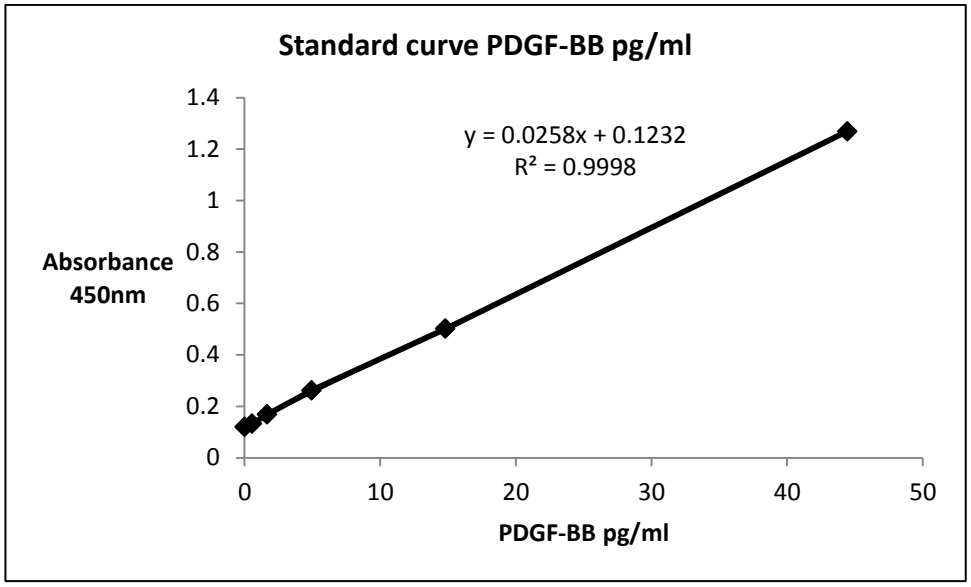

Figure 5.4 Standard curve for PDGF-BB ELISA. *The standard curve was obtained following the manufacturer's instructions. Increasing concentrations (0-44.44 pg/ml) of the standard provided with the kit were added to the test plate and plotted against the reading obtained from the spectrophotometer at 450nm. The resulting curve showed a linearity coefficient (R^2) of 0.9998 used to determine the concentrations of PDGF-BB from the optical density obtained from the samples.*

5.4.8.2 TNF-α ELISA

The release of Tumour Necrosis Factor-alpha (TNF-α) was measured using the Human TNF-α ultrasensitive kit purchased by Invitrogen Corporation (Cat. Number KHC3014C) as described in Section 4.6.3.3 and performed on n=6 samples. The use of ultrasensitive kit allowed measuring low levels (ranging from 0 to 32pg/ml) of TNF-α in the samples. In order to reach levels of TNF-α measurable with the ultrasensitive kit all samples were diluted 1:4 with standard diluents buffer supplied by the company prior loading into the wells. All samples were loaded in duplicate and two wells with culture medium (DMEM+10%FBS+penicillin/streptomycin) were prepared as background. The standard curve was prepared using the human TNF-α standard provided according to the instructions of the company producing a dilution series (0-32 pg/ml) as represented in Figure 5.5.

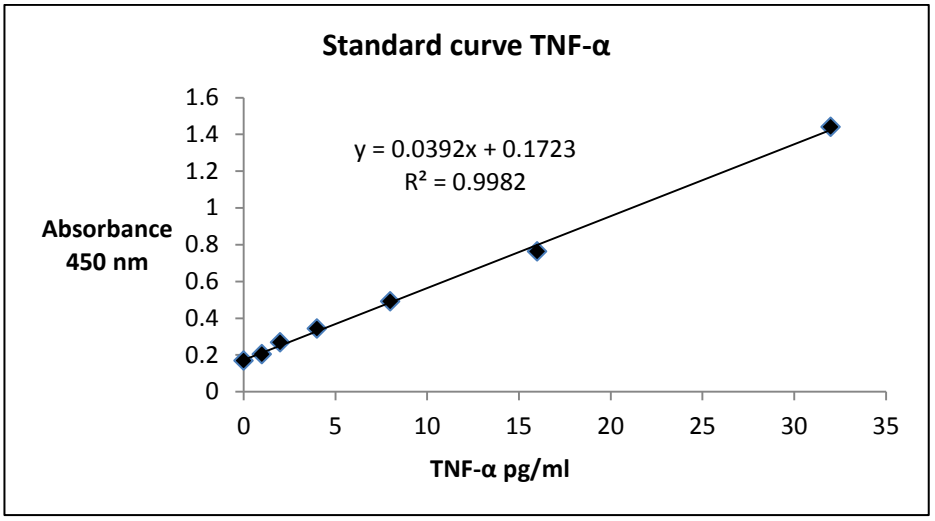

Figure 5.5 Standard curve for TNF-α ELISA. *The standard curve was obtained following manufacturer's instructions. Increasing concentrations (0-32 pg/ml) of the standard provided with the kit were added to the test plate and potted against the reading obtained from the spectrophotometer at 450nm. The resulting curve showed a linearity coefficient (R^2) of 0.9982 used to determine the concentrations of PDGF-BB from the optical density obtained from the samples.*

5.4.8.3 Protein assay (Bradford method)

In order to normalise the results obtained from the ELISA test the amount of proteins in supernatants were measured using the Bio-Rad reagent for protein assay applying the technique first described by Bradford as described in Section 4.3.6.5. The reagent was diluted 1 to 5 in deionised water and 200µl were loaded into each well of a 96-well plate with 10µl of sample or standard. Standard curve was prepared by serial dilution (0-1000 µg/ml) of a 10mg/ml solution of BSA in PBS and the results are shown in Figure 5.6.

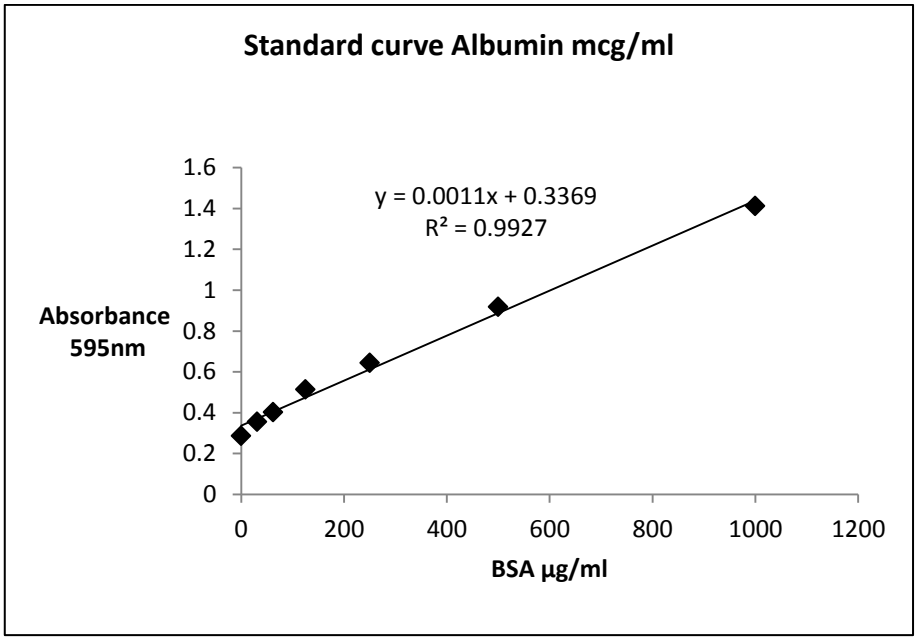

Figure 5.6 Standard curve for protein assay (Bradford method). *The standard curve was obtained plotting the absorbance read at 595 nm corresponding to a serial dilution of BSA (0-1000 µg/ml). The curve obtained showed a linearity coefficient (R^2) of 0.9927.*

5.5 RESULTS

5.5.1 Preliminary experiments

Increasing concentrations of palmitate were added to the culture medium to establish the concentration that, despite representing acute hyperlipidaemia, did not affect cell viability or proliferation.

Results after staining with HPI showed alive cells in all the experimental conditions indicating that macrophages could maintain their viability and proliferate in all the conditions. However, a general increase in dead cells with the increase of the concentration of palmitate was observed even after overnight incubation (figure 5.7).

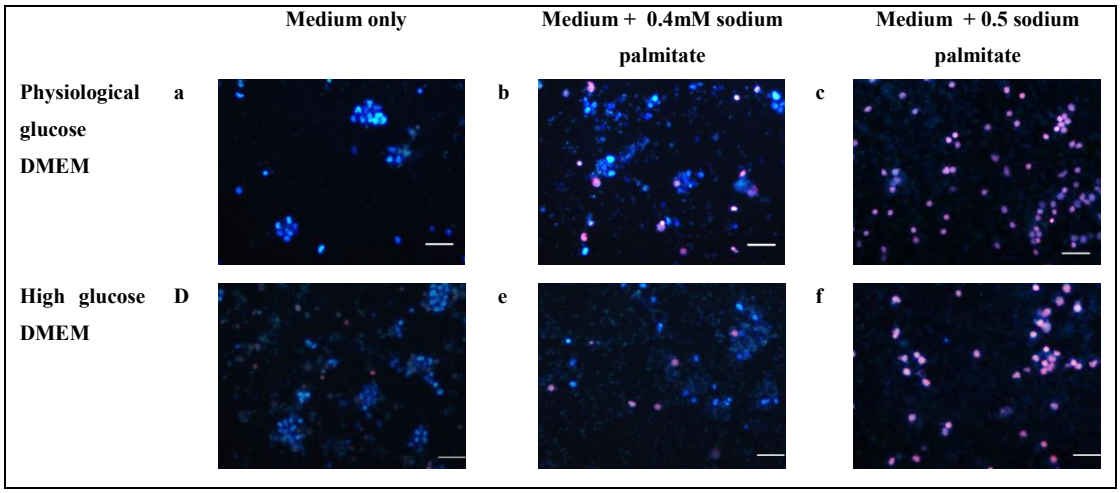

Figure 5.7 Effect of increasing concentrations of sodium palmitate on cell viability. *The images show that increased concentration of sodium palmitate in DMEM caused increase in cell death when viability was tested through staining with Hoechst and propidium iodide. Macrophages incubated in pure medium with both physiological (figure 5.7a) and high glucose (figure 5.7d) concentration were alive. The number of dead cells increased in samples added with 0.4mM of Palmitate (figures 5.7b, 5.7e) at both glucose concentrations. A greater amount of dead cells were seen in samples added with 0.5mM palmitate (figures 5.7c, 5.7f). Pictures were taken with epi-fluorescence microscope at X32 magnification. Size bars =50µm.*

In particular, in wells containing 0.5mM palmitate areas with a very high amount of dead cells (figures 5.7c, 5.7f) could be found. This suggested that at the experimental conditions for this study a concentration of 0.5mM palmitate negatively affected the viability of macrophages. A similar scenario was seen in the case of cells cultured in DMEM with both low and high glucose concentration (figure 5.7).

Results showed that macrophages were proliferating under all culture conditions. The expression of Ki-67 was seen by the totality of adhering cells cultured in medium with physiological or high glucose concentrations (figures 5.8a,b and 5.8g,h) and after addition of 0.2mM (data not shown) and 0.4mM palmitate (figures 5.8c,d and 5.8i,j). Similarly, adhering cells cultured in media spiked with 0.5mM palmitate expressed Ki-67 (figures 5.8e,f and 5.8k,l) despite the fluorescence being less intense and did not involve all of the adhering cells. This suggested that the high concentration of palmitate added to the medium might affect the proliferation of the cells.

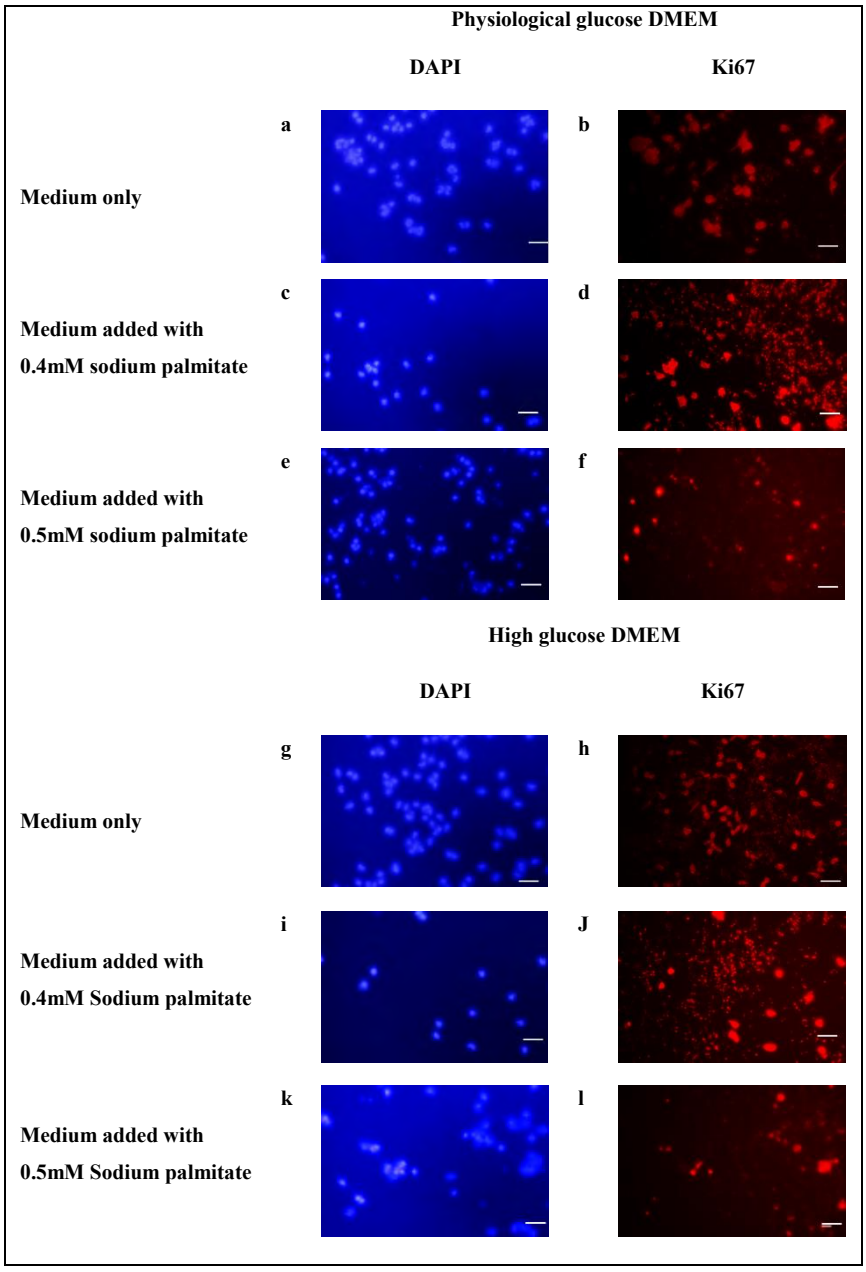

Figure 5.8 Effect of increasing concentrations of palmitate on macrophage proliferation. *Images of immunocytochemistry identifying Ki-67, a marker for cell proliferation, showed that macrophages proliferated under all culture conditions. After overnight incubation the marker was expressed by all the macrophages adhering on tissue culture plastic in physiological and high glucose concentration DMEM (figure 5.8a,d: DAPI nuclei counterstain; figure 5.8b,e: Ki-67). Cells also stained positive for Ki67, indicating proliferation, when the medium was added with o.4mM sodium palmitate (figure 5.8c,d: physiological glucose DMEM; figure 5.8i,j: high glucose DMEM). Cells were positive for Ki-67 when physiological and high glucose concentration DMEM was added with 0.5mM palmitate, although fluorescence was less intense (figure 5.8e,f and 5.8k,l respectively). Images were taken at fluorescence microscope at X20 magnification. Size bars = 50um.*

Results from SEM showed the presence of macrophages with smooth plasmalemma or spread onto the surface of the wells when cells were cultured in media with no addition of palmitate (figures 5.9a,d). In wells where palmitate was added at higher concentrations (0.4mM and 0.5mM) macrophages showed rough plasmalemma and the presence of blebs typical of activation and phagocytosis (figures 5.9b,c and 5.9e,f respectively).

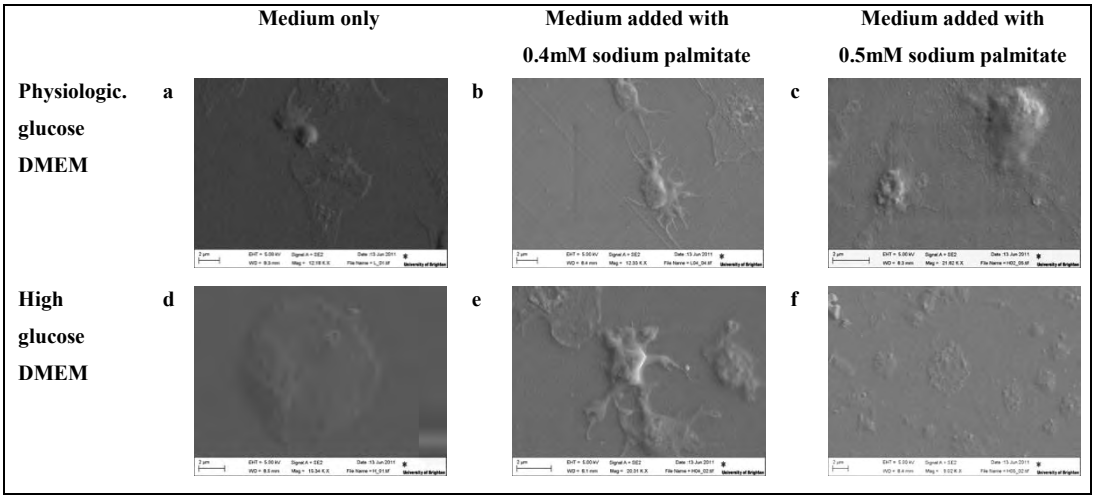

Figure 5.9 SEM images of mononuclear cells incubated on TCP at increasing concentrations of sodium palmitate. *The preliminary experiment for the evaluation of the optimal concentration of sodium palmitate revealed that when incubated overnight on TCP in DMEM with physiological (figure 5.9a) or high (figure 5.9d) glucose concentration cells spread on the surface remaining isolated. Following the addition of 0.4mM (figures 5.9b,e) and 0.5mM (figures 5.9c,f) cells showed a morphology characterised by the formation of numerous cell-cell interactions, rough plasmalemma and formation of "blebs" on their membrane. Those represent features typical of phagocytosis and macrophage activation.*

The results from preliminary experiments suggested that macrophages could proliferate under all the tested experimental conditions, although proliferation seemed to be affected when 0.5mM palmitate was added. In addition, considering the high amount of dead cells observed after HPI staining in wells where macrophages were cultured in medium with the addition of 0.5mM sodium palmitate this concentration was excluded to avoid risk of cell damage affecting the assessment of the response to the biomaterial. The addition of 0.2mM

palmitate was considered a condition not significantly different from the control (medium only). The 0.4mM palmitate concentration was chosen to represent a pathological concentration of lipids but still in a range not causing toxicity to the cells. Overnight incubation was chosen as the timescale suitable to evaluate the acute response of inflammatory cells to the biomaterial as assessed in previous part of this work.

5.5.2 Immunocytochemistry

Samples double-stained for the identification of CD34 (marker for haematopoietic progenitor cells) and CD68 (activated macrophages) revealed a variable amount of adhering cells expressing the CD34 among the adhering cells expressing CD68 (figure 5.10). Immunocytochemistry did not seem to show any significant difference in the expression of the markers between different surfaces or culture conditions.

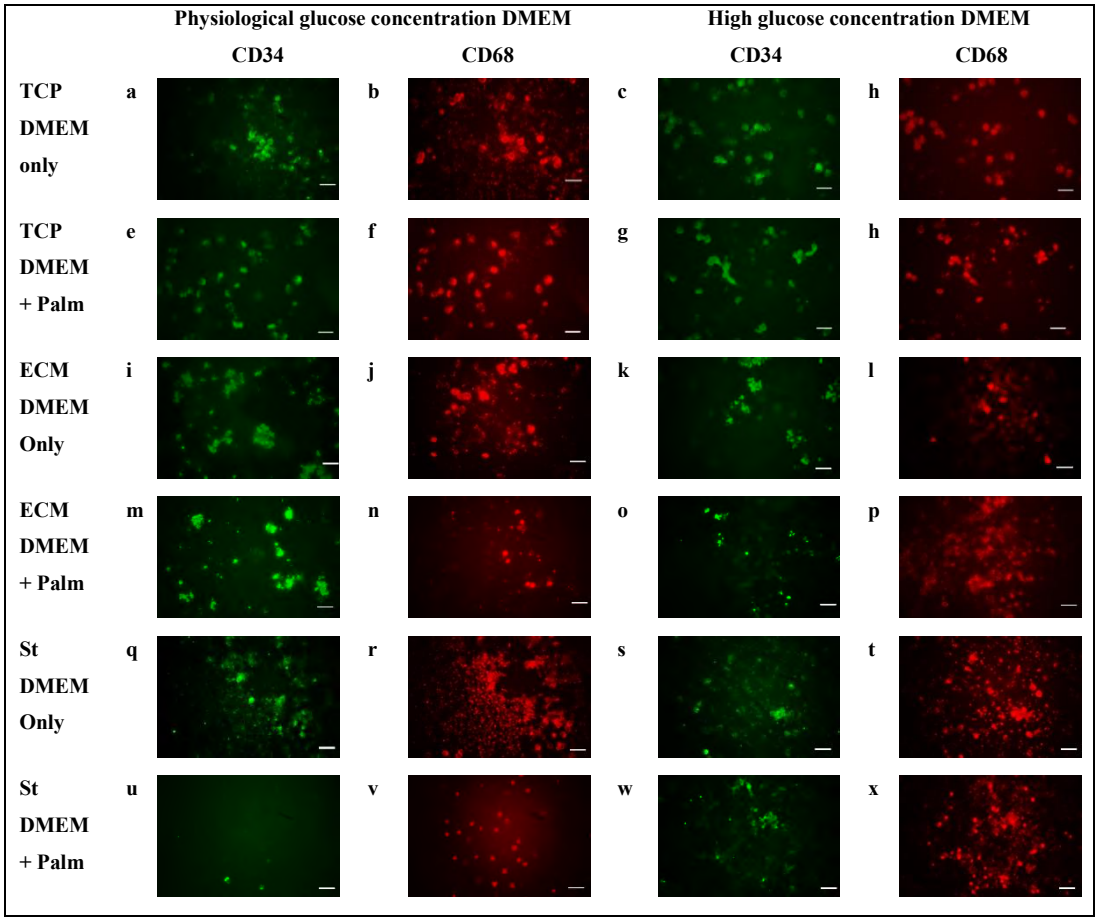

Figure 5.10 Co-expression of CD34 and CD68 in adhering mononuclear cells. *The figure shows the result of double immunostaining on adhering cells extracted from one donor after overnight incubation on tissue culture plastic (figures 5.10a-h), extra-cellular matrix-coated wells (figures 5.10i-p) and stainless steel (figures 5.10q-x) and incubated in DMEM with low and high glucose concentration and with or without the addition of 0.4mM sodium palmitate. The areas shown in the figures show that adhering expressed the marker for activated macrophages (red staining). Among the same cells the expression of the marker for haematopoietic progenitor cells (CD34) was variable (green staining). Magnification X40. Size bars = 50µm.*

The amount of cells expressing CD34 identified as endothelial progenitor cells varied across donors and areas on the surfaces but no specific trend could be identified comparing culture conditions or surfaces (figure 5.10). The double immunostaining also showed that adhering cells co-expressed the marker for monocytes (CD14) and the marker for smooth muscle cells (α-actin) on all the surfaces and under all experimental conditions (figure 5.11). Overall the immunostaining confirmed that the adhering cells expressed markers for both monocytes (CD14) and activated macrophages (CD68), thus identifying them as monocytes-derived macrophages, co-expressing the marker for smooth muscle cells and for haematopoietic progenitor cells.

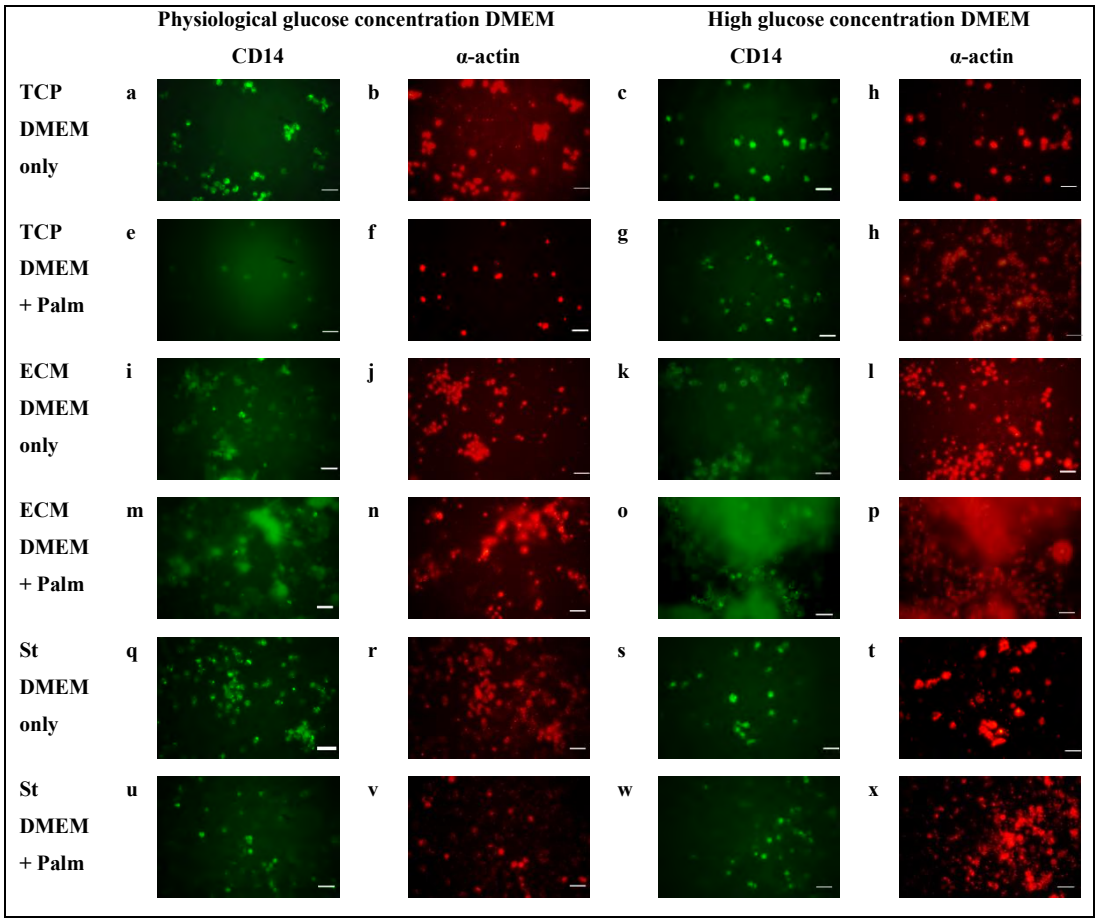

Figure 5.11 Co-expression of CD14 and α-actin in adhering mononuclear cells. *The figure shows adhering cells positive for the marker for monocytes (CD14; green staining) and for the marker for smooth muscle cells (α-actin; red staining) on tissue culture plastic (figure 5.11a-h), on extra-cellular matrix-coated wells (figure 5.11i-p) and on stainless steel (figure 5.11q-x). Cells were isolated from the same donor and nuclei counterstained with DAPI (data not shown). Magnification X40. Size bars = 50μm.*

5.5.3 Scanning electron microscopy (SEM)

SEM was used to verify the effect of surfaces and different culture conditions on the morphology of the adhering macrophages. The images of macrophages incubated overnight in DMEM, both with normal or high glucose concentration, showed that on TCP (figures 5.12a,d respectively) and ECM (figures 5.12b,e respectively) cells remained isolated appearing spread onto the surface, the majority of them losing their original round shape. The behaviour and morphology shown were typical of macrophages on tissue culture plastic, expressing a good degree of cell-material interaction and no activation of the phagocytic process (Guildford 2005). The initial cell-to-cell interaction and rougher plasmalemma (figure 5.12c,f) seen in cells adhering on stainless steel was characteristic of the initial phases of activation and phagocytosis (Guildford 2005), despite macrophages being well spread onto the surface.

The addition of sodium palmitate to the culture medium showed a completely different morphological pattern. On all surfaces cells seemed to become activated. Macrophages were in fact establishing cell-to-cell interactions forming giant cells (i.e. figure 5.12h: cells on ECM). In addition, cells showed rough plasmalemma with "blebbing" on the surface indicating activation and phagocytosis (figure 5.12k: on ECM). Similar scenario was seen in cells on tissue culture plastic (figures 5.12 g and j, respectively in normal and high glucose DMEM). The morphological alterations seemed to be more pronounced in the case of macrophages adhering on stainless steel (figures 5.12 i and l, respectively in normal and high glucose DMEM added with 0.4mM palmitate), in particular when in culture with high glucose DMEM. In this case cells appeared as a rough membrane and the integrity of the membrane structure was compromised by the phagocytic process (figure 5.12l). However, the roughness of the surface of metal discs might partially affect the interpretation of variations of the morphological features of adhering cells when compared to the morphology of cells adhering on smoother surfaces (i.e. TCP or ECM-coated TCP).

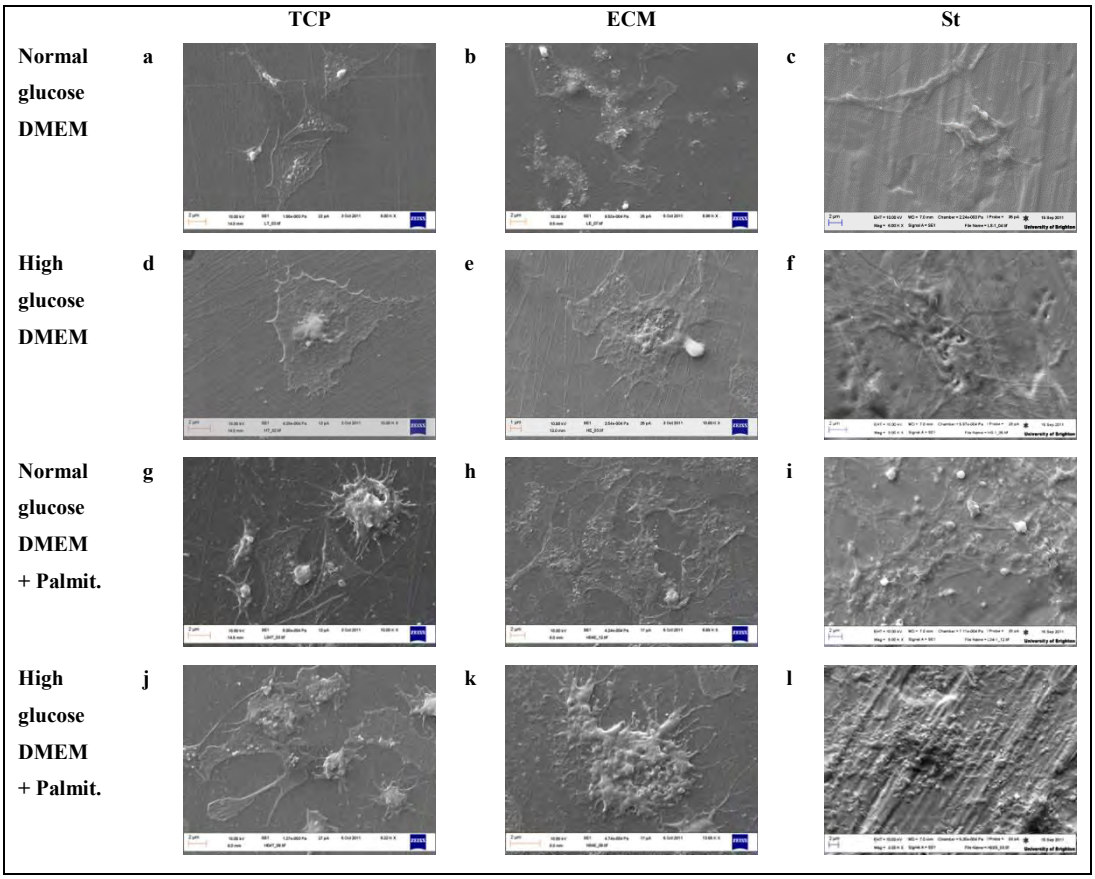

Figure 5.12 Morphology of adhering macrophages. *Images obtained with SEM showed that macrophages adhering on TCP spread onto the surface as a result of cell-material interaction in medium with low (Figure 5.12a) or high (Figure 5.12d) glucose remaining isolated after overnight incubation. Similar scenario was seen for macrophages adhering on ECM-coated wells incubated both in physiological (figure 5.12b) and high (figure 5.12e) glucose concentration. Macrophages on St seemed to spread onto the surfaces indicating a good degree of interaction cell-material. However, the morphology of these cells adhering on the metal appeared different both in physiological (figure 5.12c) and high (figure 5.12f) glucose concentration. They started to interact in the attempt to form aggregates and became activated as suggested by their rough plasmalemma and by the formation of filopodia at a greater extent compared to the cell on TCP and ECM. When cells were incubated in medium added with sodium palmitate 0.4mM cells on all surfaces and under all culture conditions showed a good degree of cell-cell communication in the process of forming giant cells. Furthermore macrophages on all the surfaces showed rough plasmalemma and "blebs" on cell surface as sign of activation and phagocytosis. Similar behaviour and morphology was seen in macrophages adhering on TCP (figures 5.12g,j), ECM (Figures 5.12h,k), and St (figures 5.12i,l). In the case of St, cell structure was difficult to identify, particularly in macrophages incubated in high glucose DMEM added with palmitate (figure 5.12l). However, the rough surface of the metal discs might affect the interpretation of morphological alterations of adhering cells.*

5.5.4 Measurement of the release of cytokines by ELISA

ELISA tests were used to quantify the release of PDGF-BB and TNF-α by macrophages incubated overnight on the experimental surfaces under different culture conditions. The raw data obtained from ELISA and Bradford tests are listed in Appendix 2.The amount of released cytokines was normalised through protein quantification in the same samples to avoid artefacts due to differences in the number of adhering cells. The statistical differences were assessed using paired t-test.

5.5.4.1 PDGF-BB ELISA

Results from ELISA test are represented in table 5.2. The table shows that the trend in PDGF-BB release was similar when comparing the values before and after normalization on the total amount of proteins obtained from the Bradford test.

Results from ELISA showed that, as a general trend, PDGF-BB release was higher from cells incubated on stainless steel (St) compared to samples from cells incubated on tissue culture plastic (TCP) under all culture conditions (figure 5.13; table 5.2). Similarly, increase in the release of PDGF-BB was seen in samples from cells incubated on extra-cellular matrix-coated wells (ECM) with the exception of cells incubated in high glucose concentration DMEM spiked with 0.4mM of sodium palmitate where the PDGF-BB released from cells on ECM was equivalent to the PDGF-BB released from cells incubated on TCP under the same conditions (figure 5.13; table 5.2).

Cells incubated on stainless steel (0.038pg/µg±0.0064) in high glucose concentration DMEM was significantly higher ($p=0.0049$) than the PDGF-BB released from cells incubated on tissue culture plastic (0.018pg/µg±0.0045) under the same conditions (tables 5.2 and 5.3). The comparison also revealed that cells adhering on stainless steel and incubated in DMEM with a physiological concentration of glucose released amounts of PDGF-BB (0.034pg/µg±0.0066)

significantly higher (p=0.013) than cells incubated on tissue culture plastic (0.015pg/µg±0.0034). Under the same conditions also cells incubated on extra-cellular matrix released a significantly higher (p=0.029) amount of PDGF-BB (0.031pg/µg±0.0069) than cells incubated on TCP (tables 5.2 and 5.3). Furthermore, among samples incubated in DMEM with high glucose concentration and spiked with 0.4mM of sodium palmitate macrophages adhering on stainless steel released a significantly higher (p=0.033) amount of PDGF-BB (0.034pg/µg±0.0071) than cells incubated on extra-cellular matrix (0.025pg/µg±0.0053) under the same conditions (tables 5.2 and 5.3).

Table 5.2 Overview of the results obtained from the ELISA test for the measurement of PDGF-BB (n=6). The table represents the means of the amount of PDGF-BB measured in the samples (pg/ml) through ELISA test and their normalization on the total amount of proteins in the same samples. This is expressed as ratio PDGF-BB/total proteins (pg/µg ± standard error).

	PDGF-BB measured in samples (pg/ml)			**PDGF-BB normalized on total amount of proteins in samples (pg/µg)**		
CONDITIONS	**TCP**	**St**	**ECM**	**TCP**	**St**	**ECM**
Physiological glucose DMEM	20.37	45.12	41.13	0.015±0.0034	0.034±0.0066	0.031±0.0069
Physiological glucose DMEM + 0.4mM palmitate	26.47	42.73	49.91	0.018±0.0048	0.029±0.0048	0.032±0.0073
High glucose DMEM	26.80	50.57	38.39	0.018±0.0045	0.038±0.0064	0.026±0.0064
High glucose DMEM + 0.4mM palmitate	35.40	51.49	43.30	0.023±0.0072	0.034±0.0071	0.025±0.0053

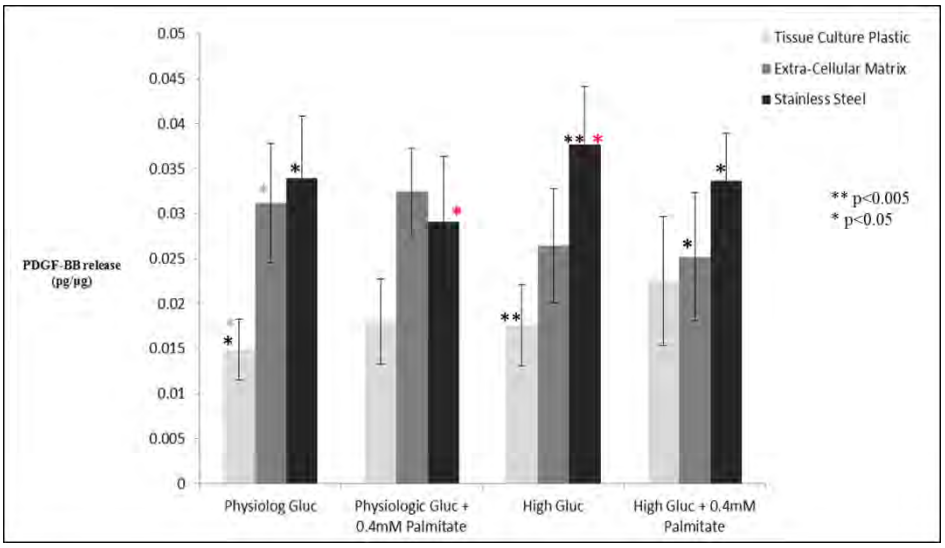

Figure 5.13 PDGF-BB release from cells incubated overnight on the experimental surfaces at different glucose and palmitate concentrations (n=6). *Values are expressed as mean ± standard error of the PDGF-BB (pg) measured by ELISA over the total amount of proteins (µg) measured in the samples by Bradford method. The incubation overnight on St and ECM seemed to release a higher amount of PDGF-BB compared to cells incubated on TCP. No relevant differences were seen comparing different cultural condition among cells incubated on the same surface.*

The comparison between the reaction to the metal under different conditions revealed that a significantly higher (p=0.046) release of the PDGF-BB from cells incubated on stainless steel in DMEM with high glucose concentration (0.038pg/µg±0.0064) was observed when compared to the release from cells incubated on stainless steel in DMEM with physiological glucose concentration added with 0.4mM sodium palmitate (0.029pg/µg±0.0048) (tables 5.2 and 5.3). As shown in figure 5.13 the addition of sodium palmitate did not seem to further affect the release of the growth factor as no further statistical significance among the data was observed. The only possible observation was that the addition of soiudm palmitate seemed to quench the differences between surfaces, thus partially masking the effect of the metal.

Table 5.3 Statistical analysis of the release of PDGF-BB from monocytes/macrophages under different culturing conditions (n=6). Summary of the statistically significant differences expressed as p values obtained from the comparison of the amount of PDGF-BB released in the samples after normalisation with the correspondent total amount of proteins in the same samples. The values were obtained after application of paired t-test in Minitab 16.

SAMPLES (Comparison between surfaces)	SIGNIFICANCE (p value)	SAMPLES (comparison between conditions)	SIGNIFICANCE (p value)
Cells in high glucose on ST HIGHER than cells in high glucose on TCP	0.0049	**Cells in high glucose on St HIGHER than cells in physiological glucose with 0.4 mM palmitate on St**	0.046
Cells in normal glucose on St HIGHER than cells in normal glucose on TCP	0.013		
Cells in normal glucose on ECM HIGHER than cells in normal glucose on TCP	0.029		
Cells in high glucose with 0.4mM of palmitate on St HIGHER than cells in high glucose with 0.4mM palmitate on ECM	0.033		

5.5.4.2 TNF-α ELISA

The measurement of the release of TNF-α in supernatants after overnight incubation of macrophages on different experimental surfaces and under different experimental conditions revealed that, as a general trend, the contact with stainless steel triggered the release of the pro-inflammatory cytokine at levels higher than those adhering on tissue culture plastic and extra-cellular matrix (figure 5.14). Results from ELISA test are represented in table 5.4 which shows that the trend in PDGF-BB release was similar when comparing the values before and after normalization on the total amount of proteins obtained from the

Bradford test. In particular, cells incubated on extra-cellular matrix showed the lower amount of TNF-α in supernatants. Cells incubated on tissue culture plastic released a higher amount of the cytokine than cells on extra-cellular matrix but lower than cells on stainless steel (figure 5.14; table 5.4).

The general trend represented in figure 5.14 as well as the values represented in table 5.4 also showed that changes in glucose concentration in the medium did not affect the release of TNF-α and the addition of 0.4mM sodium palmitate seemed to reduce the release of the growth factor in cells adhering on all surfaces (figure 5.14; table 5.4).

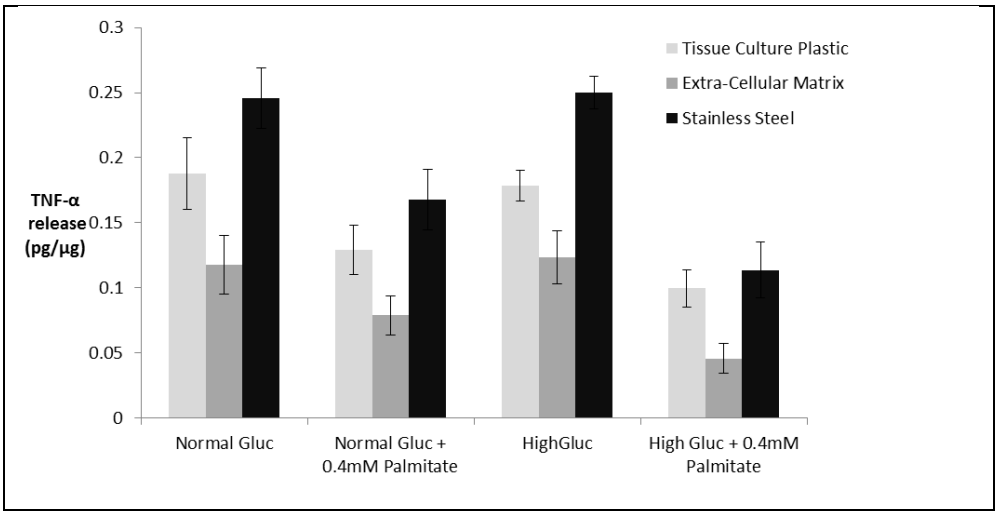

Figure 5.14 TNF-α release from cells incubated overnight on the experimental surfaces at different glucose and palmitate concentration (n=6). *Values are expressed as mean ± standard error of the TNF (pg) measured by ELISA over the total amount of proteins (µg) measured in the samples by Bradford method. Results revealed that under all culture conditions the overnight incubation of macrophages on St (black column) triggered the release of the pro-inflammatory cytokine, particularly in comparison with the release from cells incubated on ECM. Release of TNF-α from cells incubated on TCP was on average lower than the release from cells incubated on St under the same conditions but higher than the release from cells incubated on ECM. The addition of 0.4mM sodium palmitate in the medium reduced the release of the cytokine across all the experimental surfaces. Changes in glucose concentration did not seem to affect the release of TNF-α.*

Table 5.4 Overview of the results obtained from the ELISA test for the measurement of TNF-α (n=6). The table represents the means of the amount of TNF-α measured in the samples (pg/ml) through ELISA test and their normalization on the total amount of proteins in the same samples. This is expressed as ratio TNF-α /total proteins (pg/µg ± standard error).

	TNF-α measured in samples (pg/ml)			TNF-α normalized on total amount of proteins in samples (pg/µg)		
CONDITIONS	**TCP**	**St**	**ECM**	**TCP**	**St**	**ECM**
Physiological glucose DMEM	256.71	338.41	166.81	0.18±0.027	0.25±0.023	0.12±0.023
Physiological glucose DMEM + 0.4mM palmitate	186.30	240.55	124.90	0.13±0.019	0.17±0.023	0.079±0.015
High glucose DMEM	265.52	344.43	181.30	0.18±0.012	0.25±0.012	0.12±0.020
High glucose DMEM + 0.4mM palmitate	160.42	181.54	78.96	0.10±0.014	0.11±0.022	0.045±0.011

The statistical analysis comparing the effect of different surfaces on cells incubated in DMEM with physiological glucose concentration showed that cells incubated on stainless steel released a significantly higher (p=0.00012) amount of TNF-α (0.25pg/µg±0.023) than cells incubated on extra-cellular matrix (0.12pg/µg±0.023) (tables 5.4 and 5.5). Similarly, cells incubated on tissue culture plastic under the same conditions released a significantly higher (p=0.0045) amount of TNF-α (0.18pg/µg±0.027) than cells on extra-cellular matrix (tables 5.4 and 5.5). The release of TNF-α from cells incubated on stainless steel in DMEM with a physiological glucose concentration was also significantly higher (p=0.018) than the release from cells on tissue culture plastic (tables 5.4 and 5.5).

When incubated in DMEM with a high glucose concentration, cells in contact with stainless steel released a significantly higher (p=0.0078) amount of the

cytokine (0.25pg/µg±0.023) than cells in contact with extra-cellular matrix (0.12pg/µg±0.020) (tables 5.4 and 5.5). The TNF-α released by cells in contact with stainless steel was also significantly higher (p=0.010) than the release from cells on tissue culture plastic (0.18pg/µg±0.012) (tables 5.4 and 5.5). The release of TNF-α from cells incubated in DMEM with high glucose concentration on tissue culture plastic was also significantly higher (p=0.011) than the release form cells on extra-cellular matrix (tables 5.4 and 5.5).

The statistical analysis of data obtained from cells incubated in DMEM with physiological glucose concentration added with 0.4mM palmitate showed that cells in contact with stainless steel released a significantly higher (p=0.0019) amount of TNF-α (0.17pg/µg±0.023) than cells on extra-cellular matrix (0.079pg/µg±0.015) (tables 5.4 and 5.5). Also cells incubated under the same conditions on tissue culture plastic showed a significantly higher (p=0.0027) release of TNF-α (0.13pg/µg±0.019) than cells on extra-cellular matrix (tables 5.4 and 5.5).

No significant differences were found between values obtained from cells incubated on different surfaces in DMEM with high glucose concentration spiked with 0.4mM palmitate.

The comparison of the culture conditions between cells incubated on the same surface revealed that when cells were incubated on tissue culture plastic a significantly lower (p=0.0075) release of TNF-α was observed in samples incubated in DMEM with high glucose concentration and spiked with 0.4mM palmitate (0.10pg/µg±0.014) if compared to cells incubated in DMEM with high glucose concentration (0.18pg/µg±0.012) (tables 5.4 and 5.5). Release of TNF-α from cells in high glucose with palmitate was also significantly lower (p=0.027) than the amount found from cells in low glucose (0.19pg/µg±0.028) (tables 5.4 and 5.5). Among cells incubated on tissue culture plastic, the amount of TNF-α released form cells incubated in high glucose was significantly higher (p=0.040)

than the amount from cells in physiological glucose concentration DMEM spiked with 0.4mM palmitate (0.13pg/µg±0.019) (tables 5.4 and 5.5).

Similar scenario was seen among cells incubated on stainless steel. Indeed, the amount of TNF-α released from cells incubated in high glucose concentration spiked with palmitate was significantly ($p=0.00054$) lower (0.11pg/µg±0.022) than the amount released by cells in high glucose without palmitate (0.25pg/µg±0.012) and significantly lower ($p=0.014$) than the amount released by cells in physiological glucose concentration without palmitate (0.25 pg/µg±0.023) (tables 5.4 and 5.5). The TNF-α levels released in physiological glucose concentration DMEM was also significantly higher ($p=0.040$) than the amount measured from cells in physiological glucose concentration and spiked with palmitate (0.17pg/µg±0.023) (tables 5.4 and 5.5). The amount measured in those samples was in turn significantly lower ($p=0.025$) than the amount released when cells were incubated in high glucose concentration (0.25pg/µg±0.012) (tables 5.4 and 5.5).

Table 5.5 Statistical analysis of TNF-α release from monocytes/macrophages under different culturing conditions (n=6). Summary of the statistically significant differences expressed as p values obtained from the comparison of the amount of TNF-α released in the samples after normalisation with the correspondent total amount of proteins in the same samples. The values were obtained after application of paired t-test in Minitab 16.

SAMPLES (comparison between surfaces)	SIGNIFICANCE (p value)	SAMPLES (comparison between condition)	SIGNIFICANCE (p value)
Cells in physiological glucose on St HIGHER than cells in physiological glucose on ECM	0.00012	**Cells in high glucose on TCP HIGHER than cells in high glucose with 0.4mM palmitate on TCP**	0.0075
Cells in physiological glucose on TCP HIGHER than cells in normal glucose on ECM	0.0045	**Cells in physiological glucose on TCP HIGHER than cells in high glucose with 0.4mM palmitate on TCP**	0.027
Cells in high glucose on St HIGHER than cells in high glucose on ECM	0.0078	**Cells in high glucose on TCP HIGHER than cells in physiological glucose on TCP**	0.040
Cells in physiological glucose with 0.4mM palmitate on St HIGHER than cells in physiological glucose with 0.4mM palmitate on ECM	0.0019	**Cells in high glucose on St HIGHER than cells in high glucose with 0.4mM palmitate on St**	0.00054
Cells in physiological glucose with 0.4mM palmitate on TCP HIGHER than cells in physiological glucose with 0.4mM palmitate on ECM	0.0027	**Cells in physiological glucose on St HIGHER than cells in high glucose with 0.4mM palmitate on St**	0.014
Cells in physiological glucose on St HIGHER than cells in physiological glucose on TCP	0.018	**Cells in physiological glucose on St HIGHER than cells in physiological glucose with 0.4mM palmitate on St**	0.040
Cells in high glucose on TCP HIGHER than cells in high glucose on ECM	0.011	**Cells in high glucose on St HIGHER than cells in physiological glucose with 0.4mM palmitate on St**	0.025
Cells in high glucose on St HIGHER than cells in high glucose on TCP	0.010	**Cells in physiological glucose on ECM HIGHER than cells in high glucose with 0.4mM palmitate on ECM**	0.034
		Cells in high glucose on ECM HIGHER than cells in high glucose with 0.4mM palmitate on ECM	0.015

The comparison of the results obtained from cells incubated on extra-cellular matrix revealed a similar scenario although with differences less accentuated and an overall release of TNF-α lower than from cells incubated on tissue culture plastic and stainless steel. The data showed that the amount of TNF-α measured in samples derived from cells incubated in high glucose DMEM spiked with 0.4mM palmitate (0.046pg/µg±0.011) was significantly ($p=0.034$) lower than the amount of the cytokine measured in supernatants from cells in physiological glucose concentration DMEM (0.12pg/µg±0.023) and in supernatants from cells in high glucose concentration DMEM (0.12pg/µg±0.020) ($p=0.015$).

Overall, the data suggested a synergistic effect of the combination of high glucose concentration and sodium palmitate resulting in the reduction of the release of TNF-α from cells when incubated on all the experimental surfaces. The differences were more accentuated in cells incubated on stainless steel, where the overall amount of TNF-α was higher than the release form cells on extra-cellular matrix, likely due to the effect of the material.

5.6 DISCUSSION

Diabetes is a condition associated with a higher incidence of cardiovascular pathologies. The links between the primary pathology and the associated clinical conditions are represented by both the long-term damages caused by the disease on the vascular endothelium and the co-morbidities associated with metabolic dysfunctions (Miettinen 1998, Hu 2001, Peppa 2003, Price 2004, Wellen & Hotamisligil 2005, Goldin 2006, Sell 2006). Indeed, different studies have demonstrated a direct correlation between obesity, inflammation and insulin resistance. In particular, the recruitment of macrophages in the white adipose tissue has been shown to be mediated by the release of free fatty acids by the same

tissue and by the release of TNF-α by macrophages with the consequent activation of the inflammatory process (Rustan & Drevon 2005, Suganami 2005).

Other studies have shown the increase in the release of TNF-α by macrophages in culture under the influence of free fatty acids via activation of Toll-like receptor. In particular, it was shown that saturated fatty acids, but not unsaturated, were able to trigger the release of pro-inflammatory cytokines from macrophages through the action of ceramide, a product of their metabolism (Rustan & Drevon 2005, Curtiss & Tobias 2008, Haversen 2009, Dasu 2011).

Previous parts of this study showed that the amount of circulating activated macrophages and endothelial progenitor cells in blood isolated from diabetic patients was variable when compared to control subjects. Mononuclear cells are typically present in the bloodstream as monocytes, differentiating in activated macrophages once reaching the tissues in order to sustain an inflammatory reaction in response to pro-inflammatory stimuli such as injuries (Takahashi 2001, Geissman 2010). An increased amount of circulating activated macrophages (CD68+) represents therefore a basic inflammatory condition that could potentially affect the response of individuals to foreign materials. In addition, variations in the number of circulating endothelial progenitor cells (expressing CD34+), normally present in low amount in the bloodstream, have been identified as correlated to increased cardiovascular risk or cardiac events (Fadini 2006, Boilson 2008). Findings from this work have shown differences in the amount of circulating activated macrophages among donors with diabetes independently from the general health condition assessed by measuring biochemical values and clinical data. This confirmed the diabetic condition as at high risk of cardiovascular diseases, thus paving the way towards the possible identification of biomarkers for *in-stent* restenosis. In addition, the analysis of the macrophage activation by adhesion on stainless steel as described in chapter 4 highlighted the specific effect of the metal on the cytokine and growth factor release pathways. The contact with stainless steel triggered in fact a higher release of TNF-α and

PDGF-BB in comparison to macrophages incubated on control surfaces. Differences were seen between the groups of diabetic patients. However, the heterogeneity of the donors in terms of co-morbidities and clinical background did not lead to the identification of a specific trend correlating diabetic condition to the response to the biomaterial.

In this chapter, mononuclear cells were isolated from healthy donors in order to minimize the variability related to the presence of co-morbidities linked to the diabetic conditions and to evaluate solely the effect of biochemical factors altered in diabetes. Alterations in lipid metabolism and obesity (identified by BMI values above 30) are among the most relevant factors for the occurrence of cardiovascular complications (British Heart Foundation 2010). The work described in this chapter studied the effect of high concentrations of glucose and saturated fatty acids (palmitate), on the activation of macrophages induced by stainless steel. The concentration of sodium palmitate (0.4mM) added to the medium was chosen on the basis of published studies (Briaud & Poitout 2001, Haversen 2009) and after preliminary experiments allowing the identification of a concentration able to mimic hyperlipidaemia without affecting the cell viability *in vitro*.

5.6.1 Immunocytochemistry

Immunocytochemistry confirmed that the cells adhering on the surfaces were monocytes-derived macrophages co-expressing the marker for monocytes (CD14) (figure 5.11) and for activated macrophages (CD68) (figure 5.10), thus confirming the physiological activation of monocytes into activated macrophages once in contact with both the metal surface and the extra-cellular matrix substrate. Although depending on variability associated to donor and surface features, cells expressing the marker for hematopoietic progenitor cells (CD34) were consistently found among the cells expressing CD68 (figure 5.10). Interestingly,

the double staining showed that cells were co-expressing CD34 and CD68, thus confirming the presence of a sub-population with a potential to differentiate into myofibroblasts (figure 5.10) (Mesure 2010). No relevant differences in the expression of the marker could be identified across groups of donors from the images. Across surfaces and culture conditions cells expressing α-actin, identifying smooth muscle cell-like phenotype, were found. Interestingly, the double staining also allowed the identification of cells co-expressing the marker for monocytes (CD14) and α-actin, thus confirming the presence among mononuclear cells of a sub-population expressing the myofibroblast phenotype (figure 5.11). These findings support evidences recently provided in literature about the trans-differentiation potential of monocytes/macrophages (Kuwana 2003, Boilson 2008, Pilling 2009, Forte 2010, Mesure 2010) as discussed in previous chapters. No differences in the expression of the markers were seen across all the surfaces and under all experimental conditions.

5.6.2 SEM

The images obtained from scanning electron microscopy highlighted differences in the morphology of macrophages after incubation on the different surfaces and under different experimental conditions (figure 5.12). No differences were observed between macrophages incubated in normal or high glucose concentration media, thus indicating that short-term incubation in high glucose did not lead to modifications in the morphological features of macrophages. The images of macrophages adhering on stainless steel showed that cells were well spread onto the surfaces, indicating a good adherence, and more cell-to-cell interactions could be observed, thus suggesting the formation of giant cells. In addition, the cell plasmalemma appeared rough, another typical morphological features of activated macrophages (Guildford 2009). Similar behaviour was observed in cells incubated at both physiological and high glucose concentrations

(figure 5.12). Images of macrophages in high glucose concentration medium spiked with palmitate showed that the structure of the cells was barely possible to be identified due to the extent of spreading on the surface and "blebbing" (figure 5.12). The addition of palmitate to the medium emphasized the activation of macrophages that, on all of the surfaces, showed a trend towards the formation of giant cells through cell-to-cell interactions. In addition, macrophages plasmalemma showed features of "blebbing" typical of the phagocytic process. The analysis of the images seemed to suggest that the degree of activation of macrophages incubated on stainless steel was higher under the different conditions and exacerbated by the concomitant presence of glucose and palmitate. However, it must be taken into account that the roughness of stainless steel surface might affect the interpretation of changes in the morphological features of adhering cells, particularly when compared to smoother surfaces such as tissue culture plastic.

5.6.3 ELISA: release of PDGF-BB and TNF-α

The measurement of the release of cytokines confirmed that the contact with the metal triggered a significantly higher release of PDGF-BB in comparison to cells incubated on tissue culture plastic (figure 5.13; tables 5.2 and 5.3). The effect of the metal seemed to be emphasised when cells were cultured in medium (with normal or high glucose concentration) without addition of palmitate. This was likely due to the average increase in the release of PDGF-BB from cells incubated on tissue culture plastic when palmitate and high glucose were present in the culture medium, thus demonstrating that those culture conditions affected the release of the growth factor. Results from ELISA also showed that cells incubated on extra-cellular matrix-coated wells released a higher amount of PDGF-BB than cells on tissue culture plastic, although the difference was significant only in cells cultured in medium with normal glucose concentration. In those conditions the

effect of the surface was in fact particularly evident as both stainless steel and extra-cellular matrix-coated wells triggered a significantly higher release of the growth factor compared to tissue culture plastic (figure 5.13; tables 5.2 and 5.3). Therefore, the overall results obtained from the measurement of PDGF-BB in supernatants suggested that stainless steel triggered the release of the growth factor, thus indicating that, even after a short incubation time, macrophages tend to assume a post-inflammatory status producing PDGF-BB and resulting in the proliferation of smooth muscle cells and in the stimulation of the wound healing process. The effect of the surface seemed to be predominant compared to the effect of different biochemical conditions. In fact, no significant differences were recorded comparing results with or without the addition of sodium palmitate to the medium. The presence of glucose and palmitate seemed to solely have an impact on the PDGF-BB release by partially masking the effect of the surface on the release of the growth factor.

The measurement of the release of TNF-α showed that the contact of macrophages with tissue culture plastic and stainless steel triggered the release of the pro-inflammatory cytokine in comparison to cells on extra-cellular matrix-coated well (figure 5.14; tables 5.4 and 5.5). Significant differences were in fact found between cells incubated on tissue culture plastic and stainless steel in comparison to cells incubated on extra-cellular matrix under all culture conditions with the exception of samples with high glucose concentration and palmitate. Results confirmed that the contact with artificial surfaces, in particular stainless steel, triggered the activation of macrophages even after short-time incubation (overnight). The comparison of the culture conditions showed that glucose concentration did not affect the release of TNF-α from macrophages. The addition of palmitate reduced the release of the pro-inflammatory cytokine from macrophages on all the experimental surfaces. In particular, the reduction was emphasized when cells were incubated in high glucose suggesting that the combination of hyperglycaemia and hyperlipidaemia may affect the response of

macrophages (figure 5.14; tables 5.4 and 5.5). Under this condition in fact no significant differences were seen between the surfaces, thus suggesting that the environmental effect masked the effect of the surface. In particular, the presence of both cytokines in the supernatants as shown by the results from ELISA might be related to the choice of incubation time. It is likely that the TNF- α accumulated in the supernatants as consequence of the initial metal-triggered inflammatory activation. Following the initial pro-inflammatory reaction, the release of PDGF-BB suggested the switch to a post-inflammatory phenotype. In addition, the reduction in the amount of TNF- α in the presence of high glucose and palmitate suggested that the conditions affected the phenoptypical expression promoting the post-inflammatory status. Those findings reproduce results published in previous works where macrophages in contact with stainless steel were found to predominantly release PDGF-BB (Harrison 2007). However, results from the presence study seem to contradict data previously published that showed no increase in the release of TNF- α (Harrison 2007). The controversy is likely due to the choice of different experimental conditions that, in the case of this study, seemed to allow the collection of evidence of both the initial pro-inflammatory activation of adhering macrophages and their following switch to a post-inflammatory phenotype. Overall, results suggest the switch to post-inflammatory phenotype and the influence of the environment on the switch, relevant for the deposition of the restenotic plaque. Despite the PDGF-BB serum level in circulating blood were found to be in the order of thousands of picogram per ml (1000 pg/ml increasing to up to 8000 pg/ml in particular conditions) (Czarkowska-Paczek 2006, Takayama 2011, Tisato 2013), results from a previous study demonstrated that in supernatants from control macrophages the amount of PDGF-BB was around the 20.9 pg/ml (Tisato 2013). Those values are in line with the results described in both chapter 4 (table 4.3) and chapter 5 (table 5.2) reporting similar amount of PDGF-BB in supernatants from macrophages incubated on tissue culture plastic. Therefore, the significance of the difference found for the amount of PDGF-BB in supernatants collected form macrophages

incubated on stainless steel (rising to 40-50 pg/ml) (tables 4.3 and 5.2) is reinforced despite the absence of a positive control obtained by stimulating macrophages to release the growth factor.

5.7 CONCLUSIONS

The measurement of the secretion of pro- and post-inflammatory cytokines showed that overnight contact with stainless steel triggered the release of both pro-inflammatory cytokines (TNF-α) and post-inflammatory growth factors such as the PDGF-BB, considered the most potent inducer of smooth muscle cell and myofibroblast proliferation (Wight 2004, Pintucci 2005, Santin 2005). In particular, the increase in the release of PDGF-BB confirmed the switch to a post-inflammatory status of macrophages typical of wound healing and key element in the development of the restenotic plaque. The presence of glucose and palmitate seemed to have an impact on the PDGF-BB and TNF-α release partially masking the effect of the surface This biochemical pathway supports an *in-stent* restenosis mechanism whereby macrophages adhering on the stent strut surface and exposed to hyperglycaemia and hyperlipidaemia would be able to stimulate the deposition of a neointimal tissue through the PDGF-BB-induced smooth muscle cell proliferation (Wight 2004, Pintucci 2005, Santin 2005).

The synergistic effect of lipid and glucose on the activation of macrophages appeared more evident after the analysis of cell morphology. The concomitance of palmitate and high glucose showed to have a great impact on the morphological features of macrophages adhering on all of the tested surfaces.

Therefore, results from this study suggest that the control of blood glucose and lipid levels at the moment of intervention might have an impact on the response of macrophages to the contact with the metallic strut. In fact, the concomitance of

hyperglycaemia and hyperlipidaemia seemed to emphasize and accelerate the reaction to the metal, thus potentially representing a critical point for the prediction of the outcome of the procedure as mentioned in previous studies (Khosravi 2010, Nusca 2010).

The neointimal tissue is formed by hyaluronan-rich matrix with smooth muscle cells and myofibroblasts. Acquiring the phenotypical features characteristic of myofibroblasts, macrophages acquire the ability to synthesize hyaluronan through the expression of hyaluronan synthase (HAS). A recent study has shown that macrophages expressed the HAS isoform responsible for the synthesis of long molecular chain hyaluronan (HAS1), important for the tissue remodelling, after 5 days of incubation on stainless steel. The next part of study will evaluate the effect of high glucose and lipid concentrations on the expression of HAS isoforms in macrophages after overnight incubation on the metal surface. This will provide more indications on the influence on environmental effect on the response of macrophages to stainless steel and on their contribution to *in-stent* restenosis.

CHAPTER 6

EFFECT OF HIGH GLUCOSE AND HIGH FREE FATTY ACID CONCENTRATION ON THE EXPRESSION OF HAS ISOFORMS BY MACROPHAGES

6.1 INTRODUCTION

Later stages of *in-stent* restenosis are characterised by the deposition of a proteoglycan-rich extracellular matrix (ECM). The cellularity of the tissue forming the restenotic plaque progressively decreases in concomitance with the switch from inflammatory to proliferative stage. Lesions analysed 18 months following implantation appeared to be formed by a proteoglycan-rich extra-cellular matrix populated by stellated smooth muscle cells. Those features are typical of a tissue known as myoxid tissue, characteristic of the wound healing process (Chung 2002). The restenotic plaque was therefore identified by features typical of a non-healed wound (Santin 2005). In particular, high amounts of hyaluronic acid were found after histological analysis of restenotic stented arteries throughout all the stages of restenosis thus identifying hyaluronan as one of the components playing a major role in in-stent restenosis by inducing the contraction of extra-cellular matrix driven by myofibroblasts (Santin 2005).

The contribution of monocytes-derived macrophages to the restenotic process through their ability in trans-differentiating into myofibroblasts has been investigated in previous studies and discussed in chapters 3 and 4 of this study. It has been shown that macrophages are characterized by phenotypical plasticity and under particular conditions they can differentiate acquiring features typical of different cell types such as osteoclasts (Udagawa 1990) and endothelial progenitor cells (Rehman 2003). In addition, cell sub-populations of monocytic origin have been identified as precursor of endothelial cells and myofibroblasts (Kuwana 2003, Boilson 2008, Pilling 2009, Forte 2010). After contact with stainless steel macrophages acquire phenotypical features typical of smooth muscle cells (Stewart 2009), findings confirmed by the results discussed previous chapters of this work. When assuming the characteristics typical of smooth muscle cells, macrophages can produce hyaluronic acid thus providing a further contribution to

the development of in-stent restenosis. In particular, a study from Stewart et al. (2009) showed that macrophages incubated for up to seven days on stainless steel expressed the gene for the HAS1, responsible for the production of high molecular weight hyaluronic acid. This confirmed the direct contribution of macrophages to the formation of the restenotic tissue in the later stages of restenosis (Stewart 2009).

6.1.1 Hyaluronic acid

Hyaluronic acid is a glycosaminoglycan present in most human tissues. It was first isolated in the vitreous of the eye in 1934 by Meyer and Palmer and from umbilical cord tissue in 1936. The structure was first characterised by Weissman and Meyer in 1954. It represents a constitutive and regulatory component of most tissues in the human body under physiological conditions where it appears as a high molecular weight polymer (more than 10^6 Da) and maintains the integrity of the tissues (Noble 2002).

6.1.1.1 Hyaluronic acid: the structure

Hyaluronic acid is a large negatively charged polysaccharide. In particular, it is a non-sulphated glycosaminoglycan composed of repeating dimers of D-glucuronic acid β-1,3-N-acetylglucosamine-β1,4 (Noble 2001, Tammi 2002).

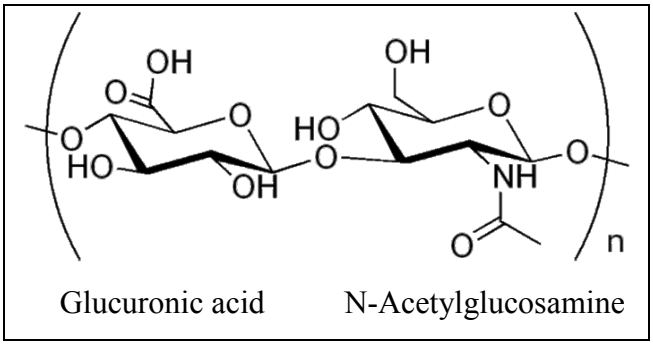

Figure 6.1 Molecular structure of the repeating dimer forming the polymer of hyaluronic acid. *Hyaluronic acid is a glycosaminoglycan formed of repeating D-glucuronic acid β-1,3-N-Acetylglucosamine-β1,4.*

Under physiological conditions hyaluronic acid is present in tissues in molecules of molecular weight ranging from 10^5 to 10^7Da as a constituent of the structure of most tissues and of the matrix of the connective tissue. Due to its size, charge and peculiar physicochemical properties hyaluronic acid is responsible for providing specific structural properties to tissues. Under inflammatory or pathological condition, hyaluronic acid encounters fragmentation due to interaction with reactive oxygen species (ROS) and enzymes in order to favour cell migration and support the progress of inflammation (Noble 2001, Tammi 2002).

6.1.1.2 Hyaluronic acid: synthesis and functions

Hyaluronic acid is produced in the vasculature at the cytoplasmic face of the cell membranes (Kennedy 2000) by the enzyme hyaluronan synthase (HAS) in the three isoforms HAS1, HAS2 and HAS3. The three isoforms were shown to be codified by three different genes (Kennedy 2000). Once synthesised, the polysaccharide is trans-located to the outer side of membrane and into the intercellular space (Chai 2005). The HAS isoforms were first characterised in Streptococcus. The different distribution and expression of the isoforms among cells and tissues suggested that each isoform performs different roles in the human

body. In particular, studies have demonstrated that HAS3 is the isoform responsible for the synthesis of low molecular weight hyaluronan (Weigel 1997, Itano 1999, Tammi 2002, Chai 2005), thus playing a fundamental role during the inflammatory reaction. Similar studies have shown that HAS1 and HAS2 participate in the synthesis of high molecular weight hyaluronic acid (Itano 1999).

One third of the total amount of HA is replaced daily through endocytotic uptake removal. Alterations in hyaluronic acid distribution associated to diseases such as cancers suggest that a delicate balance between production, sizing and removal of HA is essential for the maintenance of body homeostasis and for the protection from the occurrence of disease (Itano 1999, Liu 2001, Tammi 2002, Toole 2002, Chai 2005). During the inflammatory process the interaction of reactive oxygen species and enzymes such as hyaluronidase lead to the fragmentation of the constituent hyaluronic acid into low molecular weight chains that intervene in cell migration supporting the development of the reaction itself. In order to re-establish integrity of the tissue, the fragmentation products are generally removed by binding to cells through the receptor CD44, protein also expressed on the surface of cells from the haematopoietic lineage such as macrophages (Liang 2011). The binding of hyaluronan fragments to both CD44 receptor and toll-like receptor (TLR) on macrophages is correlated to the modulation of the inflammatory response and to the production of inflammatory cytokines. In particular, studies have shown that the pro- and anti-inflammatory response induced respectively by short and long chains of hyaluronan is correlated to the binding of the glycosaminoglycan with TLR-2 and TLR-4 that results in the modulation of the inflammatory reaction (Jiang 2005, Jiang 2007, Campo 2011, Campo 2012). Specifically, the interaction of hyaluronan fragments with TLR-2 and TLR-4 in inflammatory macrophages seems to be the solely responsible for the activation of inflammatory genes in the cells. The CD-44, representing the main hyaluronan receptor on macrophages, is related to the clearance of hyaluronan fragments in the site of the injury (Jiang 2007). This suggests the close

interaction between hyaluronan and inflammatory cells in the development of the inflammatory reaction (Itano 1999). Pro-inflammatory cytokines such as IL-1β and TNF-α, released during the inflammatory phases following injury or disease and participating in the process of wound healing, were shown to affect the expression of HAS in cells like dermal fibroblasts (Kennedy 2000, Vigetti 2010). Hyaluronan was also shown to trigger the production of cytokine by fibroblasts and macrophages during inflammatory process (Kennedy 2000, Vigetti 2010). These findings demonstrated the strict correlation of cytokines and inflammatory cells with hyaluronan providing evidence of the key role of hyaluronan in the different stages of tissue repair after injury.

6.1.1.3 Hyaluronic acid: role in atherosclerosis and *in-stent* restenosis

During the formation of the atherosclerotic plaque, the smooth muscle cells present in the vessel wall migrate into the tunica intima and proliferate switching from contractile to synthetic state, thus producing long molecular weight hyaluronan (340kDa) (Papakonstantinou 1998). The migration of smooth muscle cells and the secretion of hyaluronan seem to be driven specifically by the action of PDGF, particularly PDGF-BB (Papakonstantinou 1998). This reinforces the importance of hyaluronan in the changes occurring within the extracellular matrix in normal and pathological conditions and highlighting its role in the development of vascular disease.

Atherosclerotic and restenotic processes are both characterised by changes in the distribution of hyaluronic acid within the vessel wall structure (Travis 2001). During *in-stent* restenosis, the deposition of hyaluronan increases in the proliferating phases at early stages after angioplasty where it favours the proliferation and migration of arterial smooth muscle cells. In particular, smooth muscle cells and fibroblasts populate the injured area to remodel the extracellular matrix and favour the healing process. This can lead to changes in the structure of vessel wall resulting in shrinkage and possible restenosis (Travis 2001).

Furthermore, hyaluronan has been shown to play a fundamental role in the remodelling phase of restenosis by mediating the contraction of ECM through the binding to specific receptor (CD44) present on surface of arterial smooth muscle cells (Travis 2001, Toole 2002).

Hyaluronan plays a fundamental role during all the phases of in-stent restenosis. Low molecular weight chains favour cell migration and activation as well as influencing the production of cytokines, thus intervening in the inflammatory process characterizing the early stages following stent inflammation. Long molecular weight chains of hyaluronan represent a constitutive part of tissues and intervene in the remodelling of tissues after injury and in the later stages of the restenotic process (Tammi 2002) .

6.2 AIMS

This chapter investigated the acute effect of high glucose and free fatty acid concentration on the expression of the three isoforms of hyaluronic synthase in monocytes-derived macrophages incubated overnight on stainless steel and extracellular matrix. This contributed to unravel the impact of hyperglycaemia, hyperlipidaemia and their synergy on the response of macrophages to stainless steel, thus clarifying the importance of the control of blood levels at the moment of intervention for the prevention of in-stent restenosis following implantation of non-medicated stainless steel stent.

6.3 MATERIALS AND METHODS

6.3.1 The technique: reverse transcription-polymerase chain reaction (RT-PCR)

Polymerase chain reaction is a technique used and developed in the last few decades for the amplification of short sequences of DNA. The reaction is based upon the subsequent cyclic increase and decrease of the temperature in a mixture containing the desired DNA fragment, a temperature-resistant polymerase (enzyme able to extend and sequence the nucleotides) and two primers represented by short fragments of DNA complementary to the extremities of the DNA strands. An initial increase of the temperature to 94^{o}C causes the double stranded DNA helix to separate. The temperature is then reduced to 50-60^{o}C to allow the primers to combine to single DNA strands and a further increase of the temperature to 72^{o}C facilitate the extension of new strands of DNA by the polymerase. Every cycles leads to the production of the double amount of copies of the original DNA. Therefore the repetition of the cycle many times (generally around 30-40) multiplies the gene of interest exponentially in the sample tubes (Kendrew 1995, Karp 1999). The simplicity of the reaction and the availability of instrumentations together with the development of more accurate and more precise technical procedures have made of PCR a widely used technique for the identification and quantification of genes in research and in practical applications in different fields such as forensic sciences, virology, microbiology, medicine and diagnosis (Bustin 2005).

PCR can also be used to amplify the copy-DNA (cDNA) obtained from the reverse transcription of mRNA extracted from the cells. In this case the technique is called reverse transcription-PCR (RT-PCR) and it is used for the analysis of the expression of proteins in cells.

The products of PCR reactions can be resolved and identified through agarose gel electrophoresis. DNA fragments are generally visualised adding ethidium bromide to the agarose. Ethidum bromide is a fluorescent dye emitting in the UV range and intercalating the double stranded fragments of DNA.

The figure 6.2 shows the reactions involved in the analysis of the expression of the HAS isoforms by monocytes using RT-PCR technique.

6.3.2 Blood collection, extraction of mononuclear cells and incubation on surfaces

Recruitment of volunteers and blood collection was done as described in section 5.3.1. After extraction of mononuclear blood cells through the Boyum's method as described in section 2.3.1.2, $1x10^6$ cells were seeded onto stainless steel discs, tissue culture plastic and extra-cellular matrix coated wells as described in section 4.3.2. The culture medium (low-glucose DMEM) was replaced after 3 hours of incubation at 37^oC, 5% of CO_2 and 95% to re-create the cultural condition described in paragraph 5.3.4. Cells were then incubated for 24 hours at 37^oC, 5% of CO_2 and 95%.

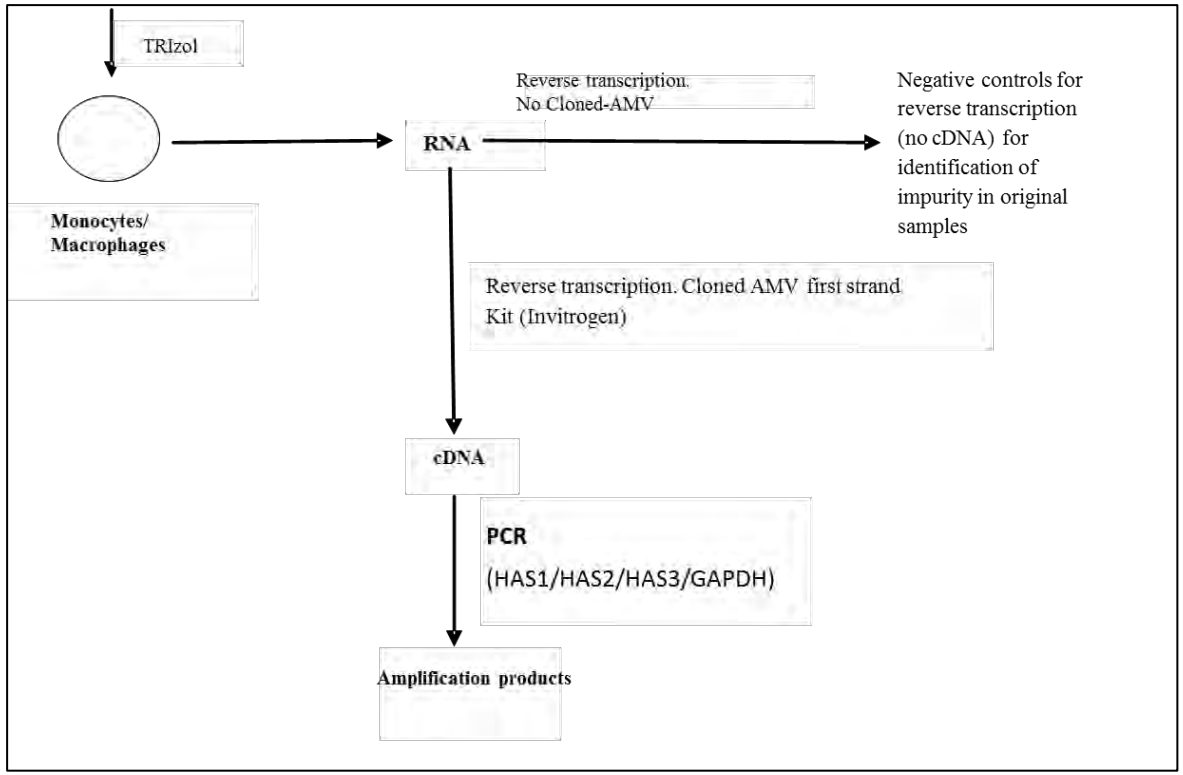

Figure 6.2 Schematic representation of the sequence of steps involved in RT-PCR reaction. *The scheme illustrates the steps involved in the reaction from the isolation of the total RNA from the adhering monocyte/macrophages to the reaction of amplification for the detection of the expression of the hyaluronic synthase (HAS) in the three isoforms. Negative controls for the reaction of reverse transcription were created in order to exclude amplification of DNA fragments contaminating the RNA samples extracted with the method based on the use of TRIzol.*

6.3.3 Extraction of RNA

Supernatants were collected after incubation and centrifuged as described in paragraph 5.3.4. Cells were rinsed with sterile PBS before proceeding to the RNA extraction using Trizol reagent (Invitrogen, Life Technologies Cat No 15596-026) as extracting mixture. Trizol is a commercial reagent containing a mixture of phenol, guanidine thiocyanate and ammonium thiocyanate to perform the first step of the extraction of nucleic acids and proteins from cells. The method is based on an original procedure described by Chomczynski and Sacchi (Chomczynski 1987) and widely utilised as RNA extraction method. 1ml of Trizol was added to each well and the solution passed several times through the pipette to favour the cell lysis. Trizol disrupts the cells dissolving cellular components but it maintains the integrity of nucleic acid. After an incubation of 5 minutes at room temperature the solution was transferred in a RNAse-free 1.5ml polypropylene tubes and added with 200µl of DNAse and RNAse free chloroform (Sigma Aldrich,UK). Before centrifuging at 12,000Xg for 15 minutes at 4^{o}C tubes were vigorously shaken by hand for 15 seconds to favour the extraction and incubated at room temperature for a few minutes. After centrifugation the aqueous phase containing RNA was gently collected and transferred in a fresh tube. RNA was precipitated by a 10 minutes incubation with RNAse-free Isopropyl-alcohol (Sigma Aldrich, UK) followed by centrifugation for 10 minutes at 12,000Xg at 4^{o}C. The resulting RNA-containing pellet was then purified by re-suspension in 75% ethanol in DEPC-treated water and centrifugation for 5 minutes at 7,500Xg at 4^{o}C. After removing the ethanol, the pellet containing RNA was air-dried and suspended in DEPC-treated water. RNA samples were stored at -70^{o}C. The amount of RNA extracted was determined through UV spectrometry (Eppendorf Biophotometer) after diluting 2µl of the final solution in 48µl of DEPC-treated water. The absorbance at 260 nm provided the concentration of RNA in the samples and the purity was represented by the ratio of absorbance measured at 260nm and 280nm. The ratio provided the amount of contaminant DNA. The

results obtained from the reading with the spectrophotometer (data not shown) revealed an average final concentration of RNA of 0.3µg/µl in the samples with a purity of around 1.38 expressed as A_{260}/A_{280} ratio. The results confirmed that considering the low amount of RNA extracted from the cells a concentration step was needed to increase the amount of RNA in a smaller amount of solution (RNA was re-suspended in 20µl of DPEC-treated water). In order to improve the purity samples were also treated with DNAse to eliminate the contaminant DNA.

6.3.4 Treatment of RNA samples with DNase and sample concentration

In order to eliminate the residues of contaminant DNA, samples were treated with RQ1 RNase-free DNase (Promega, Cat. M610A) according to the instructions provided by the manufacturer. The kit contained RNA qualified (RQ) DNase I that is an endonuclease degrading both single- and double-stranded DNA producing oligonucleotides. The kit was proven efficient for the removal of DNA from RNA samples before RT-PCR. RQ1 DNase was added to the RNA samples with RQ1 RNase-free DNase reaction buffer provided by the company and DPEC-treated water as instructed and incubated for 30 minutes at 37^{o}C. The reaction was then terminated by addition of the stop solution and incubation at 65^{o}C for 10 minutes.

In order to optimize the outcome of RT-PCR, the concentration of RNA needed increasing. This was obtained through precipitation with ethanol and re-suspension in smaller volume of water. To facilitate the identification of the pellet containing RNA 1µl of pellet paint NF co-precipitant was added into each tube. This contained a non-fluorescent dye-labelled carrier not interfering with the reactions of transcription and amplification but visualising the pellet. The tubes were then added with 1/10 of volume of sodium acetate 3M and the double volume of RNase- and DNase-free absolute ethanol and incubated for 30 minutes at -70^{o}C. Following centrifugation at 13,000Xg for 15 minutes the supernatants

were discarded and the pellets re-suspended in 70% of ethanol in DPEC-treated water. The pellets obtained after a further centrifugation at 13,000Xg for 8 minutes were dried through incubation at 65^{o}C for one minute, re-suspended in 10µl of DPEC-treated water and stored at -70^{o}C.

6.3.5 Reverse Transcritpion

RNA samples were converted in cDNA through a reverse transcription reaction using the cloned AMV first-strand cDNA synthesis kit (Invitrogen; Cat. 12328) according to the instructions provided by the manufacturer. The kit utilises cloned avian myeloblastosis virus (AMV) reverse transcriptase. The reaction consisted in a first step of denaturation of RNA and primer coupling through incubation of RNA with primers (oligo (dT)) and dNTPs in DPEC-treated water for 5 minutes at 65^{o}C. The reaction was stopped placing samples in ice and it was followed by the cDNA synthesis reaction consisting in the incubation of the samples with the reaction mixture containing cloned AMV, RNase OUT, reaction buffer and reagents in DPEC-treated water for 45 minutes at 50^{o}C. The reaction was then stopped through incubation at 85^{o}C for 5 minutes. The resulting samples containing cDNA were stored at -70^{o}C.

A negative control for the reverse transcription was obtained for each sample in order to exclude artefacts generated by the presence of contaminant DNA in the samples. The negative controls were obtained preparing tubes for the reverse transcription containing the sample RNA and all the reagents with the exception of the cloned AMV. Due to the absence of reverse transcriptase in the tubes no cDNA could be produced from the original RNA. In case some DNA would be obtained in the negative controls after PCR, this would have to be related to the presence of contaminant DNA.

6.3.6 Polymerase chain reaction

The cDNA obtained from reverse transcription of the RNA samples were used to verify the expression of the gene producing the three isoforms of hyaluronan synthase (HAS). The primers for the amplification of the three isoforms of HAS were selected and used as previously described by Stewart et al (2009) as shown in table 6.1. PCR for housekeeping gene was done to verify the presence of cDNA in all the samples. The gene for glyceraldehyde-3-phosphate dehydrogenase (GAPDH) was chosen as housekeeping gene and the primers obtained from previous publications (Wang 2004). This represents one the most common housekeeping genes used in PCR experiments due to the consistent presence in all the tissues and the repeated expression within the same tissue (Barber 2005). The expression of the gene under investigation can be compared to the expression of the housekeeping gene. The negative controls for the reaction of reverse transcription were used in a PCR reaction for GAPDH to verify the purity of samples and the presence of contaminant DNA in the original samples. All the primers were purchased from Eurofin, re-suspended in DPEC-treated water and stored at -20^{o}C.

Table 6.1 List of primers used in RT-PCR. The table shows the sequences of the primers used for the amplification of the desired genes (5'-3'), size of the amplification products and final working concentrations.

Gene	Forward primer 5'-3'	Reverse primer 5'-3'	Amplification product size (base pairs)	Concentration in reaction tubes
HAS1	ggcttgtcagagctacttc	gccacgaagaaggggaa	368 bp	0.4 µM
HAS2	atgcattgtgagaggtttct	ccatgacaactttaatcccag	354 bp	0.4 µM
HAS3	gacgacagccctgcgtgt	ttgaggttcagggaaggagat	335 bp	0.4 µM
GAPDH	aggggtctacatggcaactg	cgaccactttgtcaagctca	228 bp	0.8 µM

The PCR reaction was performed using Taq DNA polymerase gold (Biogene; Cat. D1003Y) according to the instructions provided by the manufacturer. 5µl of solution containing cDNA was added to each reaction tube with the primers at the working solution as reported in table 6.1, taq polymerase and reaction buffer containing $MgCl_2$ at a final working concentration of 1.5mM and the addition of a 10mM oligonucleotide mixture (dNTP) to obtain a final concentration of 0.8mM in the reaction tubes. The cycling conditions were determined upon previous publications (Stewart 2009) and verified through preliminary experiments were as follows:

- HAS1 : initial 5 minutes at 94^{o}C followed by 40 cycles at 94^{o}C for 30 seconds, 52^{o}C for 50 seconds and 72^{o}C for 30 seconds, followed by final extension step at 72^{o}C for 7 minutes
- HAS2: 5 minutes at 94^{o}C followed by 40 cycles at 94^{o}C for 30 seconds, 53^{o}C for 30 seconds and 72^{o}C for 30 seconds followed by extension step at 72^{o}C for 7 minutes
- HAS3: 5 minutes at 94^{o}C followed by 40 cycles at 94^{o}C for 30 seconds, 56^{o}C for 30 seconds and 72^{o}C for 30 seconds, followed by an extension step at 72^{o}C for 7 minutes.
- GAPDH: 3 minutes at 94^{o}C followed by 35 cycles at 94^{o}C for 30 seconds, 55^{o}C for 30 seconds and 72^{o}C for 30 seconds, followed by extension step at 72^{o}C for 10 minutes

Negative controls were obtained by amplifying the reaction mixture without the inclusion of cDNA in order to exclude the presence of contaminant DNA in the mixture. Positive controls for every amplification reaction were used. At this purpose a PCR-ready first strand cDNA extracted from normal human adult (68 years old, male) artery and purchased by AMS Biotechnology (Europe) Ltd was amplified. The estimated cDNA concentration provided by the company was 2.5

ng/µl and 1µl of solution was added to the reaction tube as suggested by the company.

The resulting amplification products were stored at -20^{o}C.

6.3.7 Electrophoresis on 1% agarose gel

The amplification products were resolved performing an electrophoresis on 1% agarose gel. Agarose gel was prepared dissolving agarose (Fisher Scientific) in Tris Acetate-EDTA (TAE) buffer (Sigma Aldrich; Cat T4038) and added with ethidium bromide in aqueous solution (Sigma Aldrich; Cat. E1385) at a final concentration of 0.5 µg/ml. In each gel 5 µl of PCR 100 base pairs (bp) low ladder (Sigma Aldrich; Cat. P1473) were loaded. The ladder contained 10 bands ranging from 100 bp to 1000 bp in 100 bp spaced repeats.

Each sample (10 µl) was added with 3 µl of loading dye (4g sucrose, 2.5 mg of bromophenol blue to 10 ml in Tris-EDTA buffer) and 12µl of each loaded into each well.

The gels were run in TAE buffer at 100-120V for 30-40 minutes.

The intensity of the bands were recorded using the Fluorchem software and expressed as ratio between integrated intensity value (IDV) provided by the instruments and the area selected after automatic adjustment to eliminate interference from background. Values were expressed as ratio IDV/area in order to normalise the intensity measured for different areas. Due to the limited accuracy of the software and to the experimental conditions a reliable semi-quantitative analysis of the results was not possible. Values were mainly used to emphasize differences in gene expression.

6.4 RESULTS

The products obtained from the reaction of RT-PCR were resolved and visualised through electrophoresis in 1% agarose gel. The expression of HAS isoforms in RNA extracted from monocytes incubated on stainless steel was compared to the expression in RNA extracted from macrophages incubated on extracellular matrix-coated wells in order to verify differences in the behaviour of inflammatory cells in contact with the metal in comparison with a substrate mimicking physiological environment. Results were analysed to determine whether the expression occurred on the basis of presence or absence of bands. The intensity of the bands was measured to provide a general indication of the level of expression of the different genes.

In order to confirm the presence of cDNA in test tubes, all samples were tested through PCR reactions for the amplification of GAPDH chosen as housekeeping gene. As shown in figure 6.3, all samples obtained from macrophages incubated on stainless steel confirmed the presence of an amplification product corresponding to the gene for GAPDH (227bp product size). Weak signal was obtained from tubes containing cDNA from macrophages isolated form donor 3 and incubated on stainless steel in low glucose DMEM (figure 6.3a-lane 6; table 6.2) and cDNA from macrophages from donor 1 incubated on stainless steel in high glucose (figure 6.3c-lane 1; table 6.2). Those samples were included to show the complete scenario obtained from the PCR experiment but, considering the low expression of the housekeeping gene, are not relevant for the final analysis of the results. The lack of housekeeping gene expression represents in fact a flaw in the experiment execution and the reduced amount of RNA in the samples. Negative control for the PCR reaction was represented by the reaction mixture including both primers with the exception of cDNA (figure 6.3a-lane 2). A positive control was obtained from the amplification of cDNA from human artery purchased as

described in paragraph 6.3.5 (figure 6.3a-lane 3). Similarly, cDNA obtained from RNA isolated from macrophages incubated on ECM-coated wells under the different cultural conditions confirmed the presence of an amplification product corresponding to the gene for GAPDH (figure 6.4). Weaker bands were obtained observed in cDNA obtained from macrophages from donors 4 and 6 and incubated on ECM-coated wells incubated in low glucose DMEM added with 0.4mM sodium palmitate (figure 6.4b-lanes 4-6). The intensity of the bands was generally variable among samples.

The absence of impurities due to contaminant DNA was verified through amplification for the GAPDH gene of the negative samples produced during the reverse transcription. Those samples were obtained by mixing RNA with the reagents included in the reverse transcription kit with the exclusion of the reverse transcriptase as described in paragraph 6.3.4.

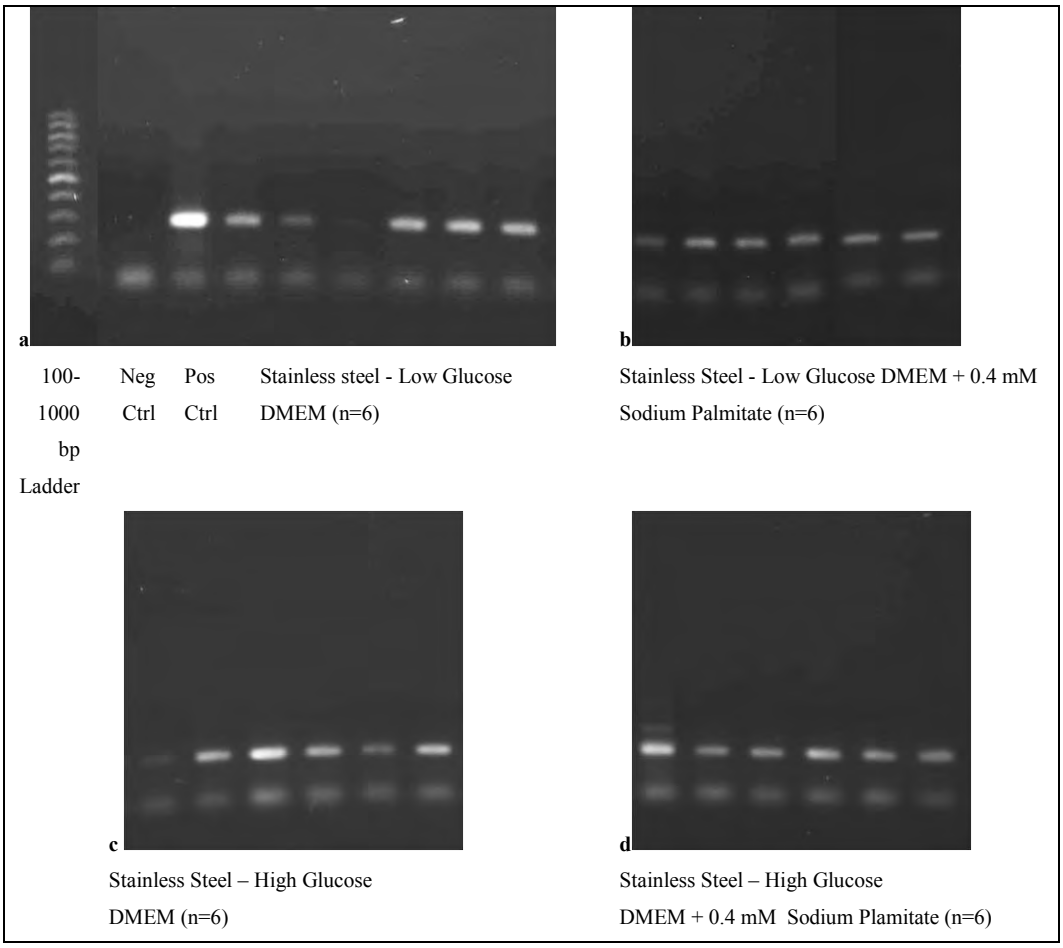

Figure 6.3. Resolution of the PCR reaction products after amplification of the gene for GAPDH in monocytes incubated on stainless steel at different culturing conditions. *The housekeeping gene was expressed in all the samples. Low expression in cells from the donor 3 incubated in low glucose concentration DMEM (Figure 6.3a-row 6). The primers chosen for GAPDH amplification originated a product of 227 bp size (figure 6.3a).*

The agarose gels obtained from these samples showed no contamination of the original samples (data not shown). Weak bands with extremely low intensity appeared on the gels in the case of samples obtained from macrophages from donors 4 and 6 and incubated on ECM-coated wells in physiological glucose concentration DMEM added with 0.4 mM palmitate (figure 6.4b).

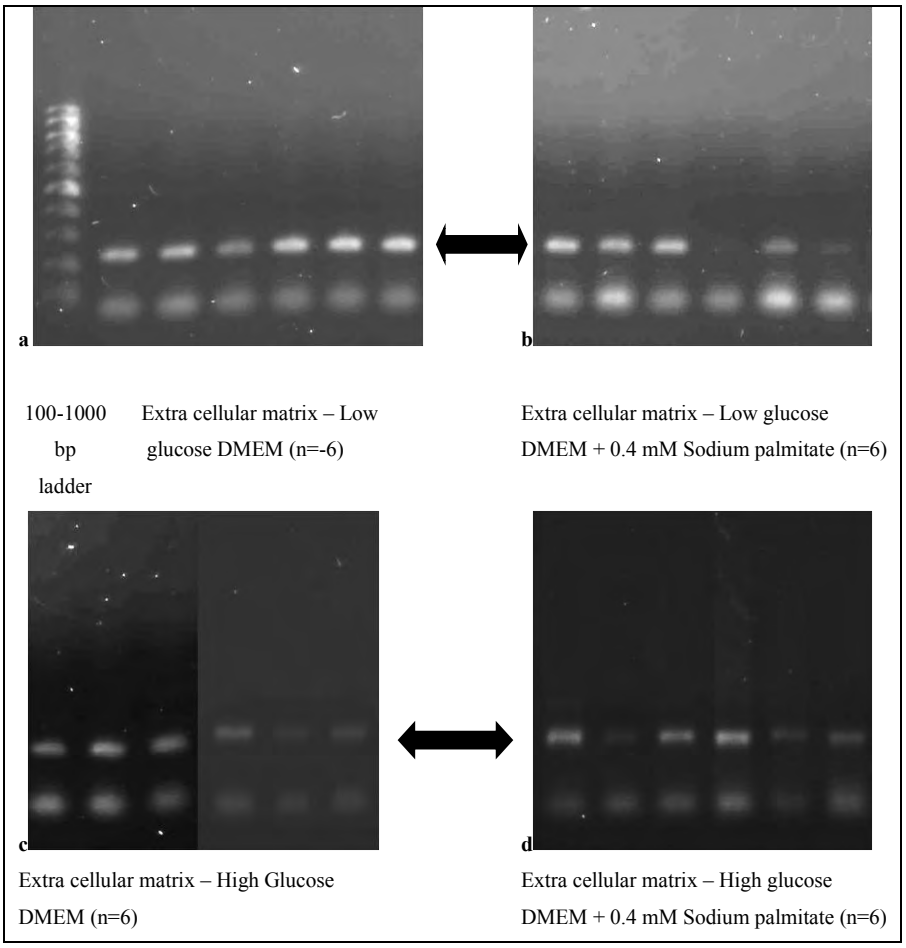

Figure 6.4 Resolution of the PCR reaction products after amplification of the gene for GAPDH in monocytes incubated on extra cellular matrix at different culturing conditions. *Housekeeping gene was expressed in all of the samples. Low expression in cells from donors 4 and 6 incubated on extra cellular matrix (ECM) in low glucose concentration DMEM added with 0.4mM sodium palmitate (Figure 6.4b-rows 4 and 6). The primers chosen for GAPDH amplification originated a product of 227 bp size as indicated by the black double arrows in the figure.*

6.4.1 Expression of HAS isoforms

RT-PCR was performed on all the samples to verify the expression of genes for the three different isoforms of hyaluronan synthase (HAS1, HAS2 and HAS3). The outcome of every RT-PCR reaction was monitored using positive and negative controls as described in section 6.3.5.

Results showed that no HAS1 was expressed when macrophages were incubated overnight on extra-cellular matrix-coated wells. Similarly, expression of HAS1 could be found only in macrophages from one donor incubated on stainless steel in low glucose DMEM and in macrophages from two donors incubated on stainless steel in high glucose concentration DMEM, although represented by weak intensity bands (table 6.2).

Similarly, the analysis of the results obtained from macrophages incubated overnight on stainless steel or extra-cellular matrix-coated wells showed no relevant expression of HAS2 in macrophages under any cultural conditions (table 6.3). In the case of RNA isolated from macrophages incubated on stainless steel, the expression of HAS2 was observed in macrophages from donor 5 and donor 1 incubated respectively in high glucose concentration DMEM and in high glucose concentration DMEM added with 0.4mM sodium palmitate (table 6.2). Low intensity bands were observed after amplification of cDNA obtained from RNA extracted from macrophages from donor 6 and incubated on stainless steel in low glucose concentration DMEM and from donor 3 and incubated in high glucose concentration DMEM added with sodium palmitate (table 6.2).

HAS3 is the isoform associated with the production of low molecular weight hyaluronan and consequently triggering the inflammatory process. Results suggest that overnight incubation of macrophages on stainless steel, particularly if incubated in high glucose concentration alone or in combination with sodium palmitate, seemed to trigger the expression of HAS3. In fact, the recurrent appearance of high intensity bands corresponding to the gene for HAS3 (product size 335bp) was observed (figure 6.5; table 6.2). The band identifying HAS3 was seen in samples obtained from macrophages from four of the six donors incubated overnight on stainless steel in high glucose concentration DMEM added with sodium palmitate (figure 6.5h). Similarly, macrophages from four donors incubated in high glucose concentration DMEM alone expressed the gene for HAS3 (figures 6.5g).

HAS3 expression was randomly seen in macrophages incubated on extra-cellular matrix-coated wells and expressed by low intensity bands (figure 6.6).

Densitometry with the software Fluorchem was performed to compare the expression of the genes although not relevant semi-quantitative analysis could be performed. Densitometry was based on the intensity of the bands as analysed by the instruments in terms of density of “light” areas in comparison to the “dark” background. This showed that the expression of the HAS3 gene was on average half of the average of intensity of the expression of the GAPDH when considering the ratio between integrated density value and area analysed. The densitometry values varied widely among samples.

Table 6.2 Summary of the expression of HAS isoforms and housekeeping gene (GAPDH) in macrophages from six donors incubated overnight on stainless steel. Values are expressed as ratio between integrity density value (IDV) and area selected as provided by FLourchem software and automatically adjusted for background.

Stainless Steel					
Condition of culture	**Donor**	**Gene expression (IDV/Area)**			
		HAS1	**HAS2**	**HAS3**	**GAPDH**
DMEM with physiological glucose concentration	**1**	-	-	-	37
	2	-	-	-	9
	3	-	-	-	3
	4	-	-	-	15
	5	6	-	1	12
	6	-	1	2	11
DMEM with physiological glucose concentration and 0.4 mM sodium palmitate	**1**	-	-	-	4
	2	-	-	-	9
	3	-	-	-	8
	4	-	-	2	9
	5	-	-	2	19
	6	-	-	-	17
DMEM with high glucose concentration	**1**	-	-	2	4
	2	-	-	-	23
	3	-	-	2	41
	4	7	-	-	21
	5	-	9	5	10
	6	1	-	3	24
DMEM with high glucose concentration and 0.4 mM sodium palmitate	**1**	-	3	17	33
	2	-	-	4	14
	3	-	4	7	15
	4	-	-	2	22
	5	-	-	-	15
	6	-	-	-	15

Table 6.3 Summary of the expression of HAS isoforms and housekeeping gene (GAPDH) in macrophages from six donors incubated overnight on extracellular matrix-coated wells. Values are expressed as ratio between integrity density value (IDV) and area selected as provided by FLourchem software and automatically adjusted for background.

Extracellular matrix-coated tissue culture plate wells					
Condition of culture	**Donor**	**Gene expression (IDV/Area)**			
		HAS1	**HAS2**	**HAS3**	**GAPDH**
DMEM with physiological glucose concentration	**1**	-	3	5	13
	2	-	1	3	13
	3	-	-	-	8
	4	-	-	-	17
	5	-	-	-	18
	6	-	-	-	17
DMEM with physiological glucose concentration and 0.4 mM sodium palmitate	**1**	-	-	-	11
	2	-	-	-	9
	3	-	-	-	10
	4	-	-	-	2
	5	-	-	-	5
	6	-	-	-	1
DMEM with high glucose concentration	**1**	-	-	2	7
	2	-	-	-	10
	3	-	-	-	9
	4	-	-	-	7
	5	-	-	-	3
	6	-	-	-	4
DMEM with high glucose concentration and 0.4 mM sodium palmitate	**1**	-	1	1	15
	2	-	-	-	3
	3	-	-	-	11
	4	-	-	-	4
	5	-	-	-	6
	6	-	-	-	8

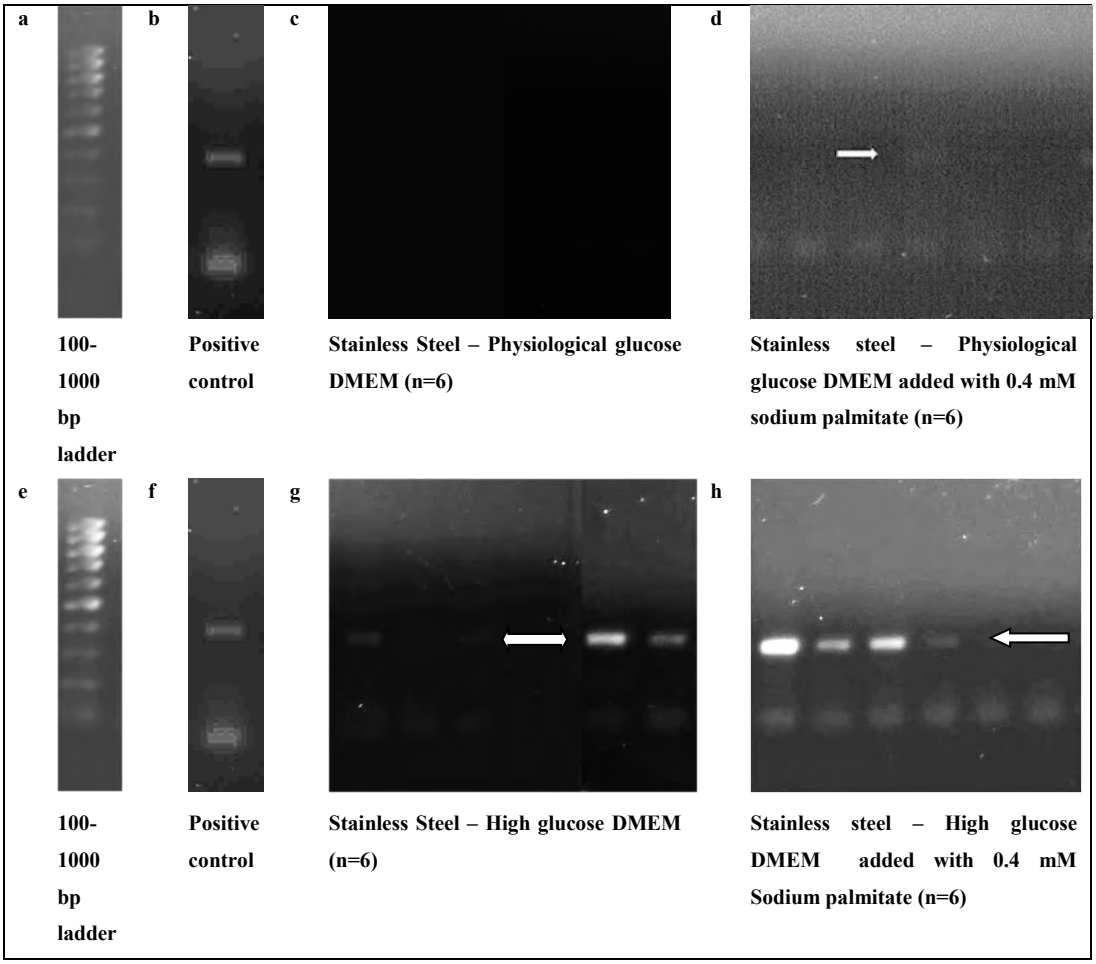

Figure 6.5 Resolution of the PCR reaction products for the identification of the gene for HAS3 in monocytes incubated on stainless steel at different culturing conditions (n=6). *The presence of high glucose (figure 6.5g) and concomitant presence of high glucose and free fatty acid represented by 0.4 mM of sodium palmitate (figure 6.5h) in the culture medium triggered the expression of the gene for the isoform of hyaluronic synthase responsible for the synthesis of short molecular weight hyaluronic acid (HAS3) in monocytes from different donors incubated for 24 hours on stainless steel. The couple of primers selected for the amplification of HAS3 gene generated an amplification product of 335 bp size (Fig. 6.5b) indicated by the with arrows in the figures. The positive control was represented by smooth muscle cells from human aorta (figures 6.5b,f).*

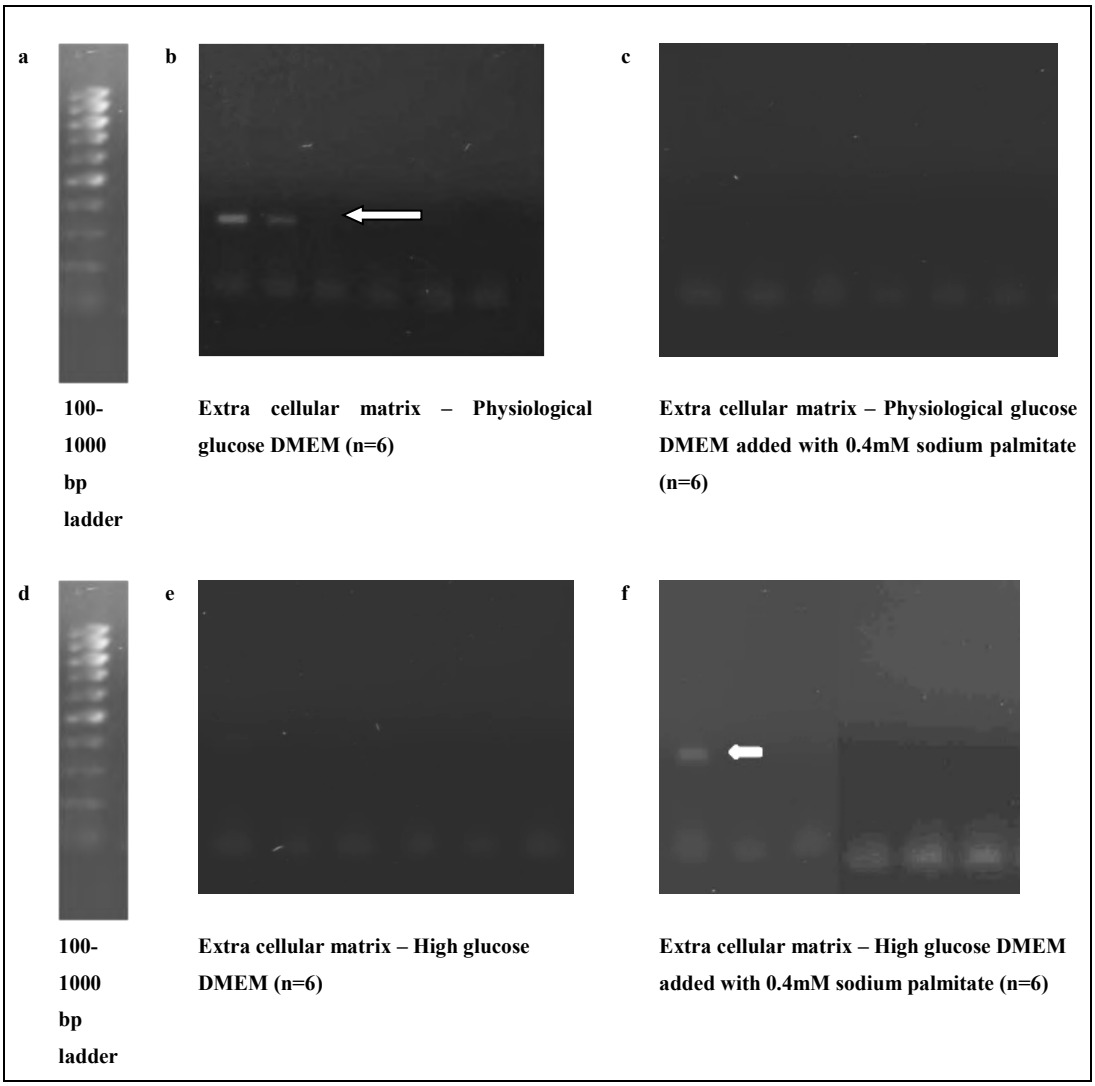

Figure 6.6 Resolution of the PCR reaction products for the identification of the gene for HAS3 in monocytes incubated on extra cellular matrix-coated wells at different culturing conditions (n=6). *The expression of the gene for the isoform of hyaluronic synthase responsible for the synthesis of short molecular weight hyaluronic acid (HAS3) in monocytes from different donors incubated for 24 hours on extra cellular matrix was seen only in two donors when cells were incubated in physiological glucose DMEM (figure 6.6b) and in one donor when cells were incubated in high glucose DMEM added with 0.4mM sodium palmitate (figure 6.6b). The couple of primers selected for the amplification of HAS3 gene generated an amplification product of 335 bp size (Fig. 6.6a) as indicated by the white arrows.*

6.5 DISCUSSION

Hyaluronic acid, one of the main components of the extra-cellular matrix conferring specific physic-chemical properties (Travis 2001), is synthesized by different cell types including endothelial cells, smooth muscle cells and fibroblasts (Weigel 1997, Itano 1999, Tammi 2002, Chai 2005). Hyaluronan intervenes in tissue remodelling and wound healing after injuries (Itano 1999, Tammi 2002, Toole 2002, Chai 2005) where it modulates the inflammatory process through the formation of low molecular weight chains obtained either through fragmentation of constituent hyaluronan or through direct synthesis by hyaluronic acid synthase 3 (HAS3) (Itano 1999, Kennedy 2000, Vigetti 2010). The process of inflammation is directly correlated to the presence and function of hyaluronan. Studies have demonstrated the accumulation of hyaluronan triggered by the presence of pro-inflammatory cytokines in culture medium of endothelial cells, thus confirming the involvement of hyaluronan in the vascular inflammatory process. The release of cytokines from inflammatory cells was demonstrated to be triggered by the presence of hyaluronan (Itano 1999, Kennedy 2000, Vigetti 2010).

In addition to representing the main component of the neointimal tissue, hyaluronan plays a fundamental role throughout all the phases of the restenotic plaque deposition. During the early stages following stent implantation the fragmentation of hyaluronan sustains the initial inflammatory process through its interaction with inflammatory cells and favouring cell migration. During the later stages of restenosis long molecular weight hyaluronan participates to tissue remodelling and to the formation the neointimal plaque deposition (Travis 2001, Tamni 2002).

A study from Stewart et al. (2009) demonstrated that macrophages in contact with stainless steel for seven days trans-differentiated into myofibroblasts expressing

the gene for HAS1 (Stewart 2009). HAS1 is responsible for the synthesis of high molecular weight hyaluronan intervening in tissue remodelling and providing fundamental contribution in the remodelling phase of restenosis. Macrophages did not show to express HAS1 when incubated on physiological-mimicking surfaces such as collagen and fibrinogen indicating that stainless steel induces phenotypical changes in macrophages reflected also in their ability to produce hyaluronan and confirming their direct involvement in the deposition of the restenotic plaque in later phases of *in-stent* restenosis following implantation of bare metal stents.

Results from this study showed that, after overnight incubation, macrophages did not express HAS1 or HAS2 when incubated on either stainless steel or extracellular matrix under any experimental conditions. However, the up-regulation of the expression of mRNA codifying for HAS3 when macrophages were incubated overnight on stainless steel was suggested by the experiment. In particular, the up-regulation seemed to be accentuated in the presence of medium with high glucose concentration with or without the addition of sodium palmitate (figure 6.5; table 6.2). No relevant expression of the mRNA for HAS3 was seen in macrophages incubated on ECM-coated well (figure 6.6; table 6.3). HAS3 is the isoform responsible for the synthesis of low molecular weight hyaluronan that has been associated with the inflammatory reaction (Itano 1999, Kennedy 2000, Vigetti 2010). Therefore, despite the importance of taking, into consideration the limited amount of samples analysed (n=6), the up-regulation of the expression of the mRNA codifying for HAS3 by macrophages incubated overnight on stainless steel suggested the activation of macrophages triggered by the contact with the metal in comparison to physiological-mimicking surfaces such as extra-cellular matrix. Overnight incubation was chosen to reflect the conditions adopted in previous experiments. Those aimed at identifying potential differences in the early inflammatory response of macrophages following the implantation of cardiovascular stents. A recent study investigated the patterns of the production of

proteoglycans constituting the extra-cellular matrix by macrophages under specific stimuli *in-vitro* (Chang 2012). The study showed that, among the complex variety of proteoglycans produced by the cells, the upregulation of mRNA for HAS2 and HAS3 was transient and detectable shortly after activaction of monocyte-derived macrophages (Chang 2012). This reinforces the validity of the potential up-regulation of the expression of mRNA for HAS3 observed after overnight incubation of macrophages activated by the contact with stainless steel in the presence of high glucose with or without palmitate. In addition, similarly to the results obtained from this experiment, the study by Chang *et al.* (2012) showed no expression of HAS1 immediately after activation of macrophages (Chang 2012).The positive control used for the PCR experiments was represented by a PCR-ready cDNA extracted from adult human artery. This provided a positive control for the presence of HAS isoforms confirming the correct execution of the amplification process. However, future experiments could benefit of a further positive control represented by fully differentiated macrophages. At this purpose, the study published by Chang *et al.* (2012) stimulated the activation of monocytes by using phorbol myristate acetate (Chang 2012). Therefore, results suggest that the contact with the metal, particularly under dysmetabolic conditions, may trigger the formation of low molecular weight hyaluronan involved in the initial inflammatory reaction following stent implantation, thus favouring cell migration and possibly initiating the deposition of the restenotic plaque. Overall, the scenario depicted by the results from this and previous chapters suggests that, following stent implantation, macrophages migrate towards the stent, activated to promote the inflammatory reaction and soon switch their phenotype to favour the wound healing thus promoting the proliferation of smooth muscle cells and the synthesis of hyaluronan.

In addition, results from this work suggested that the effect of high glucose concentration, particularly in combination with high lipid concentration, on the response of macrophages to the contact with stainless steel. The up-regulation of

the gene for HAS3 was in fact emphasized in samples obtained from macrophages incubated on stainless steel in medium with high glucose and palmitate concentration. This suggests that the control of blood glucose and lipid at the moment of intervention may represent a critical point affecting the outcome of the procedure.

6.6 CONCLUSIONS

The analysis of the response of macrophages isolated from different cohorts of donors and discussed in the chapters 2, 3 and 4 confirmed that the implantation of stainless steel non-medicated stents induces the migration of macrophages to the strut and their activation. Furthermore, soon after adhesion, macrophages change from pro- to post-inflammatory status characteristic of a wound healing process acquiring phenotypical features typical of myofibroblasts. However, the complexity of the scenario characterizing donors with diabetes did not allow identifying a clear pattern linking the pathology with the biomolecular pathways responsible for *in-stent* restenosis.

The evaluation of the effect of hyperglycaemia and hyperlipidaemia on macrophages from healthy donors suggested that the concomitance of high glucose and lipid concentration enhances the response of inflammatory cells to the metal, accelerating the phenotypical switch and emphasizing the metal-induced activation. Therefore, results suggest that the control hyperglycaemia and hyperlipidaemia at the moment of stent implantation may have an impact on the outcome of the procedure and reduce the incidence of restenosis as mentioned in previous studies based on clinical data (Khosvari 2011, Nusca 2011).

CHAPTER 7

DISCUSSION AND CONCLUSIONS

7.1 SCIENTIFIC BACKGROUND

Cardiovascular disease represents the biggest cause of death in UK. Despite an overall decrease in the number of deaths achieved through a preventive approach aiming at reducing risk factors and through improvements of available therapies, in 2008 CVD still accounted for 191,000 deaths in UK of which 50,000 were classified as premature deaths. Particularly, CVD were established to be the cause of the death of one in four men and one in five women under 75 (British Heart Foundation, 2010). Among the forms of cardiovascular disease, atherosclerosis is considered one of the major fatal pathologies of the 21st century. In particular, when the atherosclerotic plaque forms within coronary arteries it can cause partial or complete occlusion of the vessels thus leading to angina, heart attack and to a significant number of cases of death (Chapman 1998, Kannel 1998, Fan 2003, British Heart Foundation 2010).

One of the major surgical interventions adopted to re-establish the lumen patency of atherosclerotic vessels is the percutaneous transluminal coronary angioplasty (PTCA). This technique has been successfully utilized since its introduction in 1977 (Santin 2005). It is a procedure of choice as it is a less invasive technique than by-pass graft (Bertrand 1998). Despite the procedure leading to an immediate success rate of revascularization (Herrmann 1992), complications such as thrombus formation, elastic vascular recoil and restenosis still affected the outcome of the intervention in up to the 40% of cases (Liu 1999, Santin 2005).

The PTCA technique has been developed further by the deployment of a stent, an expandable tubular metallic mesh that is loaded onto the balloon and delivered during PTCA (Farb 2002, Moses 2003, Santin 2005). The stent is placed at the site of the lesion to act as a scaffold for the blood vessel and maintain the lumen patency thus ensuring the success of the revascularization procedure. Indeed, the presence of the metallic structure reduces the chances of elastic recoil consequently improving the outcome of the procedure (Gross 2000, Santin 2005).

Despite the deployment of stents having represented a significant improvement in the angioplastic procedure, ISR still affects the general outcome in up to the 35% of patients when considering the implantation of traditional bare metal stents in more complex scenarios (Gross 2000, Santin 2005, Singh 2010). In particular, bigger and more complex lesions, small calibre vessels, calcified lesions and diabetes represent risk factors for the occurrence of restenosis (Ruygrok 2001, Farb 2002, Klein 2002, Ruygrok 2003, Barlis 2007)

In-stent restenosis consists of the formation of a secondary occlusion and it represents a common complications of the procedure (Santin 2005) leading to potentially fatal cardiovascular events such as myocardial infarction and to the necessity of secondary revascularisation (Moses 2003). Partial reduction in the incidence of ISR has been achieved by improvements introduced to the surgical procedure in order to reduce the stress on the blood vessel wall and to limit the penetration of the metal strut during implantation (Farb 2002, Santin 2005). Furthermore, different technological attempts to develop new stents have been carried out over the last decades in the attempt to improve the outcome of the procedure in comparison to the traditional bare metal stents made with stainless steel.

The most relevant development has been represented by the commercially successful production of drug-eluting stents in which the metal strut is coated with polymer releasing anti-proliferative or cytostatic agents (Santin 2005, O'Brien 2009) thus inhibiting the cellular proliferation associated with the formation of the restenotic plaque. The general clinical approach in agreement with the guidelines published by the National Institute of Clinical Excellence (NICE) recommend the use of drug-eluting stents in case of the more complex scenarios mentioned above (NICE Technology appraisal 71, 2003; O'Brien & Carroll 2009). People with diabetes represent the major population at risk of cardiovascular diseases and prone to develop ISR.

The incidence of ISR in diabetic patients following implantation of BMS was significantly higher than in subjects without a diagnosis of diabetes; in particular between 41% and 70% of diabetic patients suffer of ISR when bare metal stents are implanted (Kornowski 1997). The rate of ISR and the need for a secondary revascularization have been reduced up to the 70% since DESs were chosen for the treatment of vessel occlusions in diabetic patients (Abizaid 2003, Gilbert 2004, Joner 2006, Barlis 2007, Jensen 2007, Somberg 2007, Kumbhani 2008, Patti 2008, Yan 2008, Frobert 2009, Singh 2010). Evidence of the benefits obtained in the short and intermediate period following implantation of DESs has been published in many meta-analysis studies (Mauri 2007, Yan 2008, Barlis 2006, Jensen 2007). However, data related to long-term drawbacks associated with the use of DES and mainly concerning the occurrence of late thrombosis still remain controversial (Jensen 2007, Garg 2008).

The causes of failure of bare metal stents and DES are of particular clinical relevance if framed within their higher rate of negative outcome in diabetic patients. Indeed, diabetes mellitus is a "metabolic disorder of multiple aetiology characterized by chronic hyperglycaemia with disturbances of carbohydrate, fat and protein metabolism resulting from defects in insulin secretion or action or both" (WHO Consultation, 1999). An estimated 171 million people worldwide were affected by diabetes mellitus in 2000 and the figure was predicted to increase to 366 million by 2030 (WHO 2006).

The two main forms of diabetes are represented by type 1 and type 2. They differ in terms of aetiology of the disease and mechanisms involved in the development of hyperglycaemic condition and insulin dysfunction. Type 1 diabetes is characterized by the destruction of pancreatic islets of Langerhans (beta cells), responsible for the production of insulin, mainly due to an autoimmune reaction identified by the presence of specific auto-antibodies (Lambert 2006). It has been demonstrated that the destruction of pancreatic cells is not due to the direct action of the antibodies but it is an immune process mediated by T lymphocytes and

inflammatory cells (Zacher 2002, Lamhamedi-Cherradi 2003, Homo-Delarche 2004, Lambert 2006).

Type 2 diabetes is a condition of insulin resistance characterized by lost in sensitiveness to insulin action in insulin-sensitive tissues such as muscles, fat and heart thus resulting in increased blood glucose levels (O'Rahilly, 1994, Sjoholm, 2006). A direct connection between insulin resistance, obesity and diabetes has been demonstrated in various studies that focussed on the direct connection between metabolism and immune system. Obesity has been characterized as a chronic inflammatory condition with overproduction of pro-inflammatory cytokines such as TNF-α and IL-6, and of messenger molecules known as adipokines (leptin, adiponectin) from muscles and adipose tissue of obese individuals (Wellen & Hotamisligil 2005, Sell 2006). Accumulation of macrophages in the adipose tissue participate to the activation and progression of inflammatory condition in adipocytes of obese individuals paving the way for the development of insulin resistance (Weisberg 2003, Permana 2006). Type 2 diabetes is therefore a condition affecting adult population and correlated to metabolic dysfunction. The aetiology of the disease derives from genetic predisposition and lifestyle risk factors such as low physical activity and diet (Tuomilehto 2001, Spranger 2003). The correction of lifestyle habits can control the development of type 2 diabetes in individuals with insulin resistance (Tuomilehto 2001).

Despite differences in the aetiology of the type 1 and type 2 diabetes, cardiovascular diseases represent one of the major causes of mortality among the diabetic population (Miettinen 1998). The increase of cardiovascular risk in people with diabetes has been traditionally correlated to alterations in the vascular endothelium and stiffening of the artery wall due to prolonged exposure to hyperglycaemic conditions in diabetic people as a result of the formation of advanced glycated end products (AGE) (Peppa 2003, Price 2004, Goldin 2006). Studies have shown that the increase in cardiovascular risk associated with

diabetes is the result of a more complex scenario where cardiovascular alterations are associated with inflammation, leukocyte and immune cell activation and consequent increase in the release of pro-inflammatory cytokines (Hu 2003).
The close connection between diabetes and cardiovascular disease has in fact led to the development of a "common soil" hypothesis suggesting that diabetes and cardiovascular disease share genetic and environmental circumstances, resulting from an underlying pathophysiological condition (Hu 2003).

The combination of alteration in vascular endothelium, basic inflammatory conditions and increased cardiovascular risk characterizing diabetic patients represent the background to be investigated in order identify possible connection between the disease and the increase in the development of in-stent restenosis.

In-stent restenosis is characterized by the deposition of a neointimal tissue around the stent strut. The newly formed tissue is characterized by a high content of a proteoglycan (versican and hyaluronan)-rich extracellular matrix colonised by smooth muscle cells, myofibroblasts and macrophages, a histological pattern often associated with non-healing wound tissue (Bayes-Genis 2002). Inflammatory cells (neutrophils and macrophages) have been found in the initial phases of healing following stent expansion infiltrating the thrombi deposited around the stent strut and throughout all the stages of the neointimal formation (Santin, 2005). Monocytes-derived macrophages are one of the cellular component playing a fundamental role throughout the whole restenotic process in association with smooth muscle cells responsible for the tissue deposition and of the vasculature contraction (Tashiro 2001, Santin 2005).Understanding the origin of myofibroblasts in the restenotic tissues would therefore identify the cellular components directly involved in the development of the restenotic process.

Previous studies have shown that monocyte-derived macrophages in contact with stainless steel presented phenotypical plasticity being able to differentiate into myofibroblasts thus contributing to the formation of neointima during the later

stages of ISR. These findings extended the role played by monocytes and macrophages in the development of the restenotic plaque in addition to the initial leading role of the inflammatory reaction (Santin 2005, Stewart 2009, Mesure 2010).

The trans-differentiation potential of monocytic cells has been investigated in different studies that showed the ability of monocytes, identified by the marker CD14, to differentiate, thus acting as progenitor of mesenchymal lineages under specific in-vitro culture conditions (Kuwana 2003, Gordon 2005, Varol 2009).

More recent studies have also identified sub-populations in the circulating blood derived from monocytes and able to differentiate in cells of the mesenchymal lineage, endothelial cells and smooth muscle-like cells, in particular representing precursors for the formation of myofibroblasts, main cellular component of restenotic neointimal tissue. A further characterization of the sub-populations forming the mononuclear fraction of circulating blood could therefore fully elucidate on the role of monocytes in the deposition of neointima responsible for the formation of the restenotic plaque and more in general on their role in the foreign body reaction.

7.2 HYPOTHESIS OF THE STUDY AND ITS CONTRIBUTION TO KNOWLEDGE

The present study provides insights in the mechanisms of ISR and uniquely identifies host conditions that can predispose to its development in diabetic subjects. Since the beginning of this project, papers have been published by other authors that emphasize the plastic behaviour of the mononuclear cell population of the peripheral blood and its ability to contribute to cardiovascular pathologies either through biochemical signalling or through direct cell differentiation and trans-differentiation pathways (Simper 2002, Kuvana 2003, Sugiyama 2006, Boilson 2008, Pilling 2009, Stewart 2009, Forte 2010, Mesure 2010). On this line, the present project contributes to the knowledge by identifying more in depth phenotypic plasticity and linking it to biochemical and cellular pathways in the context of the particular micro-environmental conditions determined by the presence of a typical stent material (i.e. stainless steel) and levels of glucose and lipids. The systematic study adopted in this project includes the use of samples derived from diabetic patients of type 1 and type 2. While the characterization of diabetic samples was limited to a relatively small population participating in the study, its contribution to knowledge has to be framed within the widest context of the whole project where it is linked to in vitro experiments gradually integrating three main potential determinants of ISR in diabetics; (i) foreign surface of the material, (ii) normo/hyper glycaemia, and (iii) hyperlipidaemia and how these factors contribute to the triggering of the formation of the restenotic plaque, the biochemistry of which is largely undefined. Their understanding is a fundamental step forward towards the development of new bare metal stents especially if considered the concerns about the long term outcome of drug-eluting stents and their significantly higher costs. Therefore, this study aimed to investigate the molecular mechanisms, with particular attention to the role of monocytes-derived

macrophages, leading to the adverse reaction to bare metal stents implantation and to the higher incidence of *in-stent* restenosis in patients with diabetes.

The experimental process involved:

- **Characterization of circulating cell sub-populations.** The characterization of the mononuclear cells in blood from diabetic donors in comparison to control subjects in order to evaluate the predisposition of people with diabetes to inflammatory cell activation.
- **Effect of stainless steel on monocytes-derived macrophages**. Evaluation of the differences in the acute response of inflammatory cells from people with diabetes to contact with stainless steel to identify differences in the response of inflammatory cells from diabetic people to the metal.
- **Effect of high glucose and high lipids and their synergy on the reaction of macrophages to stainless steel.** Development of an *in vitro* model of diabetes to determine the effect of high glucose and lipid concentrations alone and their synergy in the response of cells responsible for inflammation to the contact with stainless steel.

7.3 DISCUSSION

7.3.1 Characterization of circulating cell sub-populations

Any study trying to elucidate the causes of increased incidence of ISR in diabetic patients needs to comprehensively analyse the combination of potential effects driven by the basic inflammatory status and altered vascular condition affecting the patients as well as by the medical device biocompatibility. In relation to the underlying conditions affecting diabetic patients, a correlation between obesity, diabetes and inflammation has been highlighted in several studies (Spranger 2003, Weisberg 2003, Wellen & Hotamisligil 2005, Permana 2006, Sell 2006). This study provides a further contribution derived by the measurement of circulating activated macrophages in buffy coats of diabetic patients in comparison to control subjects whereby the majority of donors affected by type 1 diabetes showed higher levels of CD68 positive cells when compared to healthy individuals. As expected by their heterogeneous clinical conditions, donors with type 2 diabetes showed a mixed scenario that was not possible to harmonise even when patients relatively older and with BMI values significantly higher than donors with type 1 diabetes were singled out. Differences in the amount of CD68 (activated macrophages) positive circulating cells could be correlated to the general inflammatory status of the donor, consequently suggesting its exacerbation following implantation of the device. The combined analysis of clinical and biochemical blood parameters with the amount of circulating activated macrophages did not provide a direct relationship, especially in type 2 diabetes subjects, allowing the identification of any specific factor relevant to ISR. In fact, most of the donors with diabetes recruited in this study showed alterations in at least one of the cardiovascular risk factors measured in the study. However, some of the donors presenting well-controlled clinical conditions showed a significant increase in the amount of circulating activated macrophages. The limited amount

of donors recruited for the study did not provide sufficient data for a statistically significant analysis of the trend correlating clinical data with population distribution. The clinical scenario of people with diabetes is generally complex and particularly affected by the duration of the disease and by the use of medications that can interfere with the vascular condition of patients. These results confirm the inflammatory nature of the disease potentially identifying the basis for the predisposition of developing in-stent restenosis (Miettinen 1998, Hu 2003). This suggested that the measurement of the circulating amount of activated macrophages may not stand alone as a possible diagnostic parameter for the preventive identification of subjects at risk of developing ISR. The amount of circulating cells positive for the marker for endothelial progenitor cells mobilised during tissue repair (CD34) seems to vary rapidly following vascular injury and cardiac events increasing immediately after cardiac events. Therefore, the measurement of their circulating levels represents a realistic diagnostic or therapeutic target that could be combined with the assessment of activated circulating monocytes/macrophages to evaluate the risk of ISR in diabetic patients prior to stent procedure (Yin 1997, Boilson 2008). In this study, data obtained from the CD34 positive cells analysis of buffy coats showed a variability of results particularly among donors with type 2 diabetes suggesting that the evaluation of circulating cells positive for the marker for haematopoietic progenitor cells (CD34) could indeed be used in diagnostic procedures to assess predisposition to ISR.

Alongside these findings, the present study also identified other parameters potentially linked to the ISR risk assessments that are more closely linked to the formation of neointimal tissue around the device. These additional parameters are linked to the identification of mononuclear cell sub-populations and more specifically monocytes able to trans-differentiate into myofibroblasts capable of secreting typical ECM components of a restenotic tissue. Particular attention was paid to the differentiation potential of monocytes into myofibroblast and smooth-

muscle-like cells relevant for the restenotic process when in buffy coats and after their contact with a typical stent surface, i.e. stainless steel.

A small sub-population of monocytes (identified by the expression of CD14) co-expressed the marker for endothelial progenitor cells (CD34) alone or in combination with the general leukocyte marker (CD45) in most of the donors. These findings confirmed the results published by Kuwana *et al.* (2003) that identified a sub-population co-expressing the three markers as progenitor cells of monocytic origin that were able to differentiate in cells of the mesenchymal lineage and to participate in tissue repair and homeostasis (Kuwana 2003). In addition Boilson et al. (2008) identified a population co-expressing CD34 and CD45 as cells generating spindle-like cells in culture in opposition to the cells expressing exclusively CD34 and identified as pure precursor of endothelial cells. It was also shown that the amount of CD34+CD45+ cell sub-population, reduced in patients with endothelial dysfunctions (Boilson 2008), was the only one varying with the variation of cardiovascular conditions). Recent studies have also identified a population co-expressing the marker for endothelial progenitor cells (CD34), the general marker for leukocytes (CD45) and collagen I as fybrocytes (Pilling 2009, Forte 2010). Among the monocytic lineage, fybrocytes are considered as circulating precursors of vascular myobfibroblasts (Pilling 2009, Forte 2010). The presence of sub-populations expressing similar phenotype in buffy-coats isolated from donors recruited in the study reinforces the trans-differentiation potential of monocytes as key element to their contribution to the formation of myofibroblasts populating the restenotic plaque (Pilling 2009, Forte 2010). Due to the limited amount of data collected and to the extreme variability across individuals, a statistically significant comparison between the groups was not possible.

Results confirmed the presence among the circulating cells of co-expression of the marker for endothelial progenitor cells (CD34) and the marker for activated macrophages (CD68) alone or in combination with the general marker for

leukocytes (CD45). The identification of the CD34+CD68+ sub-population in circulating blood is particularly relevant for the understanding of the restenotic process. A recent study demonstrated that, after switching to their wound-healing phenotype during the foreign body reaction, the population of activated macrophages contained a fraction of CD34+CD68+ cells that seemed to contribute to formation of myofibroblasts (Mesure 2010).

In addition, results confirmed the presence of a circulating sub-population co-expressing the marker for monocytes (CD14) and for smooth muscle cells (α-actin) thus representing a precursor able to form smooth muscle-like cells. This confirmed findings previously published by Sugiyama et al. (2006) and by Simper et al. (2002) demonstrating the presence of precursors of smooth muscle cells in the low density fraction of monocytes isolated form human blood (Simper 2002, Sugiyama 2006). The variability across donors in addition to individual differences in blood cell distribution can also be related to the extraction procedure. It has been in fact shown that only the lower density fraction of the mononuclear cells extracted on poly-sucrose gradient contained cells positive to α-actin (Sugiyama 2006).

Results from these experiments seemed to confirm that the mononuclear fraction of circulating blood is composed of sub-populations characterized by a trans-differentiation potential that can contribute to the formation of neointima, thus representing a focal point for the understanding of the development of the restenotic process. In this study, the distribution of the different sub-populations seemed to be generally consistent across the groups. The study also suggests that a thorough analysis of cell sub-populations extended to a higher number of individual could represent the target for the full understanding of ISR mechanisms and pave the way towards a relatively rapid diagnostic protocol for its prevention in predisposed subjects.

7.3.2 Effect of stainless steel on monocytes-derived macrophages

The present project has provided more detailed evidence found in previous studies conducted on the circulating mononuclear cell population. The in vitro clinically reflective model here adopted has confirmed that after seven days of incubation on stainless steel macrophages expressed α–actin acquiring a spindle-like morphology (Stewart 2009), features typical of both smooth muscle cells and myofibroblasts, the cell types widely recognised as key players in neointimal tissue formation (Chung 2002, Farb 2002, Santin 2005).

The experimental conditions chosen for this study aimed to investigate the acute response (overnight incubation) of inflammatory cells to the material reproducing the environment surrounding the stent strut following implantation. In addition, the choice of a low glucose medium, reproducing physiological blood glucose concentrations, enabled to emphasise the effect of the material on the cells in order to highlight possible differences between donors. Immunocytochemistry confirmed that stainless steel is a good substrate for cell adhesion, thus suggesting that, following implantation, monocytes which migrate from the surrounding tissue may adhere with great affinity to the stent struts. In addition, the cells adhering on the experimental surfaces expressed CD68, thus identifying them as activated macrophages. Among those cells, a noteworthy amount were shown to express α-actin, thus confirming that even after short-term contact, the metal is able to trigger the switch to a myofibroblast-like phenotype in macrophages. Only a reduced amount of adhering cells expressed the marker for endothelial progenitor cells (CD34). Furthermore, the amount of adhering CD34+ cells was variable among donors. No relevant differences were observed among the three different groups of donors (control, type 1 and type 2 diabetes) and a similar trend was observed in cells adhering on all the experimental surfaces, although artificial surfaces like TCP and St seemed to stimulate the expression of α–actin at a greater extent.

Results from flow cytometry showed a greater increase in the amount of activated macrophages among cells retrieved after overnight incubation on stainless steel in comparison to buffy coats. This confirmed the activation of monocyte into macrophages triggered by adhesion on stainless steel as determined using immunocytochemistry. In addition, flow cytometry results identified a population among the adhering cells co-expressing the marker for smooth muscle cells (α-actin) with CD68 (identifying activated macrophages) alone or in combination with CD45, general marker for leukocytes, thus confirming the presence of a sub-population possessing the potential to trans-differentiate into myofibroblasts. Flow cytometry also identified a sub-population of cells co-expressing the marker for endothelial progenitor cells (CD34) with the marker for monocytes (CD14) and the general marker for leukocytes (CD45) thus confirming the presence of progenitors deriving from monocytes and able to trans-differentiate into cells of the mesenchymal lineage and myofibroblasts as demonstrated in various studies (Kuwana 2003, Boilson 2008, Pilling 2009, Forte 2010).

The complex cascade of events characterizing the inflammatory reaction in the early phases of the foreign body reaction is driven by the release of pro- or anti-inflammatory cytokines that regulate cell responses (Luttikhuizen 2006). Macrophages in contact with metallic or ceramic particles were shown to release TNF-α, one of the main pro-inflammatory cytokines, as a consequence of their activation (Santin 2004). However, different studies have shown that TNF-α does not represent the predominant cytokine in the restenotic process (Santin 2005). Studies have in fact shown that restenosis is mainly characterized by the presence of TGF-β and PDGF-BB, cytokines promoting smooth muscle cell proliferation and extra-cellular matrix formation (Santin 2005). This study confirmed that overnight incubation on stainless steel triggered the release of PDGF-BB by macrophages. The effect of stainless steel was particularly evident in cells from control subjects where the release of the growth factor was significantly higher compared to both tissue culture plastic and extra-cellular matrix. Increase in the

release of PDGF-BB after contact with stainless steel was also seen in donors with type 1 and type 2 diabetes. Results showed that even after overnight incubation in physiological glucose concentrations stainless steel promotes the post-inflammatory status in macrophages. Although a similar trend was observed in all the groups, it seemed emphasised in healthy donors, thus suggesting that donors with diabetes might be characterized by higher basic level of activation partially masking the effect of the metal.

Macrophages from all the groups of donors released higher amounts of TNF-α after incubation on stainless steel thus indicating the activation of the inflammatory response from the cells. The stainless steel stimulated release of TNF-α was in fact significantly higher when compared to the release from cells in contact with extra-cellular matrix ($p<0.005$) representing the physiological substrate. Higher release of TNF-α was observed also in comparison to cells incubated on tissue culture plastic with the trend being significantly different only in control subjects and in donors with type 2 diabetes. The reason for that can be in part due to the reaction to the tissue culture plastic that, representing an artificial surface, can trigger partial activation of macrophages. In addition, donors with type 1 diabetes showed a higher basic level of activation demonstrated by the significant difference in the release of TNF-α from cells from donors with type 1 diabetes when compared to the release from cells from donors with type 2 diabetes incubated on extra-cellular matrix. These data seem to contradict those previously found by Harrison et al. (2007) who suggested a propensity of the cells adhering on stainless steel to acquire a post-inflammatory phenotype secreting growth factors rather than pro-inflammatory cytokines. Differences in experimental conditions and more sensitive ELISA kits may explain this inconsistency.

In conclusion this experiment suggests that, following implantation, macrophages migrate towards the stent struts and activate to sustain the acute inflammatory

response to the foreign body. Contemporary to the activation, macrophages start to switch to their wound healing, or post-inflammatory, status producing PDGF-BB, stimulating the proliferation of smooth muscle cells. The release of cytokines was higher in patients with diabetes, thus partially masking the effect of the metal and suggesting an increased basic level of activation of inflammatory cells that could represent a further element relevant for the development of in-stent restenosis. Sub-populations derived from monocytes and macrophages potentially acting as precursors of myofibroblasts were also identified among cells adhering on surfaces. Results suggest that, after implantation, stainless steel triggers the activation of an inflammatory response from macrophages that soon switches to their post-inflammatory phenotype characterized by formation of myofibroblasts and synthesis of growth factors such as PGDF-BB driving the smooth muscle cell proliferation and potentially the formation of a restenotic plaque. The different level of activation found in some of the diabetic donors in combination with a more advanced analysis of cell sub-populations could provide a better understanding of the conditions triggering the neointimal formation in restenosis.

7.3.3 Effect of high glucose and high lipids and their synergy on the reaction of macrophages to stainless steel

The direct correlation between obesity, inflammation and insulin resistance has been shown in different studies. In particular, the recruitment of macrophages in the white adipose tissue was shown to be mediated by the release of free fatty acids by the same tissue and by the release of TNF-α by macrophages with the consequent activation of inflammatory process (Rustan 2005, Suganami 2005).

More studies have shown the increase in the release of TNF-α by macrophages in culture under the influence of free fatty acids via activation of Toll-like receptor, particularly TLR-2 and TLR-4. In particular, it was shown that saturated fatty acids, but not unsaturated, were able to trigger the release of pro-inflammatory

cytokines from macrophages through the action of ceramide, a product of their metabolism (Rustan 2005, Curtiss & Tobias 2008, Haversen 2009, Dasu 2011).

For the aim of this study an experimental model re-creating hyperlipidaemia and hyperglycaemia was created in order to eliminate the variability related to the complex scenarios characterizing the diabetic population including influences on the reaction of inflammatory cells due to therapeutic regimens and to evaluate solely the effect of the environment. Results from immunocytochemistry confirmed the activation of macrophages once in contact with stainless steel, as represented by the expression of the marker for monocytes (CD14) and for activated macrophages (CD68) from the adhering cells. Although in variable amount depending on the donor and area observed, cells expressing the marker for endothelial progenitor cells (CD34) were found. Interestingly, the double staining showed that cells were co-expressing CD34 and CD68, thus confirming the presence of a sub-population able to differentiate into myofibroblasts (Mesure 2010) as discussed above. No significant differences in the marker expression were identified from the images. Cells expressing α-actin, identifying smooth muscle cell-like phenotype were found across surfaces and culture conditions. Interestingly, the double staining also allowed the identification of cells co-expressing the marker for monocytes (CD14) and α-actin, thus confirming the presence among mononuclear cells of a sub-population expressing the phenotype of smooth muscle cells as previously found through the characterization of cells with flow cytometry. Those findings confirmed the heterogeneity of phenotype expressed by mononuclear cells adhering on surfaces. The expression of the markers was similar across all the surfaces and under all experimental conditions.

The effect of the concomitance of high lipid and glucose concentrations on macrophages was more evident when observing the images obtained from scanning electron microscopy after overnight incubation. Cells on tissue culture plastic and extracellular matrix-coated wells appeared isolated and completely spread onto the surfaces, a sign of good adherence on the surfaces without

activation of the phagocytic process (Guildford 2009). Results did not show any difference between macrophages incubated in normal or high glucose concentration media, thus indicating that high glucose did not modify the acute response of macrophages in terms of changes in morphology. Macrophages incubated on stainless steel showed a morphology characterizing the initial phases of attempted phagocytosis with the formation of giant cells through cell-cell interactions and rough surface, although the roughness of the metal surface might partially affect the interpretation of morphological variations when compared to smoother surfaces. Similar behaviour was observed in cells incubated in both normal and high glucose medium. The effect of palmitate on macrophages incubated on all type of experimental surfaces, both in normal and high glucose concentration, resulted in the expression of the morphology typical of activation of the phagocytic process (Guildford 2009) characterized by the formation of giant cells through cell-cell interactions and rough surface presenting blebs. The process seemed accentuated by the concomitance of high glucose concentration medium and palmitate suggesting their synergic effect on the response of macrophages to stainless steel. High concentration of free fatty acid seem to trigger the activation of inflammatory cells suggesting that lipid level may be critical in the acute setting for the development of restenosis.

The overall results obtained from the measurement of PDGF-BB in supernatants suggested that stainless steel triggered the release of the growth factor even after overnight incubation. The effect of the surface seemed to be predominantcompared to the effect of the different conditions.

The measurement of the release of TNF-α showed that the contact of macrophages with tissue culture plastic and stainless steel triggered the release of the pro-inflammatory cytokine in comparison to cells on extracellular matrix-coated wells with the exception of samples in medium with high glucose concentration and palmitate. The pro-inflammatory effect was emphasized in cells in contact with the metal, thus confirming the activation of inflammatory process

induced by the contact with stainless steel. The comparison of the culture conditions showed that glucose concentration did not affect the release of TNF-α from macrophages. The addition of palmitate reduced the release of the pro-inflammatory cytokine from macrophages on all the experimental surfaces. In particular, the reduction was emphasized when cells were incubated in high glucose in the presence of the fatty acid. This suggested that the combination of high glucose and palmitate affected the response of macrophages. Under this condition no significant differences were seen between the surfaces, thus suggesting that the environmental effect masked the effect of the surface.

The results obtained from the measurement of the release of TNF-α and PDGF-BB, therefore, suggested that after overnight incubation the contact with stainless steel triggered the release of TNF-α and PDGF-BB the switch of macrophages to their post-inflammatory status following the initial pro-inflammatory metal-induced activation. The concomitant increase of the cytokine and growth factors suggesting the concomitance of a pro- and post-inflammatory status of macrophages might seem contradictory, in particular when compared to data published in previous studies (Harrison 2007). However, this can be related to the choice of different experimental conditions that provided evidence of transition from an early pro-inflammatory status to a post-inflammatory one. The presence of high glucose did not have any effect on the release of the cytokines. However, the addition of palmitate, particularly in concomitance with high glucose concentration seemed to mask the effect of the surfaces and modify the response of macrophages reducing the release of TNF-α and suggesting that the presence of glucose and fatty acid impacted on macrophages accelerating the shift to a post-inflammatory status identified by the release of PDGF-BB. This would therefore represent an important point in the development of restenosis. Studies have shown that the control of diabetes and blood glucose level at the moment of intervention may influence the outcome of the procedure (Khosravi 2011, Nusca 2011). Results obtained from this study highlighted the impact of the concomitant

presence of high glucose and lipid concentration suggesting their ability to activate the macrophages and triggered the switch to post-inflammatory phenotype thus possibly promoting the neointimal formation.

The analysis of the expression of genes for the synthesis of hyaluronan, the main component of the neointimal tissue, provided further confirmation on the activation induced by concomitant presence of high glucose and high lipid in the environment. Results showed that, after overnight incubation, macrophages did not express HAS1 or HAS2 when incubated on either stainless steel or extracellular matrix-coated wells under any experimental conditions. However, results showed that incubation overnight on stainless steel induced the upregulation of the mRNA codifying for HAS3, particularly in the presence of high glucose alone or in combination with sodium palmitate. No relevant expression of HAS3 was seen in macrophages incubated on extracellular matrix-coated well. HAS3 is the isoform responsible for the synthesis of low molecular weight hyaluronan that has been associated with the inflammatory reaction. Short fragments of hyaluronan favour the migration and activation of inflammatory cells in order to activate the wound healing process as well as favouring the cell growth in certain forms of cancer (Liu 2001). In addition, studies have also demonstrated accumulation of hyaluronan triggered by the presence of pro-inflammatory cytokines, whose release from inflammatory cells is in turn triggered by the presence of hyaluronan (Itano 1999, Kennedy 2000, Vigetti 2010).

Therefore, findings from this study confirmed that the synergistic effect of high concentrations of lipid and glucose emphasizes the reaction of macrophages to the contact with stainless steel as demonstrated by SEM images and by the upegulation of the expression of the gene for HAS3. The overnight incubation of macrophages on stainless steel triggered phenotypical changes towards the acquisition of post-inflammatory status confirming the effect of the metal as discussed in Section 7.3.2. Following the trans-differentiation into myofibroblasts, macrophages were shown to secrete different isoforms of the enzyme responsible

for the synthesis of the polysaccharide depending on the exposure time to stainless steel. Longer incubation time seemed to induce the complete acquisition of myofibroblast-like morphology accompanied by the expression of HAS1, responsible for the synthesis of high molecular weight hyaluronan, thus potentially participating in the formation of the restenotic neointimal tissue (Stewart 2009). Even after short incubation time, as utilised in this study, the metal-induced phenotypical switch to post-inflammatory status on macrophages was demonstrated. However the combination of hyperglycaemic and hyperlipidaemic conditions seems to generate a synergistic effect triggering the activation of the response from macrophages in the early stages of incubation on stainless steel. This suggests that the control of blood glucose and lipid levels at the moment of stent implantation have an impact on the activation of macrophages, thus possibly influencing the deposition of the restenotic plaque and consequently the outcome of the procedure. This could indicate that the clinical fate of bare metal stents may depend on the control of these biochemical parameters in patients prior and at the time of implantation. In the case of subjects where both hyperglycaemia and hyperlipidaemia are poorly controlled the risk of ISR development might well be increased.

7.4 CONCLUSIONS AND FUTURE DIRECTIONS

This study confirmed the contribution of macrophages to the development of ISR through their ability to acquire a post-inflammatory phenotype prone to the synthesis of potent stimulators of myofibroblast proliferation (i.e. PDGF-BB) and through their potential to trans-differentiate into myofibroblasts thus directly contributing to the formation of the neointimal tissue occluding the vessel. Smooth muscle cells and myofibroblasts are in fact the major cell types populating the neointimal tissue in restenotic stents. Following contact with stainless steel, macrophages quickly switch their phenotype from pro-inflammatory to post-inflammatory. PDGF-BB and high molecular weight hyaluronic acid will determine an anti-inflammatory and proliferative environment likely to contribute to the building up of excessive neointimal tissue. The macrophages hosted in such environment and in contact with the metal strut undergo trans-differentiation into spindle-like shaped cells expressing markers typical of smooth muscle cells and fibroblasts. This study suggests that different factors can influence the activation of macrophages, thus justifying the increase in the rate of the occurrence of the complication in subjects with diabetes. The analysis of blood biochemical values and of the presence of risk factors can provide an indication of general health conditions of diabetic patients thus identifying subjects at risk of developing ISR. However, findings from this study seem to suggest that independent factors can contribute to provide a better indication of the probability of developing restenosis at the moment of intervention. Indeed, the analysis of cell sub-populations, with particular attention to the sub-populations expressing the marker for activated macrophages (CD68), could represent a key factor in the identification of basic level of inflammation and tendency to develop in-stent restenosis.

As suggested by previous studies (Khosravi 2011, Nusca 2012), blood glucose and lipid levels at the moment of intervention can play an essential role in the development of restenosis dramatically affecting the outcome of the procedure. This study confirmed that the concomitant presence of high concentrations of free fatty acid and glucose in the environment generates a synergistic effect triggering the activation of macrophages thus enhancing the response to stainless steel. This could therefore accelerate the trans-differentiation into myofibroblasts possibly initiating the deposition of the restenotic plaque.

7.5.1 Future directions

On the basis of the findings from this and previous studies, further contribution in the understanding of the factors influencing the increased rate of ISR in diabetic patients and on the role of macrophages in the development of the neointimal tissue could derive from the extension of experiments of population distribution to a greater number of individuals. A wider characterization of sub-populations and their comparison to biochemical values indicators of the general health condition could in fact identify significant trends linking diabetic condition, biochemical values and circulating sub-populations thus providing further elements for the evaluation of the predisposition of developing ISR.

A better understanding of the role of trans-differentiation of macrophages and their link to diabetic condition in the development of *in-stent* restenosis would derived by an extended characterization of the cells after contact with stainless steel, particularly focusing on the sub-populations acting as precursors of myofibroblasts. The thorough analysis of marker expression, cytokine release and phenotypical changes under different cultural conditions and at different incubation times would provide more details on the elements affecting the trans-differentiation of macrophages and their reaction to stainless steel. In addition, similar characterization applied to a broader and selected diabetic population may

provide more specific links elucidating on the effect of the pathology on the behaviour of macrophages in relation to their reaction to the metal.

In addition, results suggested that the amount of circulating macrophages and the glucose and lipid blood levels at the moment of intervention can represent independent critical factors influencing the outcome of the procedure. Therefore, the monitoring of those values in patients undergoing stent implantation in association with a follow-up monitoring of the outcome of the procedure in the same patients during the year following intervention could provide an overall understanding of the links between the different variables. The combination of biomolecular investigations with the clinical monitoring before and after stent implantation in a large group of patients could provide with the answers for an overall understanding of the key factors to be investigated in order to prevent the occurrence of the *in-stent* restenosis and assist in the selection of the stent to be implanted.

APPENDIX 1

University of Brighton

Royal Sussex County Hospital and University of Brighton
School of Pharmacy and Biomedical Sciences

DIABETES AND BIOMATERIALS

Participant Information Sheet

(Diabetic patients)

Version 3.2, May 2007

Study title

Activation of monocytes in diabetes

Invitation

You are being invited to take part in a research study which is part of a PhD project. Before you decide it is important for you to understand why the research is being done and what it will involve. Please take time to read the following information carefully and discuss it with others if you wish. Ask us if there is anything that is not clear or if you would like more information. Take time to decide whether or not you wish to take part. If you decide to take part in this study we would ask you to please sign the accompanying consent form.

Thank you for reading this.

Background

As adults age, the wall of the blood vessels (e.g. arteries) tends to harden. This process is called atherosclerosis and it is caused by deposits of fatty substances such as cholesterol within the blood vessels. This build up is called plaque. Plaques can grow large enough to significantly reduce the blood's flow through an artery. Most of the damage occurs when plaques become fragile and rupture, possibly causing a stroke or heart attack.

Many medical treatments are available which aim to prevent the deposit of fat in blood vessels. However, when the build up is too big, surgical procedures may be required. One of the surgical procedures is called angioplasty in which an expandable balloon is inserted into the blocked artery in order to re-open it. Often, better results can be obtained inserting a metal stent, which is a tubular metallic mesh used to maintain the shape of the vessel wall.

The use of stents has significantly increased the rate of success in angioplasty. However, because stents are made of metal, the body sometimes "rejects" this foreign object leading to re-blockage of the vessel. Unfortunately, research to date has suggested that this happens much more frequently among patients with diabetes. The reasons for this are not currently understood which is why we are undertaking this research project.

In this project we will study how a high amount of sugar in the blood (characteristic of diabetes) can play a role in the rejection process induced by the stent materials. This may help us to understand why the use of stents in diabetic patients is more problematic. This study can also be extended to obtain more information about the general state of inflammation characteristic of diabetes.

Location of the study

Blood will be taken at the Royal Sussex County Hospital and the experimental work with cells and the stent material will be carried out in fully equipped laboratories at the University of Brighton.

Why have I been chosen?
You have been chosen to take part in this study as you have diabetes.
We need the help from people with diabetes to determine the effect of blood sugar levels and diabetes on the reaction against stent materials.

Do I have to take part?
It is up to you to decide whether or not to take part. If you do decide to take part you will be given this information sheet to keep and be asked to sign a consent form. If you decide to take part you are still free to withdraw at any time and without giving a reason. A decision to withdraw at any time, or a decision not to take part, will not affect the standard of care you receive.

What will happen to me if I take part?
You will be asked to give a little extra blood. This will only be a small amount (20 ml) in addition to the usual blood sample (around 30 ml) taken when you attend the clinics. You will not feel any difference from your usual visit. If you have to make an extra trip for the collection of blood you will be reimbursed for your travelling expenses. A researcher will take some details concerning your age, diabetes treatment, medication and a history of your health. You will remain anonymous and we only need these details to help us interpreting the data we obtain from your blood. Besides the blood sample and the questionnaire, no further commitment is required from you and all this process will take maximum 10 minutes to be completed.

What will happen to my blood sample?
The amount blood which is destined to our study (20 ml) will be immediately processed inside laboratories of the University of Brighton to obtain the inflammatory cells which are relevant to the study. We will compare the cells from people with and without diabetes to understand their behaviour when in contact with the materials used to produce stents or other medical devices.

Subject Privacy

All data collected will be locked in filing cabinets and kept on password-protected computers. No personal information will be disclosed to the investigators. Information taken will be anonymous because every sample and the relative set of

data will be identified by the clinicians through a code. Only the clinicians at the Royal Sussex County Hospital will be able to access the database and to refer your name to the data collected. If at any stage of the study some information relevant to your health is found, it will be referred them to the clinicians of the Hospital who will, in turn, inform you through your GP. You will remain anonymous in any presentation of data and publications of findings.

Complaints

If you have a concern about any aspect of this study, you should ask to speak to the researchers who will do their best to answer your questions (Mr. Tiziano Poletti Tel N xxx). If you remain unhappy and wish to complain formally, you can contact xxx, Research and Development Manager, Royal Sussex County Hospital.

University of Brighton

Royal Sussex County Hospital and University of Brighton
School of Pharmacy and Biomedical Sciences

DIABETES AND BIOMATERIALS

Participant Information Sheet

(Control subjects)

Version 3.2, May 2007

Study title

Activation of monocytes in diabetes

Invitation

You are being invited to take part in a research study which is part of a PhD project. Before you decide it is important for you to understand why the research is being done and what it will involve. Please take time to read the following information carefully and discuss it with others if you wish. Ask us if there is anything that is not clear or if you would like more information. Take time to decide whether or not you wish to take part. If you decide to take part in this study we would ask you to please sign the accompanying consent form.

Thank you for reading this.

Background

As adults age, the wall of the blood vessels (e.g. arteries) tends to harden. This process is called atherosclerosis and it is caused by deposits of fatty substances such as cholesterol within the blood vessels. This build up is called plaque. Plaques can grow large enough to significantly reduce the blood's flow through an artery. Most of the damage occurs when plaques become fragile and rupture, possibly causing a stroke or heart attack.

Many medical treatments are available which aim to prevent the deposit of fat in blood vessels. However, when the build up is too big, surgical procedures may be required. One of the surgical procedures is called angioplasty in which an expandable balloon is inserted into the blocked artery in order to re-open it. Often, better results can be obtained inserting a metal stent, which is a tubular metallic mesh used to maintain the shape of the vessel wall.

The use of stents has significantly increased the rate of success in angioplasty. However, because stents are made of metal, the body sometimes "rejects" this foreign object leading to re-blockage of the vessel. Unfortunately, research to date has suggested that this happens much more frequently among patients with diabetes. The reasons for this are not currently understood which is why we are undertaking this research project.

In this project we will study how a high amount of sugar in the blood (characteristic of diabetes) can play a role in the rejection process induced by the stent materials. This may help us to understand why the use of stents in diabetic patients is more problematic. This study can also be extended to obtain more information about the general state of inflammation characteristic of diabetes.

Location of the study

Blood will be taken at the Royal Sussex County Hospital and the experimental work with cells and the stent material will be carried out in fully equipped laboratories at the University of Brighton.

Why have I been chosen?

You have been chosen to take part in this study because we need to compare the results from people with diabetes with data obtained from people without the condition. This is necessary to understand if the amount of sugar in the blood can influence the reaction against the stent materials.

Do I have to take part?

It is up to you to decide whether or not to take part. If you do decide to take part you will be given this information sheet to keep and be asked to sign a consent form. If you decide to take part you are still free to withdraw at any time and without giving a reason.

What will happen to me if I take part?

You will be asked to give an amount of blood (50 ml). If you have to make an extra trip for the collection of blood you will be reimbursed for your travelling expenses. A researcher will take some details concerning your age, medication and a history of your health. You will remain anonymous and we only need these details to help us interpreting the data we obtain from your blood. Besides the blood sample and the questionnaire, no further commitment is required from you. The entire process will take a maximum 10 minutes.

What will happen to my blood sample?

Part of the blood sample (20 ml) will be immediately processed inside the laboratories of the University of Brighton to obtain the inflammatory cells which are relevant to the study. We will compare the cells from people with and without diabetes to understand their behaviour when in contact with the materials used to produce stents or other medical devices.

The remaining amount of blood (30 ml) will be tested at the Hospital in order to collect clinical data relevant to our study. Among them blood cholesterol (fat blood levels) and lipids (fat) levels, blood glucose levels (sugar blood levels), CRP (C-Reactive Protein: indicator of inflammatory diseases or infection), U&E (Urea and Electrolytes: indicators of kidney function), fibrinogen (indicator of blood clot system relevant in cardiovascular diseases and inflammation), ESR (Erythrocyte Sedimentation Rate: indicator of inflammatory condition), homocysteine (indicator of cardiovascular heart disease risk).

Subject Privacy

All data collected will be locked in filing cabinets and kept on password-protected computers. No personal information will be disclosed to the investigators. Information taken will be anonymous because every sample and the relative set of data will be identified by the clinicians through a code. Only the clinicians at the Royal Sussex County Hospital will be able to access the database and to refer your name to the data collected. If at any stage of the study some information relevant to your health is found, it will be referred to the clinicians at the Hospital who will, in turn, inform you through your GP. You will remain anonymous in any presentation of data and publications of findings.

Complaints

If you have a concern about any aspect of this study, you should ask to speak to the researchers who will do their best to answer your questions (Mr. Tiziano Poletti Tel N xxx). If you remain unhappy and wish to complain formally, you can contact xxx, Research and Development Manager, Royal Sussex County Hospital.

University of Brighton

CONSENT FORM

Title of Project: **Diabetes and biomaterials. Activation of monocytes in diabetes.**

Please initial box

1. I confirm that I have read and understand the information sheet dated May 2007 ☐
2. I understand that my participation is voluntary and that I am free to withdraw at any time, ☐
3. I understand that sections of any of my medical notes may be looked at by responsible individuals from The Royal Sussex Hospital or from regulatory authorities where it is relevant to my taking part in research. I give permission for these individuals to have access to my records. ☐
4. I agree to donate my blood to be collected, processed and stored as appropriate. ☐
5. I authorise the responsible individuals from the Royal Sussex County Hospital to contact my GP if information relevant to my health emerges from the study. ☐
6. I agree to take part in the above study. ☐

Name of Patient	Date	Signature
Name of Person taking consent (if different from researcher)	Date	Signature
Researcher	Date	Signature

1 for patient; 1 for researcher; 1 to be kept with hospital notes

Version 3.2,May 2007

School of Pharmacy and Biomedical Sciences

Inflammatory response to biomaterials study

Participant Information Sheet

Study title:
In vitro assessment of the effect of artificial surfaces and increased glucose and lipid concentrations on the inflammatory reaction in freshly isolated human monocyte- derived macrophages

Invitation

You are being invited to take part in a research study. Before you decide it is important for you to understand why the research is being done and what it will involve. Please take time to read the following information carefully and discuss it with others if you wish. Ask us if there is anything that is not clear or if you would like more information. Take time to decide whether or not you wish to take part.

Thank you for reading this.

Background

As adults age, some hardening of the arteries occurs. This process is called atherosclerosis. The hardening of the arteries is caused by deposits of fatty substances such as cholesterol. This build up is called plaque. Plaques can grow large enough to significantly reduce the blood's flow through an artery. Most of the damage occurs when they become fragile and rupture. Plaques that rupture can cause a stroke or heart attack.

Many medical treatments are available which aim to prevent the build up of plaques. However, if significant amounts of plaque have accumulated,

surgical procedures may be required. One of the surgical procedures is called angioplasty in which an expandable balloon is inserted into the blocked artery in order to remove the plaque and reinforce the blood vessel wall. Often, the effect of this procedure is maximised by the deployment of a metal stent, which is used to maintain the shape of the vessel wall.

The use of stents has significantly increased the rate of success in angioplasty. However, because stents are made of metal, the body sometimes "rejects" this foreign object and can lead to re-blockage of the vessel. Unfortunately, research to date has suggested that the incidence of re-blockage is much more frequent among patients with diabetes. The reasons for this are not currently understood which is why we are undertaking this research project.

In this project we will study the role of blood sugar and lipid levels on the rejection process when in contact with materials used to produce biomedical devices. We are trying to understand why diabetic patients experience more rapid re-blockage after stents implantation than non-diabetic patients, extending this study to a more general evaluation of the basic inflammatory condition observed in this disease.

Location of the study
Blood samples will be obtained and the experimental work with cells and the material will be carried out in fully equipped laboratories at the University of Brighton

Why have I been chosen?
You have been chosen to take part in this study because you fall within the desired demographic. There is no gender exclusion in this study and the age of invited participants ranges between 20 and 65 years of age.
We exclude from this stage of the study people with diagnosed diabetes, people with cancer or conditions affecting the immune system and any individuals undergoing infections or any condition affecting their inflammatory response.
If you are willing to take part to this study please inform the recruiter in case of any doubt.

Do I have to take part?
It is up to you to decide whether or not to take part. If you do decide to take part you will be given this information sheet to keep and be asked to sign a consent form. If you decide to take part you are still free to withdraw at any time and without giving a reason. Unfortunately there is no funding available for the payment of volunteers with the exception of travel expenses if applicable.

What will happen to me if I take part?
You will be asked to sit and a qualified phlebotomist will withdraw 30ml-40ml of blood using a sterile needle and syringe, or Vacuette system. You may experience slight discomfort during this stage, but this is temporary and lasts only as long as the procedure itself (no more than one minute).
Before the blood taking procedure you may be asked to answer basic questions about yourself and your general health and lifestyle habits (age, height, weight, smoking habits, cardiovascular disease familiarity, blood pressure).

Are there any risks?
The risks you face are minimal. You may experience bruising at the injury site, this is minimised by applying firm pressure immediately after removal of the needle.
The phlebotomist will ensure that the wound has stopped bleeding before covering the site with a plaster. To avoid allergic reaction to the plaster used to protect the injection site after the procedure please inform the phlebotomist or the research in case you previously experienced adverse reactions to plasters. To minimize the risk plaster for sensitive skins will be used.
They will then ensure you are in sufficient good health to leave. The whole procedure should take no longer than 10 minutes.

What will happen to my blood sample?
The blood will be used to isolate cells which are thought to be important in inflammation. We will compare the responses of cells from donor to donor when exposed to the materials highlighted above.
As part of the research study it might be necessary to extract RNA (genetic material) from the cells to examine the expression of proteins relevant to inflammatory process after cardiovascular stents implantation.

Subject Privacy

The samples collected will be anonymised and identified by a code throughout the experimental work, the data collection, elaboration and presentation.
The traceability of the sample will be ensured as requested under the Human Tissue Act and only the authorized DI (Dr xxx) will have access to the database.

In case you are interested and willing to participate please refer to the following contact details and we will book an appointment according to your availability to discuss this further and to obtain written consent, if granted.

For experimental reasons blood will normally be taken from Monday to Thursday between 9.00 and 12.00.
There won't be the need for you to be fasting before the blood taking.

UNIVERSITY OF BRIGHTON

Participant Consent Form

Approval for volunteer blood procurement and donation for research purposes

- I volunteer to the procurement and donation of …….mls of my blood for the use in scientific research.
- The researcher has explained to my satisfaction the process of blood procurement and the possible risks involved.
- I have had the principles and the procedure explained to me and I have also read the Procedure Information sheet. I understand the principles and procedures fully.
- I understand that blood will be used to extract inflammatory cells in order to investigate their reaction to different materials and conditions. I understand that as part of the research process cells might be processed to extract nucleic acid (genetic material) to evaluate protein expression in the same cells.
- I understand that any confidential information will be logged onto a secure, restricted database and an anonymising code will be issued to identify the sample throughout all the stages of the experimental work and data publication. Personal data will not be available to the experimenter.
- I understand that I am free to withdraw from the voluntary donation at any time.

Name (please print) .....

Signed .....

Date .....

Witnessed (please print name)
.....

Signature of witness .....

Date .....

UNIVERSITY OF BRIGHTON

Standard Operating Procedure for Volunteer blood procurement and use in scientific research.

Information for all experimenters on blood donation procedure.

1. Approach and gain consent of the individual blood donor. The approach of volunteers was done by sending an email to the general mail box of the University of Brighton (as per wording submitted within the RECs application form) and consent form will be signed by the donor after reading the relevant information leaflet
2. Experimenter and volunteer donor agree to volume of blood to be donated. Donors will be asked to donate between 30 and 40 ml of blood once only during the study
3. Contact the qualified phlebotomist to arrange an appointment. Trained phlebotomists within PABS department to be contacted via email are the following:

    xxx
    xxx
    xxx

4. Contact xxx to book the room.
5. Inform volunteer donor of appointment time and location. (Reception Hall-Huxley Building)
6. Prior to appointment provide volunteer donor with a copy of the Participant Consent Form and Procedure Information sheet. Ensure that the volunteer understands the blood procurement procedure before signing Participant Consent Form.
7. Accompany volunteer donor to appointment, and stay for procedure to ensure that in the case of any difficulties a first aid can be contacted following the usual university procedure.
8. Ensure the volunteer's Participant Consent form is placed into the folder in the phlebotomy trolley in the Clinical skills lab.
9. Log the sample onto the Human Tissue Tracking database and all details as required.

Sample will be issued with an anonymising code that must be the only identifier from that point onwards.

10. Remain with volunteer during blood procurement.
11. Ensure that the patient is not allergic to plaster and inform them of the use of the plaster to stop the bleeding after the procedure.
12. Phlebotomist will either use syringe/needle or the Vacuette system to procure blood from the volunteer.

13. Treat all blood samples as potentially hazardous, the phlebotomist must wear gloves to carry out the procurement, and dispose of needles/sharps in the disposal bin provided on the phlebotomy trolley.
14. Place blood sample collection bottle containing blood, in an air-tight container for transport to the room H416 equipped with a Category II laminar flow hood.
15. Escort volunteer donor from treatment room to place of work.
16. Ensure that blood donor details are not recorded with respect to experimental results but referred to with the anonymising code at any stage of the experimental work or data elaboration and presentation.
17. Treat all blood samples as potentially hazardous, the experimenter must wear gloves and lab coat and carry out all procedures in the Category II laminar flow hood in the clean room (H416) or, in alternative in the primary cell culture room (C251).
18. Any unused blood sample or by-products will be disposed of immediately after the conclusion of the experimental work, following the standard disposal procedure for clinical/biohazard waste. After use or discard of the remaining blood, samples will have to be logged as “use at exhaustion” or discarded in the HTA Licence database referring to the samples coding.
19. If blood/blood products are intended for storage and not immediate use, additional ethical approval will need to be gained, as this will not be covered by the blood procurement ethics approval. Storage procedure is covered by the HTA-licence Number 12583 and refer to specific SOP in case of need.

APPENDIX 2

DATA FROM THE BRADFORD TEST RELATED TO RESULTS PUBLISHED IN CHAPTER 4

Raw data (O.D. 595nm)											
Controls				**Type 1 Diabetes**				**Type 2 Diabetes**			
Donor	**TCP**	**ST**	**ECM**	**Donor**	**TCP**	**ST**	**ECM**	**Donor**	**TCP**	**ST**	**ECM**
C1	1.5535	1.569	1.6545	**T1D6**	1.512	1.411	1.59	**T2D1**	1.4185	1.536167	1.6195
C6	1.482	1.5525	1.5605	**T1D7**	1.5645	1.4765	1.695	**T2D2**	1.46	1.594	1.6035
C7	1.542	1.4445	1.5755	**T1D8**	1.497	1.765	1.547	**T2D4**	1.553	1.5445	1.575
C8	1.5955	1.4595	1.6025	**T1D9**	1.5455	1.5885	1.565	**T2D7**	1.5705	1.524	1.5485
C9	1.6495	1.568	1.519	**T1D10**	1.5765	1.522	1.5555	**T2D8**	1.5975	1.6075	1.456
C10	1.5855	1.5495	1.51	**T1D11**	1.553	1.4995	1.6155	**T2D9**	1.765	1.596	1.5245
C11	1.492	1.4915	1.5845	**T1D12**	1.452	1.698	1.5255	**T2D10**	1.5545	1.49	1.6625
C12	1.582	1.55	1.629	**T1D13**	1.3835	1.576	1.578	**T2D11**	1.5735	1.556	1.628
C13	1.5655	1.6015	1.391	**T1D14**	1.5205	1.5215	1.592	**T2D12**	1.447	1.619	1.5945
C14	1.5205	1.6965	1.4995	**T1D15**	1.5905	1.5525	1.5775	**T2D13**	1.471	1.578	1.568

Total proteins in samples (µg/ml)											
Controls				**Type 1 Diabetes**				**Type 2 Diabetes**			
Donor	**TCP**	**ST**	**ECM**	**Donor**	**TCP**	**ST**	**ECM**	**Donor**	**TCP**	**ST**	**ECM**
C1	1210.8	1226.3	1311.8	**T1D6**	1169.3	1068.3	1247.3	**T2D1**	1075.8	1193.467	1276.8
C6	1139.3	1209.8	1217.8	**T1D7**	1221.8	1133.8	1352.3	**T2D2**	1117.3	1251.3	1260.8
C7	1199.3	1101.8	1232.8	**T1D8**	1154.3	1422.3	1204.3	**T2D4**	1210.3	1201.8	1232.3
C8	1252.8	1116.8	1259.8	**T1D9**	1202.8	1245.8	1222.3	**T2D7**	1227.8	1181.3	1205.8
C9	1306.8	1225.3	1176.3	**T1D10**	1233.8	1179.3	1212.8	**T2D8**	1254.8	1264.8	1113.3
C10	1242.8	1206.8	1167.3	**T1D11**	1210.3	1156.8	1272.8	**T2D9**	1422.3	1253.3	1181.8
C11	1149.3	1148.8	1241.8	**T1D12**	1109.3	1355.3	1182.8	**T2D10**	1211.8	1147.3	1319.8
C12	1239.3	1207.3	1286.3	**T1D13**	1040.8	1233.3	1235.3	**T2D11**	1230.8	1213.3	1285.3
C13	1222.8	1258.8	1048.3	**T1D14**	1177.8	1178.8	1249.3	**T2D12**	1104.3	1276.3	1251.8
C14	1177.8	1353.8	1156.8	**T1D15**	1247.8	1209.8	1234.8	**T2D13**	1128.3	1235.3	1225.3

TNF-α ELISA DATA FOR RESULTS DISCUSSED IN CHAPTER 4

RAW DATA (O.D. 450nm)											
Controls				**Type 1 Diabetes**				**Type 2 Diabetes**			
Donor	**TCP**	**ST**	**ECM**	**Donor**	**TCP**	**ST**	**ECM**	**Donor**	**TCP**	**ST**	**ECM**
C1	0.1975	0.58175	0.84275	**T1D6**	0.266	1.7625	1.186	**T2D1**	0.189	1.4045	0.428
C6	1.886	1.897	1.486	**T1D7**	1.1025	2.085	1.763	**T2D2**	0.1375	1.8905	0.1235
C7	1	1.5125	1.2035	**T1D8**	1.173	1.301	1.033	**T2D4**	0.1535	1.546	0.1385
C8	0.368	0.874	0.845	**T1D9**	1.9675	2.1295	1.24	**T2D7**	0.2305	1.824	0.1635
C9	0.925	1.6505	1.076	**T1D10**	0.759	0.822	0.5605	**T2D8**	1.4525	1.066	1.1735
C10	1.052	1.208	0.949	**T1D11**	1.5465	1.614	1.215	**T2D9**	1.9395	1.901	1.1385
C11	1.312	1.571	0.945	**T1D12**	1.4	1.655	1.0175	**T2D10**	1.718	1.4945	1.3495
C12	1.782	1.692	1.14	**T1D13**	1.0455	1.4775	1.375	**T2D11**	1.327	1.776	0.55
C13	1.766	1.608	1.1955	**T1D14**	1.258	1.1995	1.1245	**T2D12**	0.634	1.03	1.1045
C14	0.4625	0.492	0.265	**T1D15**	1.5535	1.474	1.397	**T2D13**	1.1565	1.3845	0.224

TNF-α (pg/ml) in original samples (before dilution 1:4)											
Controls				**Type 1 Diabetes**				**Type 2 Diabetes**			
Donor	**TCP**	**ST**	**ECM**	**Donor**	**TCP**	**ST**	**ECM**	**Donor**	**TCP**	**ST**	**ECM**
C1	26.62595	143.9542	223.6489	**T1D6**	47.54198	504.4885	328.458	**T2D1**	24.03053	395.1756	97.00763
C6	542.1985	545.5573	420.0611	**T1D7**	302.9618	602.9618	504.6412	**T2D2**	8.305344	543.5725	4.030534
C7	271.6641	428.1527	333.8015	**T1D8**	324.4885	363.5725	281.7405	**T2D4**	13.19084	438.3817	8.610687
C8	78.68702	233.1908	224.3359	**T1D9**	567.084	616.5496	344.9466	**T2D7**	36.70229	523.2672	16.24427
C9	248.7634	470.2901	294.8702	**T1D10**	198.0763	217.313	137.4656	**T2D8**	409.8321	291.8168	324.6412
C10	287.542	335.1756	256.0916	**T1D11**	438.5344	459.145	337.313	**T2D9**	558.5344	546.7786	313.9542
C11	366.9313	446.0153	254.8702	**T1D12**	393.8015	471.6641	277.0076	**T2D10**	490.9008	422.6565	378.3817
C12	510.4427	482.9618	314.4122	**T1D13**	285.5573	417.4656	386.1679	**T2D11**	371.5115	508.6107	134.2595
C13	505.5573	457.313	331.3588	**T1D14**	350.4427	332.5802	309.6794	**T2D12**	159.9084	280.8244	303.5725
C14	107.542	116.5496	47.23664	**T1D15**	440.6718	416.3969	392.8855	**T2D13**	319.4504	389.0687	34.71756

Tnf-α divided by total of proteins (pg/µg)											
Controls				**Type 1 Diabetes**				**Type 2 Diabetes**			
Donor	**TCP**	**ST**	**ECM**	**Donor**	**TCP**	**ST**	**ECM**	**Donor**	**TCP**	**ST**	**ECM**
C1	0.021999	0.117389	0.17049	**T1D6**	0.040659	0.472235	0.263335	**T2D1**	0.022337	0.331116	0.075977
C6	0.475905	0.450948	0.344934	**T1D7**	0.247964	0.531806	0.373173	**T2D2**	0.007433	0.434406	0.003197
C7	0.226519	0.388594	0.270767	**T1D8**	0.281113	0.255623	0.233945	**T2D4**	0.010899	0.364771	0.006987
C8	0.062809	0.208803	0.178073	**T1D9**	0.47147	0.494903	0.282211	**T2D7**	0.029893	0.442959	0.013472
C9	0.190361	0.383816	0.250676	**T1D10**	0.160542	0.184273	0.113346	**T2D8**	0.326611	0.230722	0.291603
C10	0.231366	0.277739	0.219388	**T1D11**	0.362335	0.39691	0.265016	**T2D9**	0.392698	0.436271	0.265658
C11	0.319265	0.388244	0.205243	**T1D12**	0.355	0.348015	0.234197	**T2D10**	0.4051	0.368392	0.286696
C12	0.41188	0.400035	0.244431	**T1D13**	0.274363	0.338495	0.312611	**T2D11**	0.301846	0.419196	0.104458
C13	0.413442	0.363293	0.316092	**T1D14**	0.29754	0.282135	0.247882	**T2D12**	0.144805	0.22003	0.242509
C14	0.091308	0.086091	0.040834	**T1D15**	0.353159	0.344187	0.318177	**T2D13**	0.283125	0.314959	0.028334

PDGF-BB ELISA DATA FOR RESULTS PRESENTED IN CHAPTER 4

Raw data (O.D. 450nm)											
Controls				**Type 1 Diabetes**				**Type 2 Diabetes**			
Donor	**TCP**	**ST**	**ECM**	**Donor**	**TCP**	**ST**	**ECM**	**Donor**	**TCP**	**ST**	**ECM**
C1	0.895	0.878	0.906	**T1D6**	0.378	1.263	0.4445	**T2D1**	0.959	1.039	1.3035
C6	0.9485	1.218	1.0185	**T1D7**	0.4055	0.4455	0.5125	**T2D2**	0.5395	0.7935	1.09
C7	0.395	0.4605	0.701	**T1D8**	0.379	0.607	0.3875	**T2D4**	0.627	1.195	0.8025
C8	0.3635	0.551	0.4885	**T1D9**	1.4055	2.0445	1.662	**T2D7**	1.0035	1.677	0.81
C9	0.644	0.931	0.6885	**T1D10**	0.297	0.3875	0.23	**T2D8**	1.0005	0.8515	0.7485
C10	0.726	1.186	0.7125	**T1D11**	0.827	0.603	0.451	**T2D9**	0.8805	0.913	0.6165
C11	0.843	1.469	0.803	**T1D12**	1.066	1.122	0.783	**T2D10**	0.6185	0.874	0.48
C12	0.857	0.931	0.907	**T1D13**	0.6555	0.902	0.6085	**T2D11**	0.4535	0.749	0.4435
C13	0.7065	1.2245	0.625	**T1D14**	0.704	0.5615	0.6195	**T2D12**	0.3115	0.3275	0.2345
C14	0.2965	0.4535	0.2835	**T1D15**	0.5695	0.5505	0.532	**T2D13**	0.316	0.3655	0.2935

PDGF-BB in original samples (raw data entered in standard curve) (pg/ml)											
Controls				**Type 1 Diabetes**				**Type 2 Diabetes**			
Donor	**TCP**	**ST**	**ECM**	**Donor**	**TCP**	**ST**	**ECM**	**Donor**	**TCP**	**ST**	**ECM**
C1	41.34615	40.41209	41.95055	**T1D6**	12.93956	61.56593	16.59341	**T2D1**	44.86264	49.25824	63.79121
C6	44.28571	59.09341	48.13187	**T1D7**	14.45055	16.64835	20.32967	**T2D2**	21.81319	35.76923	52.06044
C7	13.87363	17.47253	30.68681	**T1D8**	12.99451	25.52198	13.46154	**T2D4**	26.62088	57.82967	36.26374
C8	12.14286	22.44505	19.01099	**T1D9**	69.3956	104.5055	83.48901	**T2D7**	47.30769	84.31319	36.67582
C9	27.55495	43.32418	30	**T1D10**	8.489011	13.46154	4.807692	**T2D8**	47.14286	38.95604	33.2967
C10	32.06044	57.33516	31.31868	**T1D11**	37.60989	25.3022	16.95055	**T2D9**	40.54945	42.33516	26.04396
C11	38.48901	72.88462	36.29121	**T1D12**	50.74176	53.81868	35.19231	**T2D10**	26.15385	40.19231	18.54396
C12	39.25824	43.32418	42.00549	**T1D13**	28.18681	41.73077	25.6044	**T2D11**	17.08791	33.32418	16.53846
C13	30.98901	59.45055	26.51099	**T1D14**	30.85165	23.02198	26.20879	**T2D12**	9.285714	10.16484	5.054945
C14	8.461538	17.08791	7.747253	**T1D15**	23.46154	22.41758	21.4011	**T2D13**	9.532967	12.25275	8.296703

Ratio PDGF-BB/Total proteins in samples (pg/µg)											
Controls				**Type 1 Diabetes**				**Type 2 Diabetes**			
Donor	**TCP**	**ST**	**ECM**	**Donor**	**TCP**	**ST**	**ECM**	**Donor**	**TCP**	**ST**	**ECM**
C1	0.034148	0.032954	0.031979	**T1D6**	0.011066	0.05763	0.013303	**T2D1**	0.041702	0.041273	0.049962
C6	0.038871	0.048846	0.039524	**T1D7**	0.011827	0.014684	0.015033	**T2D2**	0.019523	0.028586	0.041292
C7	0.011568	0.015858	0.024892	**T1D8**	0.011257	0.017944	0.011178	**T2D4**	0.021995	0.048119	0.029428
C8	0.009693	0.020098	0.01509	**T1D9**	0.057695	0.083886	0.068305	**T2D7**	0.03853	0.071373	0.030416
C9	0.021086	0.035358	0.025504	**T1D10**	0.00688	0.011415	0.003964	**T2D8**	0.03757	0.0308	0.029908
C10	0.025797	0.04751	0.02683	**T1D11**	0.031075	0.021873	0.013318	**T2D9**	0.02851	0.033779	0.022038
C11	0.033489	0.063444	0.029225	**T1D12**	0.045742	0.03971	0.029753	**T2D10**	0.021583	0.035032	0.014051
C12	0.031678	0.035885	0.032656	**T1D13**	0.027082	0.033837	0.020727	**T2D11**	0.013884	0.027466	0.012867
C13	0.025343	0.047228	0.02529	**T1D14**	0.026194	0.01953	0.020979	**T2D12**	0.008409	0.007964	0.004038
C14	0.007184	0.012622	0.006697	**T1D15**	0.018802	0.01853	0.017332	**T2D13**	0.008449	0.009919	0.006771

DATA FROM THE BRADFORD TEST RELATED TO RESULTS PUBLISHED IN CHAPTER 5

Raw data (O.D. 595nm)												
Donor	**LT**	**L04T**	**HT**	**H04T**	**LS**	**L04S**	**HS**	**H04S**	**LE**	**L04E**	**HE**	**H04E**
1	2.0415	1.864	1.721	2.1115	1.698	1.657	1.757	1.7455	1.922	2.1015	1.908	2.33
2	1.697	1.8445	1.945	2.28	1.9925	2.2115	2.1305	2.113	2.179	2.0505	1.9515	2.4175
3	1.87	1.9705	2.112	2.3355	2.1935	2.1225	2.0675	2.406	1.592	2.211	1.872	2.001
4	1.878	2.15	2.174	2.1955	1.6	1.8035	1.602	1.828	1.5625	1.8065	1.8085	2.3605
5	1.849	1.863	2.0795	1.807	1.739	2.01	1.8535	1.985	1.6625	1.969	1.8975	1.971
6	1.857	1.9525	1.7825	2.166	1.854	1.9825	1.724	2.333	2.3075	2.4625	2.3945	2.52

Total Protein µg/ml												
Donor	**LT**	**L04T**	**HT**	**H04T**	**LS**	**L04S**	**HS**	**H04S**	**LE**	**L04E**	**HE**	**H04E**
1	1549.636	1388.273	1258.273	1613.273	1237.364	1200.091	1291	1280.545	1441	1604.182	1428.273	1811.909
2	1236.455	1370.545	1461.909	1766.455	1505.091	1704.182	1630.545	1614.636	1674.636	1557.818	1467.818	1891.455
3	1393.727	1485.091	1613.727	1816.909	1687.818	1623.273	1573.273	1881	1141	1703.727	1395.545	1512.818
4	1401	1648.273	1670.091	1689.636	1148.273	1333.273	1150.091	1355.545	1114.182	1336	1337.818	1839.636
5	1374.636	1387.364	1584.182	1336.455	1274.636	1521	1378.727	1498.273	1205.091	1483.727	1418.727	1485.545
6	1381.909	1468.727	1314.182	1662.818	1379.182	1496	1261	1814.636	1791.455	1932.364	1870.545	1984.636

Key to samples		
LT: cells on TCP in physiological glucose concentration DMEM	**LS:** cells on St in physiological glucose concentration DMEM	**LE:** cells on ECM in physiological glucose concentration DMEM
L04T: cells on TCP in physiological glucose concentration DMEM added with Palmitate	**L04S:** cells on St in physiological glucose concentration DMEM added with Palmitate	**L04E:** cells on ECM in physiological glucose concentration DMEM added with Palmitate
HT: cells on TCP in high glucose concentration DMEM	**HS:** cells on St in high glucose concentration DMEM	**HE:** cells on ECM in high glucose concentration DMEM
H04T: cells on TCP in high glucose concentration DMEM added with Palmitate	**H04S:** cells on St in high glucose concentration DMEM added with Palmitate	**H04E:** cells on ECM in high glucose concentration DMEM added with Palmitate

DATA FROM TNF-α ELISA TEST AS DISCUSSED IN CHAPTER 5

Raw data (O.D. 450nm)												
Donor	**LT**	**L04T**	**HT**	**H04T**	**LS**	**L04S**	**HS**	**H04S**	**LE**	**L04E**	**HE**	**H04E**
1	1.348	1.466	1.16	0.763	1.894	1.716	1.706	0.729	1.107	1.255	1.203	0.756
2	2.061	1.252	1.84	0.889	2.712	1.382	1.969	0.837	1.871	0.825	1.695	0.512
3	1.247	0.958	1.446	1.037	1.864	1.051	1.989	1.143	0.799	0.56	0.922	0.484
4	1.001	1.069	1.571	0.726	1.314	1.45	1.485	0.564	0.513	0.506	0.904	0.909
5	1.597	1.165	1.618	1.228	1.582	1.474	2.246	1.7	0.973	0.921	0.752	0.522
6	1.327	0.601	1.205	1.107	1.617	1.033	1.765	1.398	0.675	0.639	0.888	0.168

TNF-alpha (pg/ml) in test plate (OD in standard curve)												
Donor	**LT**	**L04T**	**HT**	**H04T**	**LS**	**L04S**	**HS**	**H04S**	**LE**	**L04E**	**HE**	**H04E**
1	29.99235	33.00255	25.19643	15.06888	43.92092	39.3801	39.125	14.20153	23.84439	27.6199	26.29337	14.89030612
2	48.18112	27.54337	42.54337	18.28316	64.78827	30.85969	45.83418	16.95663	43.33418	16.65051	38.84439	8.665816327
3	27.41582	20.04337	32.49235	22.05867	43.15561	22.41582	46.34439	24.76276	15.98724	9.890306	19.125	7.951530612
4	21.14031	22.875	35.68112	14.125	29.125	32.59439	33.48724	9.992347	8.691327	8.512755	18.66582	18.79336735
5	36.34439	25.32398	36.8801	26.93112	35.96173	33.20663	52.90051	38.97194	20.42602	19.09949	14.78827	8.920918367
6	29.45663	10.93622	26.34439	23.84439	36.85459	21.95663	40.6301	31.26786	12.82398	11.90561	18.25765	0

TNF-α (pg/ml) in original samples (before dilution 1:8)												
Donor	**LT**	**L04T**	**HT**	**H04T**	**LS**	**L04S**	**HS**	**H04S**	**LE**	**L04E**	**HE**	**H04E**
1	239.9388	264.0204	201.5714	120.551	351.3673	315.0408	313	113.6122	190.7551	220.9592	210.3469	119.122449
2	385.449	220.3469	340.3469	146.2653	518.3061	246.8776	366.6735	135.6531	346.6735	133.2041	310.7551	69.32653061
3	219.3265	160.3469	259.9388	176.4694	345.2449	179.3265	370.7551	198.102	127.898	79.12245	153	63.6122449
4	169.1224	183	285.449	113	233	260.7551	267.898	79.93878	69.53061	68.10204	149.3265	150.3469388
5	290.7551	202.5918	295.0408	215.449	287.6939	265.6531	423.2041	311.7755	163.4082	152.7959	118.3061	71.36734694
6	235.6531	87.4898	210.7551	190.7551	294.8367	175.6531	325.0408	250.1429	102.5918	95.2449	146.0612	0

Ratio TNF-α/Total proteins (pg/mcg)												
Donor	**LT**	**L04T**	**HT**	**H04T**	**LS**	**L04S**	**HS**	**H04S**	**LE**	**L04E**	**HE**	**H04E**
1	0.154836	0.190179	0.16019693	0.074725	0.283965	0.262514	0.242448	0.088722	0.132377	0.137739	0.147274	0.065744
2	0.311737	0.160773	0.23280992	0.082802	0.344369	0.144866	0.224878	0.084015	0.207014	0.085507	0.211712	0.036652
3	0.157367	0.107971	0.16107 9744	0.097126	0.204551	0.110472	0.235659	0.105317	0.112093	0.046441	0.109635	0.042049
4	0.120716	0.111025	0.17091 8228	0.066878	0.202913	0.195575	0.232936	0.058972	0.062405	0.050975	0.111619	0.081726
5	0.211514	0.146026	0.18624 1764	0.161209	0.225707	0.174657	0.306953	0.208 09	0.135598	0.102981	0.083389	0.048041
6	0.170527	0.059568	0.16036982	0.114718	0.213777	0.117415	0.257764	0.137847	0.057267	0.049289	0.078085	0

DATA FROM PDGF-BB ELISA TEST AS DISCUSSED IN CHAPTER 5

Raw data (O.D. 450nm)												
Donor	**LT**	**L04T**	**HT**	**H04T**	**LS**	**L04S**	**HS**	**H04S**	**LE**	**L04E**	**HE**	**H04E**
1	0.1085	0.125	0.112	0.1225	0.7445	0.6705	0.776	0.8395	0.796	0.8595	0.75	0.964
2	0.4615	0.551	0.7325	0.837	1.0075	0.9745	1.175	1.1185	0.716	0.9455	0.79	0.753
3	0.7335	0.6855	0.6585	0.87	1.188	1.2765	1.2595	1.3695	0.8285	1.204	0.877	0.99
4	0.859	1.0215	0.9675	1.1215	1.9845	1.8195	1.852	2.43	1.801	2.278	2.1215	2.2185
5	0.826	1.304	1.4715	1.9385	1.196	1.523	1.8445	1.7475	1.4905	1.883	1.0075	1.5895
6	0.889	1.1495	0.9345	1.329	1.6025	1.09	1.6605	1.205	1.4735	1.295	1.1355	0.9265

PDGF-BB (pg/ml) in samples												
Donor	**LT**	**L04T**	**HT**	**H04T**	**LS**	**L04S**	**HS**	**H04S**	**LE**	**L04E**	**HE**	**H04E**
1	0	0.069767	0	0	24.0814	21.21318	25.30233	27.76357	26.07752	28.53876	24.29457	32.58915
2	13.1124	16.5814	23.61628	27.66667	34.27519	32.99612	40.76744	38.57752	22.97674	31.87209	25.84496	24.41085
3	23.65504	21.79457	20.74806	28.94574	41.27132	44.70155	44.04264	48.3062	27.33721	41.89147	29.21705	33.5969
4	28.51938	34.81783	32.72481	38.6938	72.14341	65.74806	67.00775	89.41085	65.03101	83.51938	77.45349	81.21318
5	27.24031	45.76744	52.25969	70.36047	41.5814	54.25581	66.71705	62.95736	52.99612	68.2093	34.27519	56.83333
6	29.68217	39.77907	31.44574	46.73643	57.33721	37.47287	59.58527	41.93023	52.33721	45.4186	39.23643	31.13566

Ratio PDGF-BB/Total proteins in original samples (pg/mcg)												
Donor	**LT**	**L04T**	**HT**	**H04T**	**LS**	**L04S**	**HS**	**H04S**	**LE**	**L04E**	**HE**	**H04E**
1	0.00000	0.00005	0.00000	0.00000	0.01946	0.01768	0.01960	0.02168	0.01810	0.01779	0.01701	0.01799
2	0.01060	0.01210	0.01615	0.01566	0.02277	0.01936	0.02500	0.02389	0.01372	0.02046	0.01761	0.01291
3	0.01697	0.01468	0.01286	0.01593	0.02445	0.02754	0.02799	0.02568	0.02396	0.02459	0.02094	0.02221
4	0.02036	0.02112	0.01959	0.02290	0.06283	0.04931	0.05826	0.06596	0.05837	0.06251	0.05790	0.04415
5	0.01982	0.03299	0.03299	0.05265	0.03262	0.03567	0.04839	0.04202	0.04398	0.04597	0.02416	0.03826
6	0.02148	0.02708	0.02393	0.02811	0.04157	0.02505	0.04725	0.02311	0.02921	0.02350	0.02098	0.01569

REFERENCES AND BIBLIOGRAPHY

- Aas V., et al. (2006). “Eicosapentaenoic acid (20:5 n-3) increases fatty acid and glucose uptake in cultured human skeletal muscle cells”. *The journal of lipid research* **47**: 366-374
- Abizaid A., et al. (2003). “Sirolimus-eluting stents inhibit neointimal hyperplasia in diabetic patients. Insight from the RAVEL trial”. *European heart journal* **25** (2): 107-112
- Alderman E.L., et al. (The BARI Investigators) (2000). “Seven-Year Outcome in the Bypass Angioplasty Revascularization Investigation (BARI) By Treatment and Diabetic Status”. *Journal of the American college of cardiology* **35**(5): 1122–1129
- Almeida M., et al. (2000). “A Simple Method for Human Peripheral Blood Monocyte Isolation”. *Memorias do Instituto Oswaldo Cruz* **95**: 221-223
- American diabetes association (2002). “Implications of the United Kingdom Prospective Diabetes Study”. *Diabetes care* **25**(1): 528-532
- Anderson J.M., Rodriquez A., Chang D.T. (2008). “Foreign body reaction to biomaterials”. *Seminars in Immunology* **20**(8): 86-100
- Barber R. D., et al. (2005). "GAPDH as a housekeeping gene: analysis of GAPDH mRNA expression in a panel of 72 human tissues." *Physiological Genomics* **21**(3): 389-395
- Barlis P., et al. (2007). “Still a future for the bare metal stent?”. *International journal of cardiology* **121**: 1-3
- Battegay E. J., et al. (1994). "PDGF-BB modulates endothelial proliferation and angiogenesis in vitro via PDGF-beta receptors". *The Journal of Cell Biology* **125**: 917-928
- Bayes-Genis A. C. J., et al. (2002). "Macrophages, myofibroblasts and neointimal hyperplasia after coronary artery injury and repair". *Atherosclerosis* **163**(1): 89-98
- Beilby J. *(2004).* **“**Definition of Metabolic Syndrome: Report of the National Heart, Lung, and Blood Institute/American Heart Association

Conference on Scientific Issues Related to Definition". *Circulation* **109**: 433-438

- Bertrand M. E., et al. (1998). "Randomized multicentre comparison of conventional anticoagulation therapy in unplanned and elective coronary stenting". *Circulation* **98**: 1597-1603
- Bocksteins E. S. A., et al. (2012). Study of Cellular Components and Analysis of Cellular Processes by Immunocytochemistry. *Applications of Immunocytochemistry*. [Online] H. Dehghani, Intech Books and Journals. Available from: www.intechopen.com. [Accessed 4th September 2012].
- Boilson B. A., et al. (2008). "Circulating CD34+ Cell Subsets in Patients with Coronary Endothelial Dysfunction". *Nature Clinical Practice Cardiovascular Medicine* **5**(8): 489-496
- Boyce D.E., et al. (1997). "Hyaluronic acid induces tumour necrosis factor-alpha production by human macrophages in vitro". *British Journal of Plastic Surgery* **50**(5): 362-368
- Boyum A. (1968). "Isolation of mononuclear cells and granulocytes from human blood. Isolation of monuclear cells by one centrifugation and of granulocytes by combining centrifugation and sedimentation at 1 g". *Scandinavian Journal of Clinical Laboratory Investigation* Supplement **97**: 77-89
- Bradford, M. M. (1976). "A Rapid and Sensitive Method for the Quantitation of Microgram Quantities of Protein Utilizing the Principle of Protein-Dye Binding". *Analytical Biochemistry* **72**: 248-254
- Briaud I., Poitout V., et al. (2001). "Lipotoxicity of the pancreatic beta-cell is associated with glucose-dependent esterification of fatty acids into neutral lipids". *Diabetes* **50**(2): 315-321
- British Heart Foundation, (2010). "Coronary heart disease statistics". *British Heart Foundation Statistics Database*. Available from: www.heartstats.org. 2010 Edition

- Brown M. W. C. (2000). "Flow Cytometry:Principles and Clinical Applications in Hematology". *Clinical Chemistry* **46**(8(B)): 1221-1229
- Buhagiar J., et al. (2012). “Corrosion properties of S-phase layers formed on medical grade austenitic stainless steel” *Journal of materials science: materials in medicine* **23**(2): 271-281
- Bunch, T. J., et al. (2002). "Effects of statins on six-month survival and clinical restenosis frequency after coronary stent deployment." The American Journal of Cardiology **90**(3): 299-302
- Bustin S.A.V., et al. (2005). “Quantitative real-time RT-PCR – a perspective”. *Journal of Molecular Endocrinology* **34**: 597–601
- Campo G. M., et al. (2011). “Hyaluronan reduces inflammation in experimental arthritis by modulating TLR-2 and TLR-4 cartilage expression”. *Biochimica et Biophysica acta* **1812**(9): 1170-1181
- Campo G. M., et al. (2012). “Hyaluronan differently modulates TLR-4 and the inflammatory response in mouse chondrocytes”. *Biofactors* **38**(1): 69-76
- Catelas I., et al. (1999). "Cytotoxicity and Macrophage Cytokine Release Induced by Ceramic and polyethylene Particles in vitro". *The Journal of Bone and Joint Surgery* **81**(b): 516-521
- Chai S. C. Q., et al. (2005). "Overexpression of Hyaluronan in the Tunica Media Promotes the Development of Atherosclerosis". *Circulation Research* **96**(5): 583-591
- Chait A., et al. (2010). “Editorial. Saturated fatty acids and inflammation: who pays the toll?”. *Arteriosclerosis, thrombosis and vascular biology* **30**: 692-693
- Chang M. Y., et al. (2012). “Monocyte-to-macrophage differentiation. Synthesis and secretion of a complex extracellular matrix”. *The journal of biological chemistry* **287**: 14122-14135

- Chapman M. J., et al. (1998). “Atherogenic, dense low-density lipoproteins. Pathophysiology and new therapeutic approaches”. *European Heart Journal* Supplement **A**: 24-30
- Czarkowska-Paczek B., et al. (2006). “The serum levels of growth factors: PDGF, TGF-beta and VEGF are increased after strenuous physical exercise”. *The journal pf physiology and pharmacology* **57**(2): 189-97
- Chomczynski P. S. N. (1987). "Signal-step method of RNA isolation by acid guanidinium thiocyanate-phenol-chloroform extraction". *Analytical Biochemistry* **162**: 156-159
- Chung I.-M., et al. (2002) “Enhanced extracellular matrix accumulation in restenosis of coronary arteries after stent deployment”. *Journal of the American College of Cardiology* **40**(12): 2072-2081
- Collier B., et al. (2008). “Glucose control and the inflammatory response”. *Nutrition in clinical practice* **23**(1): 3-15
- Crowther, J., Ed. (2001). The ELISA Guidebook. Methods in Molecular Biology. Totowa, New Jersey, Humana Press Inc.
- Curtiss L. K., Tobias P. S. (2009). “Emerging role of Toll-like receptors in atherosclerosis”. *The Journal of Lipid Research* **50**(Suppl): S340-S345
- Dahlke M.H., et al. (2004). “The biology of CD45 and its use as a therapeutic target”. *Leukemia and Lymphoma* **45**(2): 229-236
- Dasu M. R., et al. (2008). “High glucose induces Toll-like receptor expression in human monocytes: mechanism of activation”. *Diabetes* **57**(11): 3090-3098
- Dasu M. R., et al. (2011). “Free fatty acids in the presence of high glucose amplify monocyte inflammation via Toll-like receptors”. *The American Journal of Physiology. Endocrinology and Metabolism* ***3*00**(1): E145-154
- Delia D., et al. (1993). “CD34 expression is regulated reciprocally with adhesion molecules in vascular endothelial cells in vitro”. *Blood* **81**(4): 1001-1008

- Di Gregorio G. B., et al. (2005). "Expression of CD68 and Macrophage Chemoattractant Protein-1 Genes in Human Adipose and Muscle Tissues". *Diabetes* **54**: 2305-2313
- Dinarello, C. (2000). "Proinflammatory Cytokines". *Chest* **118**(2): 503-508
- Dinarello, C. (2007). "Historical Review of Cytokines". *European Journal of Immunology* (Supplement 1) **37**: S34-S45
- Dinnes D.L., et al. (2007). "Material surfaces affect the protein expression patterns of human macrophages: a proteomics approach". *Journal of Biomedical Materials Research Part A* **80A**(4):895-908
- Fadini G.P., et al. (2006). "Circulating CD34+ cells, metabolic syndrome, and cardiovascular risk." *European Heart Journal* **27**: 2247-2255
- Fan J., Watanabe T. (2003). "Inflammatory reactions in the pathogenesis of atherosclerosis". *Journal of atherosclerosis and thrombosis* **10**(2): 63-71
- Farb A., et al. (2002). "Morphological predictors of restenosis after coronary stenting in humans". *Circulation* **105**: 2974-2980
- Forte A., et al. (2010). "Role of myofibroblasts in vascular remodelling: focus on restenosis and aneurysm". Review article. *Cardiovascular Research* **88**: 395-405
- Frobert O., et al. (2009). "Differences in restenosis rate with different drug-eluting stents in patients with and without diabetes mellitus: a report from the SCAAR (Swedish Angiography and Angioplasty Registry)". *Journal of the American college of cardiology* **53**(18): 1660-1667
- Gabbiani G. (2004). "The evolution of the myofibroblasts concept: a key cell for wound healing and fibrotic diseases". *Giornale di Gerontologia* **52**:280-282
- Garg P. et al. (2008). "Balancing the risks of restenosis and stent thrombosis in bare-metal versus drug-eluting stents: results of a decision

analytic model". *Journal of the American College of Cardiology* **51**(19): 1844-1853

- Geissmann F., et al. (2010). "Development of monocytes, macrophages and dendritic cells". *Science* (327(5966)): 656-661
- Gilbert J., et al. (2004). "Meta-analysis of the effect of diabetes on restenosis rates among patients receiving coronary angioplasty stenting". *Diabetes care* **27** (4): 990-994
- Glatz J. F., et al. (2010). "Membrane fatty acid transporters as regulators of lipid metabolism: implications for metabolic disease". *Physiological reviews* **90**(1): 367-417
- Goldin A., et al. (2006). "Advanced Glycation End Products: Sparking the Development of Diabetic Vascular injury". *Circulation* **114**: 597-605
- Gordon S., Taylor P.R. (2005) "Monocyte and macrophage heterogeneity". *Nature reviews. Immunology* (5): 953-964
- Gotman I. (1997). "Characteristics of metals used in implants". *Journal of Endourology* **11**(6): 383-389
- Greenberg D., et al. (2004). "Can we afford to eliminate restenosis? Can we afford not to?". *Journal of the American college of cardiology* **43**(4): 513-518
- Gregg E.W., et al. (2005). "Secular trends in cardiovascular disease risk factors according to body mass index in US adults". *The journal of the American medical association* **293**(15): 1868-1874
- Gross C.M., et al. (2000). "Clinical and angiographic outcome in patients with in-stent restenosis and repeat target lesion revascularisation in small coronary arteries". *Heart* **84**: 307–313
- Hammacher, A., et al. (1988). "A major part of platelet-derived growth factor purified from human platelets is a heterodimer of one A and one B chain". *Journal of Biological Chemistry* **263**(31): 16493-16498
- Hansen B.C. (1999). "The metabolic syndrome X". *Annals of the New York Academy of Science* **892**: 1-24

- Harrison M., et al. (2007). "Stent material surface and glucose activate mononuclear cells of control, type 1 and type 2 diabetes subjects." *Journal of Biomedical Material Research* A **83**(1): 52-57
- Haston W.S., Wilkinson P.C. (1982). "Lymphocyte locomotion and attachment on two-dimensional surfaces and in three-dimensional matrices." *The Journal of Cell Biology* **92**: 747-752
- Håversen L., et al. (2009). "Induction of proinflammatory cytokines by long-chain saturated fatty acids in human macrophages". *Atherosclerosis* **202**(2): 382-93
- Herrmann H.C., et al. (1992). "Emergent Use of Balloon-Expandable Coronary Artery Stenting for Failed Percutaneous Transluminal Coronary Angioplasty". *Circulation* **86**:812-819
- Hinz B., et al. (2007). "The myofibroblasts: one function, multiple origins". *American Journal of Pathology* **170**(6):1807-1816
- Holness C.L., Simmons D.L. (1993). "Molecular cloning of CD68, a human macrophage marker related to lysosomal glycoproteins". *Blood* **81**(6): 1607-1613
- Homo-Delarche F., Drexhage H.A. (2004). "Immune cells, pancreas development, regeneration and type 1 diabetes". *Trends in immunology* **25**(5): 222-229
- Honess C., et al. (2006). "Importance of surface finish in the design of stainless steel". *Stainless steel industry. Engineering utility*: 14-15
- Hu F. B, et al. (2001). "Diet, lifestyle, and the risk of type 2 diabetes mellitus in women". *New England Journal of Medicine* **345**(11): 790-797
- Hu F.B. (2011). "Globalization of diabetes. The role of diet, lifestyle and genes". *Diabetes Care* **34**(6): 1249-1257
- Huang S., et al. (2012). "Saturated fatty acids activate TLR-mediated proinflammatory signalling pathways". *The journal of lipid research* **53**(9): 2002-2013

- Inaba T, S. H., et al. (1993). "Expression of platelet-derived growth factor beta receptor on human monocyte-derived macrophages and effects of platelet-derived growth factor BB dimer on the cellular function". *The Journal of Biological Chemistry* **268**(32): 24353-24360
- Itano N., et al. (1999). "Three Isoforms of Mammalian Hyaluronan Synthases Have Distinct Enzymatic Properties." *Journal of Biological Chemistry* **274**(35): 25085-25092
- Jensen L.O. et al. (2007). "Stent thrombosis, myocardial infarction and death after drug-eluting and bare-metal stent coronary interventions". *Journal of the American college of cardiology* **50**(5): 463-470
- Jiang D., et al. (2005). "Regulation of lung injury and repair by Toll-like receptors and hyaluronan". *Nature. Medicine* **11**(11): 1173-1179
- Jiang D., et al. (2007). "Hyaluronan in tissue injury and repair". *Annual review of cell and developmental biology* **23**:435-461
- Joner M., et al. (2006). "Pathology of drug-eluting stents in humans". *Journal of the American college of cardiology* **48**(1):193-202
- Kahn B. B., Flier J. S. (2000). "Obesity and insulin resistance". *The Journal of Clinical Investigation* **106**(4): 473-481
- Kannel W. B. (1998) "Overview of atherosclerosis". *Clinical therapeutics* 20:supplement B
- Kannel W. B. (1998). "Overview on atherosclerosis". *Clinical Therapeutics* **20** Suppl B: 2-17
- Kendrew J. (1995). *The encyclopedia of molecular biology*. Blackwell Science.
- Kennedy A., et al. (2008). "Saturated fatty acid-mediated inflammation and insulin resistance in adipose tissue: mechanisms of action and implications". *The Journal of Nutrition* **139**: 1-4
- Kennedy C. I., et al. (2000). "Proinflammatory cytokines differentially regulate hyaluronan synthase isoforms in foetal and adult fibroblasts". *Journal of Pediatric Surgery* **35**(6): 874-879

- Kerber S. J., et al. (2000). “Stainless steel surface analysis. AES and XPS analysis of the passivation layer on stainless steel can help determine how well it will resist corrosion”. *Advanced materials and processes*: 33-36
- Khosravi A., et al. (2011). “Does Lipoprotein (a) level have a predictive value in restenosis after coronary stenting?”. *International Journal of Preventive Medicine* **2**(3): 158-163
- King P., et al. (1999). “The UK prospective study (UKPDS): clinical and therapeutic implications for type 2 diabetes”. *British Journal of Clinical Pharmacology* **48(**5): 643-648
- Kitoga M., et al. (2008). “Coronary in-stent restenosis in diabetic patients after implantation of sirolimus or paclitaxel drug-eluting coronary stents”. *Diabetes and Metabolism* **34**(1): 62-67
- Klein L.W., et al. (2002). "Percutaneous coronary interventions in octogenarians in the american college of cardiology-National cardiovascular data registry*". Journal of the American College of Cardiology* **40**(3): 394-402
- Kornowski R., et al. (1997). ” Increased Restenosis in Diabetes Mellitus After Coronary Interventions Is Due to Exaggerated Intimal Hyperplasia. A Serial Intravascular Ultrasound Study”. *Circulation* **95**: 1366-1369
- Krettek A., et al. (2001). “Expression of PDGF receptors and ligand-induced migration of partially differentiated human monocyte-derived macrophages influence of IFN-γ and TGF-β”. *Atherosclerosis* **156**:267-275
- Kumbhani D.J., et al. (2008). “The effect of drug-eluting stents on intermediate angiographic and clinical outcomes in diabetic patients: insights from randomized clinical trials”. *American heart journal* **155**: 640-647
- Kuwana M, et al. (2003). "Human Circulating CD14+ Monocytes as a Source of Progenitors that Exhibit Mesenchyma Cell Differentiation". *Journal of Leukocyte Biology* **74**: 833-845

- Lakka H.-M., et al. (2002). “The Metabolic Syndrome and Total and Cardiovascular Disease Mortality in Middle-aged Men”. *Journal of the American Medical Association* **288**(21): 2709-2716
- Lambert P., Bingley PJ (2006). “What is type 1 diabetes?”. *Medicine* **34**(2): 47-51
- Lamhamedi-Cherradi S.E., et al. (2003). “Transcriptional regulation of type 1 diabetes by NF-kB”. *The Journal of Immunology* **171**:4886-4892
- Lee J. M., et al. (2006). “Prevalence and determinants of insulin resistance among U.S. adolescents”. *Diabetes Care* **29**: 2427-2432
- Li Z., *et al*. (2008). “The lysosomal-mitochondrial axis in free fatty acid–induced hepatic lipotoxicity”. *Hepatology* **47**(5): 1495–1503
- Liang J., et al. (2011). “The role of hyaluronan and hyaluronan-binding proteins in human asthma”. *Journal of Allergy and Clinical Immunology* **128**(2): 403-411
- Libby P., et al. (2009). “Inflammation in atherosclerosis. From pathophysiology to practice. State of the art paper”. *Journal of the American College of Cardiology* **54**: 2129-2138
- Lilly J., et al. (2011). “Review article. The haematopoietic stem cell niche: new insights into the mechanisms regulating haematopoietic stem cell behaviour”. *Stem Cells International* Volume, Article ID 274564, 10 pages
- Liu N., et al. (2001). “Hyaluronan synthase 3 overexpression promotes the growth of TSU prostate cancer cells”. *Cancer Research* **61**: 5207-5214
- Luttikhuizen M. C., et al. (2006). "Cellular and molecular dynamics in the foreign body reaction". *Tissue Engineering* **12**(7): 1955-1970
- Marieb EN. (1991). In: “Human anatomy and physiology”. *Blood*. Heyden R, Schmid J eds. The Benjamin/ Cumming Publishing Company: 596-597
- Mauri L., et al. (2007). “Stent thrombosis in randomized clinical trials of drug-eluting stents”. *New England Journal of Medicine* **356**(10): 1020-1029

- Mazzone T. (2010). “Diabetes and Cardiovascular Disease. Intensive Glucose Lowering and Cardiovascular Disease Prevention in Diabetes. Reconciling the Recent Clinical Trial Data”. *Circulation* **122**: 2201-2211
- Mesure, L., et al. (2010). "Gene Expression Study of Monocytes/Macrophages during Early Foreign Body Reaction and Identification of Potential Precursors of Myofibroblasts". *PLoS ONE* **5**(9): e12949
- Miettinen H., et al. (1998). “Impact of diabetes on mortality after the first myocardial infarction. The FINMONICA Myocardial Infarction Register Study Group”. *Diabetes Care* **21**(1): 69-75
- Mlinar B., et al. (2007). “Molecular mechanisms of insulin resistance and associated diseases”. *Clinica Chimica Acta* **375**: 20-35
- Moller D.E. (2000). “Potential role of TNF-α in the pathogenesis of insulin resistance and type 2 diabetes”. *Trends in Endocrinology and Metabolism* **11**(6): 212-217
- Moses J.W., et al. (2003). “Sirolimus-eluting stents versus standard stents in patients with stenosis in a native coronary artery”. *The New England journal of medicine* **349**(14): 1315-1323
- Moustapha A., et al. (2001). “Percutaneous and surgical interventions for in-stent restenosis: long-term outcomes and effect of diabetes mellitus”. *Journal of the American college of cardiology* **37**(7): 1877-1882
- Nathan D.M. (1993). “Long-term complications of diabetes mellitus”. *The New England Journal of Medicine* **328**(23):1676-1685
- Newson T. (2002) Stainless steel – *A family of medical device materials on British Stainless Steel Association* [Online] Available: http://www.bssa.org.uk/cms/File [16 November 2013]
- Nicholson J. W. (2002). “Metals”. Chapter 4 in *The chemistry of medical and dental materials*. RSC Publishing, Chemspider: 104-147

- Nicholson J. W. (2002). “Biological interactions with materials”. Chapter 6 in The chemistry of medical and dental materials. RSC Publishing, Chemspider: 104-147
- Noble P.W. (2002). "Hyaluronan and its catabolic products in tissue injury and repair". *Matrix Biology* **21**: 25-29
- Nusca A., et al. (2012). “Prognostic role of preprocedural glucose levels on short- and long-term outcome in patients undergoing percutaneous coronary revascularization”. *Catheterization and Cardiovascular Interventions* **80**(3): 377-384
- O’Brien B., Carroll W. (2009). “The evolution of cardiovascular stent materials and surfaces in response to clinical drivers: A review”. *Acta Biomaterialia* **5**: 945–958
- O’Rahilly S., et al. (1994). “Insulin resistance as the major cause of impaired glucose tolerance: a self-fulfilling prophesy?”. *The Lancet* **344**: 585-589
- Orkin S.H., Zon L. (2008). **“**Hematopoiesis: An Evolving Paradigm for Stem Cell Biology”. *Cell* **132**(4): 631–644
- Papakonstantinou E., et al. (1998). "A 340 KDa hyaluronic aci secreted by human vascular smooth muscle cells regulates their proliferation and migration". *Glycobiology* **8**(8): 821-830
- Park J. B., Lakes R. S. (1992). In *Biomaterials. An introduction.* Springer Verlagh GmbH. Second edition.
- Park J. B., Bronzino J. D. (2002). In *Biomaterials: principles and applications*. CRL Press.
- Patti G., et al. (2008). “Meta-analysis comparison (nine trials) of outcomes with drug-eluting stents versus bare metal stents in patients with diabetes mellitus”. *The American journal of cardiology* **102**(10):1328-1334
- Peppa M., et al. (2003). “Glucose, advanced glycation end products, and diabetes complications: what is new and what works”. *Clinical diabetes* **21** (4): 186-187

- Perfetto S.P., et al. (2004). "Seventeen-colour flow cytometry: unravelling the immune system". *Nature Reviews. Immunology* **4**: 648-655
- Perfetto S.P., et al. (2006). "Quality assurance for polychromatic flow cytometry". *Nature Protocols* **1**(3): 1522-1530
- Permana P.A., et al. (2006). "Macrophage-secreted factors induce adipocyte inflammation and insulin resistance". *Biochemical and Biophysical Research Communications* **341**(2): 507-514
- Pilling D., et al. (2009). "Identification of markers that distinguish monocyte-derived fibrocytes from monocytes, macrophages, and fibroblasts". *PLoS one* **4**(10): e7475
- Pintucci G., et al. (2005). "PDGF-BB Induces Vascular Smooth Muscle Cell Expression of High Molecular Weight FGF-2, Which Accumulates in the Nucleus". *Journal of Cellular Biochemistry* **95**(6): 1292-1300
- Price C.L., et al. (2004). "Advanced glycation end products modulate the maturation and function of peripheral blood dendritic cells". *Diabetes* **53**: 1452-1458
- Rehman J, et al. (2003). "Peripheral Blood "Endothelial Progenitor Cells" Are Derived From Monocyte/Macrophages and Secrete Angiogenic Growth Factors". *Circulation* **107**: 1164-1169
- Riddle M. (2000). "Managing Type 2 Diabetes Over Time: Lessons From the UKPDS ". *Diabetes Spectrum* **13**(4): 194
- Rokicki R., et al. (2008). "Corrosion characteristic of medical grade AISI type 316L stainless steel surface after electropolishing in a magnetic field". *Corrosion* **64**(8): 660-665
- Ross R. (1999). "Atherosclerosis-An inflammatory disease". New England *Journal of Medicine* **340**(2): 115-126
- Royal Society of Chemistry. (2013) Chemspider. Search and share chemistry. [Online] Available from: http://www.chemspider.com/Chemical-Structure.960.html?rid=9b5cae5f-66c8-4d54-9179-8e88f5da62cc#. [Accessed: 4th June 2013].

- Rustan A. C., Drevon C. A. (2005). “Fatty acids: structures and properties”. *Encyclopedia of Life Sciences. Introductory article.* John Wiley & Sons, Ltd. Available from: www.els.net: 1-7. [Accessed 15th May 2012]
- Ruygrok P. N., et al. (2001). “Clinical and angiographic factors associated with asymptomatic restenosis after percutaneous coronary intervention”. *Circulation* **104**: 2289-2294
- Ruygrok P.N., et al. (2003). “Vessel calibre and restenosis: a prospective clinical and angiographic study of NIR stent deployment in small and large coronary arteries in the same patient”. *Catheterization and cardiovascular interventions* **50**: 165-171
- Sack M. (2002). "Tumor Necrosis Factor-alpha in cardiovascular biology and the potential role for anti-tumor necrosis factor-alpha therapy in heart disease". *Pharmacology and Therapeutics* **94**: 123-135
- Samuel V. T., et al. (2010). “Lipid-induced insulin resistance: unravelling the mechanism”. *Lancet* **375**(9733): 2267-2277
- Santin M., Bruschi G. (2005). "Interfacial biology of in-stent restenosis". *Expert Review of Medical Devices* **2**(4): 429-443
- Santin M., et al. (2004). “In vitro host response assessment of biomaterials for cardiovascular stent manufacture”. *Journal of materials science: materials in medicine* **15**: 473-477
- Schachtrupp A. et al. (2003). “Individual inflammatory response of human blood monocytes to mesh biomaterials”. *British Journal of Surgery* **90**(1): 114-120
- Scholzen T., Gelden J. (2000). “The KI-67 protein: from the known and the unknown”. *Journal of Cell Physiology* **182**(3): 311-322
- Schwenk R. W., et al. (2010). “Fatty acid transport across the cell membrane: regulation by fatty acid transporters”. *Prostaglandins, leukotrienes and essential fatty acids* **82**(4-6): 149-154

- Sell H., et al. (2006). “The adipocyte–myocyte axis in insulin resistance”. *Trends in Endocrinology and Metabolism* **17**(10): 416-422
- Sharma C. P. (2005). “Biomaterials and Artificial Organs: Few Challenging Areas”. *Trends Biomaterials and Artificial Organs* **18** (2):
- Shimada M., et al. (1992). "Platelet-derived growth factor bb-dimer suppresses the expression of macrophages colony-stimulating factor in human vascular smooth muscle cells". *The Journal of Biological Chemistry* **267**(22): 15455-15458
- Simper D., et al. (2002). "Smooth Muscle Progenitor Cells in Human Blood". *Circulation* **106**: 1109-1204
- Singh I.M., et al. (2010). “Drug-eluting stents versus bare-metal stents for treatment of bare-metal in-stent restenosis”. *Catheterization and cardiovascular interventions* **76**: 257-262
- Sjoholm A., Nystrom T. (2006). “Inflammation and the etiology of type 2 diabetes. Review article”. *Diabetes Metabolism Research and Reviews* **22**: 4-10
- Somberg J., Weinberger J. (2007). “Late stent thrombosis: problem or not?”. *The American journal of cardiology* **99**(7):1020-1023
- Spector A. A. (1975). “Fatty acid binding to plasma albumin”. *Journal of Lipid Research* **16**(3): 165-179
- Spector A. A., et al. (1969). “Binding of long-chain fatty acids to bovine serum albumin”. *Journal of Lipid Research* **10**: 56-67
- Spranger J., et al. (2003). “Inflammatory cytokines and the risk to develop type 2 diabetes. Results of the prospective population-based European prospective investigation into cancer and nutrition (EPIC)-Potsdam study”. *Diabetes* **52**: 812-817
- Stewart H. J. S., et al. (2009). "Substrate-induced phenotypical change of monocytes/macrophages into myofibroblast-like cells: A new insight into the mechanism of in-stent restenosis". *Journal of Biomedical Materials Research* **90A**(2): 465-471

- Strobl H., et al. (1998). “Identification of $CD68^{+}Lin^{-}$ peripheral blood cells with dendritic precursor characteristic”. *The journal of immunology* **161**(2): 740-748
- Suganami T., et al. (2005). “A paracrine loop between adipocytes and macrophages aggravates inflammatory changes: role of free fatty acids and tumor necrosis factor alpha”. *Arteriosclerosis, Thrombosis and Vascular Biology* **25**(10):2062-2068
- Sugiyama S., et al. (2006). "Characterization of smooth muscle-like cells in circulating human peripheral blood". *Atherosclerosis* **187**(2): 351-362
- Suska, F., et al. (2003). "IL-1α, IL-1β and TNF-α secretion during in vivo/ex vivo cellular interactions with titanium and copper". *Biomaterials* **24**(3): 461-468
- Takahashi K. (2001). “Development and differentiation of macrophages and related cells: historical review and current concepts. Review article”. *Journal of Clinical and Experimental Hematopathology* **41**(1): 1-33
- Takayama H., et al. (2011). “Serum levels of platelet-derived growth factor-BB and vascular endothelial growth factor as prognostic factors for patients with fulminant hepatic failure”. *The journal of gastroenterology and hepatology* **26**(1): 116-121
- Tammi M.I., et al. (2002). "Hyaluronan and homeostasis: a balancing act." *The Journal of Biological Chemistry* **277**(7): 4581-4584
- Tashiro H., et al. (2001). “Role of cytokines in the pathogenesis of restenosis after percutaneous transluminal coronary angioplasty”. *Coronary artery disease* **12**: 107-113
- Teo Z.Y.P. (2003). “The role of macrophages in apoptosis: initiator, regulator, scavenger”. *Reviews in undergraduate research* **2**: 7-11
- Tiirikainen M. (1995). "Evaluation of Red Blood Cell Lysing Solutions for the Detection of Intracellular Antigens by Flow Cytometry". *Cytometry* **20**: 341-348

- Tisato V., et al. (2013). “Patients affected by metabolic syndrome show decreased levels of circulating platelet derived growth factor (PDGF-BB)”. *Clinical nutrition* **32**: 259-264
- Toole B.P., Tammi M.I. (2002). "Hyaluronan-cell interactions in cancer and vascular disease". *The Journal of Biological Chemistry* **277**(7): 4593-4596
- Travis J.A., et al. (2001). "Hyaluronan enhances contraction of collagen by smooth muscle cells and adventitial fibroblasts. Role of CD44 and implications for constrictive remodelling". *Circulation Research* **88**: 77-83
- Tuomilehto J., et al. (2001). “Prevention of type 2 diabetes mellitus by changes in lifestyle among subjects with impaired glucose tolerance”. *The New England Journal of Medicine* **334**(18):1343-1350
- Turley E.A. (2001). “Extracellular matrix remodelling: multiple paradigms in vascular disease”. *Circulation Research* **88**: 2-4
- Udagawa N., et al. (1990). “Origin of osteoclasts: mature monocytes and macrophages are capable of differentiating into osteoclasts under a suitable microenvironment prepared by bone marrow-derived stromal cells”. *Proceeding of the National Academy of Sciences* **87**: 7260-7264
- Umoru I., et al. (2009). “Monitoring, Control and Prevention Practices of Biomaterials Corrosion– An Overview”. *Trends in Biomateials and Artificial Organs* ***23****(2):93-104*
- Varol C., et al. (2009). “Origins and tissue-context-dependent fates of blood monocytes”. *Immunology and Cell Biology* **87**: 30-38
- Vigetti, D., et al. (2010). "Proinflammatory Cytokines Induce Hyaluronan Synthesis and Monocyte Adhesion in Human Endothelial Cells through Hyaluronan Synthase 2 (HAS2) and the Nuclear Factor-κB (NF-κB) Pathway". *Journal of Biological Chemistry* **285**(32): 24639-24645
- Waksman R., Pakala R. (2009). “Drug-Eluting Balloon. The Comeback Kid?”. *Circulatory Cardiovascular Intervention* **2**:352-358

- Waldo S. W., et al. (2008). "Heterogeneity of Human Macrophages in Culture and in Atherosclerotic Plaque". *The American Journal of Pathology* **172**(4): 1112-1126
- Wang Z.-N., et al. (2004). "Expression of survivin in primary and metastatic gastric cancer cells obtained by laser capture microdissection". *World Journal of Gastroenterology* **10**(21): 3094-3098
- Wannamethee, S. G., et al. (1997). "Serum Creatinine Concentration and Risk of Cardiovascular Disease: A Possible Marker for Increased Risk of Stroke". *Stroke* **28**(3): 557-563
- Weigel, P. H., et al. (1997). "Hyaluronan Synthases". *Journal of Biological Chemistry* **272**(22): 13997-14000
- Weisberg S. P., et al. (2003). "Obesity is associated with macrophage accumulation in adipose tissue". *The Journal of Clinical Investigation* **112**(12): 1796-1808
- Weisberg S.P., et al. (2003). "Obesity is associated with macrophage accumulation in adipose tissue". *The journal of clinical investigation* **112**(12): 1796-1808
- Wellen K.E., Hotamisligil G.S. (2005). "Inflammation, stress and diabetes". *The journal of clinical investigation* **115** (5): 1111-1119
- Welt F.G.P., Rogers C. (2002). "Inflammation and restenosis in the stent era". *Arteriosclerosis Thrombosis Vascular Biology* 22: 1769-1776
- WHO media centre. "Cardiovascular diseases (CVDs)". Available from: www.who.int. Factsheet 317 (September 2012) [Accessed 1st October 2012]
- WHO, D. P. S. (2006). "Definition and diagnosis of diabetes mellitus and intermediate hyperglycaemia". *Report of a WHO consultation.* W. D. P. Services. Geneva, Switzerland, WHO Document Production Services.
- WHO, D.P.S. (1999). "Definition, diagnosis and classification of diabetes mellitus and its complications". *Report of a WHO consultation* Part 1.

WHO Department of Non-communicable Disease Surveillance, Geneva 1999

- Wight, T. N., et al. (2004). "The pro-inflammatory nature of the vascular extracellular matrix". *International Congress Series* **1262**(0): 404-406
- Wilcox J. N., et al. (2001). "Perivascular responses after angioplasty which may contribute to post angioplasty restenosis: a role for circulating myofibroblast precursors?". *Annals of the New York Academy of science* **947**: 68-92
- Williams D.F. (2008). "On the mechanisms of biocompatibility". *Biomaterials online:* 1–13
- Wynn T.A. (2008). "Cellular and molecular mechanisms of fibrosis". *Journal of Pathology* **214**(2): 199–210
- Yan B.P., et al. (2008). "Rates of stent thrombosis in bare-metal versus drug-eluting stents (from a large Australian multicentre registry)". *The American journal of cardiology* **101**(12): 1716–1722
- Yang K., et al. (2010). "Nickel-free austenitic stainless steel for medical applications. Topical review". *Science and technology of advanced materials* **11**: 1-13
- Yin A. H., et al. (1997). "AC133, a Novel Marker for Human Hematopoietic Stem and Progenitor Cells". *Blood* **90**: 5002-5012
- Zacher T., et al. (2002). "Characterization of monocyte-derived dendritic cells in recent-onset diabetes mellitus type 1". *Clinical immunology* **105**(1): 17-24
- Zammaretti P., et al. (2005). "Adult endothelial progenitor cells. Renewing vasculature". *The International Journal of Biochemistry & Cell Biology* **37**:493-503
- Zhao H., et al. (2003). **"**Electrochemical polishing of 316L stainless steel slotted tube coronary stents: an investigation of material removal and surface roughness". *Progress in Biomedical Research* **8**(2): 70-81